

**VALORISATION OF RUBBER AND GLASS WASTE AS FINE  
AGGREGATE FOR THE PRODUCTION OF CONCRETE**

**Ph.D. THESIS**

**Kunal**

**2015RCE9046**



**DEPARTMENT OF CIVIL ENGINEERING**

**MALAVIYA NATIONAL INSTITUTE OF TECHNOLOGY**

**JAIPUR - 302017**

**FEBRUARY 2019**

**VALORISATION OF RUBBER AND GLASS WASTE AS FINE  
AGGREGATE FOR THE PRODUCTION OF CONCRETE**

*Submitted in*

*fulfilment of the requirements for the degree of*

***Doctor of Philosophy***

by

**Kunal**

**ID: 2015RCE9046**

Under the supervision of

**Dr. P. V. Ramana**



**DEPARTMENT OF CIVIL ENGINEERING  
MALAVIYA NATIONAL INSTITUTE OF TECHNOLOGY  
JAIPUR - 302017  
FEBRUARY 2019**

**© Malaviya National Institute of Technology Jaipur – 2019.**

**All rights reserved.**

*This thesis is dedicated to*

***My Grandmother***

*Late Smt. Himachali Bisht*

*&*

***My Beloved Parents***

*Mrs. Neelam Bisht & Mr. P.R. Bisht*



**MALAVIYA NATIONAL INSTITUTE OF TECHNOLOGY  
JAIPUR, INDIA-302017**

**DECLARATION**

I **Kunal**, declare that this thesis titled, “**Valorisation of Rubber and Glass Waste as Fine Aggregate for the Production of Concrete**” and the work presented in it, are my own. I confirm that:

- This work was done wholly or mainly while in candidature for a research degree at this university.
- Where any part of this thesis has previously been submitted for a degree or any other qualification at this university or any other institution, this been clearly stated.
- Where I have consulted the published work of others, this is always clearly attributed.
- Where I have quoted from the work of others, the source is always given. With the exception of such quotations, this thesis is entirely my own work.
- I have acknowledged all main source of help.
- Where the thesis is based on work done by myself, jointly with others, I have made clear exactly what was done by other and what I have contributed myself.

Date:

Kunal

(Student ID: 2015RCE9046)



**MALAVIYA NATIONAL INSTITUTE OF TECHNOLOGY  
JAIPUR, INDIA-302017**

**CERTIFICATE**

This is to certify that the thesis entitled '**Valorisation of Rubber and Glass Waste as Fine Aggregate for the Production of Concrete**' being submitted by **Kunal (2015RCE9046)** is a bonafide research work carried out under my supervision and guidance in fulfillment of the requirement for the award of the degree of Doctor of Philosophy in the Department of Civil Engineering, Malaviya National Institute of Technology, Jaipur, India. The matter embodied in this thesis is original and has not been submitted to any other University or Institute for the award of any other degree.

Place: Jaipur

Date:

**Dr. P. V. Ramana**

Assistant Professor

Department of Civil Engineering

MNIT, Jaipur

## ACKNOWLEDGEMENT

Time has provided me the cherished opportunity to express my heartfelt gratitude to my guide Dr. P. V. Ramana, Assistant Professor, MNIT Jaipur, who permitted me to carry out my thesis work under his able guidance. I shall ever remain indebted to him for his meticulous guidance, constructive criticism, clear thinking, keen interest, constant encouragement and forbearance right from the beginning of this thesis to its completion.

I wish to express my sincere thanks to Prof. Mahesh Kumar Jat, Professor and Head, CED, MNIT Jaipur, who has been a constant source of inspiration for me throughout this thesis work. I also like to thank Prof. M. K. Shrimali, Prof. S. D. Bharti, Prof. T. K. Dutta and Prof. Gunwant Sharma, members of the review committee for their valuable comments which helped me a lot in completing the work.

Special words of appreciation for Mr. Sapan Prasad Gaur and Mr. Pukhraj Leelawat, who helped me in my experimental work. I am also thankful to all the staff members of Civil Engineering Department Mr. Rajesh Saxena, Mr. R.S. Mandolia, Mr. Sita Ram Jat, Mr. Sadiq Ansari and Mr. Nitesh Kumar Sunaria, for their full cooperation and indispensable help. A special thanks also to the help provided by technical and support staff of Material Research Centre, MNIT Jaipur. I would also like to acknowledge Central Library and Departmental Library of MNIT Jaipur for providing access to International Journals.

I would acknowledge the support of Ms. Prachi Gupta Assistant Sales Manager West1, BASF Mumbai for providing chemical admixture for my research work. I am also thankful towards my material suppliers, Mr. Abhishek Jain (Savita Scientific and Plastic Products, Jaipur), Ankur Speciality Gases and Technologies (Jaipur), Shree Stones Crusher (Jaipur) and Gupta Rubbers (Jaipur).

I would like to express my deepest gratitude and love to my parents Mrs. Neelam Bisht and Mr. Pushp Raj Bisht, without whom I am nothing, for providing me everlasting support, big encouragement and lots of love. I am lucky to have countless support of my cousin sister Mrs. Apra Mohan and brother – in – law Mr. Bharat Mohan thorough out the process. It is an honour to acknowledge the love shown by my cousin brother Mr. Saket Vaidya and sister - in - law Mrs. Neha Vaidya throughout the completion of my research work. My understanding towards microstructural analysis has been significantly influenced

by the guidance of my cousin Ms. Surbhi Kapoor. The support of my cousin Ms. Radhika Kapoor in my life is more than sublime during the difficult times.

The contribution made by my dearest friends Ms. Shivangi Srivastava, Ms. Mahati Gurazada, Mrs. Ruchi Aswal, Ms. Ekta Tripathi, Ms. Divya Chopra, Ms. Priyanka Kumari, Mr. Kuldeep Singh, Mr. Bhanu Pratap Singh Thakur, Mr. Arpit Jindal, Mr. Varun Jain, Mr. Sushank Singla, Mr. Vikaran Mahajan, Mr. Ankit Kumar Abrol, Mr. Vipin Sharma, Mr. Rahul Khurana and Mr. Kamal Anand to my life is also profound, who inspired me to take up this doctoral degree. So just thanking them will be an understatement.

The cheerful support of my friends Ms. Priyam Tewari, Mrs. Anusha Sharma, Mr. K.I. Syed Ahmed Kabeer and Mr. Salman Siddique for their priceless guidance throughout my ups and downs is sincerely appreciated. I also thank, Mr. Shailesh Gupta, Mr. Rakesh Choudhary, Mr. Arigela Surendranath, Mr. Gyan Prakash, Mr. Ramesh Kumar, Mr. Mukesh Kuldeep, Mr. Manish Meena, Mr. Lalit Kumar Gupta, Mr. Abhishek Jain, Mr. Sumit Choudhary, Mr. Hashvardhan, Mr. Nishant Roy, Mr. Mohit Bhandari, Mr. Deepak Kumar Prajapat, Mr. Om Prakash, Mr. Rahisuddin, Ms. Ankita Saxena, Ms. Suchi Mala, Ms. Premlata Meena, Ms. Vinod Tanwar, Ms. Aishwarya Narang and Ms. Falti Teotia for their great help and support.

**Kunal**



## ABSTRACT

River sand acts as a filling agent between cement and coarse aggregate. However, ban enforced by State Government for its extraction from river bed beyond certain depth causes its scarcity. As a consequence of which price rise has been observed. To overcome this issue concrete industry has compelled to explore a substitute for fine aggregate (river sand) which is cheaper and locally available. Vast amount of discarded waste rubber and waste glass are being generated every year and their uncontrolled dumping contributes to landfilling problem. Hence, re-use of these discarded materials can protect barren lands and prevent associated health issues. Utilization of these waste materials as fine aggregate in construction industry for production of concrete also shows a positive step to diminish the cost of disposal of these superfluous materials.

Most of the researchers have studied the performance of waste rubber and waste glass individually in concrete and proved their usage as fine aggregate in concrete mixes at wide ranging percentage variation. Previous studies only talk about the proficiency of these waste materials to enhance the mechanical and durability performance of ordinary Portland cement (OPC) based concretes. In line with this, in present study, a proper study is needed to arrive at an exact optimum substitution level of fine aggregate by waste rubber (4 – 5.5% at an increment of 0.5%) and waste glass (18 – 24% at an increment of 1%) for fly-ash based concrete mixes separately.

Hence, in this study single water / cement ratio of 0.4 was adopted to verify hardened (compressive strength, flexural strength and pull-off strength), durability (abrasion resistance, water absorption, chloride penetration, carbonation, acid attack, freeze and thaw, drying shrinkage), microstructural properties (XRD, FTIR, TGA / DTA, FESEM) and Nano-structural properties (AFM) containing crumb rubber (mechanically grinded vehicle tyres) and waste glass (mechanically grinded beverage bottles) individually as partial substitute of fine aggregate. Study has also been carried out to check the performance of concrete under the exposure of natural fire at varied temperatures.

The outcome of present study indicates that bulk and apparent density of crumb rubber concrete mixes are negatively affected. Gradual fall in hardened properties were noticed however, 4% substitution level shows that strength achieved was under acceptable limit in comparison to target mean strength. Water absorption by immersion and under constant pressure shows adverse performance. On contrary to this, capillary suction of

water shows positive effect at higher substitution level. Behaviour of concrete under extreme conditions (freeze and thaw and acid attack) show improvement in performance with incorporation of crumb rubber in concrete mixes. The depth of chloride penetration remains almost constant up to 5% substitution level beyond which it increases. After 12 months of exposure, half-cell potential was less than 350  $\mu$ A. This proves that no substantial corrosion occurs in specimens. Increase in carbonation depth was noticed for crumb rubber incorporated concrete mixes at each exposure age. At 5.5% substitution level 8.4 mm penetration was recorded as compared with 7.6 mm for reference samples.

When waste glass was incorporated in concrete mixes fresh density reduced. However, apparent hardened density increases up to 21% substitution level. Incorporation of waste glass has led to the enhancement in quality of microstructure up to 21% substitution of fine aggregate. This has improved the mechanical properties of such concrete mixes. However, with rise in substitution level water absorption (immersion, constant pressure and capillary suction) shows negative performance due to increase in voids percentage. On the other hand, due to lower reactivity of waste glass higher resistance to acidic environment was observed. Due to increased porosity, resistance to rapid freezing and thawing also improved. In line with this, when exposed to chloride solution (immersion and corrosion) lesser changes have been monitored. Carbonation was also within limits, when substitution was restricted to 20%.

In a nut shell, crumb rubber and waste glass concrete can be used up to 4% and 21% substitution level of river sand respectively, without significant fall in any mechanical and durability properties. Hence, when crumb rubber and waste glass are used up to the above-mentioned levels, will reduce the dependency on fine aggregate (river sand) for the manufacture of concrete for structural elements.

# CONTENTS

<b>DECLARATION .....</b>	<b>i</b>
<b>CERTIFICATE.....</b>	<b>ii</b>
<b>ACKNOWLEDGEMENT.....</b>	<b>iii</b>
<b>ABSTRACT.....</b>	<b>v</b>
<b>LIST OF TABLES .....</b>	<b>v</b>
<b>LIST OF FIGURES .....</b>	<b>xiv</b>
<b>ABBREVIATIONS.....</b>	<b>xviii</b>
<b>CHAPTER 1.....</b>	<b>1</b>
<b>INTRODUCTION.....</b>	<b>1</b>
1.1 Background .....	1
1.2 Waste Rubber.....	2
1.3 Waste Glass .....	5
1.4 Problem Origination .....	8
1.5 Objectives .....	9
1.6 Thesis Outline.....	9
<b>CHAPTER 2.....</b>	<b>11</b>
<b>LITERATURE REVIEW .....</b>	<b>11</b>
2.1 General .....	11
2.2 Part – A: Rubber.....	11
2.2.1 Workability.....	11
2.2.2 Compressive Strength.....	12
2.2.3 Flexural Strength .....	13
2.2.4 Density.....	15
2.2.5 Abrasion Resistance .....	15
2.2.6 Water Absorption .....	16
2.2.7 Water Permeability .....	17
2.2.8 Shrinkage.....	18
2.2.9 Carbonation .....	18
2.2.10 Corrosion, Chloride Penetration and Chloride Diffusion .....	19
2.2.11 Acid Attack.....	20
2.2.12 Fire Behaviour .....	21
2.2.13 Freeze - Thaw Resistance .....	21
2.3 Part – B: Glass.....	22
2.3.1 Workability.....	22
2.3.2 Compressive Strength.....	24

2.3.3 Flexural Strength.....	25
2.3.4 Abrasion Resistance.....	26
2.3.5 Water Absorption.....	26
2.3.6 Water Permeability .....	27
2.3.7 Shrinkage .....	27
2.3.8 Carbonation.....	28
2.3.9 Corrosion, Chloride Penetration and Chloride Diffusion .....	28
2.3.10 Acid Attack.....	29
2.3.11 Fire Exposure .....	29
2.3.12 Alkali Silica Reaction .....	29
2.4 Concluding Remarks.....	30
<b>CHAPTER 3 .....</b>	<b>32</b>
<b>CHARACTERIZATION OF CRUMB RUBBER, WASTE GLASS AND CONCRETE MIXES.....</b>	<b>32</b>
3.1 General .....	32
3.2 Research Methodology .....	32
3.3 Classification of Materials .....	34
3.3.1 Cement.....	34
3.3.2 Fine Aggregate.....	34
3.3.3 Coarse Aggregate.....	35
3.3.4 Crumb Rubber.....	35
3.3.5 Waste Glass.....	35
3.3.6 Super Plasticizer.....	36
3.4 Concrete Mix Proportions.....	36
3.4.1 Crumb Rubber.....	36
3.4.2 Waste Glass.....	37
3.5 Material Preparation.....	37
3.6 Experimental Method.....	38
3.6.1 Field Emission Scanning Electron Microscopy (FESEM).....	38
3.7 Results and Discussion .....	38
3.7.1 Cement.....	38
3.7.2 Fine Aggregate.....	40
3.7.3 Crumb Rubber.....	41
3.7.4 Waste Glass.....	42
3.8 Concluding Remarks.....	43
<b>CHAPTER 4 .....</b>	<b>44</b>
<b>FRESH AND HARDENED PROPERTIES OF CONCRETE.....</b>	<b>44</b>

4.1 General .....	44
4.2 Experimental Procedure .....	45
4.2.1 Fresh Property .....	45
4.2.1.1 Workability.....	45
4.2.1.2 Fresh Bulk Density .....	46
4.2.2 Mechanical Property.....	46
4.2.2.1 Compressive Strength.....	46
4.2.2.2 Flexural Strength .....	47
4.2.2.3 Abrasion Resistance .....	47
4.2.2.4 Pull-off Strength .....	48
4.2.2.5 Density and Voids .....	48
4.2.3 Microstructure .....	49
4.2.3.1 XRD Analysis.....	49
4.2.3.2 FESEM Analysis .....	49
4.2.3.3 TGA Analysis.....	49
4.2.3.4 FTIR Analysis .....	49
4.2.3.5 AFM Technique.....	49
4.3 Results and Discussion of Part – A: Crumb Rubber .....	51
4.3.1 Fresh Property .....	51
4.3.1.1 Workability.....	51
4.3.1.2 Fresh Bulk Density .....	52
4.3.2 Mechanical Property.....	52
4.3.2.1 Compressive Strength.....	52
4.3.2.2 Density and Voids .....	54
4.3.2.3 Flexural Strength .....	55
4.3.2.4 Abrasion Resistance .....	56
4.3.2.5 Pull-off Strength .....	57
4.3.3 Microstructure .....	57
4.3.3.1 XRD Analysis.....	57
4.3.3.2 FESEM Analysis .....	60
4.3.3.3 TGA / DTA Analysis.....	60
4.3.3.4 FTIR Analysis .....	62
4.3.3.5 AFM Technique.....	63
4.4 Results and Discussion of Part - B: Glass Waste .....	65
4.4.1 Fresh Property .....	65
4.4.1.1 Workability.....	65
4.4.1.2 Fresh Bulk Density .....	66

4.4.2 Mechanical Properties.....	67
4.4.2.1 Compressive Strength.....	67
4.4.2.2 Density and Voids.....	69
4.4.2.3 Flexural Strength.....	70
4.4.2.4 Abrasion Resistance.....	71
4.4.2.5 Pull-off Strength.....	71
4.4.3 Microstructure.....	72
4.4.3.1 XRD Analysis.....	72
4.4.3.2 FESEM Analysis.....	76
4.4.3.3 TGA / DTA Analysis.....	77
4.4.3.4 FTIR Analysis.....	78
4.4.3.5 AFM Technique.....	80
4.5 Concluding Remarks.....	83
<b>CHAPTER 5.....</b>	<b>85</b>
<b>DURABILITY EFFECTS OF WATER ON CONCRETE.....</b>	<b>85</b>
5.1 General.....	85
5.2 Experimental Procedure.....	85
5.2.1 Water Absorption.....	85
5.2.1.1 Immersion.....	86
5.2.1.2 Constant Pressure.....	86
5.2.1.3 Capillary Action.....	87
5.2.2 Drying Shrinkage.....	87
5.2.3 Freeze and Thaw.....	87
5.3 Results and Discussion of Part - A: Crumb Rubber.....	88
5.3.1 Water Absorption.....	88
5.3.1.1 Immersion.....	88
5.3.1.2 Constant Pressure.....	89
5.3.1.3 Capillary Action.....	90
5.3.2 Drying Shrinkage.....	91
5.3.3 Freeze and Thaw.....	91
5.3.3.1 Mass Loss.....	91
5.3.3.2 Change in Compressive Strength.....	92
5.4 Results and Discussion of Part - B: Waste Glass.....	93
5.4.1 Water Absorption.....	93
5.4.1.1 Immersion.....	93
5.4.1.2 Constant Pressure.....	94
5.4.1.3 Capillary Action.....	95

5.4.2 Drying Shrinkage.....	95
5.4.3 Freeze and Thaw.....	96
5.4.3.1 Mass Loss .....	96
5.4.3.2 Change in Compressive Strength .....	98
5.5 Concluding Remarks.....	98
<b>CHAPTER 6.....</b>	<b>100</b>
<b>LONG TERM DURABILITY PROPERTIES AND RESISTANCE TO FIRE .....</b>	<b>100</b>
6.1 General .....	100
6.2 Experimental Procedure .....	101
6.2.1 Chloride Penetration.....	101
6.2.2 Half-cell Current.....	101
6.2.3 Carbonation .....	103
6.2.4 Acid Attack.....	104
6.2.5 Fire Attack.....	105
6.3 Results and Discussion of Part - A: Crumb Rubber .....	105
6.3.1 Corrosion .....	105
6.3.1.1 Chloride Penetration.....	105
6.3.1.2 Half-cell Potential.....	107
6.3.1.3 Carbonation .....	108
6.3.2 Acid Attack.....	109
6.3.2.1 Weight Loss.....	110
6.3.2.2 Change in Compressive Strength .....	111
6.3.2.3 XRD Analysis.....	112
6.3.2.4 FESEM Analysis .....	114
6.3.2.5 TGA / DTA Analysis.....	115
6.3.2.6 FTIR Analysis .....	116
6.3.3 Fire Test.....	118
6.3.3.1 Mass Loss .....	118
6.3.3.2 Compressive Strength.....	119
6.4 Results and Discussion of Part - B: Waste Glass .....	122
6.4.1 Corrosion .....	122
6.4.1.1 Chloride Penetration.....	122
6.4.1.2 Corrosion .....	124
6.4.1.3 Carbonation .....	125
6.4.2 Acid Attack.....	126
6.4.2.1 Weight Loss.....	126
6.4.2.2 Change in Compressive Strength .....	127

6.4.2.3 XRD Analysis .....	128
6.4.2.4 FESEM Analysis.....	130
6.4.2.5 TGA / DTA Analysis .....	132
6.4.2.6 FTIR Analysis.....	135
6.4.3 Fire Test .....	137
6.4.3.1 Mass Loss.....	137
6.4.3.2 Compressive Strength .....	138
6.5 Concluding Remarks.....	141
<b>CHAPTER-7 .....</b>	<b>142</b>
<b>CONCLUSIONS &amp; FUTURE SCOPE.....</b>	<b>142</b>
7.1 Summary .....	142
7.2 Conclusions.....	142
7.2.1 Part – A: Crumb Rubber .....	142
7.2.2 Part – B: Waste Glass.....	144
7.3 Future Scope .....	146
<b>REFERENCES .....</b>	<b>149</b>



## LIST OF TABLES

Table 1.1: Size distribution of rubber products manufacturing units .....	3
Table 1.2: State wise production of waste rubber .....	3
Table 3.1: Physical and mechanical properties of cement, aggregates, crumb rubber and waste glass.....	36
Table 3.2: Concrete mix proportions in kg/m <sup>3</sup> for a constant w/c ratio .....	37
Table 3.3: Concrete mix proportions in kg/m <sup>3</sup> for a constant w/c ratio .....	37
Table 3.4: Elemental composition of cement .....	39
Table 3.5: Elemental composition of fly-ash .....	40
Table 3.6: Elemental composition of fine aggregate .....	41
Table 3.7: Elemental composition of crumb rubber .....	42
Table 3.8: Elemental composition of waste glass .....	43
Table 4.1: Test matrix for mechanical and microstructure properties of concrete samples.....	45
Table 4.2: Workability of fresh crumb rubber concrete .....	51
Table 4.3: TGA investigated on water cured crumb rubber concrete samples.....	62
Table 4.4: FTIR analysis on water cured crumb rubber concrete samples.....	63
Table 4.5: Average length and depth of voids at ITZ.....	64
Table 4.6: Workability of fresh waste glass concrete mixes .....	66
Table 4.7: TGA investigated on water cured waste glass concrete samples .....	78
Table 4.8: FTIR analysis on waste glass concrete samples.....	80
Table 4.9: Average length and depth of voids at ITZ.....	82
Table 5.1: Test matrix for durability effects of water on concrete sample.....	86
Table 6.1: Test matrix for long term durability effects.....	101
Table 6.2: TGA investigated on crumb rubber concrete samples .....	116
Table 6.3: FTIR wave numbers investigated on crumb rubber concrete samples.....	117
Table 6.4: TGA investigated on waste glass concrete samples.....	134
Table 6.5: FTIR wave numbers investigated on waste glass concrete samples .....	136
Table 7.1: List of concluding results .....	147

## LIST OF FIGURES

Fig. 1.1: Waste rubber.....	3
Fig. 1.2: Import of waste rubber .....	4
Fig. 1.3: Production of waste rubber .....	4
Fig. 1.4: Production of sheet and float glass .....	5
Fig. 1.5: Production of bottles and glassware .....	6
Fig. 1.6: Waste glass.....	6
Fig. 1.7: Re-cycling of waste glass .....	8
Fig. 2.1: Literature review flowchart for rubber .....	23
Fig. 2.2: Literature review flowchart for glass .....	31
Fig. 3.1: 28 day compressive strength of crumb rubber concrete specimens .....	32
Fig. 3.2: 28 day compressive strength of waste glass concrete specimens.....	33
Fig. 3.3: List of raw materials.....	34
Fig. 3.4: Particle size distribution of river sand .....	34
Fig. 3.5: Crumb rubber .....	35
Fig. 3.6: Waste glass.....	35
Fig. 3.7: Concrete mixer .....	38
Fig. 3.8: FESEM image of cement particles .....	39
Fig. 3.9: EDAX of cement.....	39
Fig. 3.10: EDAX of fly-ash .....	40
Fig. 3.11: FESEM image of fine aggregate .....	40
Fig. 3.12: EDAX of fine aggregate.....	41
Fig. 3.13: FESEM image of crumb rubber .....	41
Fig. 3.14: EDAX of crumb rubber.....	42
Fig. 3.15: FESEM image of waste glass.....	42
Fig. 3.16: EDAX of waste glass.....	43
Fig. 4.1: List of experiments.....	44
Fig. 4.2: Compaction factor apparatus.....	46
Fig. 4.3: Compressive strength apparatus.....	46
Fig. 4.4: Flexural strength apparatus.....	47
Fig. 4.5: Abrasion resistance apparatus .....	47
Fig. 4.6: Pull-off strength apparatus .....	48
Fig. 4.7: Optical image obtained for concrete specimen.....	50
Fig. 4.8: Cantilever arm in tapping mode .....	50
Fig. 4.9: Percentage of admixture for crumb rubber concrete mixes.....	51
Fig. 4.10: Fresh density of crumb rubber concrete mixes.....	52

Fig. 4.11: Compressive strength of crumb rubber concrete specimens .....	53
Fig. 4.12: Hardened density of crumb rubber concrete specimens .....	54
Fig. 4.13: Voids ratio of crumb rubber concrete specimens .....	54
Fig. 4.14: Flexural strength of crumb rubber concrete specimens .....	55
Fig. 4.15: Abrasion resistance of crumb rubber concrete specimens .....	56
Fig. 4.16: Pull-off strength of crumb rubber concrete specimens .....	57
Fig. 4.17: XRD analysis of crumb rubber concrete samples .....	59
Fig. 4.18: FESEM analysis of crumb rubber concrete specimens .....	60
Fig. 4.19: TGA / DTA analysis of crumb rubber concrete samples .....	61
Fig. 4.20: FTIR analysis of crumb rubber concrete samples .....	62
Fig. 4.21: Surface topography with roughness distribution curve of CR concrete specimens .....	64
Fig. 4.22: Average roughness of crumb rubber concrete samples .....	65
Fig. 4.23: Percentage of admixture in waste glass concrete mixes .....	66
Fig. 4.24: Fresh density of waste glass concrete specimens .....	67
Fig. 4.25: Compressive strength of waste glass concrete specimens .....	68
Fig. 4.26: Hardened density of waste glass concrete specimens .....	69
Fig. 4.27: Voids ratio of waste glass concrete specimens .....	69
Fig. 4.28: Flexural strength of waste glass concrete specimens .....	70
Fig. 4.29: Abrasion resistance of waste glass concrete specimens .....	71
Fig. 4.30: Pull-off strength of waste glass concrete specimens .....	72
Fig. 4.31: XRD analysis of waste glass concrete samples .....	75
Fig. 4.32: FESEM analysis of waste glass concrete specimens .....	77
Fig. 4.33: TGA / DTA analysis of waste glass concrete samples .....	78
Fig. 4.34 FTIR analysis of waste glass concrete samples .....	79
Fig. 4.35: Surface topography with roughness distribution curve of WG concrete samples .....	81
Fig. 4.36: Average roughness of waste glass concrete samples .....	83
Fig. 5.1: List of experiments .....	85
Fig. 5.2: DIN permeability apparatus with specimens .....	86
Fig. 5.3: Drying shrinkage of specimens .....	87
Fig. 5.4: Freeze and thaw apparatus .....	88
Fig. 5.5: Water absorption of crumb rubber concrete specimens .....	89
Fig. 5.6: Water permeability of crumb rubber concrete specimens .....	89
Fig. 5.7: Sorptivity of crumb rubber concrete specimens .....	90
Fig. 5.8: Drying shrinkage of crumb rubber concrete prisms .....	91
Fig. 5.9: Mass loss of crumb rubber concrete specimens .....	92
Fig. 5.10: Freeze and thaw exposure for crumb rubber concrete specimens .....	92
Fig. 5.11: Change in compressive strength of crumb rubber concrete specimens .....	93

Fig. 5.12: Water absorption of waste glass concrete specimens .....	94
Fig. 5.13: Water permeability of waste glass concrete specimens.....	94
Fig. 5.14: Sorptivity of waste glass concrete specimens.....	95
Fig. 5.15: Drying shrinkage of waste glass concrete specimens.....	96
Fig. 5.16: Mass loss of waste glass concrete specimens .....	97
Fig. 5.17: Freeze and thaw exposure for waste glass concrete specimens.....	97
Fig. 5.18: Change in compressive strength of waste glass concrete specimens .....	98
Fig. 6.1: List of experiments .....	100
Fig. 6.2: Corrosion specimens .....	102
Fig. 6.3: Half-cell potential.....	102
Fig. 6.4: Carbonation chamber .....	103
Fig. 6.5: Carbonated specimens .....	103
Fig. 6.6: Specimens exposed to acidic environment.....	104
Fig. 6.7: Fire test apparatus.....	105
Fig. 6.8: Chloride penetration of crumb rubber concrete specimens .....	106
Fig. 6.9: Chloride penetration in crumb rubber concrete specimens .....	106
Fig. 6.10: Half-cell measurements for crumb rubber concrete specimens.....	107
Fig. 6.11: Depth of carbonation for crumb rubber concrete prisms.....	109
Fig. 6.12: Carbonation depth of crumb rubber concrete prisms after exposure to 28 days .....	109
Fig. 6.13: Change in weight for crumb rubber concrete specimens .....	110
Fig. 6.14: Change in compressive strength for crumb rubber concrete specimens.....	111
Fig. 6.15: Acid attacked crumb rubber concrete samples .....	112
Fig. 6.16: XRD analysis of crumb rubber concrete samples .....	113
Fig. 6.17: FESEM analysis for crumb rubber concrete specimens.....	114
Fig. 6.18: TGA / DTA analysis for crumb rubber concrete samples .....	116
Fig. 6.19: FTIR analysis for crumb rubber concrete samples.....	117
Fig. 6.20: Mass loss for crumb rubber concrete specimens exposed to fire .....	119
Fig. 6.21: TGA / DTA analysis of crumb rubber.....	119
Fig. 6.22: Change in compressive strength for CR concrete specimens exposed to fire .....	120
Fig. 6.23: XRD analysis of crumb rubber concrete samples exposed to 800°C.....	121
Fig. 6.24: Chloride penetration for waste glass concrete specimens .....	123
Fig. 6.25: Depth of chloride penetration in waste glass concrete specimens.....	123
Fig. 6.26: Half-cell measurements for waste glass concrete specimens .....	124
Fig. 6.27: Depth of carbonation for waste glass concrete prisms .....	125
Fig. 6.28: Carbonation depth of waste glass concrete prisms after exposure to 90 days.....	125
Fig. 6.29: Change in weight for waste glass concrete specimens .....	126
Fig. 6.30: Change in compressive strength for waste glass concrete specimens .....	128

Fig. 6.31: Acid attacked waste glass concrete samples .....	128
Fig. 6.32: XRD analysis of waste glass concrete samples.....	130
Fig. 6.33: FESEM analysis of waste glass concrete specimens .....	132
Fig. 6.34: TGA / DTA analysis of waste glass concrete samples .....	134
Fig. 6.35: FTIR analysis of waste glass concrete samples .....	136
Fig. 6.36: FTIR analysis of with and without exposed waste glass and river sand.....	136
Fig. 6.37: Mass loss of waste glass concrete specimens exposed to fire.....	138
Fig. 6.38: Compressive strength of waste glass concrete specimens exposed to fire.....	139
Fig. 6.39: XRD analysis of waste glass samples exposed to 800°C .....	141

## ABBREVIATIONS

<b>AFM</b>	: Atomic Force Microscopy
<b>ASTM</b>	: American Society for Testing and Materials
<b>B</b>	: Brucite
<b>BIS</b>	: Bureau of Indian Standards
<b>C</b>	: Calcite
<b>CASH</b>	: Calcium Aluminium Silicate Hydrate
<b>CPHEEO</b>	: Central Public Health and Environmental Engineering Organization
<b>CR</b>	: Crumb Rubber
<b>CR0</b>	: Crumb Rubber zero percent
<b>CR4</b>	: Crumb Rubber four percent
<b>CR4.5</b>	: Crumb Rubber four point five percent
<b>CR5</b>	: Crumb Rubber five percent
<b>CR5.5</b>	: Crumb Rubber five point five percent
<b>CS / CSH</b>	: Calcium Silicate Hydrate
<b>CuK<math>\alpha</math></b>	: Copper K- $\alpha$
<b>DC</b>	: Direct Current
<b>DTA</b>	: Differential Thermal Analysis
<b>EDAX</b>	: Energy-dispersive X-ray Spectroscopy
<b>E<sub>t</sub></b>	: Ettringite
<b>FESEM</b>	: Field Emission Scanning Electron Microscopy
<b>FTIR</b>	: Fourier Transform Infrared Spectroscopy
<b>GC</b>	: Glass Concrete
<b>G<sub>y</sub></b>	: Gypsum
<b>ISO</b>	: International Organization for Standardization
<b>ITZ</b>	: Interstitial Transition Zone
<b>KBr</b>	: Potassium Bromide
<b>Mm</b>	: Millimetre
<b>ml</b>	: Millilitre
<b>Mv</b>	: Millivolts
<b>N</b>	: Newton
<b>N<sub>0</sub></b>	: Normality
<b>OH</b>	: Free Water
<b>OPC</b>	: Ordinary Portland Cement
<b>O-Si-O</b>	: Free Silica

<b>pH</b>	: pouvoir Hydrogene
<b>PPC</b>	: Portland Pozzolana Cement
<b>Q</b>	: Quartz
<b>R<sub>q</sub></b>	: Mean square roughness
<b>RW</b>	: Rubber Waste
<b>S</b>	: Surface area of specimen
<b>T</b>	: Change in thickness
<b>TGA</b>	: Thermal Gravimetric Analysis
<b>UTM</b>	: Universal Testing Machine
<b>V</b>	: Volts
<b>V<sub>1</sub></b>	: Original volume of sample
<b>W</b>	: Wollastonite
<b>W<sub>1</sub></b>	: Weight of empty cylinder
<b>W<sub>2</sub></b>	: Weight of fully compacted cylinder minus weight of empty cylinder
<b>W<sub>3</sub></b>	: Initial weight of specimen
<b>W<sub>4</sub></b>	: Weight of specimen after completion of test
<b>W<sub>5</sub></b>	: Oven dry weight of specimens
<b>W<sub>6</sub></b>	: Weight of specimen after boiling
<b>W<sub>7</sub></b>	: Apparent weight of specimen after boiling
<b>WG</b>	: Waste Glass
<b>WG0</b>	: Waste Glass zero percent
<b>WG18</b>	: Waste Glass eighteen percent
<b>WG19</b>	: Waste Glass nineteen percent
<b>WG20</b>	: Waste Glass twenty percent
<b>WG21</b>	: Waste Glass twenty one percent
<b>WG22</b>	: Waste Glass twenty two percent
<b>WG23</b>	: Waste Glass twenty three percent
<b>WG24</b>	: Waste Glass twenty four percent
<b>WR</b>	: Waste Rubber
<b>XRD</b>	: X-ray Diffraction
<b>Y</b>	: Density of water
<b>µm</b>	: Micrometre
<b>AgCl</b>	: Silver Chloride
<b>AgNO<sub>3</sub></b>	: Silver Nitrate
<b>AgO</b>	: Silver Oxide
<b>CaSO<sub>4</sub></b>	: Calcium Sulphate

<b>CaSO<sub>4</sub>.0.5H<sub>2</sub>O</b>	:	Bassanite
<b>Ca(OH)<sub>2</sub></b>	:	Calcium Hydroxide
<b>CaSiO<sub>3</sub></b>	:	Wollastonite
<b>CO<sub>3</sub><sup>2-</sup></b>	:	Carbonate
<b>NaCl</b>	:	Sodium Chloride
<b>SiO<sub>2</sub></b>	:	Silica
<b>ZnCSH</b>	:	Zinc Silicate Calcium Hydrate
<b>ZnSH</b>	:	Zinc Silicate Hydrate



### INTRODUCTION

---

#### 1.1 Background

Concrete has been widely accepted as a prominent invention in the world of science, due to its performance and affordability by the society. It is widely used across the globe because of its versatile nature as it can acquire any shape, making people realise that their imagination can be framed in the field of construction. Constituents used to prepare concrete are cement, aggregates, water and admixtures. Out of these the most crucial material in concrete is cement (grey powder) which imparts strength. Interfacial bonding between cement and aggregates (gravel and river sand) leads to enhancement of microstructural characteristics thus improves the performance of concrete specimens (Simon and Chandra (2016)). However, significant volume of concrete (around 60 to 75 percentage) is made up of aggregates.

Presently, scarcity of river sand is creating trouble across the world. This is a consequence of drying rivers due to which Government has banned the excavation of river sand from river bed. As a result of which price rise has been observed for river sand because of its non-availability at local areas. Therefore, construction industry has been compelled to consider other materials as a substitute of river sand as fine aggregate in concrete (Syed and Quadri (2013)). A material can be considered as a substitute of fine aggregate in concrete only after conducting a comprehensive study.

Central Public Health and Environmental Engineering Organization (CPHEEO) stated that in India production of superfluous materials was nearly 0.00065 tons per person per day. However, the number is comparatively small as compared to waste produced by the United States (0.0023 tons per person per day). Population of India (1.2 billion) is four times more than United States (307 million) which proves that India generates more waste (27 million tons) as compared to United States.

Generation of surplus waste has led to a desperate and outrageous measure of converting cultivable and forest lands to dumping sites (Murari et al. (2014) and Pappu et al. (2007)). The degraded material is afflicting ecological balance across the globe (Sivakumar Babu et al. (2013)). Industrial by-products such as marble waste, rice husk ash,

plastic waste, stone wastes, ceramic waste, glass waste, copper slag, waste tyre rubber, etc., are some examples of solid waste materials which are harmful for atmosphere. Being non-biodegradable in nature the damage caused to the environment are very sever. In 2002, amount of waste produced was recorded around 12 billion tons annually and this quantity is projected to increase to 19 billion by the end of 2025 (Dasgupta (2014)).

## 1.2 Waste Rubber

Like other rubber producing nations, manufacturing of rubber in India during initial stages of 20<sup>th</sup> century was specifically related with its export business. However, rise in rubber industry marked subsequent progress in later 1930s. In India this growth in rubber industry mainly circled around some correlated advancements:

- a) In 1934 execution of International Rubber Regulation Agreement (IRRA) following to locally accessibility of natural rubber at lesser rate.
- b) Granting permits for overseas industries to establish in India owing to cheaper raw materials and helpers.
- c) Government support to enhance the commercial sector necessities during Second World War.

Post-World War witnessed huge rise in rubber industry sector. Mainly the in-take of rubber was controlled by some bigger organisations. However, survival of small-scale industries was also observed during that period due to fair turnover through manufacturing of rubber-based merchandise.

Basically, rubber industry is broadly divided into two parts, viz as the tyre sector and non-tyre sector. Mainly, tyre sectors are governed by bigger commercial groups whereas, non-tyre sector was directed by small and medium scale industries. Particulars about rubber merchandise units in India are mentioned in **Table 1.1** out of which consumption of small-scale units are less than 10 tonnes. It has also been noticed that total number of rubber manufacturing groups noticed a reduction from 5066 in 2001 - 02 to 4327 units in 2008 - 09 due to increase in cost of raw materials. In order to match the requirements in automobile sector rubber is also imported in India.

On the other hand, due to rapid industrialization, change has been observed in living standard of people which has resulted in steady rise in utilization of vehicles. It has been

chronicled that nearly 1000 million tyres are cast-off every year and upsurge of this count to about 1200 million is possible by 2030 (Pacheco-Torgal et al. (2012)).

**Table 1.1: Size distribution of rubber products manufacturing units (Mathew (2010))**

Years / Type of Unit	2006 - 07	2007 - 08	2008 - 09
<b>Tyre Factories</b>	58	58	58
<b>Large / Medium Non-Tyre Units</b>	471	490	490
<b>Small Units</b>	4121	4093	3779

Out of which, India individually contributes around 112 million waste tyres every year (Mukul (2010)). The discarded rubber is shown in **Fig. 1.1**. In addition to this rubber was also imported (**Fig. 1.2**) which after completion of its service life adds to waste production. The production of waste rubber (WR) in India is graphically presented in **Fig. 1.3**. Increase in production of discarded rubber has been amplified from 2010 till February 2018. However, maximum production of waste rubber was recorded by southern states of India as shown in **Table 1.2**.



**Fig. 1.1: Waste rubber**

**Table 1.2: State wise production of waste rubber (tonnes) (V.Sanjeev Kumar (2018))**

Years / States	2011 - 12	2012 - 13	2013 - 14	2014 - 15	2015 - 16	2016 - 17
<b>Kerala</b>	798890	800050	681100	565000	492000	606000
<b>Tamil Nadu</b>	25220	25350	21700	18075	15750	19500
<b>Karnataka</b>	27890	31250	24800	21950	18500	22750
<b>Others</b>	51700	57050	46400	39975	35750	42750

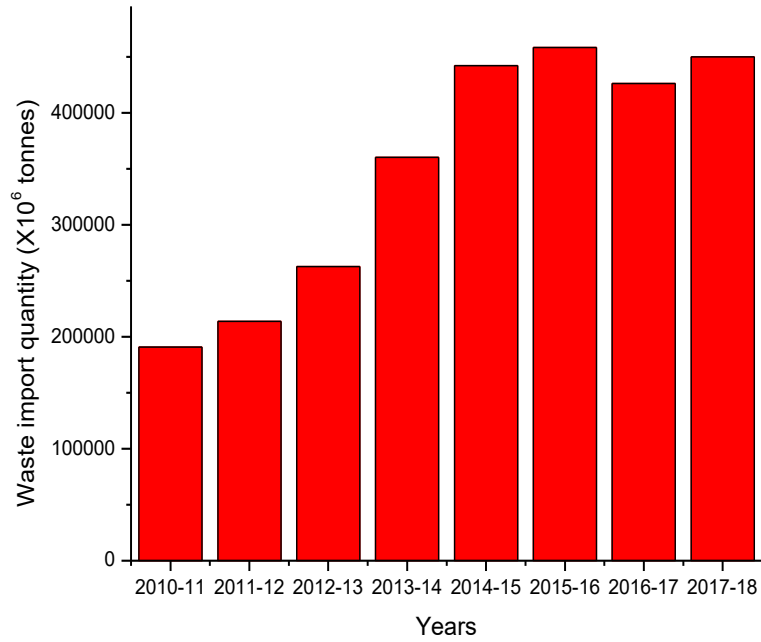


**Fig. 1.2: Import of waste rubber (V.Sanjeev Kumar (2018))**

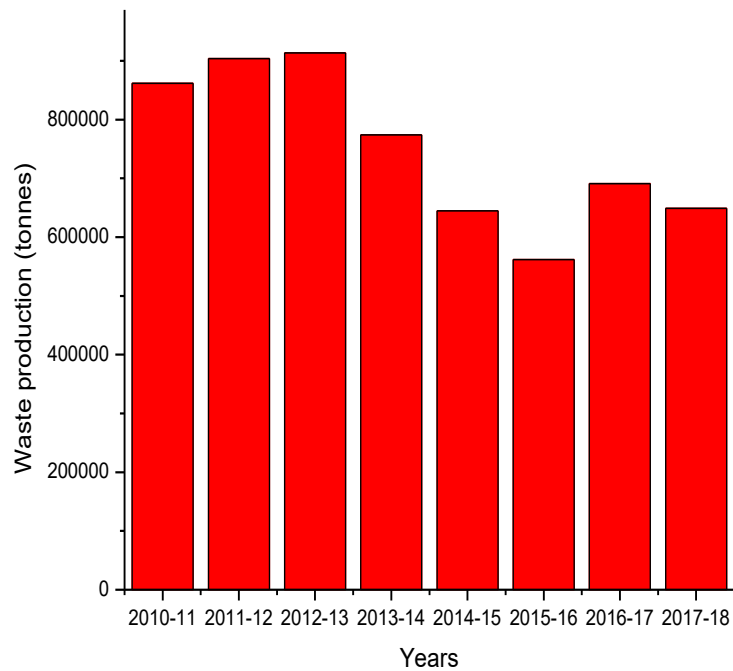


**Fig. 1.3: Production of waste rubber (V.Sanjeev Kumar (2018))**

As an outcome of this, disposal of tyre waste also increased concern towards landfilling problem as it provides space for rodents to breed (Eldin and Senouci (1994)). Incineration of disposed rubber does not prove to be a sustainable approach, since this practice is accompanied by emission of toxic fumes (Guo et al. (2014)). With 75% hollow space in waste tyres, accumulated with allowed oxygen. It was mentioned that severe fire occurs in Wales where 10 million tyres were leftover. Those tyres were burnt endlessly for

nearly 15 years results into life-threatening problems and its residue contaminates the soil (Pacheco-Torgal et al. (2012)).

Recycling of waste rubber can be done by using pyrolysis process in which tyre waste is heated in reactor which is exposed to environment. The drawback of this method is emission of carbon black which pollutes the air. Hence, alternative approaches need to be designed in order to carry out utmost usage of rubber waste (RW). The construction industry can be very crucial in doing so. RW can be consumed as fuel in cement kilns or as a substitute of fine aggregate in concrete (Correia et al. (2012)). These noteworthy steps might lessen the extent of dumping and also reduce the associated ecological issues.

### 1.3 Waste Glass

Glass being non-biodegradable in nature is manufactured by melting nearly 75% of sand, almost 15% of soda ash and approximately 10% of calcium materials. Glass production units mainly comprise of fabrication of flat glass, packaging glass, vacuum flasks, fibre glass and laboratory appliances. In 1908, first glass manufacturing unit was established in India and with due course of this industry is fully developed. From ancient hand working methods, this industry has come a long way to get fully modernised. From 2001 to 2005 maximum growth (around 67%) has been recorded in the manufacturing process of sheet and float glass as shown in **Fig. 1.4**. This progress is mainly associated with the boom in automobile and construction industries. Additionally, glass containers and bottles also resulted in upsurge at that time by 5 – 6% as presented in **Fig. 1.5**.

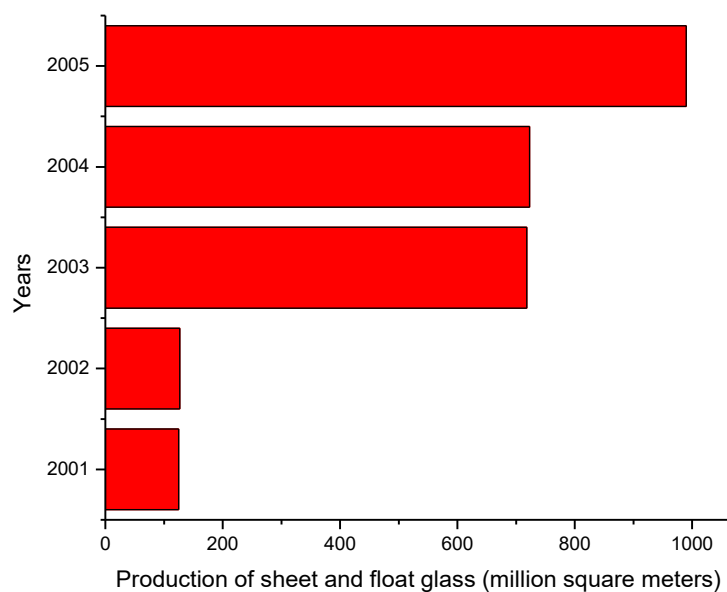


**Fig. 1.4: Production of sheet and float glass (KPMG (2007))**

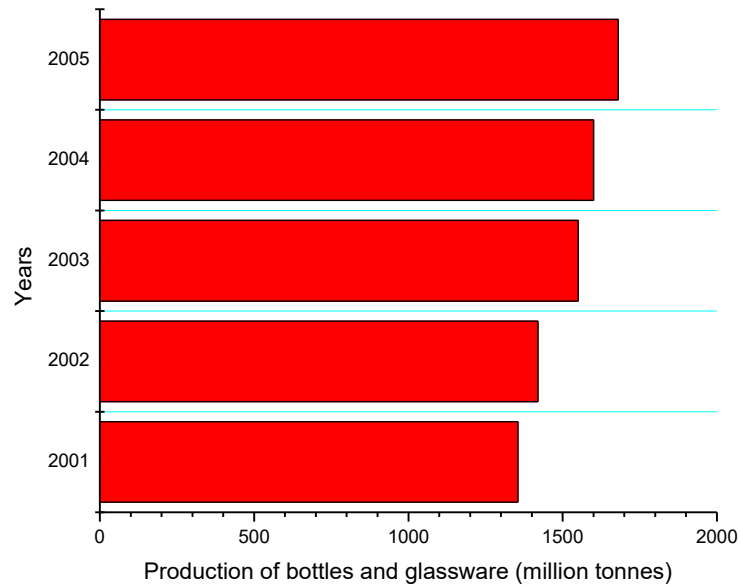


**Fig. 1.5: Production of bottles and glassware (KPMG (2007))**

From last two decades researchers have shown keen interest to reuse glass waste. This is consequence of generation of glass waste in alarming quantities and in different forms such as beverage glass, electric appliances glass etc. as shown in **Fig. 1.6**. Out of complete waste generated only certain percentage of waste glass can be recycled.



**Fig. 1.6: Waste glass**

Although recycling of glass can be done several times by sustaining its chemical characteristics (Kou et al. (2008)). For that waste glass (WG) must be segregated according to its colour (blue, green, flint etc.) which is the first prime criteria behind reprocessing method. Secondly, reprocessing can be prejudiced by adulterates attack on stockpiled WG.

Lastly, a number of cities are equipped with glass recycling amenities. Transportation of WG to other places with the available recycling infrastructure is also not preferred due to high shipping charges. Hence, the generated waste is landfilled.

CPHEEO has listed the percentage consumption of WG for different countries after recycling process which is mentioned in **Fig. 1.7**. Switzerland, Turkey, Sweden, Finland and Belgium are countries which consume maximum amount of discarded WG. However, concern of re-utilization of this discarded material is still point of concern for some countries including India, where consumption of WG is less than half of the total waste generated.

Waste glass's that can't be reprocessed are generally landfilled which is not a sustainable approach. Being non-biodegradable in nature it does not decay easily and occupies virgin land which can be used for other purpose. Anti-dumping rule for soda ash, has driven hike in manufacturing cost by 5 - 15%. In September 2017, the Gujrat High Court in; India increases duty charges on soda ash import from several markets. The United States of America and China were imposed with utmost duty charges. To overcome this, Indian glass manufactures (glass production hub - Agra) are looking for economical foreign imports in order to reduce the import expenses. In India, nearly half of the consumption of glass goods used as containers and its demand increases by 6 -7% annually. With rising concern over food quality packed and stored in plastic containers, people have started preferring glass for packaging. Another boost in glass containers was noticed when National Green Tribunal banned plastic containers in towns and cities located on the banks of the River Ganga. All such factors have led to steep rise in utilization of glass products and consequent generation of wastes.

To overcome this issue of excessive generation, utilization of WG in construction materials is one of the many possible approaches. Utilization of WG in construction industry for production of concrete also shows a positive step to diminish the cost of WG disposal (Chen et al. (2006)). WG being rich in silica improves the cementitious properties of concrete. Concrete prepared with glass generally referred as Glass Concrete (GC) can be utilized as substitute for conventional concrete in construction of road pavement and parking areas (Yuksel et al. (2013)). Such consumption of WG in concrete, reduces the environmental issues and also enhances the effective use of resources (R. Siddique (2008)).

WG is also used in the form of glass fibers in construction, owing to their low cost (Belarbi et al. (2016)).

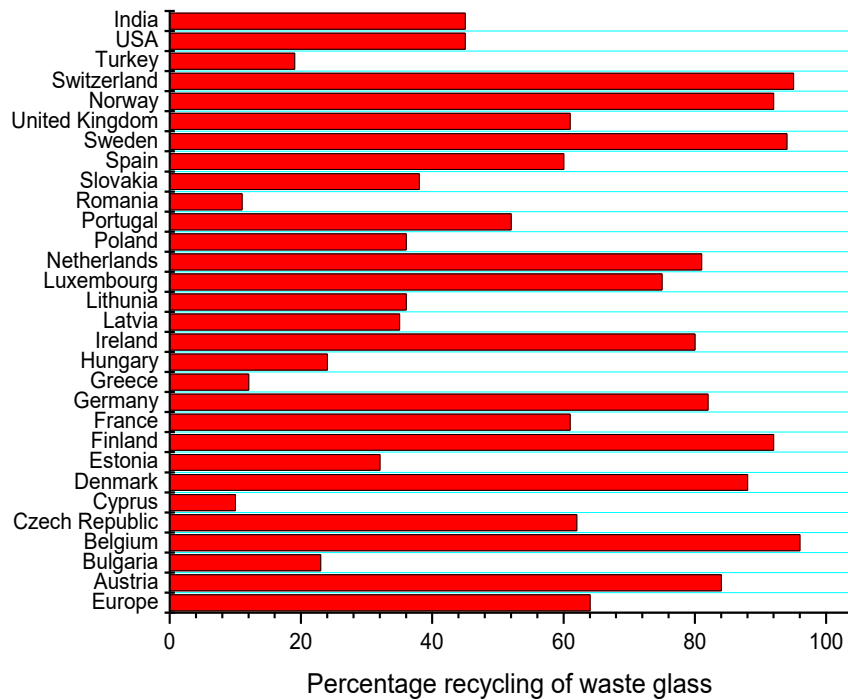


**Fig. 1.7: Re-cycling of waste glass (AIGFM (2011))**

Construction industry utilizes nearly 30 billion tonnes of natural resources for the production of building materials. Since extraction of these materials is associated with environmental degradation, governing authorities have imposed restriction on their usage. Such restrictions demand assessing alternative materials that can be used to replace conventional ones. Hence, material scientists have adopted the waste to resource conversion route through which both dependency on natural resources is reduced along with finding a suitable disposal procedure of waste generated by other industries. In order to utilize waste materials in concrete, the durability characteristics are a point of concern during a structures life span (Vipulanandan and Amani (2018)).

### 1.4 Problem Origination

Various researchers have monitored the effects of waste materials (rubber and glass) individually on concrete properties. These degraded materials have been utilised as a substitute for cement, fine and coarse aggregate. There are studies which speak about the ability of these degraded materials to modify the hardened and durability properties of ordinary Portland cement (OPC) based concretes. As per author best understanding, there is no study which brings out the change in performance of fly-ash based cement composite.



Previous studies have verified the suitability of WR and WG individually as fine aggregate in concrete mixes at wide ranging percentage variation. In line with this outcome, in this present work an attempt has been made to arrive at an exact optimum substitution level for rubber (4 – 5.5% at an increment of 0.5%) and glass (18 – 24% at an increment of 1%) in concrete mixes separately. Hence, this study was carried out to monitor the mechanical and durability effects of concrete properties of M25 grade with single water/cement ratio (0.4) containing waste glass and rubber. In addition to this, microstructural properties of prepared composites were also investigated to justify the observed results.

### **1.5 Objectives**

The objectives of this research work are as follows:

- To characterize crumb rubber and waste glass in terms of properties that supplement the modifications noted in the behaviour of concrete mixes on their utilization.
- To investigate the influence of waste rubber and waste glass individually as a partial replacement of fine aggregate on fresh & hardened physical and mechanical properties.
- Examine the behaviour of waste rubber and waste glass concrete individually under action of portable water, chemical agents, rapid freezing and thawing and fire.

### **1.6 Thesis Outline**

This thesis is structured in seven sections. Each section comprises of tables and figures which are elucidated along with text. The overview behind drawbacks of non-biodegradable waste materials which includes tyre waste and glass waste and their usage in field of construction were already presented in chapter 1. Further, research objectives are also framed in this section.

Chapter 2 illustrates the analysis on studies already carried out by using non-biodegradable waste like rubber waste and glass waste in concrete as a substitute of fine and coarse aggregates.

Chapter 3 explains physical and chemical characterization of raw materials used to prepare the concrete mixes. Microstructural study was also carried out using Field Emission Scanning Electron Microscopy (FESEM) to monitor the elemental composition of raw materials.

Chapter 4 demonstrates the fresh and hardened properties of crumb rubber and waste glass concrete mixes individually. Microstructural analysis was also conducted to judge the microstructure behaviour of concrete properties.

Chapter 5 presents the effect of water on concrete samples prepared with crumb rubber and waste glass individually. Tests like water absorption, drying shrinkage and freeze and thaw is described in this section.

Chapter 6 explains the performance of concrete samples prepared with inclusion of waste rubber and waste glass individually when exposed to simulated saline environment. The behaviour of concrete specimens, when exposed to aggressive environmental conditions such as acid attack and fire exposure is also presented.

Chapter 7 depicts the significant conclusions arrived through present study and the suggestions for future study have also been mentioned.

## **2.1 General**

This chapter presents a comprehensive analysis on the effect of waste rubber and waste glass as a partial replacement of coarse and fine aggregate on concrete properties. Thorough review on the influence of these waste materials on mechanical and durability performance has been listed in this chapter.

## **2.2 Part – A: Rubber**

### **2.2.1 Workability**

Changes have been observed in the nature of concrete mixes with incorporation of waste rubber (WR). Hernández-Olivares and Barluenga (2004), Batayneh et al. (2008), Oikonomou and Mavridou (2009), Ozbay et al. (2011), Gupta et al. (2014) and Skariah et al. (2014) mentioned fall in workability whereas, Khaloo et al. (2008) and Aiello and Leuzzi (2010) illustrates better performance.

Sukontasukkul and Chaikaew (2006) reported reduced workability for concrete mixes with decreasing the average size of WR (passing sieve 6 and 20 as per ASTM). Al-Tayeb et al. (2013) also noticed fall in workability with inclusion of WR (1 – 5 mm) as a substitute of river sand. Batayneh et al. (2008) also reported similar observation when crumb rubber (CR) (0.075 - 4.75 mm) of varying percentage from 0% to 100% was incorporated in concrete. Oikonomou and Mavridou (2009) proved that as the rubber content increases up to 15% workability decreases. The usage of CR in concrete prolongs setting time and increase the viscosity of concrete. The use of fly ash in concrete reduces this undesirable outcome with CR which reduces viscosity. Gupta et al. (2014) substituted rubber ash (0.15 to 1.9 mm) from 0% to 20% in steps of 5% with replacement of fine aggregates. The researchers concluded that as the content of rubber ash increases, concrete workability decreases. However, no change in workability was reported by Skariah et al. (2014) by replacing fine aggregate with CR (0.6 mm, 0.8 – 2 mm, 2 – 4 mm).

Khaloo et al. (2008) noticed conflicting behaviour of workability with inclusion of fine (0.15 mm) and coarse (15 mm) WR as a substitute of river sand. Improved workability was monitored up to 15% substitution with fine WR, beyond which it decreases. However,

minimum workability was detected for coarse WR at same substitution level. Aiello and Leuzzi (2010) testified insignificant progress in workability when coarse aggregate were partially replaced by WR shreds (8 - 20 mm).

### **2.2.2 Compressive Strength**

Inclusion of WR content in concrete shows steady decrease in compressive strength. By et al. (1999) noticed fall in compressive strength with substitution of aggregate (fine and coarse) with CR and tire chips respectively. This fall in strength was mainly related with agglomeration of WR around aggregates and lack of bonding between WR and cement paste. Güneyisi et al. (2004) also observed similar reduction by using WR (10 - 40 mm) as a substitute of fine aggregate.

Benazzouk et al. (2007) noticed 77% fall in compressive strength with incorporation of shredded rubber (< 1 mm) up to 50% substitution level. The reduced trend was due to lower stiffness of shredded rubber in comparison with nearby cement matrix and also due to propagation of cracks around settled rubber particles.

Batayneh et al. (2008) used CR (0.075 – 4.75 mm) as a substitute of fine aggregate and reported 90% fall in compressive strength at 100% substitution level. The decrease in strength was due to weaker bonding between aggregate and CR. This is due to smooth texture of CR as compared with fine aggregate.

Khaloo et al. (2008) observed 98% drop in compressive strength by using CR and chipped rubber as an alternative for fine and coarse aggregate. The reduction in trend was due to increase in air voids in concrete samples. However, Taha et al. (2009) observed 78% and 67% fall in compressive strength with 100% substitution of coarse aggregate and fine aggregate respectively.

Ozbay et al. (2011) stated 26% fall in compressive strength after replacing 25% of fine aggregate by CR (0 – 3 mm). This occurs due to improper bond at interface as mentioned by Shah et al. (2014) due to increased porosity of concrete hence, reduces the density. Thus, results in drop in compressive strength. Son et al. (2011) also observed similar outcome after replacing fine aggregates with CR (0.6 mm and 1 mm). Grinys et al. (2012) used CR (1mm, 1 – 2 mm and 2 – 3 mm) as a substitute of fine aggregate and noticed 85% reduction in strength at 30% replacement level. The decline in strength was attributed to substitution of higher density (fine aggregate) constituent with low density CR waste.

Turki et al. (2012) observed 84% reduction in compressive strength at 50% substitution of fine aggregate with CR (1 – 4 mm). The drop in strength shows similar reason as mentioned by Grinys et al. (2012).

Mohammed et al. (2012) observed reduced compressive strength for hollow concrete blocks when 50% of fine aggregate was replaced with CR (0.06 – 0.6 mm). Decrease in strength was due to lower adhesion between CR and cement matrix.

Xue and Shinozuka (2013) detected 47% drop in compressive strength when coarse aggregate was substituted up to 20% by CR (6 mm). The fall in strength was due to substitution of coarse aggregate with lower load taking CR and also due to weaker interfacial bonding. Al-Tayeb et al. (2013) also reported fall in compressive strength by utilizing CR (0.16 - 2.36 mm) as fine aggregate (10% and 20%) in concrete.

Onuaguluchi and Panesar (2014) also showed drop in compressive strength by substituting fine aggregate with CR (< 2.3 mm) up to 15% replacement level and monitored 40% fall in strength. This reduction owing to lower adhesive strength between CR and cement matrix.

Gupta et al. (2014) substituted rubber ash (0.15 to 1.9 mm) from 0% to 20% in steps of 5% with replacement of fine aggregates. Fall in compressive strength was noticed due to generation of voids.

Skariah et al. (2014) replaced fine aggregate with (0.6 mm, 0.8 – 2 mm, 2 – 4 mm) up to 20% substitution level with increment of 2.5%. The results noticed fall in compressive strength due to poor bonding between CR and cement paste.

### **2.2.3 Flexural Strength**

The inclusion of WR in concrete mixes show contradictory behaviour. Rise and fall of this parameter depends upon the size of WR used.

Benazzouk et al. (2003) noticed enhanced flexural strength by incorporating two different types of WR, compact WR (1 – 4 mm) and expanded WR (4 – 12 mm). Inclusion of these two different types of WR enhances the flexural strength of samples up to 20% replacement of fine aggregate. Further incorporation of WR reduced the flexural strength due to splitting of rubber and cement matrix bond. With replacement of cement up to 20%

by WR (0.25 mm, 0.5 mm and 1 mm), Yilmaz and Degirmenci (2009) monitored rise in flexural strength. However, further inclusion of WR shows decline in flexural strength. Ganesan et al. (2013) also mentioned 15% improved flexural strength with 20% replacement of river sand by shredded rubber (4.75 mm).

Turatsinze and Garros (2008) replaced coarse aggregate up to 25% with WR (4 - 10 mm) and examined 42% fall in flexural strength. This decline in strength was related with reduced mechanical performance of WR in concrete. Ganjian et al. (2009) also reported 37% decrease in flexural strength by replacing river sand with CR (0.425 – 4.75 mm). Fall in this parameter was related with weaker connection between CR particles and cement matrix.

Aiello and Leuzzi (2010) examined decrease in flexural strength by replacing coarse aggregate with rubber shreds (8 – 20 mm). At 75% replacement of coarse aggregate 28% loss in flexural strength was monitored whereas, 7% reduction was observed at same substitution level for fine aggregate. This reduction was due to poor mechanical performance of WR.

Uygunoğlu and Topçu (2010) observed 55% decline in flexural strength by replacing fine aggregate up to 50% with WR (1 – 4 mm). The rapid failure was not monitored under bending loading condition. Turki et al. (2012) investigated decreased performance of flexural strength by replacing fine aggregate up to 50% with WR (1 – 4 mm). Nearly, 72% decline in flexural strength was noticed which due to lower density of WR. Grinys et al. (2012) observed drop in flexural strength by replacing 30% fine aggregate with CR (1mm, 1 – 2 mm and 2 – 3 mm) and showed 72% fall in flexural strength at highest replacement level. Liu et al. (2013) reported 18% fall in flexural strength with 15% substitution of fine aggregate by WR (2 mm). Su et al. (2015) mentioned reduced trend for flexural strength by replacing river sand up to 20% by WR and examines 12% reduction in flexural strength.

Gupta et al. (2014) substituted rubber ash (0.15 to 1.9 mm) from 0% to 20% in steps of 5% with replacement of fine aggregates. Decrease in flexural strength was noticed which generally depends on the shape of CR. Due to irregular shape of crumb rubber particles, the interface between these and cement paste act as a bed for water during vibration and curing. Similar observation was made by Skariah et al. (2014) by replacing fine aggregate

with CR (0.6 mm, 0.8 – 2 mm, 2 – 4 mm) up to 20% substitution level and noticed fall in flexural strength due to smooth texture of CR.

#### **2.2.4 Density**

Incorporation of WR in concrete influences its hardened density. Taha et al. (2009) noticed that when fine aggregates are replaced up to 50% with WR (1 – 5 mm) density of concrete sample decreases by 12%. This drop in density was due formation of air voids and also because of lesser specific gravity of WR as compared to river sand it replaces.

Zheng et al. (2008) investigated that when coarse aggregates up to 45% are replaced by ground rubber (4 – 15 mm) and powdered rubber (< 2.6 mm) 16% drop in density was observed.

Yilmaz and Degirmenci (2009) replaced cement with rubber waste (0.0 - 0.25 mm, 0.25 - 0.5 mm, 0.5 – 1.0 mm) and noticed decrease in density. This reduction shows similar reason as mentioned by Taha et al. (2009).

Pelisser et al. (2011) mentioned that when river sand was replaced with WR (< 4.8 mm) 13% drop in density was observed. However, incorporation of 15% silica fume and WR together this reduction reduces to 9%.

Xue and Shinozuka (2013) monitored 16% fall in density when 20% substitution of coarse aggregate was made with CR (6 mm). Decrease in density was associated with lower specific gravity of CR.

#### **2.2.5 Abrasion Resistance**

Abrasion resistance specifies the durability of concrete sample by performing wear and tear action on concrete surface. Greater the abrasion resistance higher will be the durable performance of the concrete sample.

Segre and Joekes (2000) reported decrease in weight of concrete specimen when exposed to wear and tear action. Around 300% loss in weight was observed when powdered rubber (0.500 mm) was incorporated in concrete as a substitute for fine aggregate.

Ozbay et al. (2011) noticed 20% improved abrasion resistance when 25% fine aggregate was substituted by CR (0 - 3 mm) in cement mortar. However, when aggregate (coarse and fine) are replaced with CR (2 mm & 3.36 mm) upsurge in weight loss due to

wear and tear action was observed by Sukontasukkul and Chaikaew (2006). Weight loss greater than 90% was recorded at 20% substitution of fine aggregate with CR.

Gesoğlu et al. (2014) mentioned increase in depth of wear, when coarse aggregates are substituted with tire chips (4 mm) and fine aggregate by CR (1 mm). Abrasion resistance reduced by 81% at 20% substitution level. This drop was due to failure in binding action of WR with cement paste.

Gupta et al. (2014) substituted rubber ash (0.15 to 1.9 mm) from 0% to 20% in steps of 5% with replacement of fine aggregates and noticed fall in abrasion resistance for rubber ash concrete mixes. Most adverse situation occurs at 0.55 w/c ratio where, abrasion resistance was even less than allowable limits as per IS 1237 (2012).

### **2.2.6 Water Absorption**

The water absorption delivers an idea regarding porosity inside the concrete sample and also presents an overview for microstructural morphology.

Turatsinze and Garros (2008) reported that when 25% coarse aggregate was replaced with WR (4 – 10 mm) porosity increases by 30%. This occurs due to presence of air voids which reduces the compaction of concrete.

Yilmaz and Degirmenci (2009) noticed fall in water absorption when cement was replaced by WR (> 0.25 mm, 0.25 – 0.50 mm and 0.50 – 1.0 mm). This occurs because of poor water absorption nature of WR.

Ganjian et al. (2009) mentioned rise in water absorption when fine aggregate was replaced with CR (0.425 – 4.75 mm) whereas, cement with WR (0.075 – 0.475 mm). Rapid rise of water absorption was noticed owing to lack of adhesion between the constituents. Oikonomou and Mavridou (2009) monitored reduction in water absorption when 15% fine aggregate was substituted by waste tyre (< 1 mm).

Uygunoğlu and Topçu (2010) noticed rise in water absorption up to 50% substitution level of fine aggregate with WR (1 – 4 mm). Approximately 18% rise in water absorption was detected at highest substitution level. Rise in water absorption was associated with air voids and poor adhesion between WR and cement matrix.



Bjegović et al. (2011) observed reduced water absorption when 15% fine aggregate was substituted with WR (0.5 – 2 mm, 2 – 3.5 mm and 2 - 4 mm). About 78% fall in water absorption was observed at 15% substitution of fine aggregate.

Bravo and De Brito (2012) noticed upsurge in water absorption by replacing 15% river sand with WR (passing 4 mm). Rise in water absorption (2.5%) was monitored due to poor connection between cement matrix and WR.

Sukontasukkul and Chaikaew (2006) investigated rise in water absorption up to 30% substitution of fine aggregate with CR (2 mm & 3.36 mm). This was due to formation of air bubbles at the time of mixing which get trapped inside the concrete as a consequence more voids were formed near cement paste and CR.

Onuaguluchi and Panesar (2014) monitored increased water absorption with substitution of river sand by CR (< 2.3 mm). When 15% of fine aggregate was replaced around 7% rise in water absorption was recorded. Rise in water absorption was related with increased proportion of void content in concrete.

Gupta et al. (2014) noticed rise in water absorption with inclusion of rubber ash in concrete mixes. Change in water absorption was noticed approximately 169.1% for 0.35 w/c ratio, 16.3% for 0.45 w/c ratio and -9.1% for 0.55 w/c ratio at 20% substitution level.

### **2.2.7 Water Permeability**

Water permeability is essential parameter which defines the durability of concrete. Ganjian et al. (2009) monitored the behaviour of CR (0.425 – 4.75 mm) by replacing coarse aggregate and cement with WR (0.075 – 0.475 mm). At 10% replacement level, 150% rise in water permeability was noticed and 114% with replacement of cement at same substitution level. Rise in water permeability was due to reduced bonding between constituents.

Bjegović et al. (2011) studied the effect of water permeability with replacement of 15% aggregate with WR (0.5 – 2 mm, 2 – 3.5 mm and 2 - 4 mm) and noticed 100% rise in water permeability at 10% substitution level. This rise was mainly related with increase in air voids around WR which allows the water to penetrate at greater depth.

Su et al. (2015) reported 215% rise in water permeability when 20% crushed rubber (0.3 mm, 0.5 mm & 3 mm) was used as a substitute of fine aggregate. This rise in water permeability was associated with intensified porosity of concrete.

### **2.2.8 Shrinkage**

The extent of shrinkage depends upon amount of moisture vanished (Jun et al. (2011)). Rapid shrinkage was observed for lower w/c ratio due to early departure of water present in concrete specimen. Turatsinze and Garros (2008) observed fall in shrinkage for self-compacting concrete when coarse aggregate was replaced up to 25% by WR (4 – 10 mm). This better performance of shrinkage was due to improved strain capacity. Uygunoğlu and Topçu (2010) reported rise in shrinkage when scrap rubber (1 – 4 mm) was used in place of river sand up to 50% replacement level for self-compacting concrete. The researchers monitored increase in porosity due to presence of scrap rubber.

Bravo and De Brito (2012) noticed upsurge in total shrinkage when fine aggregate was replaced with WR. However, drying shrinkage was very less affected with incorporated WR.

Sukontasukkul and Tiamlom (2012) noticed rise in shrinkage up to 30% substitution of fine aggregate with CR (< 0.5 mm). This increase in shrinkage was due to flexible nature of CR.

Yung et al. (2013) mentioned uplift in drying shrinkage by substituting fine aggregate up to 20% with rubber powder (0.3 mm and 0.6 mm). At 20% substitution level 95% rise in shrinkage was noticed. Lesser distortion capacity of rubber powder displays main intention behind increased shrinkage.

### **2.2.9 Carbonation**

Insertion of carbon dioxide in concrete via connecting pores which reacts with hydrated compound and results into carbonation (Papadakis et al. (1992)). Carbonation lessens the pH of concrete and also intensifies the probability of corrosion. Roy et al. (1999) reported that extreme carbonation occurs when relative humidity was in range of 50 – 75%.

Bravo and De Brito (2012) noticed rise in carbonation depth when fine aggregate was replaced up to 15% with WR. At 15% substitution level carbonation depth increases

by 56%. This hike in carbonation depth was due to reduced workability of WR concrete and formation of pores between WR and cement matrix.

Thomas et al. (2016) mentioned lower depth of carbonation by substituting fine aggregate with CR up to 10% replacement level. Further incorporation of CR causes upsurge in depth of carbonation. Drop in carbonation up to 10% substitution level was due to improved quality of concrete with CR. This occurs due to similar size of fine aggregate it replaces. Increase in carbonation depth after 10% substitution was due to lack of adhesion between constituents.

### **2.2.10 Corrosion, Chloride Penetration and Chloride Diffusion**

Exposure of concrete to chloride is a foremost reason behind corrosion of steel bars as mentioned by Ababneh (2002). Voids present in concrete eases the movement of chloride ions inside concrete. Existence of oxygen from atmosphere results into anodic and cathodic reactions. This initiates the corrosion on steel bars.

Al-Akhras and Smadi (2004) noticed resistance against chloride ions by replacing fine aggregate with WR. This was due to fact that WR restrict the entry of chloride ions by settling down in voids.

Gesoğlu and Güneyisi (2007) mentioned upsurge in penetration of chloride ions when river sand was replaced with CR and coarse aggregate with tire chips. Rise in chloride permeability was observed up to 59% at 25% substitution of total aggregate.

The fall in chloride penetration was observed by Oikonomou and Mavridou (2009) by substituting fine aggregate with WR. At 15% substitution level, 35% fall in chloride penetration was noticed. Bjegović et al. (2011) also reported drop in chloride penetration when 15% total aggregate was replaced with WR. This fall in chloride penetration was due to better filling ability of WR in concrete.

Bravo and De Brito (2012) does not observe any pattern for chloride penetration when fine aggregate was replaced by WR. Fall in chloride penetration was noticed by researchers up to 5% substitution of fine aggregate beyond which it increases.

J. F. Dong et al. (2013) mentioned rise in chloride penetration on replacing fine aggregate with CR and noticed 40% hike in chloride penetration at 30% substitution of fine

aggregate. This upsurge in chloride penetration was due to presence of voids at CR and cement paste interface.

Onuaguluchi and Panesar (2014) monitored irregular trend for chloride penetration with inclusion of CR. Nearly, 18%, 25% and 12% fall in chloride penetration was noticed at 5%, 10% and 15% substitution of fine aggregate.

Gupta et al. (2014) indicates lesser penetration of chloride ions for all CR modified concrete mixes. Thus results into higher resistance towards the penetration of chloride ions.

Thomas et al. (2016) detected similar or nearly equal diffusion of chloride ions when 10% CR was used as fine aggregate as compared with control mix. However further incorporation causes adverse effect. The lesser penetration of chloride ions was due to lower water absorption of CR which does not allow chloride ions to penetrate. However, beyond 10% increased chloride penetration was observed due to lack of adhesion between constituents.

### **2.2.11 Acid Attack**

The exposure of concrete materials to aggressive conditions through their service span is a point of concern (Vidya Sagar and Raghu Prasad (2012)). The performance of concrete on exposure to acidic environment (sulphuric acid) is also one such durability concern. Exposure of concrete to this medium degrades the quality and also reduces its service life as mentioned by Araghi et al. (2015). When subjected to an acidic medium, degradation of concrete occurs due to dissolution of hydrogen ions which depends upon the pH of acidic medium. Based on this pH value, extent of deterioration of concrete can vary.

Joseph et al. (1997) observed gain in mass of concrete specimens with decrease in the pH of sulphuric acid solutions. Specimens immersed in acid solutions with pH values of 1.0, 2.5 and 4.0 show the formation of reaction products which peel out the surface layers and causes change in volume. The maximum change in mass was recorded for pH 1.0 where specimens undergo 13% mass loss before completion of three months.

Azevedo et al. (2012) reported rise in mass loss after exposure to acidic environment up to 15% substitution of fine aggregate with WR (1mm and 2.4 mm). Around 35% mass loss was noticed at 15% replacement level.

Thomas et al. (2016) noticed positive outcome for rubberized concrete after exposure to acidic environment. Change in mass and compressive strength was lesser with inclusion of WR up to 20% in steps of 2.5%. This might be due to proper bonding of WR with constituents of concrete which prevents their material separation.

### **2.2.12 Fire Behaviour**

The exposure of concrete structures to elevated temperature show fall in mass loss as well as reduces mechanical performance. These variations are also noticed by various researchers Akçaözoğlu (2013) and Nadeem et al. (2014).

Peng et al. (2008) mentioned that decrease in mechanical performance of concrete depends upon method of cooling after exposure to elevated temperature. Akçaözoğlu (2013) and Nadeem et al. (2014) reported that fast cooling causes higher mass and compressive strength loss.

Hernández-Olivares and Barluenga (2004) reported the effect on concrete cubes (fine aggregate was replaced by WR fibers up to 8%), when exposed to elevated temperature. No spalling was observed on the surface of exposed concrete cubes due to burning of WR fibers which allows the vapours to take exit from concrete cube. After exposure to elevated temperature small gaps were observed on WR concrete cube surface however, no such gap was noticed on control cube. At 3% substitution level of fine aggregate with rubber fibers compressive strength reduces by 10%.

Marques et al. (2013) observed the behaviour of WR concrete samples when exposed to fire attack. After exposure to 800°C the burnt WR left behind voids which degrades its mechanical property as compared to control samples. Maximum loss was observed after 15% substitution of fine aggregate with WR.

### **2.2.13 Freeze - Thaw Resistance**

Raghavan et al. (1998) observed that incorporation of 0.6% of CR in concrete enhances the performance after exposure to freeze and thaw. Weight loss for rubber incorporated concrete mixes was lower as compared to control concrete sample.

Zhu et al. (2012) investigated size effect of CR on freezing and thawing resistance. Increasing the fineness of CR, resistance towards freezing and thawing action also increases

was showed by researchers. The maximum resistance was observed by incorporating CR of size (0.250 mm) in concrete mix.

Gesoğlu et al. (2014) reported no strong difference in mass loss for CR concrete as well as control concrete when exposed to 240 cycles. On completion of 300 cycle's mass loss was monitored more for control concrete as compared with CR concrete.

## **2.3 Part – B: Glass**

### **2.3.1 Workability**

Variations have been noticed in concrete properties with incorporation of waste glass (WG) in concrete. Rise and fall of workability depends on the size of WG utilized in concrete mix.

Park et al. (2004) reported decrease in workability with increase in substitution level of fine aggregate (up to 70%) with recycled glass (5 mm) of different colours (amber, emerald green and flint). This fall in workability was related with sharp edges of recycled glass.

Chen et al. (2006) examined the behaviour of workability when E-glass (38 – 300  $\mu\text{m}$  and 40% < 150  $\mu\text{m}$ ) was replaced with fine aggregate up to 50%. This was due to decrease in efficiency of workability with rise in substitution level.

Batayneh et al. (2007) substituted fine aggregates at an interval of 5% up to 20% with crushed glass (75 micron - 9.5 mm). No change has been observed in workability with inclusion of crushed glass in concrete mixes.

Metwally (2007) noticed negative effect on workability when finely milled WG (passing 0.045 mm) used as a substitute for fine aggregate.

Taha and Nounu (2009) reported reduction in workability when WG (< 5 mm) was used as a substitute of fine aggregate at 50% and 100% substitution level. About 28.83% and 33.33% fall in slump value was observed at higher replacement levels respectively.

Limbachiya (2009) noticed no effect on workability with replacement of fine aggregate (0%, 5%, 10%, 15%, 20%, 30% and 50%) by mixed coloured WG (< 5 mm) up to 30%. However, after 30% substitution level fall in slump value was observed.

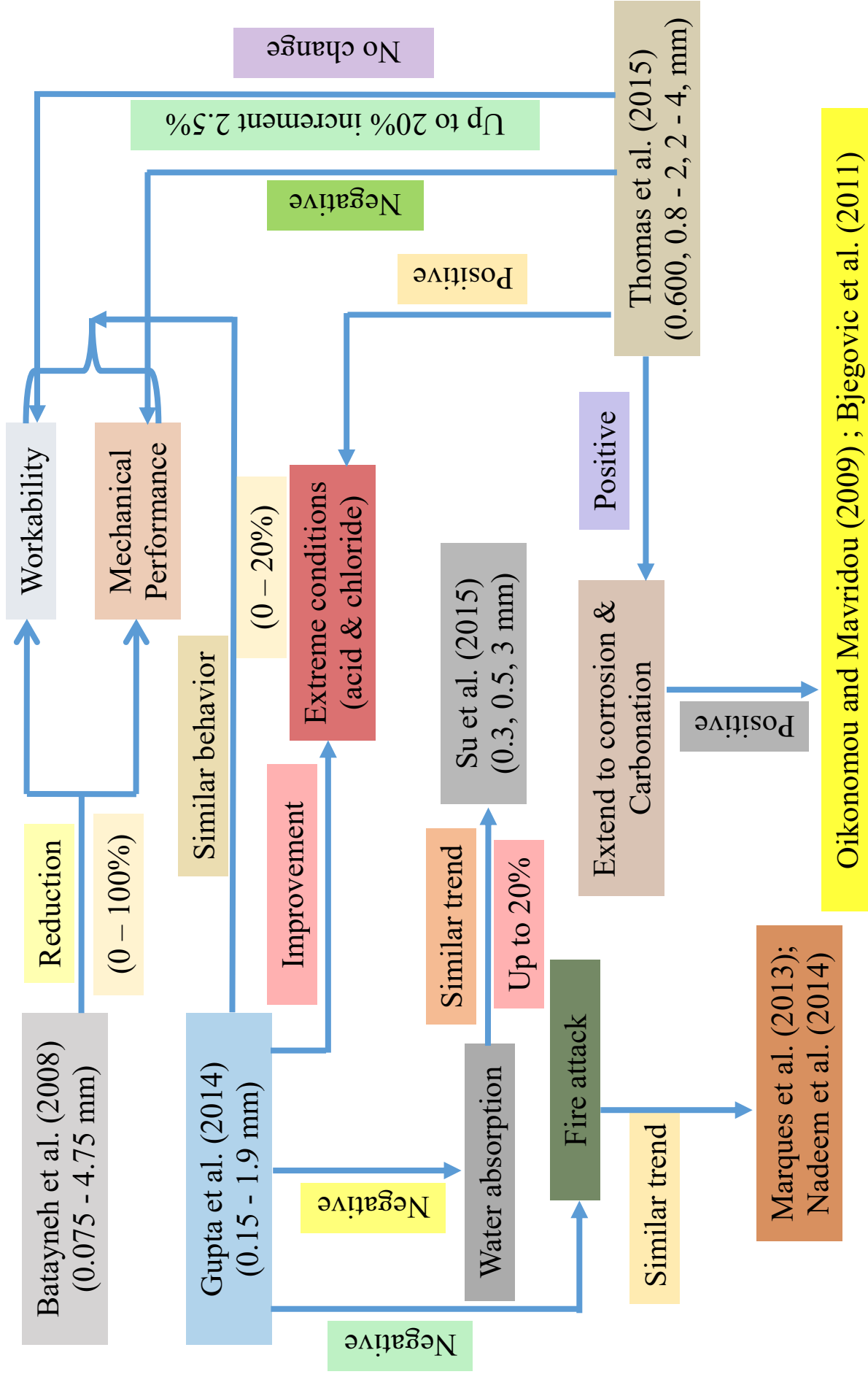


Fig. 2.1: Literature review flowchart for rubber

Ismail and AL-Hashmi (2009) substituted fine aggregate (0%, 10%, 15% and 20%) with WG (0.15 - 4.75 mm). Researchers examined 23.33%, 30% and 33.33% fall in workability with incorporation of waste at different substitution levels respectively.

De Castro and De Brito (2013) noticed reduced workability by replacing fine aggregate with WG (< 4 mm) from 5% to 20%. At 20% substitution level 4.33% fall in workability was recorded.

### **2.3.2 Compressive Strength**

Enhancement in compressive strength was reported by Shao et al. (2000) by replacing fine aggregate (40%) with waste E-glass (75 µm). Rise in compressive strength was observed by 17%, 27% and 43% at 28, 90 and 365 days respectively. This upsurge in compressive strength was due to presence alumina-silicate in E-glass which improves the properties of concrete. Chen et al. (2006) also monitored considerable progress in compressive strength during later ages when fine aggregate was replaced by fine WG (< 75 µm).

Metwally (2007) substituted finely milled WG (passing 0.045 mm) with fine aggregate (5, 10, 15 and 20%) in concrete mixtures and monitored delayed improved compressive strength. Compressive strength of concrete shows positive effect up to 20% substitution of fine aggregate with WG (75 micron – 9.5 mm) as reported by Batayneh et al. (2007).

Ismail and AL-Hashmi (2009) used WG (150 microns - 4.75 mm) as replacement of fine aggregate (10%, 15% and 20%). The researchers observed that with addition of WG, strength increases up to 20% replacement. Borhan (2012) reported that, as compared with control samples, concrete specimens containing WG (0.5 – 3 mm) at 20% replacement of fine aggregate showed enhanced compressive strength. Malik et al. (2013) substituted fine aggregate with WG (1.18 mm) up to 40%. Around 9.8% rise in compressive strength was noticed up to 30% replacement level however, further inclusion of WG reduces the performance of concrete by 8.5% as compared to control mix.

The study reported by Du and Tan (2014) depicts that as the fineness of WG as a substitute of fine aggregate increases, compressive strength illustrates superior performance. This increase in strength is basically due to high pozzolanic activity.



Park et al. (2004) substituted river sand (0%, 30%, 50% and 70%) with amber, emerald green and flint WG (< 5mm) together. The researchers noticed that with rise in substitution level compressive strength decreases. This mechanical performance did not present any remarkable change with respect to the colour of WG.

Terro (2006) noticed that at 10% replacement of fine aggregate with WG (0.075 – 4.75 mm) illustrates nearly equal compressive strength as compared to control mix. However, with further incorporation of WG (25%, 50% and 100%) fall in compressive strength was monitored.

Taha and Nounu (2008) reported the usage of mixed coloured contaminated WG (< 5 mm) as fine aggregate at 50 and 100% substitution level as a consequence of which negative behaviour was observed for its mechanical performance. Limbachiya (2009) found that utilization of mixed coloured beverage glass and containers (< 5 mm) showed improved compressive strength up to 20% replacement level of fine aggregate with WG, however further inclusion of WG showed decrement at all curing ages.

Gautam et al. (2012) partially used WG (0.15 – 4.75 mm) as a substitute of fine aggregate at an increment of 10% up to 40%. They noticed maximum compressive strength at 20% substitution level beyond which it decreases.

De Castro and De Brito (2013) also noticed reduced compressive strength by using crushed building and car window glasses (< 4mm) as fine aggregate in concrete at 5, 10 and 20% replacement level.

### **2.3.3 Flexural Strength**

As seen in compressive strength, flexural strength also shows contradictory observations with use of WG in concrete mixes. The rise or fall of this parameter is mainly dependent on the surface texture of glass used as reported by Jani and Hogland (2014). When the surface of WG was sufficiently rough, improved resistance has been observed (Topçu and Canbaz (2004)).

Rise in flexural strength was recorded up to a substitution level of 20% only. Beyond this percentage, fall in strength was observed (Ismail and AL-Hashmi (2009)). Particle size has also determined the extent of variation of this mechanical property (Du and Tan (2014)). Turgut and Yahlizade (2009) substituted white WG (4.75 mm) from 10

to 30% with increment of 10%. This study also shows that flexural strength increases up to 20% replacement. Du and Tan (2014) stated that clear WG displayed lower strength as compared to other coloured WG.

#### **2.3.4 Abrasion Resistance**

Su and Chen (2002) substituted fine aggregate at an interval of 5% up to 15% with WG ( $\leq 4.75$  mm). Improvement in skid resistance was examined in both the directions with inclusion of WG in concrete.

Turgut and Yahlizade (2009) also noticed improvement in abrasion resistance when fine aggregate was replaced by white WG (1.18 mm) at an interval of 10% up to 30% substitution level. Increase in abrasion resistance was monitored about 9.45%, 14.81% and 8.53% as compared to control concrete.

However, drop in abrasion resistance has been investigated by Ling et al. (2011) when fine aggregate was replaced by WG (5 - 10 mm) at an interval of 25% up to 100%. Fall in abrasion resistance was noticed with increase in proportion of WG. In line with this outcome, Ling and Poon (2011) also noticed reduced abrasion resistance by replacing river sand with coloured WG (60%  $< 2.36$  mm and 40% 2.36 – 5 mm).

#### **2.3.5 Water Absorption**

Taha and Nounu (2008) noticed similar behaviour when mixed coloured WG ( $< 5$  mm) was used as a substitute for fine aggregate at same substitution level.

Reduced trend for water absorption was also monitored by Taha and Nounu (2009) when fine aggregate was substituted with WG ( $< 5$  mm) to the tune of 50% and 100%. This reduction in water absorption was mainly related with impermeable nature of WG. Reduced trend for water absorption was also reported by Ling and Poon (2013) when fine aggregate (100%) was replaced with waste beverage glass ( $< 5$  mm). They noticed nearly 14.49% fall in water absorption. Further reduction in size of WG (1.18 mm) when used up to 40% also demonstrates decrease in water absorption as mentioned by (Malik et al. (2013)).

De Castro and De Brito (2013) substituted river sand at different proportions (0%, 5%, 10% and 20%) with WG ( $< 4$ mm). Reduction in water absorption at 5 and 10% substitution level was monitored. However, inclusion of 20% WG resulted into higher water absorption as compared with control concrete.

On contrary to this, Turgut and Yahlizade (2009) noticed rise in water absorption when fine aggregate was replaced with white glass (1.18 mm) up to 30% replacement level. The researchers observed 16.67% more water absorption as compared to control mix samples.

Limbachiya (2009) observed rise in initial surface absorption when fine aggregate was replaced at an interval of 5%, 10%, 15%, 20%, 30% and 50% with WG (< 5 mm). Increase in water absorption was noticed with incorporation of WG beyond 15%. Similar study has been reported by Ling and Poon (2011) by replacing fine aggregate with blue coloured WG (60% < 2.36 mm and 40% 2.36 – 5 mm) and noticed more water absorption at higher substitution level.

Rise in water absorption was also noticed by Penacho et al. (2014) by replacing fine aggregate (20%, 50% and 100%) with WG (0.149 – 2.38 mm) and monitored rise in water absorption with increase in proportion of WG in concrete mix. This upsurge in water absorption was due to increased portion of porous matrix and also due to in-built segregation characteristic of WG in concrete mixes.

### **2.3.6 Water Permeability**

Su and Chen (2002) mentioned rise in asphalt concrete permeability by substituting fine aggregate with WG ( $\leq 4.75$  mm) at an interval of 5% up to 15%. Upsurge in water permeability with inclusion of WG was noticed.

Oliveira (2008) replaced fine aggregate with amber WG (4.76 mm) at an interval of 25% up to 100%. The researchers showed higher water penetration at 25 and 50% substitution level for 28 and 63 days whereas, 100% substitution illustrates lower water penetration at 28 days. After 63 days depth of penetration for 100% substitution remains almost constant as compared with control concrete.

Penacho et al. (2014) noticed higher water permeability for mortar mixes by replacing fine aggregate with WG (0.149 – 2.38 mm).

### **2.3.7 Shrinkage**

Limbachiya (2009) reported drying shrinkage by replacing fine aggregate at 5%, 10%, 15%, 20%, 30% and 50% with mixed coloured WG (< 5mm). Results illustrates that

no effect was monitored up to 20% substitution level. However, further inclusion of WG increases shrinkage.

Ling and Poon (2013) also noticed fall in drying shrinkage at 100% substitution level of fine aggregate with WG (< 5mm) for mortar samples. This reduction in shrinkage was related with impermeable nature of WG.

Du and Tan (2014) noticed minor change in shrinkage when fine aggregate was substituted with WG at an interval of 25% up to 100%. The minor change was monitored as a consequence of its lower water absorption capacity.

On contrary to this, De Castro and De Brito (2013) monitored shrinkage effect on concrete prisms with inclusion of WG (< 4mm) by replacing river sand at 5%, 10% and 20%. Around 12.77% and 18% growth in shrinkage at 5% and 20%. However, anomaly was noticed at 10% substitution level where shrinkage decreases by 7.28% as compared to control sample.

### **2.3.8 Carbonation**

De Castro and De Brito (2013) noticed better performance towards carbonation resistance with inclusion of WG (< 4 mm) as a substitute of river sand at 5%, 10% and 20% substitution level. Initially higher depth of carbonation was monitored for 7 and 28 days as compared with reference sample. No change in carbonation depth was observed for WG concrete mixes with increased exposure duration.

### **2.3.9 Corrosion, Chloride Penetration and Chloride Diffusion**

Chen et al. (2006) incorporated WG (< 75  $\mu\text{m}$ ) in mortar as fine aggregate at an interval of 25% up to 100% which proves its resistance towards chloride ions penetration. Du and Tan (2014) also investigated at same percentage replacement for concrete samples and noticed similar results as reported by Chen et al. (2006). Hence, resistance improved with rise in WG content in concrete mixes.

However, contradictory observation was noticed by De Castro and De Brito (2013) with incorporation of WG (< 4mm) as fine aggregate at 5%, 10% and 20% replacement level. This is due to increase in chloride ion penetration by 28.88%, 34.4% and 7.77% respectively.

### **2.3.10 Acid Attack**

Chen et al. (2006) reported positive effect for concrete specimens prepared with waste E-glass ( $< 75 \mu\text{m}$ ) as substitute for fine aggregate at different substitutions (10%, 20%, 30%, 40% and 50%) after exposure to sulphate attack. The researchers proved that waste E-glass improves the performance of concrete in terms of weight loss and strength reduction as compared to control concrete.

Ling et al. (2011) reported that WG acts as barrier against acid attack (3% sulphuric acid) when used as fine aggregate up to 100% substitution level in mortar samples. After exposure to 12 weeks, higher substitution levels performs better as compared to control samples. This was due to better resistance capacity of WG to acid attack as compared to fine aggregate it replaces. Ling and Poon (2011) noticed positive effect for concrete mixes prepared with WG as a substitute of fine aggregate. Prepared samples were exposed in 3% sulphuric acid for 12 weeks. The results illustrate that glass concrete mixes shows better performance in terms of lower mass and strength loss as compared to control concrete.

### **2.3.11 Fire Exposure**

Terro (2006) substituted fine aggregate with crushed WG (0.075 – 4.75 mm) at 0%, 10%, 25%, 50% and 100% substitution level. The samples were made to undergo at different elevated temperature (60, 150, 300, 500, 700°C). Results illustrates that at 10% substitution level demonstrates greater residual compressive strength beyond 150°C as compared to other mixes.

### **2.3.12 Alkali Silica Reaction**

Zingg et al. (2013) substituted river sand with 10% WG and presents that on reducing the size of WG effect of alkali silica reaction (ASR) reduces. Here, after 14 days maximum expansion was noticed for gradation 1.18 – 2.36 mm whereas, sizes finer than this show similar expansion as of control samples.

Xie et al. (2003) substituted 10% river sand with WG in mortar mixes and observed that coarser particles (0.3 mm) shows higher ASR expansion as compared with finer (0.3 mm) glass particles. Similar observation was also noticed by Corinaldesi et al. (2005) when river sand was replaced by glass particles (100  $\mu\text{m}$ ) at 30% and 70% substitution levels. Thus increases the possibility of using WG as substitute of river sand.

Rajabipour et al. (2010) also noticed similar variation by replacing mixed coloured glass waste with river sand up to 100% substitution level. Idir et al. (2010) also noticed reduced ASR expansion by replacing marble sand with waste glass at 20% and 40% replacement level.

Tan and Du (2013) replaced river sand with mixed coloured waste glass up to 25% substitution level where size varies from 0.15 to 2.36 mm. The researchers proved that rise in ASR expansion occurs by increasing the size of waste glass.

## **2.4 Concluding Remarks**

In this section, research done so far by utilizing WR and WG as fine and coarse aggregate in concrete mixes was discussed. It is clear from literature that changes were observed in mechanical and durability performance with usage of these materials in concrete mixes. For rubber incorporated concrete, fall in mechanical performance was noticed at very minimum substitution level (around 5%). However, with inclusion of waste glass enhancement in mechanical performance was observed between substitution levels 15 - 25%. Apart from this, there isn't a single study traced which presents the effect of standard fire on rubber and waste glass based concrete mixes. Also, all studies discussed above have used ordinary Portland cement (OPC) based concrete only. In the next chapter, characterization of CR, WG and concrete mixes are discussed

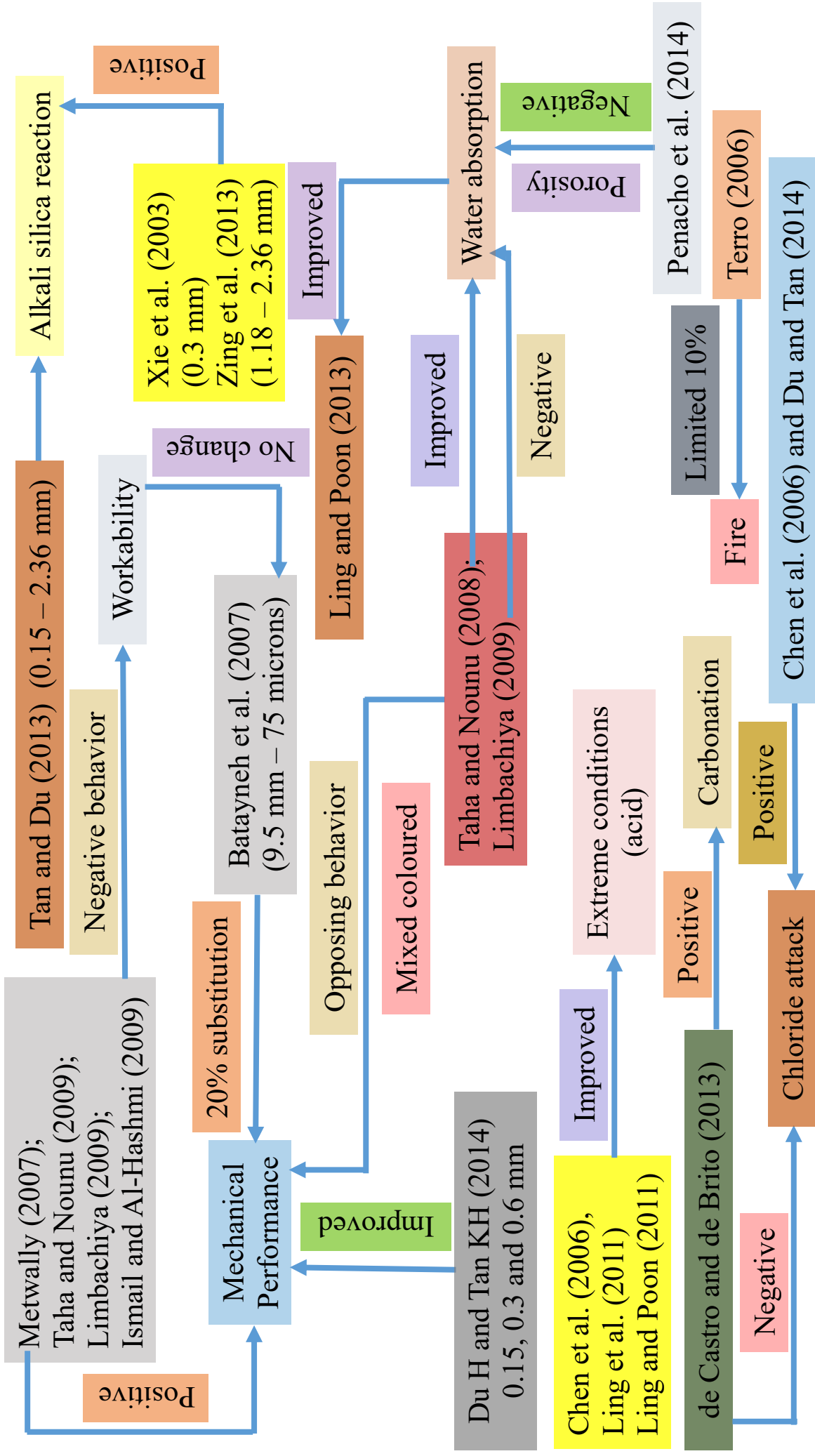


Fig. 2.2: Literature review flowchart for glass

---

**CHARACTERIZATION OF CRUMB RUBBER,  
WASTE GLASS AND CONCRETE MIXES**

---

**3.1 General**

This chapter illustrates physical and chemical characterization of cement, fine aggregate, coarse aggregate and waste materials (crumb rubber and waste glass). Microstructural analysis was also investigated through Field Emission Scanning Electron Microscopy (FESEM) to judge the nature and elemental composition of crumb rubber and waste glass.

**3.2 Research Methodology**

Previous studies have verified the suitability of waste rubber and waste glass individually as fine aggregate in concrete mixes at wide ranging percentage variation. Preliminary study was also carried out to affirm the optimum substitution level for CR and WG incorporated concrete mixes. CR concrete mixes were varied at an increment of 2.5% up to 7.5% substitution level of fine aggregate (river sand) and noticed near-by mechanical performance at 5% substitution level as compared with reference mix, beyond which huge fall in strength was observed (**Fig. 3.1**). For waste glass concrete mixes percentage variation was made at a substitution level of 5% up to 25%. Performance of hardened properties improved up to 20% substitution level (**Fig. 3.2**). These percentage substitution levels were varied as per literature.

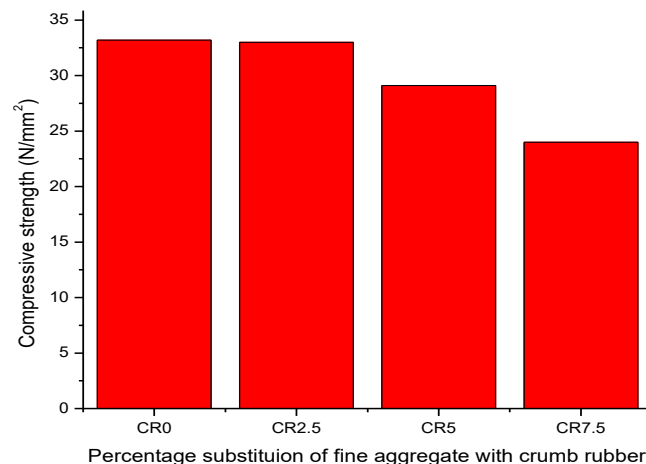


**Fig. 3.1: 28 day compressive strength of crumb rubber concrete specimens**



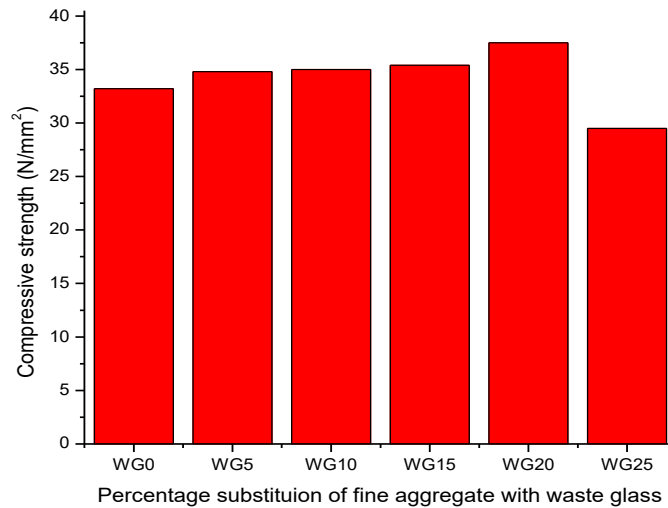


**Fig. 3.2: 28 day compressive strength of waste glass concrete specimens**

At 5% replacement level of CR in Portland pozzolana cement (PPC) based concrete the strength achieved is 33 N/mm<sup>2</sup>. However, the previous study show similar strength at 2.5% replacement level in OPC based concrete (Skariah et al. (2014)). In a similar manner, strength achieved for WG concrete mix is 37.5 N/mm<sup>2</sup> at 20% substitution level for fly-ash based cement concrete whereas, Batayneh et al. (2007) proved huge fall in strength at same substitution level for OPC based cement concrete as compared to reference sample.

In line with the outcome from this preliminary study, in this present work an attempt has been made to arrive at an exact optimum substitution level for rubber (4 – 5.5% at an increment of 0.5%) and glass (18 – 24% at an increment of 1%) concrete mixes separately. Hence, apposite study needed to be carried out to monitor the mechanical properties such as compressive and flexural strength as well as durability effects like exposure to chemical agents (Sulphate and chloride) on concrete properties using M25 grade for single water/cement ratio (0.4). Test like behaviour of concrete specimens with CR and WG exposed to standard fire has not been studied before. Hence, in addition to this, specimens were exposed to different elevated temperature (200°C - 800°C) to study the mechanical performance of concrete mixes. Microstructural properties of prepared composites were also investigated through X-ray Diffraction (XRD), Field Emission Scanning Electron Microscopy (FESEM), Thermal Gravimetric Analysis / Differential Thermal Analysis (TGA/DTA) and Fourier Transform Infrared Spectroscopy (FTIR). Additionally, Atomic Force Microscopy (AFM) method was also used to examine on concrete mixes to retrospectively analyse the property of concrete at Nano scale.

### 3.3 Classification of Materials

Raw materials used in present work are presented in flowchart (Fig. 3.3) and their characterizations are shown in below section.

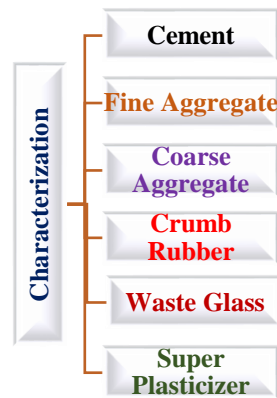


Fig. 3.3: List of raw materials

#### 3.3.1 Cement

Portland pozzolana cement (PPC) of “Ambuja” brand conforming to IS 1489 (2015) was used in present study. Consistency, soundness, Initial and final setting time, specific gravity, and compressive strength of cement was governed as per IS 4031 (1988) as mentioned in Table 3.1.

#### 3.3.2 Fine Aggregate

Locally accessible natural river sand (Banas River) proving to Zone II as per IS 383 (2016) was utilized as fine aggregate. The gradation analysis and physical properties of fine aggregate are shown in Fig. 3.4 and Table 3.1 respectively.

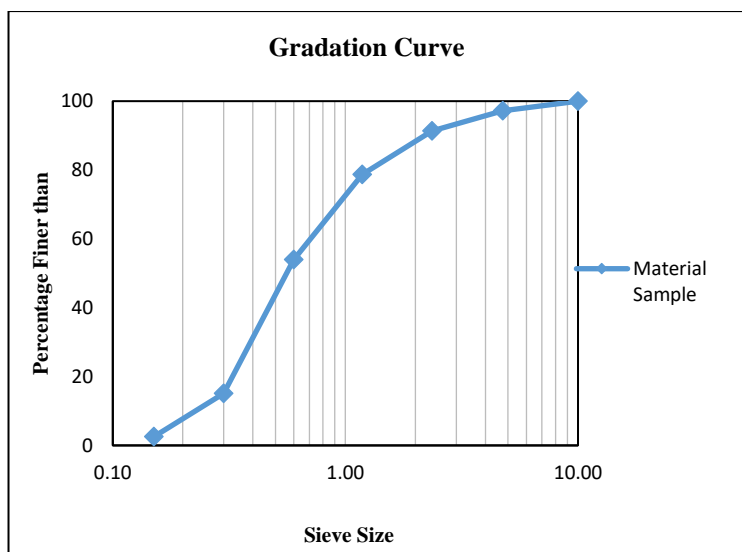


Fig. 3.4: Particle size distribution of river sand

### 3.3.3 Coarse Aggregate

Coarse aggregate with nominal size of 10 mm and 20 mm was used as per IS 383 (2016). Gravels of size 10 mm and 20 mm used in concrete mixes are in proportion of 60% and 40%.

### 3.3.4 Crumb Rubber

Crushed crumb rubber (CR) of size 0.600 mm was produced from scrap tyre rubber by mechanical grinding. **Fig. 3.5** shows image of crumb rubber used in this study. The physical properties of crumb rubber are presented in **Table 3.1**.



**Fig. 3.5: Crumb rubber**

### 3.3.5 Waste Glass

Waste glass (WG) was obtained from mechanical grinding of beverage bottles of different colours. The crushed form of WG was passed through 600 micron and retained on 150 micron sieve. The WG used in present work is shown in **Fig. 3.6** and physical properties are presented in **Table 3.1**.



**Fig. 3.6: Waste glass**

**Table 3.1: Physical and mechanical properties of cement, aggregates, crumb rubber and waste glass**

Analysis	Property	Results
PPC	Setting Time IS 4031 (Part V) (1988)	Initial time – 115 min Final time – 248 min
	Compressive Strength IS 516 (1959)	3 Day – 24.5 MPa 7 Day – 34.5 MPa 28 Day – 45.2 MPa
	Coarse Aggregate	0.5%
Fine Aggregate	Water Absorption	0.5%
Crumb Rubber	ASTM C 642 (2008)	0.3%
Waste Glass		0.3%
Coarse Aggregate		2.59
Fine Aggregate	Specific Gravity	2.66
Crumb Rubber	IS 2386 (Part III) (1963)	1.05
Waste Glass		2.33
Cement		3.11
Coarse Aggregate		10, 20 mm
Fine Aggregate	Size	> 4.75 mm
Crumb Rubber	IS 383 (2016)	0.600 mm
Waste Glass		0.150 – 0.600 mm
Coarse Aggregate	Crushing Value IS 2386 (Part IV) (1963)	24.03%
Waste Glass	Strength Activity ASTM C311 (2003)	82%
Waste Glass	Alkali Silica Reaction IS 2386-7 (1963)	Not deleterious

### 3.3.6 Super Plasticizer

Modified polycarboxylic ether based super plasticizer was procured from BASF. This admixture satisfies the norms set by IS 9103 (1999). Specific gravity was measured to be around 1.1. Necessary quantity of the superplasticizer was added to achieve the desired workability to prepare concrete specimens.

## 3.4 Concrete Mix Proportions

In the following section quantities of raw materials were tabulated by substituting river sand at different percentages by CR and WG separately.

### 3.4.1 Crumb Rubber

Four concrete mixes with crumb rubber particles were casted at single water/cement ratio of 0.40. The substitution of fine aggregates by CR was made in proportions of 0% (CR0), 4% (CR4), 4.5% (CR4.5), 5% (CR5) and 5.5% (CR5.5) in order

to prove the exact optimum substitution level. Substitution of fine aggregates with crumb rubber was made by volume basis. The dosage of superplasticizer was varied from 1.5% to 2.4% to achieve compaction factor of 0.9 as shown in **Table 3.2**.

**Table 3.2: Concrete mix proportions in kg/m<sup>3</sup> for a constant w/c ratio (0.4)**

Percentage of CR	Cement	Fine Aggregate	Crumb Rubber	Coarse Aggregate	Admixture (%) by Weight of Cement
0	384	811.2	0	1122.7	1.5
4	384	778.75	12.81	1122.7	2.0
4.5	384	774.69	14.40	1122.7	2.1
5	384	770.69	16.01	1122.7	2.2
5.5	384	766.58	17.61	1122.7	2.4

### 3.4.2 Waste Glass

Seven concrete mixes with WG particles were casted at single water / cement ratio of 0.40. The substitution of fine aggregates by WG was made in proportions of 0% (WG0), 18% (WG18), 19% (WG19), 20% (WG20), 21% (WG21), 22% (WG22), 23% (WG23) and 24% (WG24) in order to prove the exact optimum substitution level. Substitution of fine aggregates with WG was made by volume basis. The dosage of superplasticizer was varied from 1.5% to 2% to achieve compaction factor of 0.9 as shown in **Table 3.3**.

**Table 3.3: Concrete mix proportions in kg/m<sup>3</sup> for a constant w/c ratio (0.4)**

Percentage of WG	Cement	Fine Aggregate	Waste Glass	Coarse Aggregate	Admixture (%) by Weight of Cement
0	384	811.2	0	1122.7	1.50
18	384	665.2	127.9	1122.7	1.70
19	384	657.1	135.0	1122.7	1.70
20	384	648.9	142.1	1122.7	1.75
21	384	640.8	149.2	1122.7	1.80
22	384	632.7	156.3	1122.7	1.90
23	384	624.6	163.4	1122.7	1.95
24	384	616.5	170.5	1122.7	2.0

### 3.5 Material Preparation

Materials were mixed, casted and cured as per IS 516 (1959). The measured quantities of cement, fine and coarse aggregates with CR and WG were individually dry mixed. The weighed quantity of superplasticizer was mixed with water and added to concrete mix. Mixing was done for five minutes (**Fig. 3.7**) after which prepared concrete was placed in pre-oiled moulds.



**Fig. 3.7: Concrete mixer**

Compaction was done by using vibrating table for sufficient time to ensure removal of air voids. After 24 hours cubes were demoulded and placed for curing in tank for remaining 27 days.

### **3.6 Experimental Method**

CR was obtained from mechanical grinding of scrap rubber and WG was procured from crushing of mixed coloured beverage bottles. In order to justify the compatibility of these waste materials in concrete mix complete microstructural and chemical analysis was taken into picture.

#### **3.6.1 Field Emission Scanning Electron Microscopy (FESEM)**

The FESEM JSM6510LV was used for identification of the changes occurred in microstructure of powdered samples. EDAX (Energy-dispersive X-ray Spectroscopy) was also done on the same sample to find out the elemental composition of the sample.

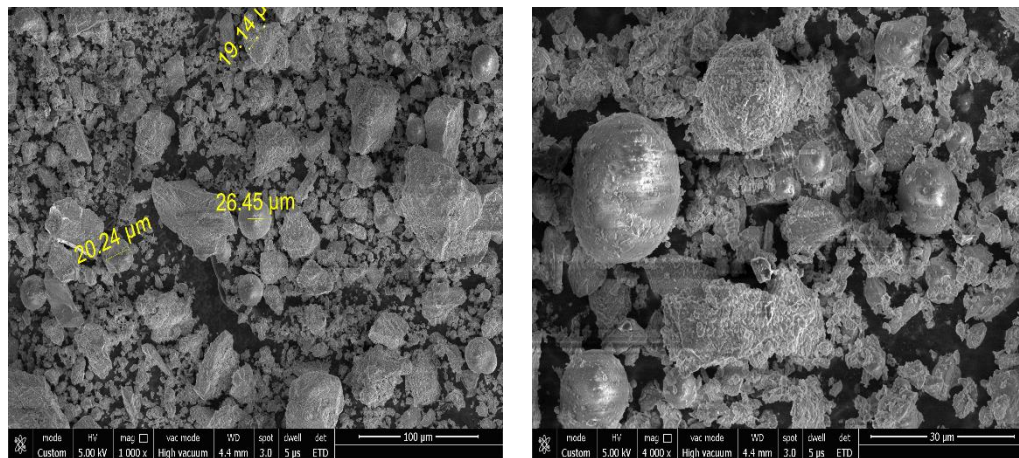
### **3.7 Results and Discussion**

#### **3.7.1 Cement**

FESEM analysis of cement powder was presented in **Fig. 3.8**. The images display irregular profile for cement particles whereas, fly-ash particles are circular in shape at different magnifications.

EDAX examination of cement particles are presented in **Fig. 3.9** and **Table 3.4**. The peaks having high intensity specifies higher amount of element. It has also been observed from above mentioned figure and table that presence of calcium (Ca) was

maximum which act as a backbone behind hydration process. EDAX for fly-ash was monitored and shown in **Fig. 3.10** and **Table 3.5**.



(a) Sizes of cement particles

(b) Higher magnification

**Fig. 3.8: FESEM image of cement particles**

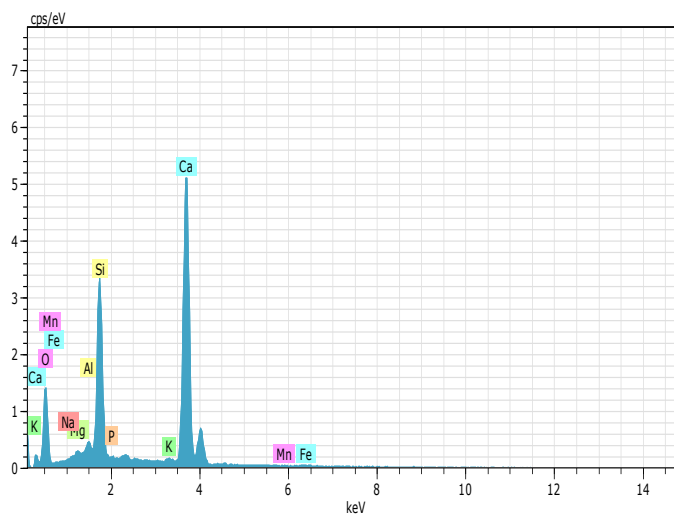


**Fig. 3.9: EDAX of cement**

**Table 3.4: Elemental composition of cement**

Element Composition	Symbol	Percentage
Calcium	Ca	45.91
Oxygen	O	38.57
Silica	Si	12.73
Aluminium	Al	1.11
Iron	Fe	0.65
Magnesium	Mg	0.55
Potassium	K	0.39
Sodium	Na	0.04
Phosphorous	P	0.03
Manganese	Mn	0.03

**Table 3.5: Elemental composition of fly-ash**

Element Composition	Symbol	Percentage
Oxygen	O	41.88
Silica	Si	31.99
Aluminium	Al	18.38
Calcium	Ca	3.11
Titanium	Ti	1.63
Iron	Fe	1.61
Potassium	K	1.39

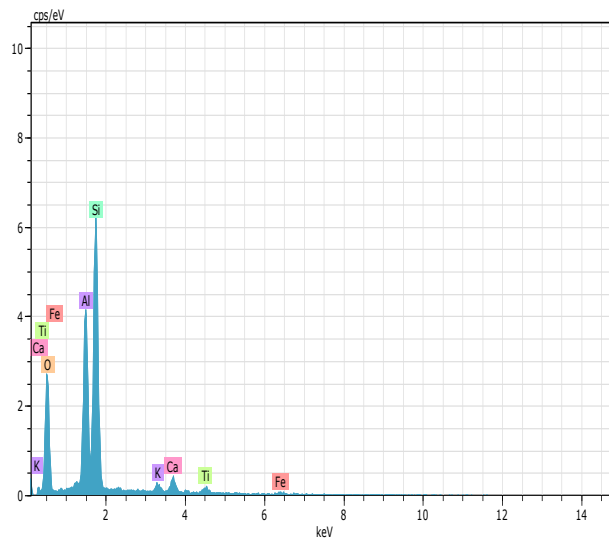
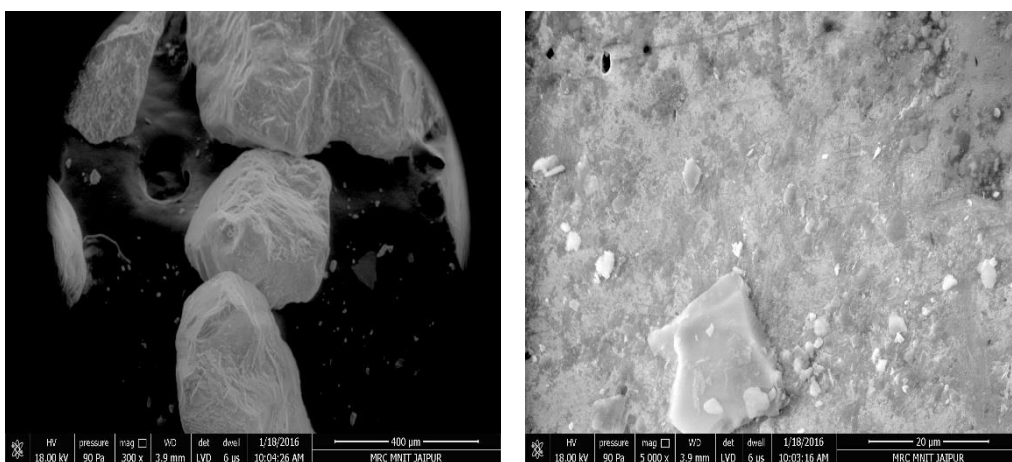


**Fig. 3.10: EDAX of fly-ash**

### 3.7.2 Fine Aggregate

FESEM analysis of fine aggregate was presented in **Fig. 3.11**. The images present smooth texture with irregular shape.



**(a) Lower magnification**

**(b) Higher magnification**

**Fig. 3.11: FESEM image of fine aggregate**



In addition to this EDAX analysis was also presented in **Fig. 3.12** and **Table 3.6**. EDAX analysis show maximum percentage of oxygen and silica in fine aggregate.

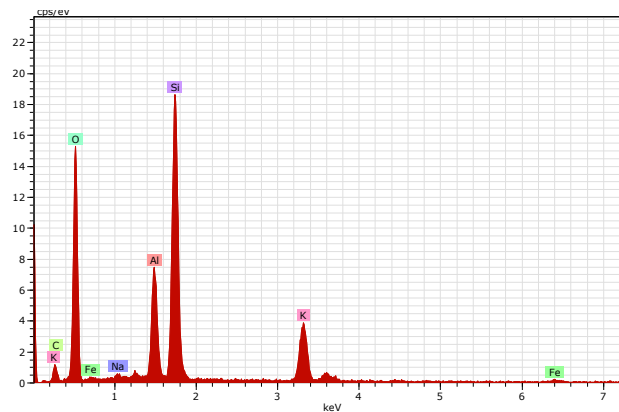


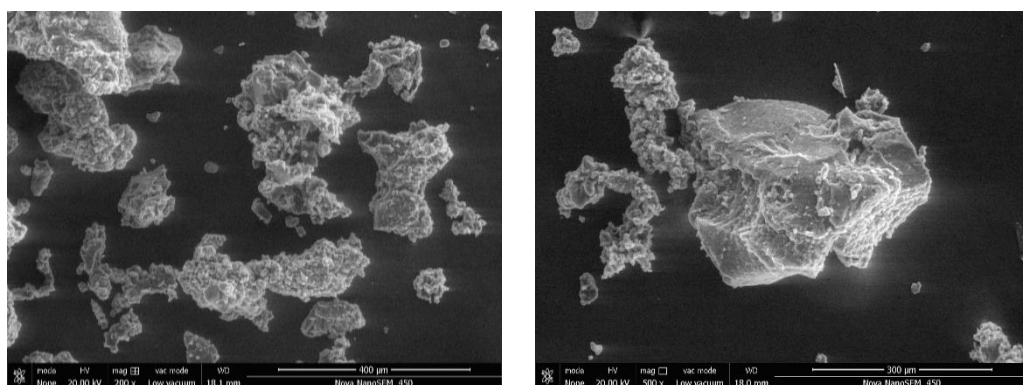
**Fig. 3.12: EDAX of fine aggregate**

**Table 3.6: Elemental composition of fine aggregate**

Element Composition	Symbol	Percentage
Oxygen	O	54.07
Silica	Si	19.09
Potassium	K	10.09
Carbon	C	8.57
Aluminium	Al	7.20
Iron	Fe	0.67
Sodium	Na	0.31

### 3.7.3 Crumb Rubber

**Fig. 3.13** presents the FESEM images of CR which shows the smooth texture. Energy Diffraction X-ray Analysis (EDAX) was performed to determine elemental composition of CR as shown in **Fig. 3.14**. Elemental composition of CR has been presented in **Table 3.7**.



**(a) Lower magnification**

**(b) Higher magnification**

**Fig. 3.13: FESEM image of crumb rubber**

**Table 3.7: Elemental composition of crumb rubber**

Element Composition	Symbol	Percentage
Carbon	C	87.50
Oxygen	O	9.24
Zinc	Zn	1.77
Sulphur	S	1.07
Silicon	Si	0.20
Magnesium	Mg	0.14
Aluminium	Al	0.08

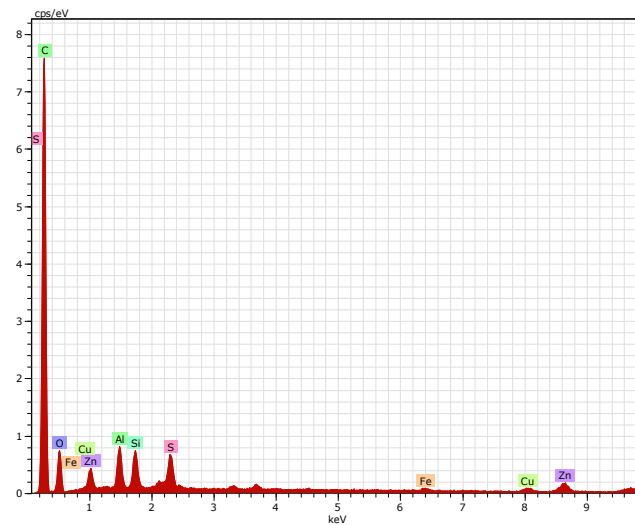
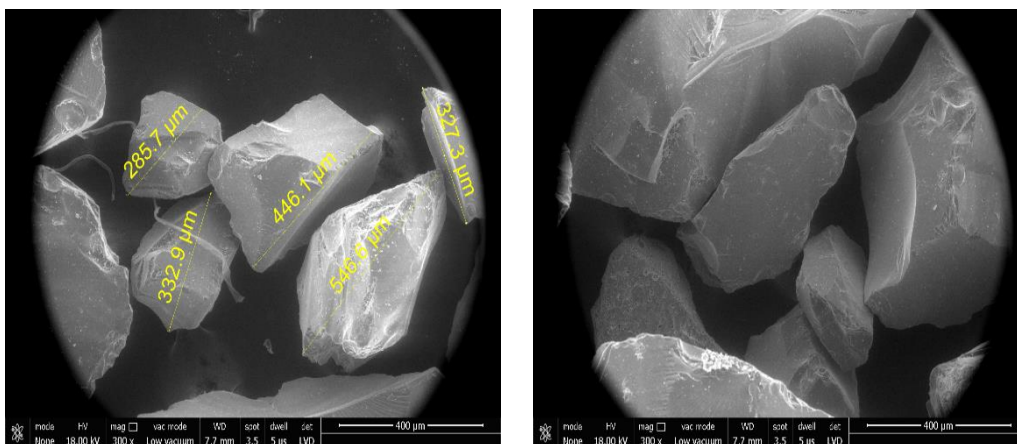


**Fig. 3.14: EDAX of crumb rubber**

### 3.7.4 Waste Glass

The morphology of WG used in present work is shown in **Fig. 3.15** by conducting FESEM of WG which shows the smooth texture with sharp edges.



**(a) Size of waste glass**

**(b) Texture of waste glass**

**Fig. 3.15: FESEM image of waste glass**

Energy Diffraction X-ray Analysis (EDAX) was performed to determine elemental analysis of WG as shown in **Fig. 3.16**. Elemental composition of WG which was evaluated using EDAX presented in **Table 3.8**.

**Table 3.8: Elemental composition of waste glass**

Element Composition	Symbol	Percentage
Oxygen	O	54.35
Silicon	Si	24.80
Sodium	Na	8.74
Calcium	Ca	7.41
Aluminium	Al	1.68
Magnesium	Mg	1.31
Potassium	K	1.26
Iron	Fe	0.27
Sulphur	S	0.19

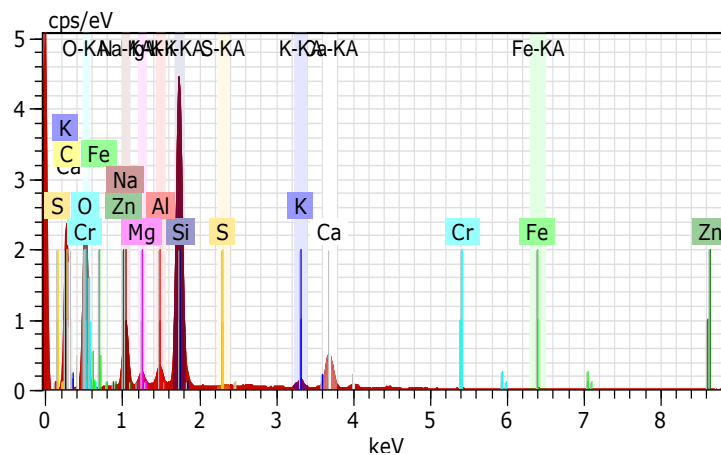


**Fig. 3.16: EDAX of waste glass**

### 3.8 Concluding Remarks

The material properties of cement, fine aggregate, crumb rubber and waste glass were evaluated by carrying out the experiments for specific gravity, water absorption, elemental composition and microstructure. Following important conclusions are drawn:

- The specific gravity of crumb rubber and waste glass is less than that of fine aggregate which can be helpful in production of low-density concrete.
- The crumb rubber is irregular shape with smooth texture as compared to fine aggregate; however, waste glass has more angular shape with sharp edges.
- Crumb rubber have high carbon content which leads to production of softer concrete.

FRESH AND HARDENED PROPERTIES OF CONCRETE

4.1 General

This chapter illustrates the effect of crumb rubber and beverage waste glass individually on concrete properties (Fig. 4.1) with partial substitution of fine aggregate. Fresh properties on concrete mixtures were evaluated by performing compaction factor and fresh bulk density. Mechanical performance of concrete mixes was evaluated in terms of compressive strength, flexural strength, abrasion resistance and pull-off strength. In addition to this, microstructural properties of prepared composites were also investigated through X-ray Diffraction (XRD), Field Emission Scanning Electron Microscopy (FESEM), Thermal Gravimetric Analysis / Differential Thermal Analysis (TGA / DTA) and Fourier Transform Infrared Spectroscopy (FTIR), Atomic Force Microscopy (AFM).

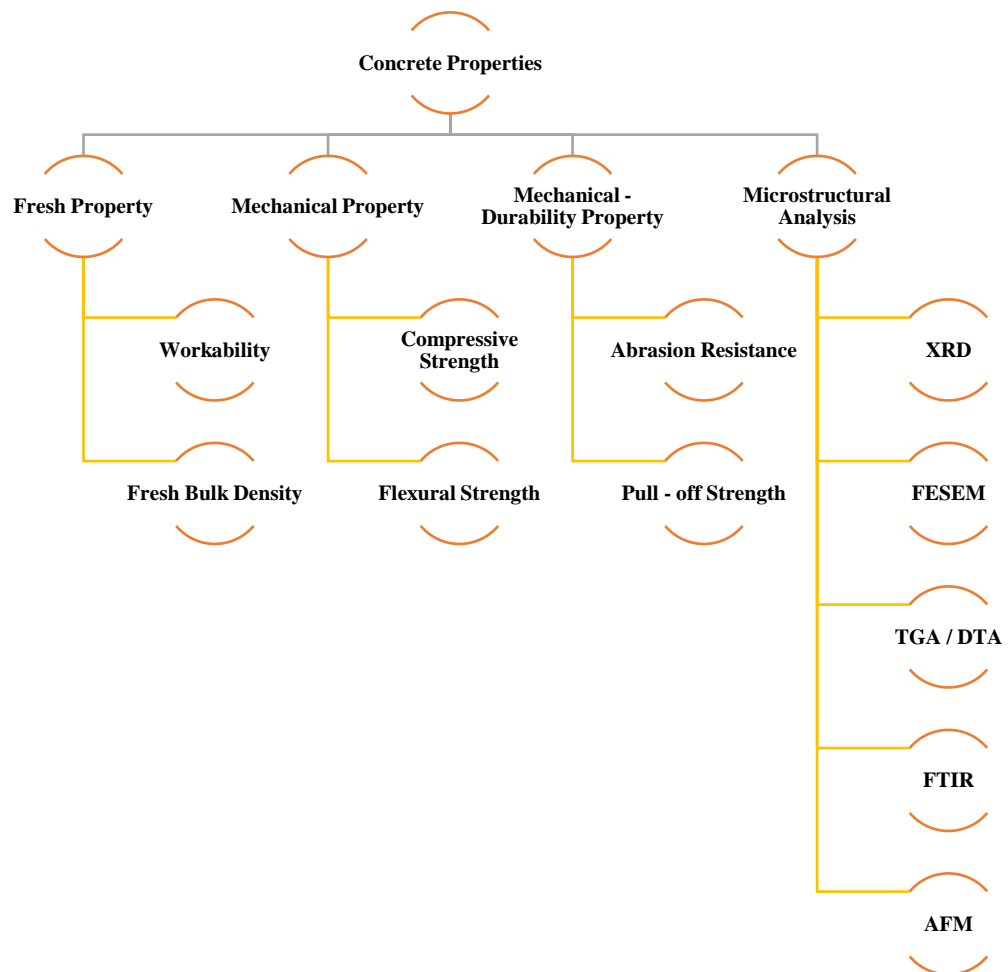


Fig. 4.1: List of experiments

## 4.2 Experimental Procedure

The techniques employed for performing the experiments listed above are explained in the following sections. The test matrix is listed in **Table 4.1**.

**Table 4.1: Test matrix for mechanical and microstructure properties of concrete samples**

Type of test	Size of specimen / Form	No of specimens tested for each mix	Designation of samples			
<b>Compressive Strength</b>	100×100×100 mm	3	Mix 1	CR0	Mix 1	WG0
<b>Flexural Strength</b>	100×100×500 mm	3	Mix 2	CR4	Mix 2	WG18
<b>Abrasion Resistance</b>	100×100×100 mm	3	Mix 3	CR4.5	Mix 3	WG19
<b>Pull-off Strength</b>	100×100×500 mm	3	Mix 4	CR5	Mix 4	WG20
<b>Microstructure</b>			Mix 5	CR5.5	Mix 5	WG21
• <b>XRD</b>	Powder				Mix 6	WG22
• <b>FESEM</b>	10×10×10 mm	3			Mix 7	WG23
• <b>TGA</b>	Powder				Mix 8	WG24
• <b>FTIR</b>	Powder					
• <b>AFM</b>	2×10×10 mm	3				

### 4.2.1 Fresh Property

Freshly mixed concrete can be shaped to any form. Proper compaction of freshly placed concrete is the main criteria to achieve strength of concrete which can only be achieved if concrete mix is workable. There are several techniques such as slump test, compaction factor test etc. to measure its workability.

#### 4.2.1.1 Workability

Workability of concrete mixes has been investigated by performing compaction factor test as per IS 1199 (1959). Compaction factor apparatus presented in **Fig. 4.2** comprises of two hopper vessels having hinge at base of each hopper and cylinder at bottom. Concrete sample was placed in pre-oiled top hopper. Hinge of top hopper was opened and allows the concrete to fall into lower hopper. Hinge of lower hopper was opened, so that concrete falls in cylinder. Top surface of cylinder was flattened and weight of cylinder plus concrete was measured which was deducted with weight of empty cylinder ( $W_1$ ). Then cylinder with concrete was allowed to vibrate on vibrating table. Weight ( $W_2$ ) was measured as weight of fully compacted concrete minus weight of empty cylinder.

$$\text{Compaction factor} = W_1 / W_2 \quad (4.1)$$



**Fig. 4.2: Compaction factor apparatus**

#### **4.2.1.2 Fresh Bulk Density**

Fresh density of concrete mixtures was verified as per IS 1199 (1959). Freshly prepared concrete mixture was placed in cylinder (150 × 300 mm) and compacted by using table vibrator. Then weight of compacted concrete with cylinder was noted which was divided by volume of cylinder, expressed in kg/m<sup>3</sup>.

#### **4.2.2 Mechanical Property**

In the following segments, procedure adopted to examine the hardened properties of concrete samples are listed.

##### **4.2.2.1 Compressive Strength**

Compressive strength was executed on three concrete cube (100 mm) specimens of each mix after 28, 90 and 180 days of curing (**Fig. 4.3**) as per IS 516 (1959). The rate of loading 140 kg/cm<sup>2</sup>/min was applied till the sample fails to sustain any further load. The maximum failure load was noted and compressive strength was computed by dividing measured load with cross-sectional area.



**Fig. 4.3: Compressive strength apparatus**

#### 4.2.2.2 Flexural Strength

The third point loading arrangement was used to evaluate flexural strength on universal testing machine (UTM) as shown in **Fig. 4.4** using three 100 × 100 × 500 mm specimen of each concrete mix after 28 and 90 days of curing. The loading rate on the beam was 180 kg/cm<sup>2</sup>/min capacity as per IS 516 (1959).



**Fig. 4.4: Flexural strength apparatus**

#### 4.2.2.3 Abrasion Resistance

The abrasion test was performed after 28 day of curing as per IS 1237 (2012). Three 100 mm concrete cube specimens of each mix were oven dried at temperature 110 ± 5°C for 24 hours and after that specimen are initially weighed ( $W_3$ ) and ( $W_4$ ) was weight after completion of test. Abrasive sand about twenty grams was used for abrasion test as shown in **Fig. 4.5**. After every twenty-two cycles cube sample was rotated 90° in clockwise direction and again cycle was repeated with new abrasive sand. After completion of total 10 cycles weight of cube sample was measured.

The change in thickness was concluded with the use of formula mentioned below:

$$t = (W_3 - W_4) \times V_1 / (W_3 \times S) \quad (4.2)$$

where,  $w_2$  is the weight measured after testing,  $V_1$  is the original volume of the sample in mm<sup>3</sup> and  $S$  is the surface area of the specimen in mm<sup>2</sup>.



**Fig. 4.5: Abrasion resistance apparatus**

#### 4.2.2.4 Pull-off Strength

Pull-off strength was executed according to BS 1881 (2003). The experiment was implemented on 28 days water cured concrete specimens. The face of concrete sample was properly cleaned in order to fix an iron disc of 50 mm diameter by using epoxy resin. Test was conducted after 24 hours so that iron disc get properly fixed on concrete specimen. The rate of loading 5 - 10 kN/min was applied till the disc get completely removed from specimen. The technique applied in whole process is shown in **Fig. 4.6**.



(a) Specimen attached with machine

(b) Failed specimen

**Fig. 4.6: Pull-off strength apparatus**

#### 4.2.2.5 Density and Voids

The density and voids of concrete was determined on three cube (100 mm) specimens as per ASTM C 642 (2008). Cube specimens in saturated condition are allowed to boil for 5 hours. Allow cube specimens to cool down by natural cooling process such that temperature of boiling water reaches to room temperature. External faces of specimens were soaked by using cloth and the weight of specimens were noted.

Suspended mass of cube specimen was recorded after water immersion and boiling using wire. From this apparent mass was evaluated.

$$\text{Bulk density} = [W_5/W_6 - W_7]\rho \quad (4.3)$$

$$\text{Apparent density} = [W_5/W_5 - W_7]\rho \quad (4.4)$$

$$\text{Voids ratio} = [W_6 - W_5/W_6 - W_7] \times 100 \quad (4.5)$$

Where,  $W_5$  = Oven dry weight of specimens;  $W_6$  = Weight of specimen after boiling;

$W_7$  = Apparent weight of specimen after boiling;  $\rho$  = Density of water



### **4.2.3 Microstructure**

To verify the microstructural properties of concrete mixes different techniques such as XRD, FESEM, TGA, FTIR and AFM were implemented and their experimental parameters are stated below.

#### **4.2.3.1 XRD Analysis**

After performing compressive strength test, the specimens were crushed. The crushed powder was allowed to sieved through 90  $\mu$  IS sieve. The collected powdered samples of all mixes were tested by X-ray Diffraction technique for phase identification at an angle of 10 - 80° using Philips Xpert-Pro PANalytical with (CuK $\alpha$ ) radiation of wavelength 1.54 Å.

#### **4.2.3.2 FESEM Analysis**

The FESEM JSM6510LV was used for identification of the changes occurred in microstructure of the formed phases. The concrete samples of size 10 × 10 × 10 mm were cut by using concrete cutter. The refined smooth samples were attained by wet grinding on Buhler disks. After that samples were polished with use of diamond paste. Then samples were dried in oven for 24 hours at 100°C and then cleaned with acetone to remove the foreign particles.

#### **4.2.3.3 TGA Analysis**

Thermal analysis was conducted on powdered samples by using PerkinElmer thermal analyzer at a heating rate of 10°C/min from 25°C up to 900°C. The test was conducted under nitrogen atmosphere having flow rate of 50 ml/min.

#### **4.2.3.4 FTIR Analysis**

FTIR transmission was conducted on PerkinElmer between the scan range of 400 – 4000 cm<sup>-1</sup>. 1mg of concrete powder was mixed with 300 mg of KBr (Potassium bromide) powder. Grinding of both the samples were done thoroughly in order to form pellets. These pellets were used to classify the presence of molecular groups in concrete samples.

#### **4.2.3.5 AFM Technique**

The concrete samples of size 10 × 10 × 10 mm were cut by using concrete cutter. The refined smooth samples of size 2 × 10 × 10 mm were attained by wet grinding on Buhler disks with paper grits of 120, 320, 600, 800, 1000, 1200 and 1500 respectively. To attain the depth of 2 mm concrete samples were grinded on 120 grit paper for 15 minutes

and for smoothing the surface of concrete samples grit paper of sizes 320, 600, 800, 1000, 1200 and 1500 was used. After that samples were dried in oven for 24 hours at 100°C and then cleaned with acetone to remove the foreign particles.

Bruker Multimode 8 HR AFM system with silicon probe clipped with cantilever arm was used to generate LFM images. Optical micrograph was employed to choose the suitable region of Interstitial Transition Zone (ITZ) as shown in **Fig. 4.7**. Tapping mode was adopted as shown in **Fig. 4.8** for imaging under scan range of 10 μm, 5 μm and 2 μm.

NanoScope analysis was considered to obtain the results from images and also to verify roughness at ITZ at 1/2<sup>th</sup> interval from top to bottom under considered scan range.

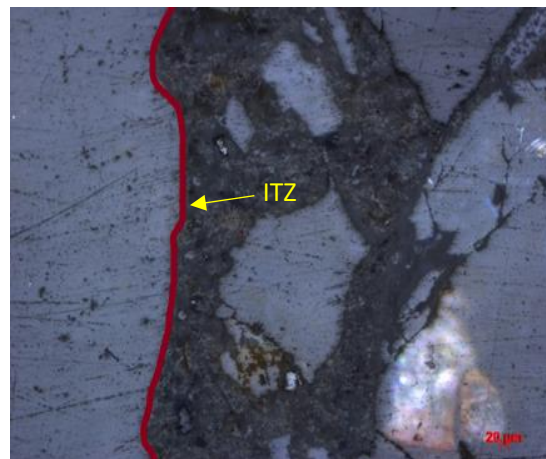


**Fig. 4.7:** Optical image obtained for concrete specimen

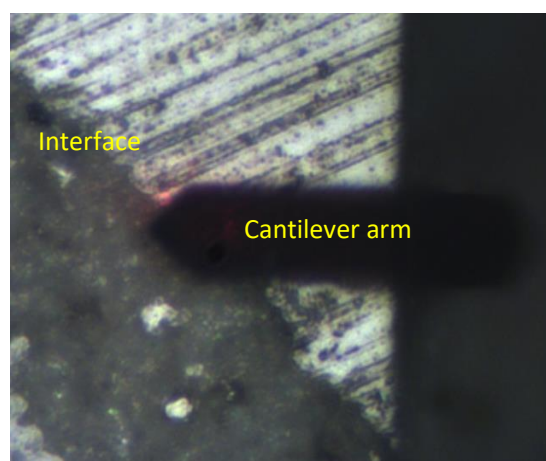


**Fig. 4.8:** Cantilever arm in tapping mode

### 4.3 Results and Discussion of Part – A: Crumb Rubber

In this section results of test such as workability, compressive strength, flexural strength, pull – off, abrasion resistance and microstructural analysis are explained in two parts A & B. Part A discusses about utilization of crumb rubber in concrete mixes and Part B about usage of waste glass in concrete mixes as mentioned below.

#### 4.3.1 Fresh Property

Fresh properties were observed in terms of workability and fresh bulk density which are described below.

##### 4.3.1.1 Workability

In this study, an appropriate amount of superplasticizer was taken to attain a compaction factor of 0.9 (**Table 4.2**) for different mixes with varying percentage of CR. From **Fig. 4.9**, it has been monitored that admixture content increases with rise in CR percentage. This might be because, high surface area of CR. Similar observation have also been noticed by (Batayneh et al. (2008) and Ganjian et al. (2009)) with inclusion of (0.075 - 4.75 mm) and (0.425 - 4.75 mm) CR in concrete.

**Table 4.2: Workability of fresh crumb rubber concrete**

Mix No.	Admixture (%) by Weight of Cement	Compaction Factor
CR 0	1.5	0.9
CR 4	2.0	0.9
CR 4.5	2.1	0.9
CR 5	2.2	0.9
CR 5.5	2.4	0.91

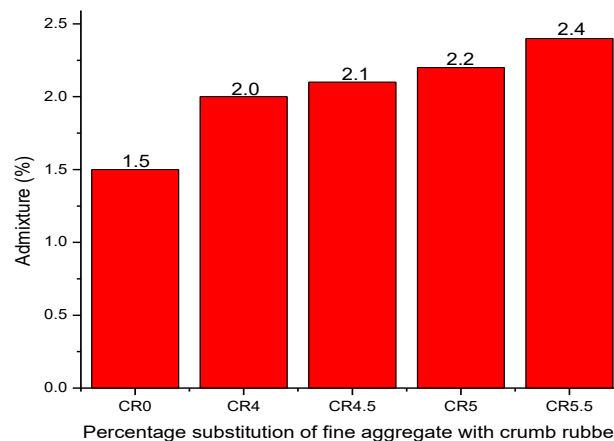


**Fig. 4.9: Percentage of admixture for crumb rubber concrete mixes**

### 4.3.1.2 Fresh Bulk Density

The fresh bulk density of CR concrete mixes presented in **Fig. 4.10**. It has been observed from same figure that with increase in substitution level of fine aggregate with CR fresh density decreases. The fall in fresh density at 4% and 5.5% substitution levels are 1.37% and 1.8% respectively. The specific gravity of CR is 1.05 which is lesser as compared to the specific gravity of fine aggregates (2.66). Hence, this reduction in density of CR concrete may be due to lesser specific gravity of CR (Batayneh et al. (2008)). Batayneh et al. (2008) noticed 27% decrease in density when fine aggregate are totally replaced with rubber fiber due to lower density of rubber fiber as compared to fine aggregate it replaces.

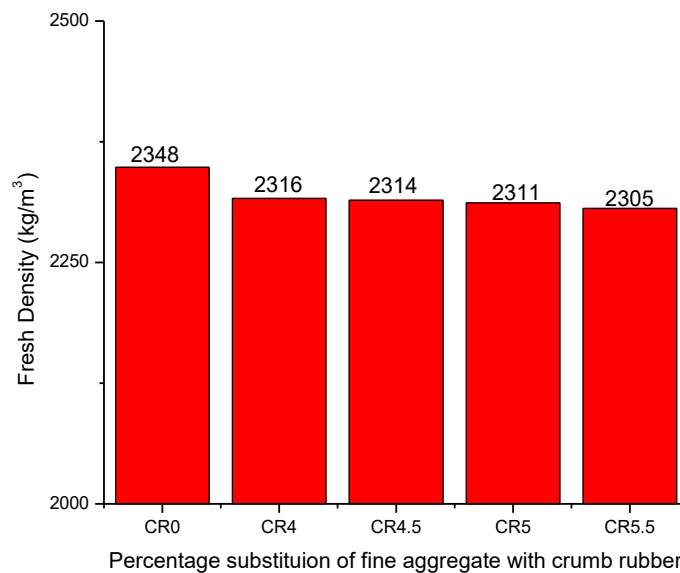


**Fig. 4.10: Fresh density of crumb rubber concrete mixes**

### 4.3.2 Mechanical Property

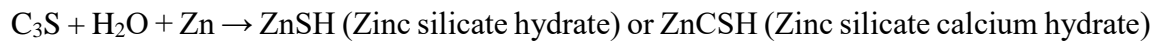
The hardened properties of CR based concrete mixes are examined in terms of compressive strength, flexural strength, abrasion resistance and pull-off strength which are explained in the subsequent sections.

#### 4.3.2.1 Compressive Strength

Compressive strength recorded for concrete samples with and without CR have been shown in **Fig.4.11** after 28, 90 and 180 days of curing. It has been observed from above mentioned figure that concrete strength deteriorates with inclusion of CR in concrete mixes. Results obtained with substitution of fine aggregate by CR4 and CR5.5

in concrete, a decrement of 3.79% and 17.8% for 28 days of curing respectively, in comparison with CR0 mix. With increase in curing period rise in strength was observed for all mixes, however as compared with control mix reduced progress in compressive strength was monitored for 90 and 180 days water cured specimens. The decrease in mechanical performance of concrete mixes might be due to poor bonding between the smooth CR constituents and cement matrix. Cracks grow rapidly around CR particles at the time of loading which causes quick rupture of concrete. Decrease in compressive strength might be also due to generation of voids which might have been developed due to excess fine characteristic of CR.

Gupta et al. (2014) also noticed reduced compressive strength due to generation of voids by consuming CR in concrete. Benazzouk et al. (2007) observed similar performance as packing of rubber particles becomes difficult with rise in replacement level due to the generation of voids. The decrease in compressive strength might also be due to retardation of the hydration reaction due to the interference of zinc to form zinc silicate hydrate instead of calcium silicate hydrate (Weeks et al. (2008)).



Arliguie et al. (1982) also observed formation of calcium zinc hydrate instead of formation of Portlandite. This occurs due to utilization of  $Ca^{2+}$  and  $OH^-$  ions to form an insoluble zincate compound, thus delays the formation of Portlandite and CSH.

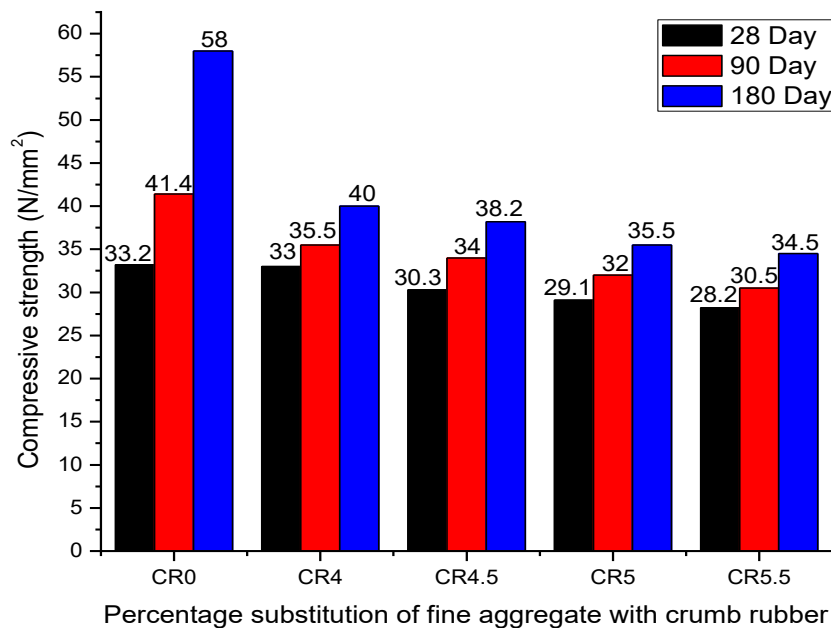


**Fig. 4.11: Compressive strength of crumb rubber concrete specimens**

### 4.3.2.2 Density and Voids

The addition of CR in concrete influences its hardened density as shown in **Fig. 4.12**. With inclusion of 5.5% of CR density of concrete decreases by 10% as compared to CR0 mix. From the same figure it has also been observed that bulk density decreases for all mixes which results into high porosity (**Fig. 4.13**). The increase in void ratio is due to poor bonding between smooth crumb rubber constituents and cement matrix. This is also associated with fine characteristic of crumb rubber. The specific gravity of CR is 1.05 which is lesser as compared to the specific gravity of fine aggregates (2.66). Hence, this reduction in density of CR concrete may be due to lesser specific gravity of CR (Batayneh et al. (2008)). Pelisser et al. (2011) reported 13% fall in hardened density with inclusion of CR as compared with control mix. Drop in density has also been noticed by different authors with substitution of natural aggregates by waste rubber at different percentages (Gupta et al. (2014) ; Q. Dong et al. (2013) and Xue and Shinozuka (2013)).

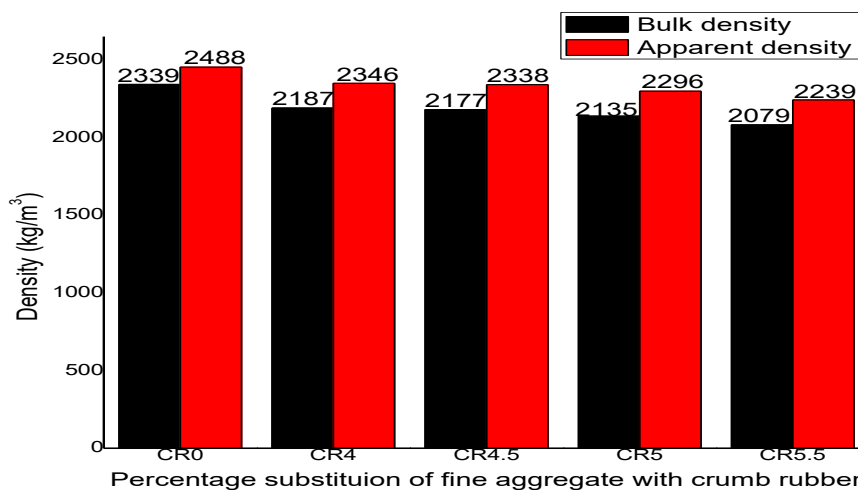


**Fig. 4.12: Hardened density of crumb rubber concrete specimens**

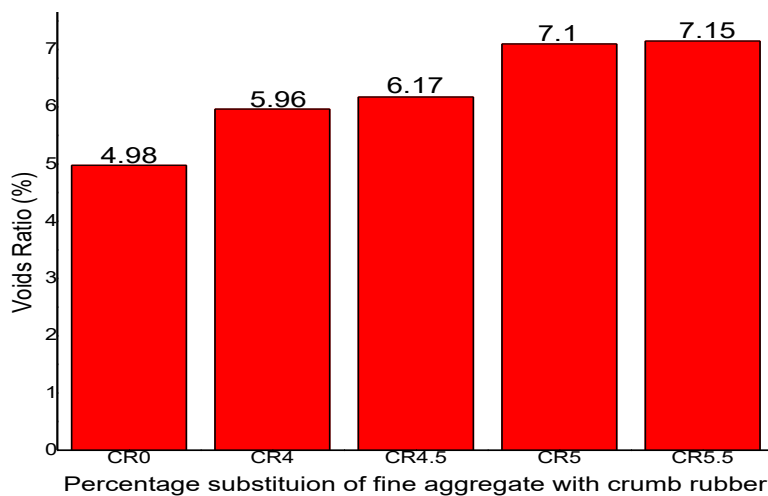


**Fig. 4.13: Voids ratio of crumb rubber concrete specimens**

### 4.3.2.3 Flexural Strength

The outcomes of 28 and 90 days flexural strength with and without CR at different proportions are shown in **Fig. 4.14**. Results of flexural strength are in line with variation observed in compressive strength values. With rise in percentage of CR in concrete mixes, drop in flexural strength was observed. The below mentioned figure presents that with incorporation of 4% and 5.5% of CR, strength decreases by 2.9% and 16.5% respectively. Inclusion of 4% and 5.5% of CR as a substitute of fine aggregate shows 11.47% and 24.17% fall in flexural strength as compared to control sample after 90 days of water curing. The shape of CR utilized in this study was highly irregular as shown in **Fig. 3.13** which does not allow bonding between cement paste and CR.

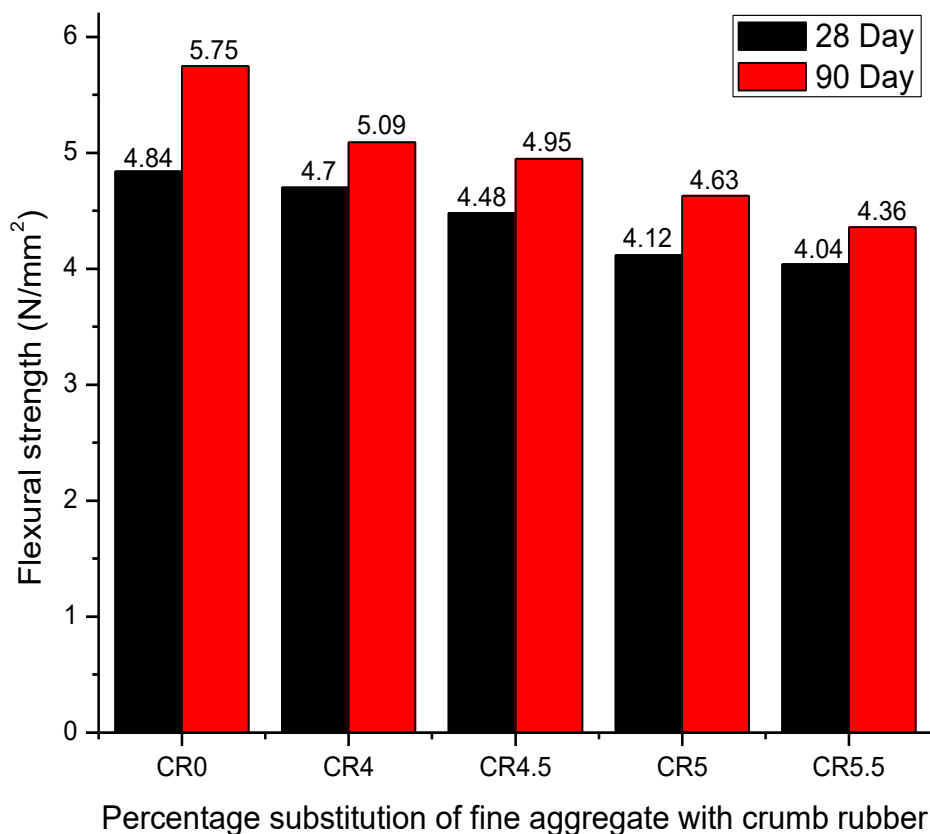


**Fig. 4.14: Flexural strength of crumb rubber concrete specimens**

Gupta et al. (2014) reported that decrease in flexural strength generally depends on the shape and size of CR. Due to irregular shape of CR particles, the interface between these and cement paste act as a bed for water during vibration and curing. Additionally, due to the smooth texture of CR the strength of this interface is further reduced. This leads to easier propagation of cracks on loading. Ganjian et al. (2009) also observed decrease in strength with incorporation of CR, shredded rubber and ground rubber as compared to

control mix samples. This occurs due to weak interlocking between the materials results in a decrease of flexural strength.

#### 4.3.2.4 Abrasion Resistance

The wear and tear of concrete occurs due to abrasion under different exposures such as skidding on the face of concrete. Employing codal recommendations, abrasion resistance can be calculated in terms of thickness of cube as per IS 1237 (2012). The variation of CR concrete abrasion resistance is shown in **Fig. 4.15**. It has been observed from same figure that with the incorporation of 5.5% of CR depth of wear increases up to 0.93 mm which shows an increment of 0.14 mm as compared with CR0 sample. During vibration of CR concrete, CR tend to move towards surfaces of concrete cube, due to lesser specific gravity of CR. This results into lower adhesive strength between CR particle and cement paste, allows easier abrasion as compared with control concrete. However, change in volume of CR concrete is basically due to reduced resistance to compression (Gupta et al. (2014)). Hence, it has been observed that CR concrete can be utilized for heavy duty applications and concrete tiles, as depth of wear was less as per IS 1237 (2012).

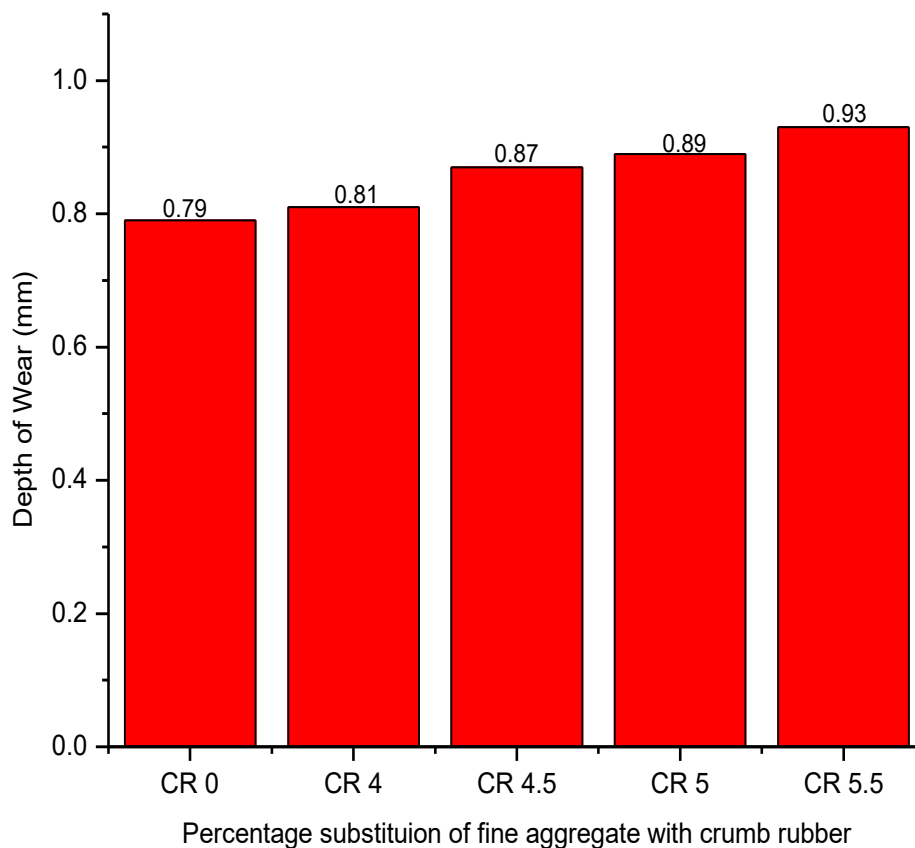


**Fig. 4.15: Abrasion resistance of crumb rubber concrete specimens**



#### 4.3.2.5 Pull-off Strength

Pull-off strength test was performed on concrete specimens with and without CR after 28 days of curing as shown in **Fig. 4.16**. It has been monitored from same figure that pull-off strength reduces with increase in substitution level of fine aggregate with CR. The highest pull-off strength was noticed for CR0 samples (2.688 N/mm<sup>2</sup>) and lowest value was obtained at 5.5% substitution level (2.056 N/mm<sup>2</sup>). As mentioned earlier, similar variation was noticed for compressive and flexural strength also. Results also signify that pull-off strength remains nearly close to control mix up to 4.5% substitution level which indicates that inclusion of CR does not have any adverse effect on concrete tensile properties. Pereira and Medeiros (2012) also verified that compressive strength and pull off strength follows similar pattern.

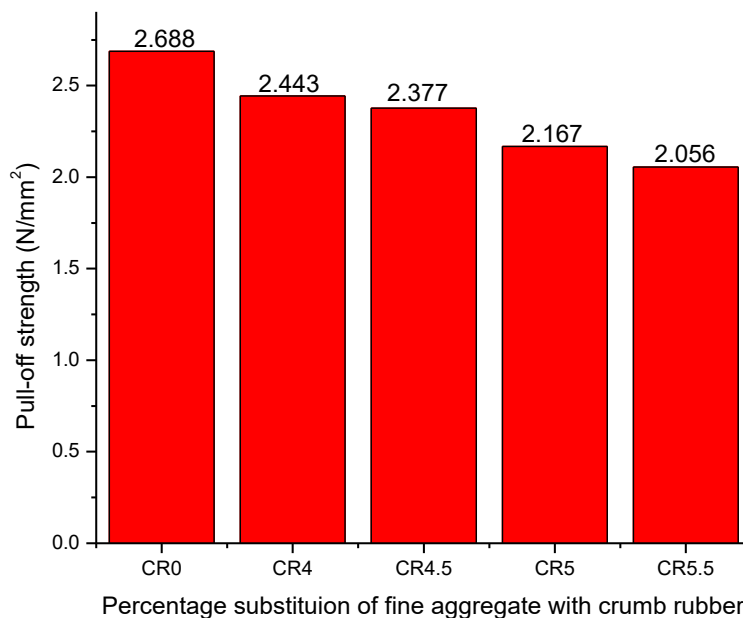


**Fig. 4.16: Pull-off strength of crumb rubber concrete specimens**

#### 4.3.3 Microstructure

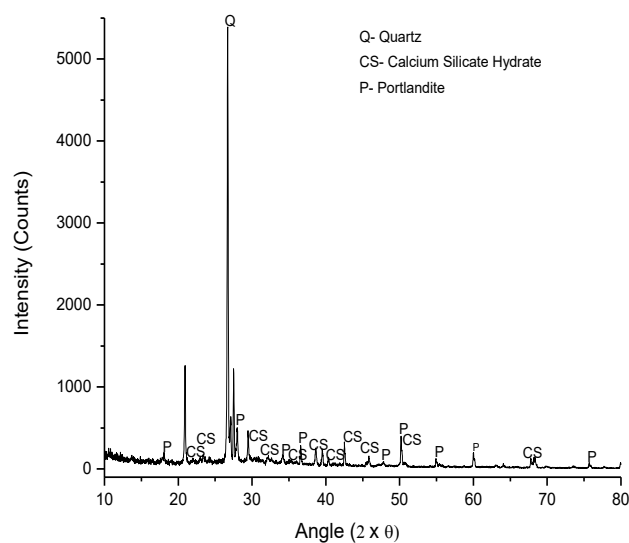
Microstructural skeleton of concrete samples were established by conducting XRD, FESEM, TGA, FTIR and AFM analyses.

##### 4.3.3.1 XRD Analysis

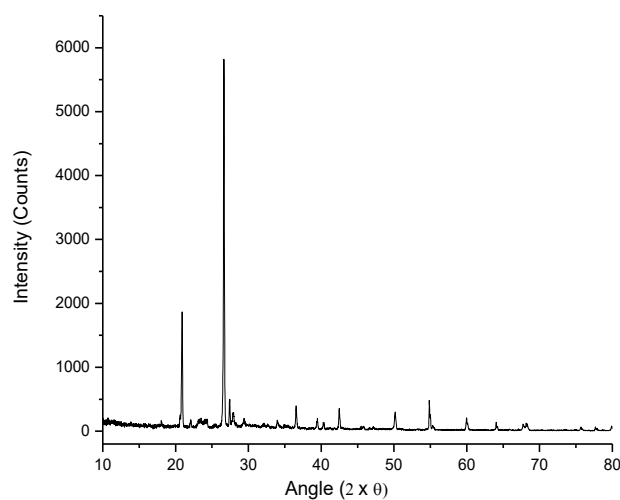
XRD analysis effect after 28 days of hydration was conducted to identify the mineralogical composition of concrete mixes with and without CR. In **Fig. 4.17**, three important phases are observed; Quartz (SiO<sub>2</sub>) (PDF 01-085-0798), calcium silicate hydrate (CSH) (PDF 01-089-7639) and Portlandite (Ca(OH)<sub>2</sub>) (PDF 01-070-7009).

### a) Effect on Quartz

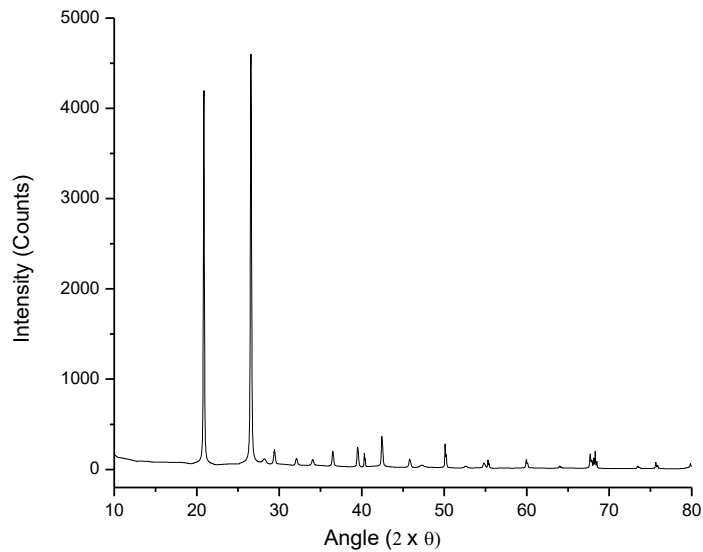
For CR0 mix the peak of quartz ( $\text{SiO}_2$ ) was at ( $2\theta = 26.28^\circ$ ) having intensity of 5380 cts. Variations were monitored in terms of intensity with substitution of fine aggregate with CR for CR4 (5485 cts) and CR5.5 (4598 cts) mixes around  $26.28^\circ$ . Through experimental investigation (**Fig. 4.11**) fall in compressive strength was monitored. The ideal usage of fine aggregate was noticed which results into formation of hydration products. However, the negative effect of CR degrades the performance of concrete sample. This might be due to formation of voids and also due to lack of bonding between the smooth CR constituents and cement matrix.



(a) CR0



(b) CR4



(c) CR5.5

**Fig. 4.17: XRD analysis of crumb rubber concrete samples**

#### **b) Effect on CSH**

CSH gel is the main hydration product which act as binder between cement & aggregate which governs the mechanical properties of concrete (Jamil et al. (2013)). Mixes with and without CR illustrates different number of peaks for CSH gel at different diffraction angles ( $2\Theta = 22.08^\circ, 36.44^\circ, 39.38^\circ$ ) as shown in **Fig. 4.17**. However, the intensities of these peaks are much lesser for CR incorporated concrete mixes as compared with control mix. Here, at 5.5% substitution level maximum intensity of 188.24 cts was monitored as compared to maximum intensity of 544.96 cts was observed at  $2\Theta = 50.07^\circ$  for control mix. Formation of lower intensities of CSH gel retards the bonding properties between constituents which results in fall of mechanical performance of concrete.

#### **c) Effect on Portlandite**

**Fig. 4.17** presents concentration of calcium hydroxide crystals after 28 days of curing for control mix having highest peak intensity of 357.82 cts at  $2\Theta = 27.95^\circ$ . At 4% substitution level peak intensity of 343 cts and for 5.5% replacement level 117 cts were noticed around  $27.95^\circ$  which is lower than control mix. However, for defining the strength of concrete formation of CSH is most important parameter i.e. more the formation of CSH gel greater will be the compressive strength of concrete.

#### 4.3.3.2 FESEM Analysis

FESEM micrograph for CR0, CR4 and CR5.5 mixes after 28 days of curing was observed as shown in **Fig. 4.18**. CSH and CASH gel were noticed in above mentioned figure and their presence is also verified through XRD (**Fig. 4.17**) analysis. The black spots are voids, fibrous portion which is dense in appearance is CSH and CASH gel. In CR0 mix, strong interfaces have been observed as compared to CR4 and CR5.5 mixes. Inclusion of CR in concrete mixes causes major changes in morphology, such as increase in voids and cracks as compared to CR0 mix as shown in **Fig. 4.18**. This affects the mechanical performance of concrete mixes as shown in **Fig. 4.11**. It has also been observed that with inclusion of CR in concrete mixes does not result in formation of any new compound. This has been verified through XRD analysis as shown in **Fig. 4.17**.

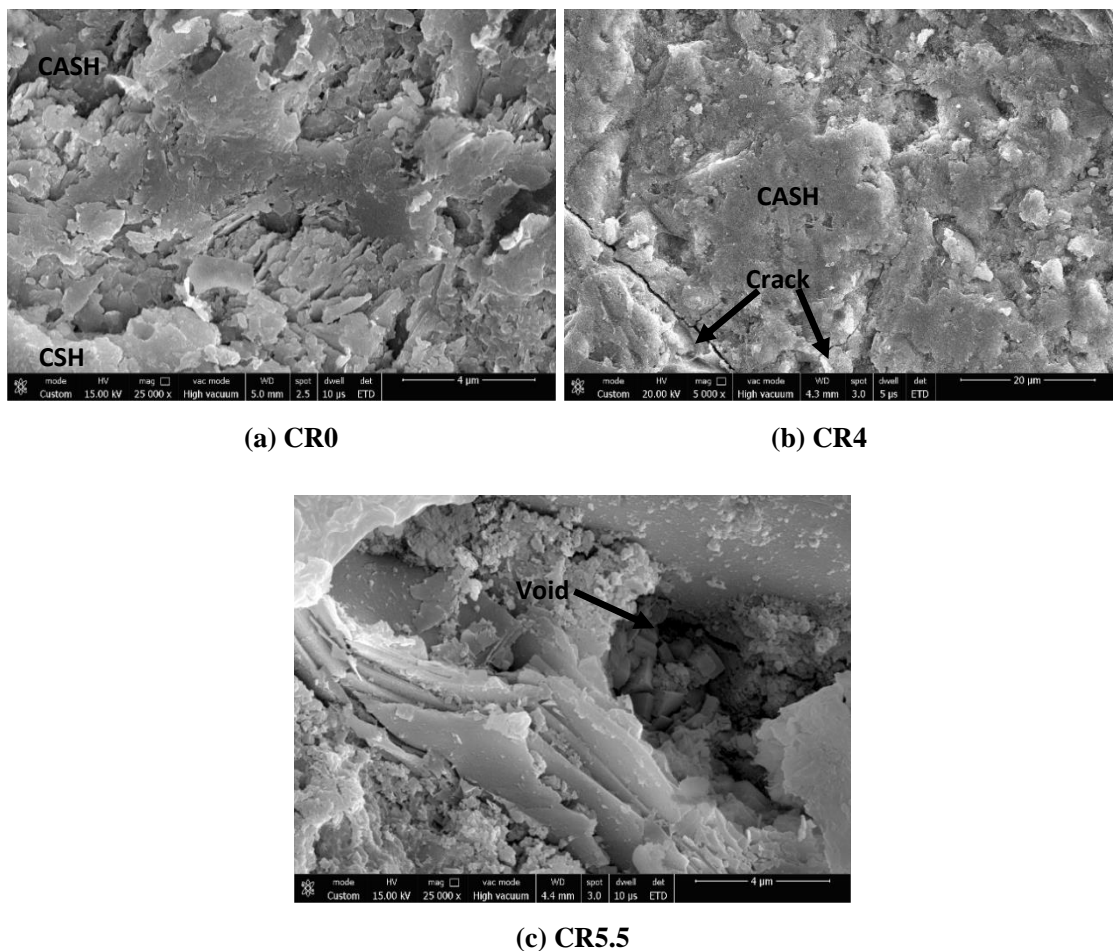
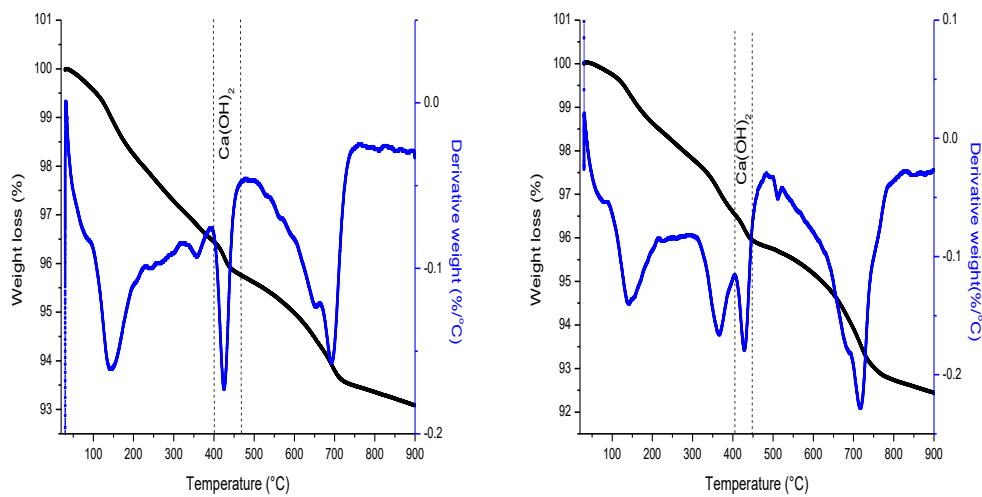


**Fig. 4.18: FESEM analysis of crumb rubber concrete specimens**

#### 4.3.3.3 TGA / DTA Analysis

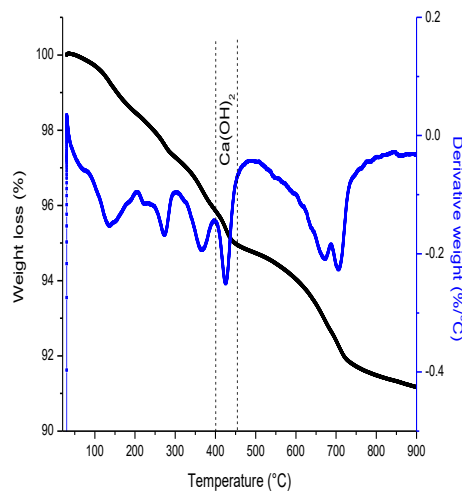
TGA / DTA thermograms were investigated on CR0, CR4 and CR5.5 mixes after 28 days of curing. The DTA curves (**Fig. 4.19**) show the typical reactions occurring in the

cement matrix, when subjected to a progressive temperature increase from room temperature up to 900°C. Evidently, DTA profile of the selective samples shows three endothermic peaks. The first peak was observed between 70°C and 170°C, corresponding to the mass loss on the TGA curve up to 170°C that attributed to the departure of weakly bound water in hydrates like CSH and ettringite (Wongkeo and Chaipanich (2010)). The second endothermic peak observed between 225°C and 320°C presents the decomposition of Calcium Aluminium Hydrate (CAH). The third endothermic peak was detected between 410°C and 470°C, that corresponds to the dehydration of  $\text{Ca(OH)}_2$ ; where, Portlandite decomposes into free lime (de-hydroxylation) (Sha et al. (1999)).



(a) CR0

(b) CR4



(c) CR5.5

**Fig. 4.19: TGA / DTA analysis of crumb rubber concrete samples**

After 28 days of water curing, the percentage weight loss of weakly bound water (CSH, ettringite etc.) in CR0, CR4 and CR5.5 mixes were calculated as 1.20%, 0.96% and 0.69% respectively. This signifies that formation of weakly bound water is more pronounced in control mix as compared to other mixes. From **Table 4.3** it has been observed that initially after 28 days of water curing formation of  $\text{Ca}(\text{OH})_2$  decreases with inclusion of CR due to reduced hydration process.

**Table 4.3: TGA investigated on water cured crumb rubber concrete samples**

MIX No.	Weight Loss (%)		
	70 - 170°C	225 - 320°C	410 - 470°C
CR0	1.20	0.90	0.64
CR4	0.96	0.79	0.57
CR5.5	0.69	0.69	0.48

#### 4.3.3.4 FTIR Analysis

FTIR spectroscopy was performed in order to examine the molecular groups present in concrete mixes for with and without CR after 28 days of curing as shown in **Fig.4.20**.

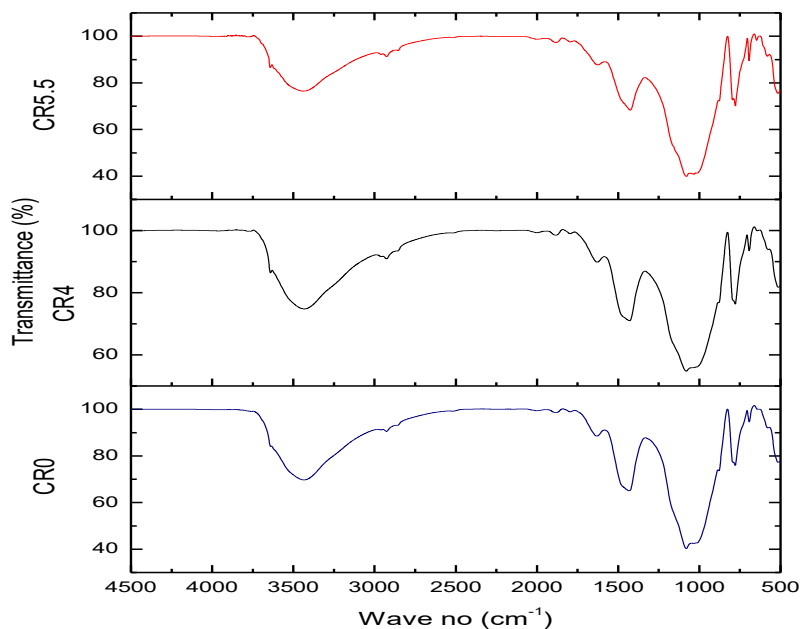


**Fig. 4.20: FTIR analysis of crumb rubber concrete samples**

FTIR spectrum can be divided into four regions. These regions are observed in ranges of  $3500 - 1600 \text{ cm}^{-1}$ ,  $1600 - 1400 \text{ cm}^{-1}$ ,  $1100 - 900 \text{ cm}^{-1}$  and  $800 - 400 \text{ cm}^{-1}$ . These bands are characterized to the presence of molecular groups  $\text{Ca}(\text{OH})_2$  (Calcium

Hydroxide), OH (Free water),  $\text{CO}_3^{2-}$  (Carbonate), CSH (Calcium Silicate Hydrate) and O-Si-O (Free Silica) respectively. It has also been clear from **Table 4.4** that molecular groups remain almost interminable with respect to their wave number for with and without CR. With rise in the percentage of CR as a substitute of fine aggregate free water band decreases due to consumption of this water which delayed hydration process. It has also been noticed that although formed molecular groups show nearly same wave numbers but reduction in mechanical performance was mainly occurs due to formation of voids.

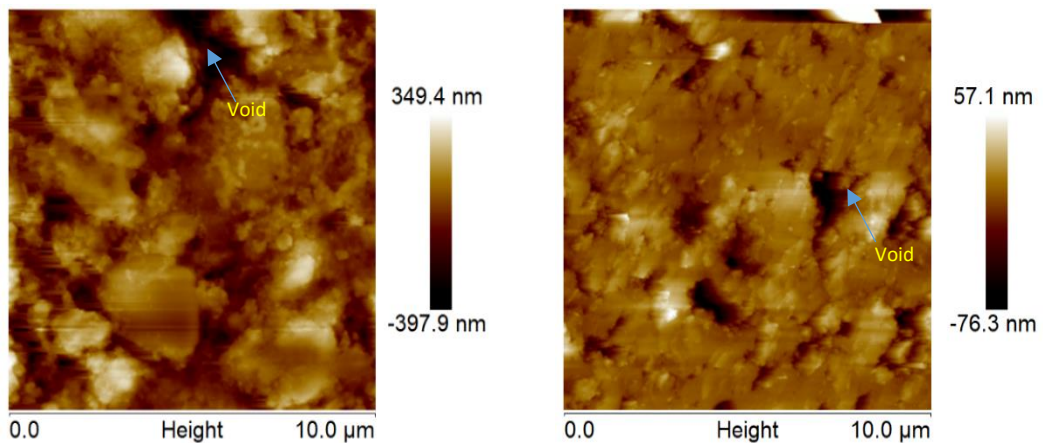
**Table 4.4: FTIR analysis on water cured crumb rubber concrete samples**

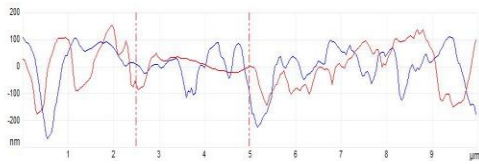
MIX No.	Molecular Groups ( $\text{cm}^{-1}$ )	
	Portlandite	Si-O-Al
CR0	3641	1017
CR4	3642	1015
CR5.5	3640	1014

#### 4.3.3.5 AFM Technique

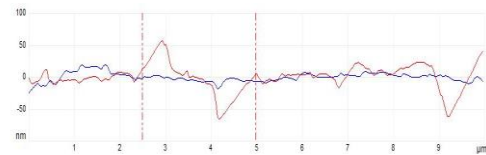
##### a) Surface Topography

**Fig. 4.21** presents surface topography for CR0, CR4 and CR5.5 samples. Dark spots have been observed in the images which shows the presence of voids at ITZ (Siddique et al. (2017)). NanoScope software was used to identify length and depth of these voids. The average values of length and depth was reported in **Table 4.5**. **Fig. 4.21(a)** shows the surface topography for CR0 sample. The largest void at top-middle portion of length  $0.278 \mu\text{m}$  and  $0.049914 \mu\text{m}$  depth at scan range of  $10 \mu\text{m}$  was noticed in the same figure. These voids were randomly placed throughout ITZ due to improper bonding between cement matrix and aggregate. This causes variations in surface roughness which has been observed at ITZ layer.

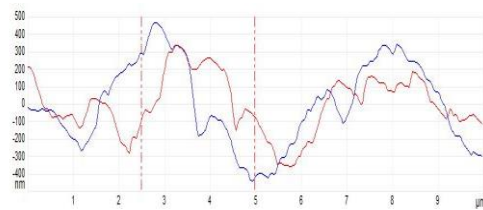
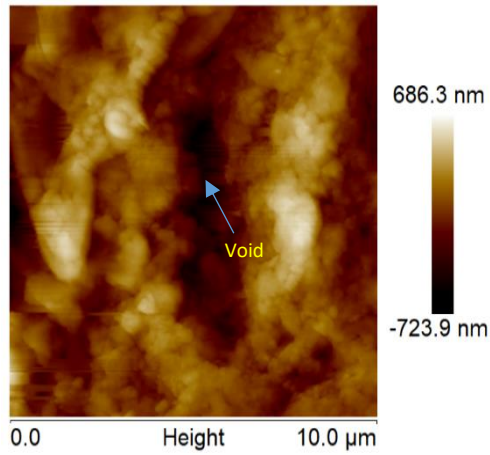




(a) CR0



(b) CR4



(c) CR5.5

**Fig. 4.21: Surface topography with roughness distribution curve of crumb rubber concrete specimens**

**Table 4.5: Average length and depth of voids at ITZ**

Sample	Length ( $\mu\text{m}$ )	Depth ( $\mu\text{m}$ )
CR0	0.278	0.049914
CR4	0.343	0.113790
CR5.5	0.368	0.153406

### b) Roughness

NanoScope software was used to quantify the surface property by calculating root mean square roughness ( $R_q$ ). This parameter was calculated by taking average value of surface height profile. The average value of roughness obtained from examination was reported in **Fig. 4.22**. It has been observed that with inclusion of CR in concrete, roughness



value increases up to 5.5% replacement level as compared to CR0. This change in roughness value is directly proportional to compressive strength. **Fig. 4.11** shows maximum compressive strength for CR0 sample and minimum roughness value (**Fig. 4.22**). Similar trend for roughness value and compressive strength were also observed by Siddique et al. (2017) for ceramic concrete. This rise in roughness value might be due to irregular shape and smooth texture of CR which reduces the adhesive strength between CR and cement paste. Decrease in compressive strength might be also due to generation of voids which might have been developed due to excess fine characteristic of CR.

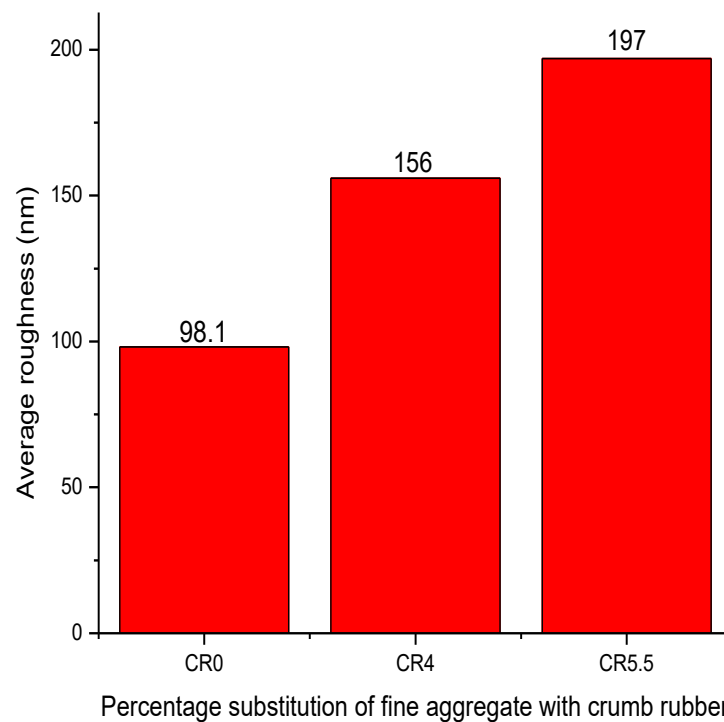


**Fig. 4.22: Average roughness of crumb rubber concrete samples**

## **4.4 Results and Discussion of Part - B: Glass Waste**

### **4.4.1 Fresh Property**

Fresh properties of WG concrete mixes are examined in terms of workability and fresh bulk density which are explained in this part of the chapter.

#### **4.4.1.1 Workability**

In the present work, amount of superplasticizer to be added in concrete mixes was strictly scrutinized in order to keep the compaction factor of 0.9 as shown in **Fig. 4.23**. This might be because WG particles were more angular in shape which reduces the fluidity of concrete mix. However, Taha and Nounu (2008) observed that reduction in workability

was due to smooth surface and lower water absorption of WG which reduces the cohesive force inside concrete mixture. Also, this reduction can be due to the sharp edges of WG used in concrete mix (Tan and Du (2013)).

**Table 4.6: Workability of fresh waste glass concrete mixes**

Mix No.	Admixture (%) by Weight of Cement	Compaction Factor
WG 0	1.50	0.90
WG 18	1.65	0.91
WG19	1.70	0.90
WG20	1.75	0.92
WG21	1.80	0.90
WG22	1.90	0.91
WG23	1.95	0.90
WG24	2.0	0.91

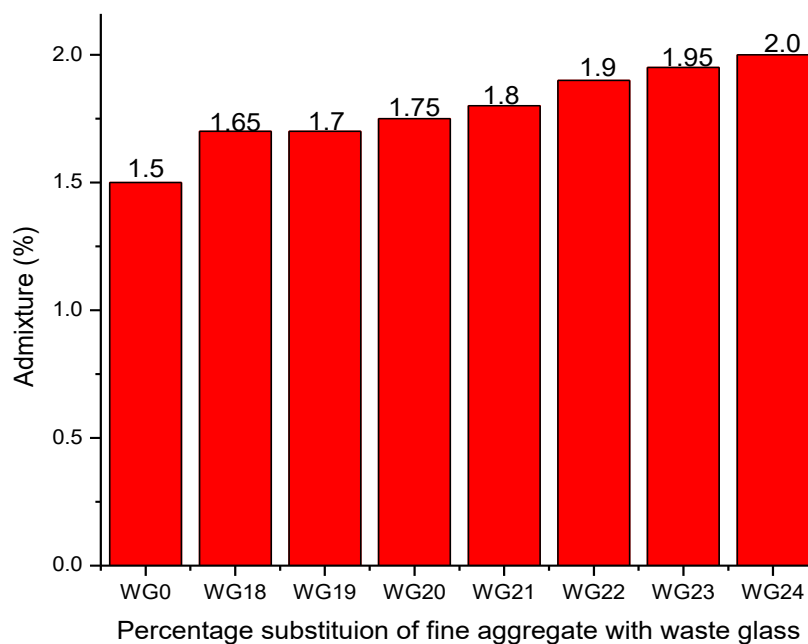


**Fig. 4.23: Percentage of admixture in waste glass concrete mixes**

#### 4.4.1.2 Fresh Bulk Density

Fresh density of WG concrete mixes illustrates a decreasing trend as shown in **Fig. 4.24**. It has been monitored from above mentioned figure that with rise in substitution level fresh density of concrete mixes decreases. The reduction in fresh density at 20% and 24% substitution levels are 2.89% and 2.97% respectively.

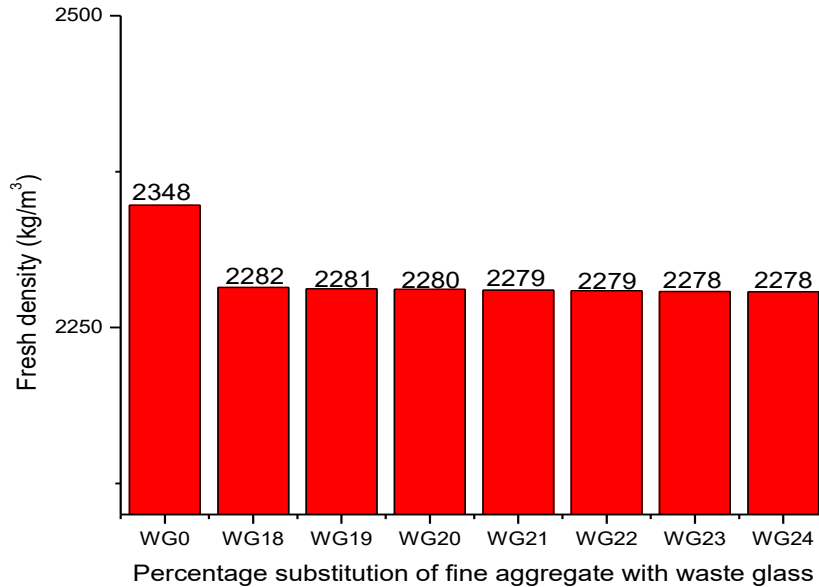


**Fig. 4.24: Fresh density of waste glass concrete specimens**

The fall in density of WG concrete may be due to lower specific gravity of WG (Du and Tan (2014)). The specific gravity of WG is 2.39 which is lower as compared to the specific gravity of fine aggregate (2.66). Similar behaviour for decrease in density of mortar has also been reported by Penacho et al. (2014) with substitution of fine aggregate from WG at different proportions due to lower specific gravity of WG.

#### 4.4.2 Mechanical Properties

In this section mechanical behaviour of WG concrete specimens are described by conducting tests like compressive strength, flexural strength, abrasion resistance and pull-off strength.

##### 4.4.2.1 Compressive Strength

The compressive strength of concrete mixes with and without WG after 28, 90 and 180 days are presented in **Fig. 4.25**. It has been observed from same figure that strength of concrete mixes deteriorates at higher percentages (22 – 24%) in concrete mix. Results obtained in the range of 18 – 20% replacement level shows rise in compressive strength as compared to reference mix. Replacement of 20% of fine aggregate by WG in concrete mix results in 12.75%, 12.32% and 11.11% increase in compressive strength for 28, 90 and 180 days cured samples. Incorporation of 21% WG in concrete mix, a decrement of 3.47%, 9.6% and 0.8% for 28, 90 and 180 days of curing respectively, in comparison with 20% replacement level. However, in comparison to WG0 mix, an increment of 9.04% and

9.90% was observed. The increase in compressive strength was due to higher apparent density of WG incorporated mixes, as compared with control mix's apparent density. It might be also due to densification of microstructure at interstitial transition zone. Reaction between calcium hydroxide present from cement hydration and silica present from WG might result into more formation of CSH gel which imparts better compressive strength to the concrete mixes.

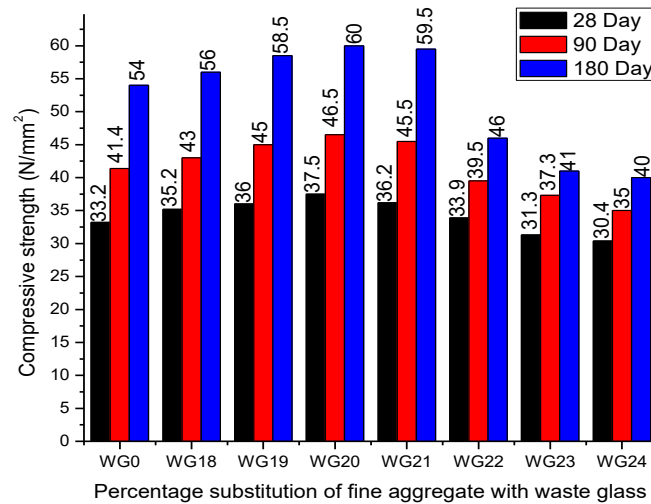


**Fig. 4.25: Compressive strength of waste glass concrete specimens**

It has also been observed from **Fig. 4.26** that at 21% substitution level apparent density is more than control mix's apparent density. This implies that inclusion of WG has increased impermeable pore spaces density, which ultimately increases the compressive strength of concrete (**Fig. 4.25**). A comparable observation was made by Ismail and AL-Hashmi (2009) for 20% replacement of fine aggregate by WG particles of size 150 microns – 4.75mm. Increase in strength was noticed due to pozzolanic activity of WG which improves the compressive strength by 4.32% as compared with control mix samples. Chen et al. (2006) also reported higher compressive strength due to pozzolanic activity of WG in the concrete mix which generated a denser microstructure.

**Fig.4.25** presents that with inclusion of 24% of WG strength decreases by 8.43%, 15.46% and 25.93% for 28, 90 and 180 days as compared to control mix. The decrease in strength might be due to presence of excessive fine waste glass which increases the void content. This negate the positive effect of denser impermeable pore space. It has been observed from **Fig.4.27** that voids ratio for different mixes increases with increase in percentage of WG. Limbachiya (2009) reported decrease in compressive strength above 20% replacement level due to generation of voids.

#### 4.4.2.2 Density and Voids

The inclusion of WG in concrete affects its hardened density as presented in **Fig.4.26**. With incorporation of 24% of WG, bulk density of concrete decreases by 7.11% as compared to control mix. From the same figure it can be seen that apparent density increases up to 20% substitution level and also results into high porosity. After which apparent density tends to reduce with further inclusion of WG. However, 21% substitution level also shows higher apparent density as compared with control samples. This increase in apparent density signifies denser impermeable pores, improves compressive resistance of concrete samples.

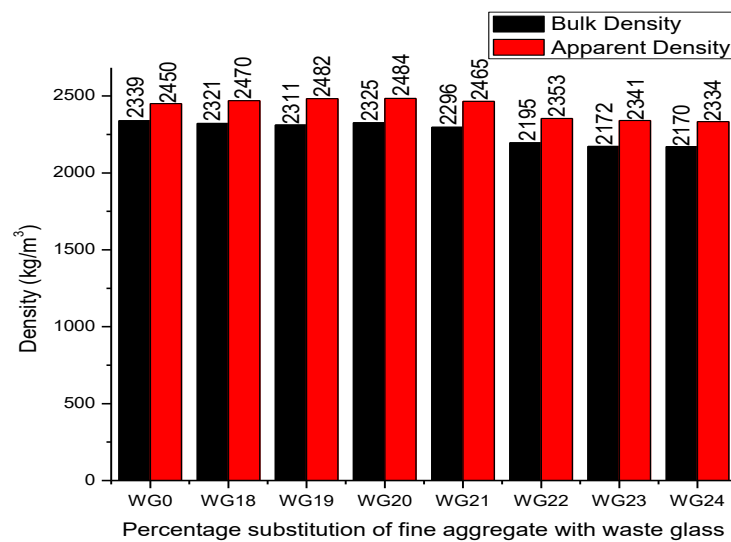


**Fig. 4.26: Hardened density of waste glass concrete specimens**

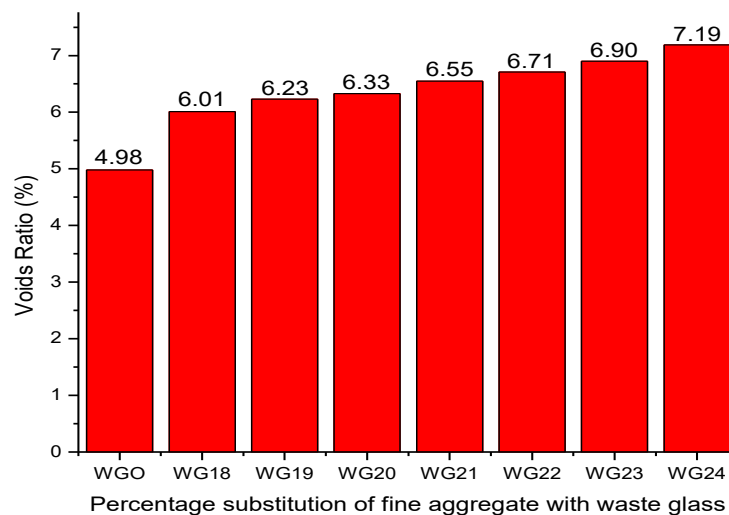


**Fig. 4.27: Voids ratio of waste glass concrete specimens**

The lower density of WG concrete may be due to lesser specific gravity of WG (Du and Tan (2014)) and also due to generation of voids (**Fig. 4.27**). The specific gravity

of WG is 2.39 which is lower as compared to the specific gravity of fine aggregate (2.66). Lee et al. (2013) observed 7.28% decrease in density of WG concrete as compared with control mix. Similar behaviour for decrease in density of mortar has also been reported by Penacho et al. (2014) with substitution of fine aggregate from WG at different proportions due to lower specific gravity of WG.

#### 4.4.2.3 Flexural Strength

The results of flexural strength after 28 and 90 days of water curing with and without WG at different percentages are reported in **Fig. 4.28**. It has been observed from same figure that flexural strength of WG concrete increases up to a substitution level of 20% as compared with WG0 mix. Inclusion of 20% of WG as a substitute of fine aggregate shows 7.85% and 7.58% increase in flexural strength for 28 and 90 days respectively. Rise in flexural strength might be due to substantial pozzolanic reaction that might have occurred during hydration which has resulted into better bonding between cement paste and WG at interstitial transition zone (ITZ). Metwally (2007) reported that enhancement in flexural strength was observed due to pozzolanic effect in the cement matrix during later age of 28 day.

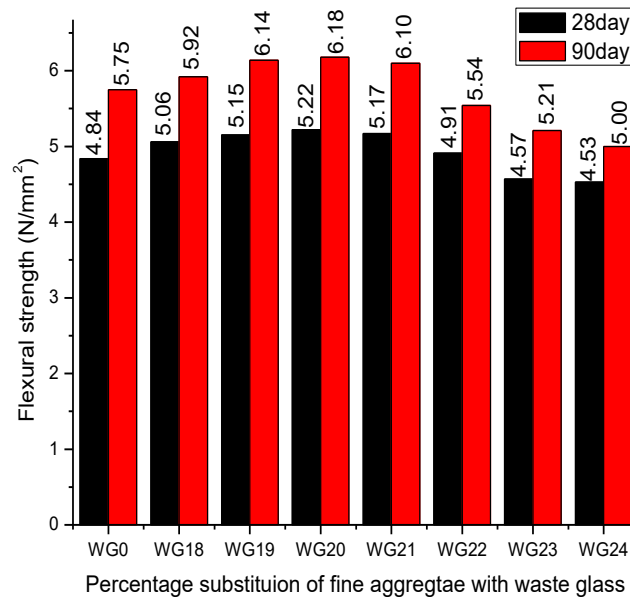


**Fig. 4.28: Flexural strength of waste glass concrete specimens**

As the percentage of WG in concrete increases after 20%, decrease in flexural strength was observed. At 24% inclusion of WG in concrete mix, 6.4% and 13.04% reduction in flexural strength for 28 and 90 days were recorded respectively. The reduction in flexural strength is mainly due to generation of cracks which developed due

to sharper edges of WG particles as shown in **Fig. 3.15**. This results into weaker bonding between WG particles and cement paste at ITZ. Tan and Du (2013) also reported decrease of flexural strength due to sharp edges of WG in concrete mix which resulted into weaker bonding at interface.

#### 4.4.2.4 Abrasion Resistance

The changes in WG concrete abrasion resistance is presented in **Fig. 4.29**. It has been monitored from same figure that with inclusion of WG depth of wear decreases up to 20% substitution level however, further inclusion of WG illustrates adverse effects. Decrease in abrasion resistance might be due to lower specific gravity of WG, during vibration of WG concrete, WG tend to move toward surfaces of concrete cube. This results into lower adhesion between WG particle and cement matrix, allows easier abrasion as compared with control concrete. However, change in volume of WG concrete was basically due to reduced resistance to compression above 20% substitution level (Topçu and Canbaz (2004)). Ling and Poon (2011) also noticed reduced abrasion resistance when fine aggregate was totally replaced with blue colour WG (60% < 2.36 mm and 40% 2.36 - 5mm).

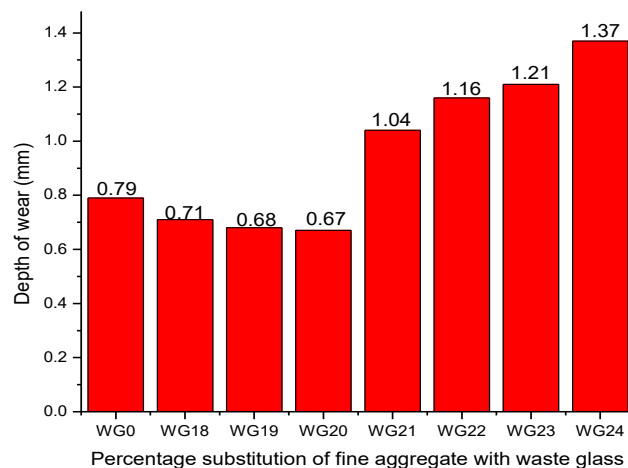


**Fig. 4.29: Abrasion resistance of waste glass concrete specimens**

#### 4.4.2.5 Pull-off Strength

Pull-off strength test was investigated on concrete specimens with and without WG after 28 days of curing as shown in **Fig. 4.30**. It has been monitored from above mentioned figure that pull-off strength increases with increase in substitution level of fine aggregate with WG. The highest pull-off strength was noticed at 20% substitution level (3.819 N/mm<sup>2</sup>) as compared to WG0 samples (2.688 N/mm<sup>2</sup>).

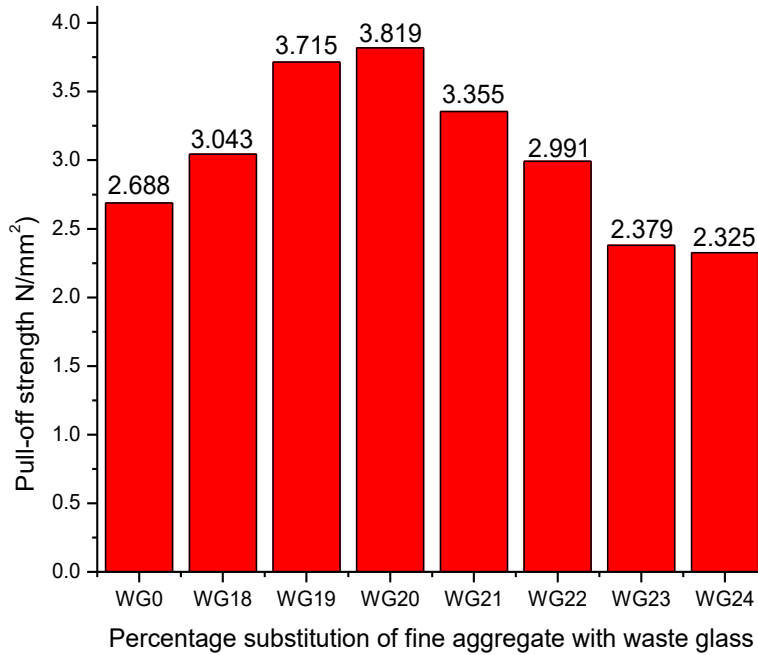


**Fig. 4.30: Pull-off strength of waste glass concrete specimens**

With incorporation of 21% of WG in concrete mix, decrease ( $3.355 \text{ N/mm}^2$ ) in pull-off strength was noticed in comparison with 20% replacement level. As mentioned earlier, similar variation was noticed for compressive and flexural strength also. Results implies that pull-off strength increases up to 21% substitution level. This implies that inclusion of WG does not show any adverse influence on concrete tensile property.

#### 4.4.3 Microstructure

Microstructural properties of WG concrete samples were examined and explained in the following sections by conducting XRD, FESEM, TGA, FTIR and AFM analyses.

##### 4.4.3.1 XRD Analysis

XRD analysis after 28 days of hydration was conducted to identify the mineralogical composition of concrete mixes with and without WG. In **Fig. 4.31**, three important phases are observed; Quartz ( $\text{SiO}_2$ ) (PDF 01-085-0798), calcium silicate hydrate (CSH) (PDF 01-089-7639) and Portlandite ( $\text{Ca}(\text{OH})_2$ ) (PDF 01-070-7009). It has been observed from above mentioned figure that peaks of di-calcium silicate, tri-calcium silicate and tetra calcium alumino ferrite are not available which shows the consumption of these compounds after 28 days of hydration.



### a) Effect on Quartz

For WG0 mix the peak of quartz ( $\text{SiO}_2$ ) was at ( $2\Theta = 26.28^\circ$ ) having intensity of 5380 cts. Changes have been observed in terms of intensity with rise in the substitution level of fine aggregate with WG for WG18 (2027 cts), WG20 (2153 cts), WG22 (1936 cts) and WG24 (1186 cts) mixes around  $26^\circ$ . Through experimental study the maximum compressive strength was monitored for WG20 mix out of all the mixes. Reaction between silica and  $\text{Ca}(\text{OH})_2$  (hydration product) enhances the compressive strength of concrete. This clearly signifies that ideal usage of silica has taken place which leads to greater generation of CSH gel and improves the bonding at cement and aggregate interface. However, after WG20 substitution level negative effect on compressive strength has been observed. This might be due to increase in percentage of WG which negate the positive binding action between cement matrix and aggregate due to decrease in distance between  $\text{SiO}_2$  particles (Singh et al. (2016)). The less space between  $\text{SiO}_2$  crystals causes reduction in the growth of CH crystal which declines its quantity.

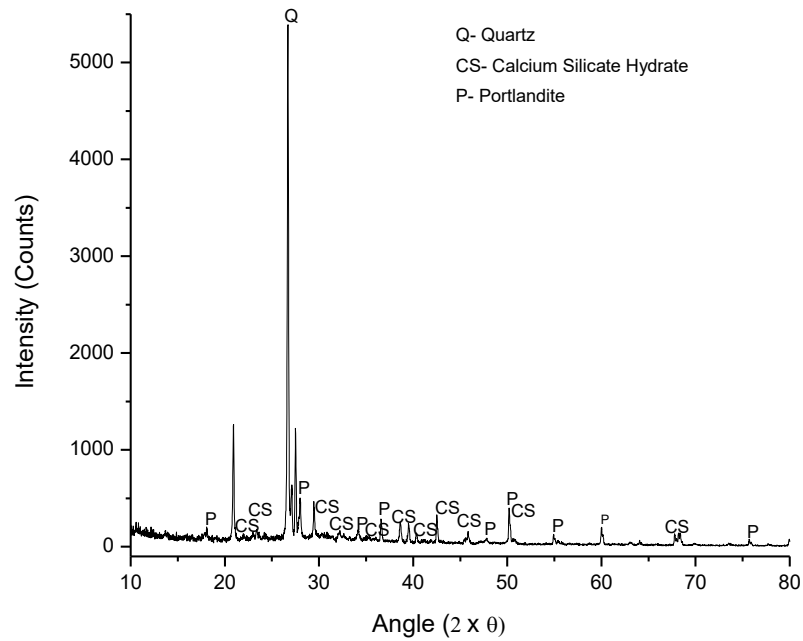
### b) Effect on CSH

CSH gel is the main hydration product which act as binder between cement and aggregate and governs the mechanical properties of concrete (Jamil et al. (2013) and Avirneni et al. (2016)). Mixes with and without WG show different number of peaks for CSH gel as shown in **Fig. 4.31**. WG20 sample has maximum count of CSH gel at different diffraction angles ( $2\Theta = 22.08^\circ, 36.44^\circ, 39.38^\circ$ ) however, maximum intensity of 544.96 cts was observed at  $2\Theta = 50.07^\circ$  as compared WG0 mix which is having maximum intensity of 367.30 cts at  $2\Theta = 50.17^\circ$ . The concentration of CSH gel is higher for all mixes as compared to calcium hydroxide. Hence, the optimal concentration of CSH gel was noticed for WG20 mix as compared to other mixes as a consequence of improved compressive strength. This might also be due to improved pozzolanic reaction with inclusion of WG as seen above by the decrease in silica content.

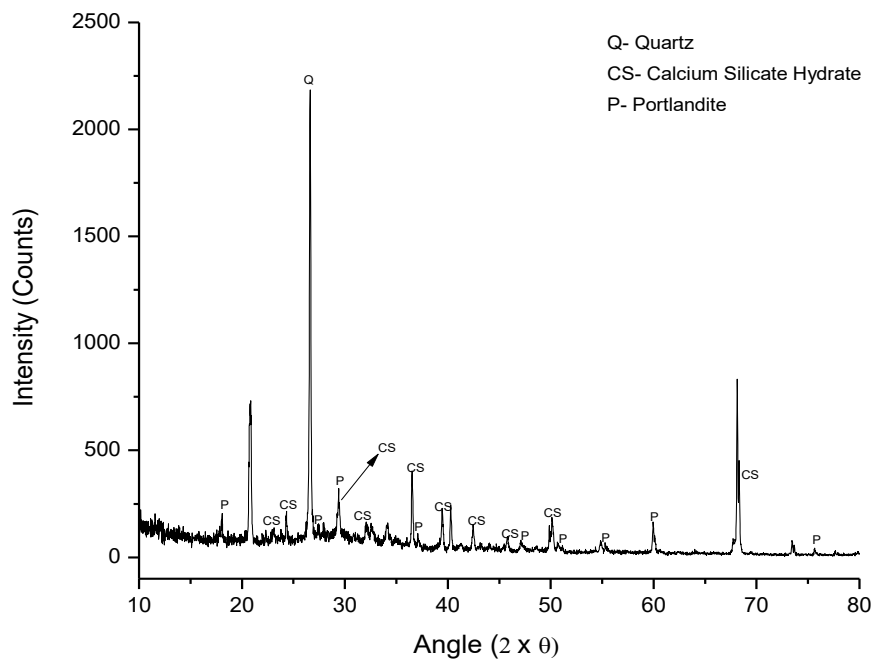
### c) Effect on Portlandite

**Fig. 4.31** presents well defined concentration of CH crystals after 28 days of curing for WG0 mix having highest peak intensity of 357.82 cts at  $2\Theta = 27.95^\circ$ . For WG18 mix peak intensity of 182 cts was observed around  $27^\circ$  which is lower than WG0 mix. In addition to this peak intensity of 80.10, 76.80 and 140.91 cts were noticed for WG20, WG22 and WG24 mixes around  $28^\circ$ . Another promising peak was also identified around

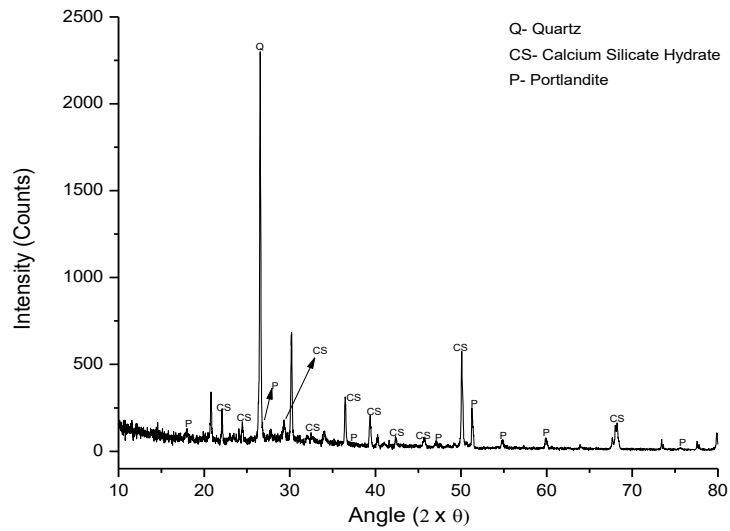
17° for all mixes. XRD analysis for WG20 mix shows lesser number of calcium hydroxide counts as compared to other mixes. However, for defining the strength of concrete formation of CSH is most important parameter i.e. more the formation of CSH gel greater will be the compressive strength of concrete.



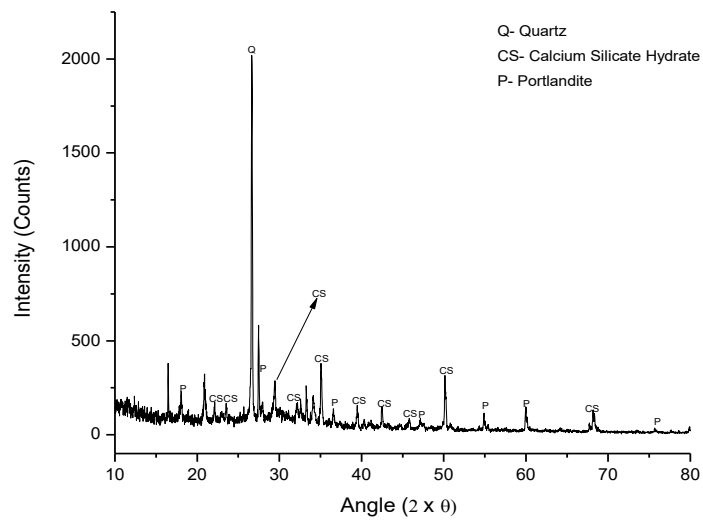
(a) WG0



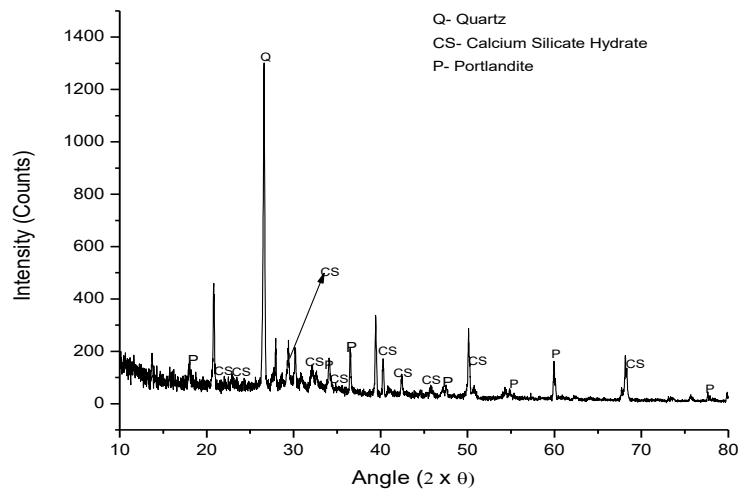
(b) WG18



(c) WG20



(d) WG22



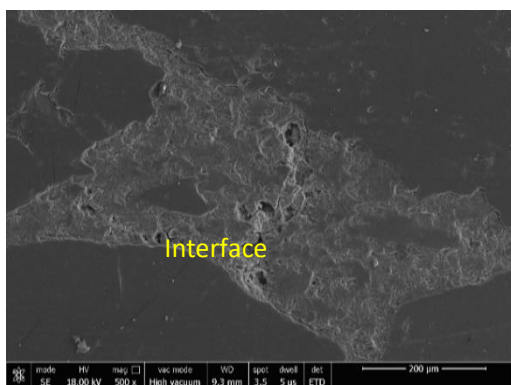
(e) WG24

Fig. 4.31: XRD analysis of waste glass concrete samples

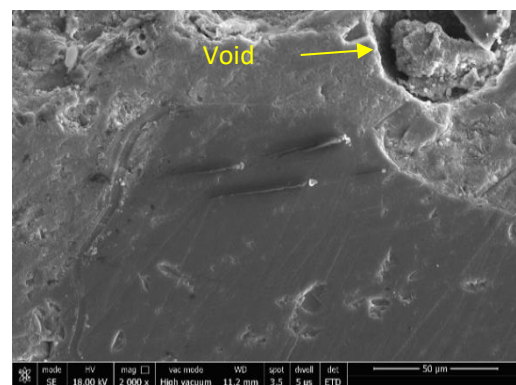
#### 4.4.3.2 FESEM Analysis

To characterize the microstructure, FESEM images of concrete mixes with and without WG were captured after 28 days of water curing. **Fig. 4.32 (a)** presents the microstructure of control concrete mix which shows the interface between cement mortar and aggregates. Hairline cracks and voids are also seen passing through these interfaces. With inclusion of WG as a replacement of fine aggregate in concrete depicts the formation of dense matrix. The particles of WG were dispersed properly throughout the cement matrix.

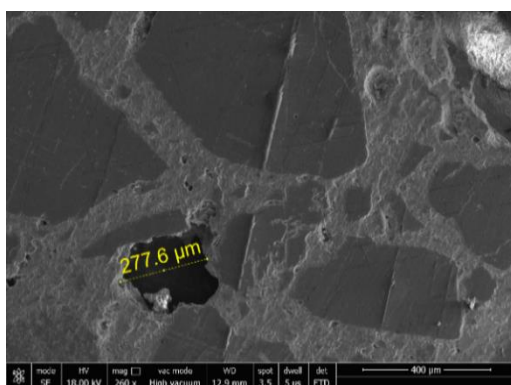
**Fig. 4.32 (b, c, d)** shows denser interface which results into improved compressive resistance of concrete specimen as shown in **Fig. 4.25**. The negative effect of WG plays dominant role at higher percentages, where percentages of voids increases as well as increase in width of crack. **Fig. 4.32** shows as the percentage of WG in concrete increases width of voids also increases. The increment of cracks leads to reduction in bonding between WG particles and cement matrix which mainly occurs due to sharper edges which leads to reduction in flexural strength as shown in **Fig. 4.28**.



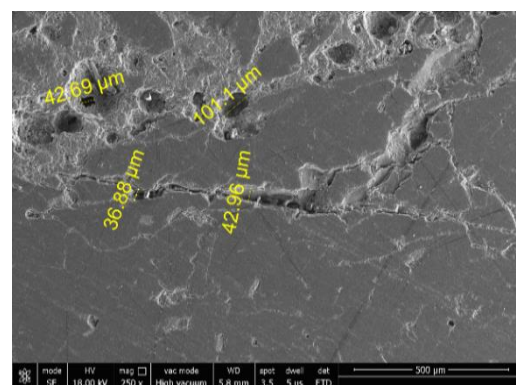
(a) WG0



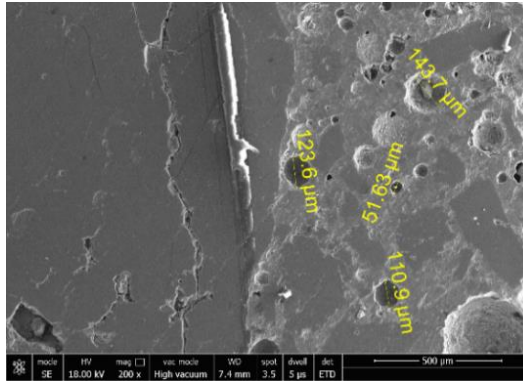
(b) WG18



(c) WG20



(d) WG22

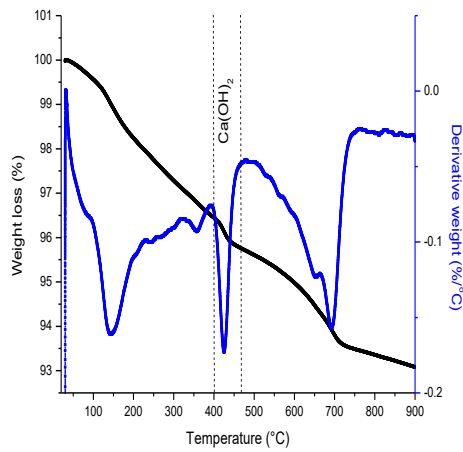


(e) WG24

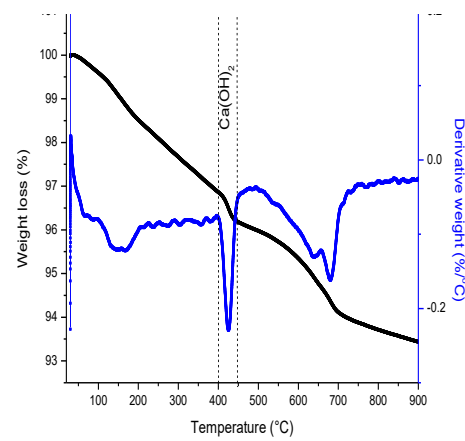
Fig. 4.32: FESEM analysis of waste glass concrete specimens

#### 4.4.3.3 TGA / DTA Analysis

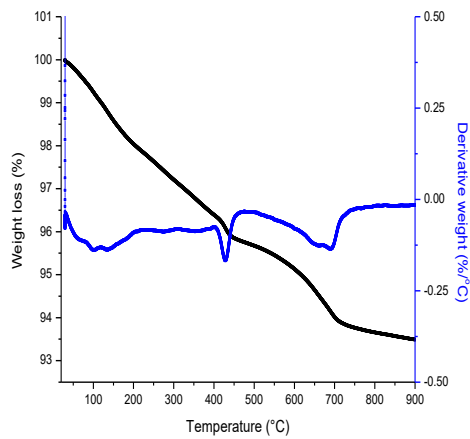
TGA / DTA thermograms were investigated for WG0, WG18, WG20, WG22 and WG24 samples after 28 days of water curing.



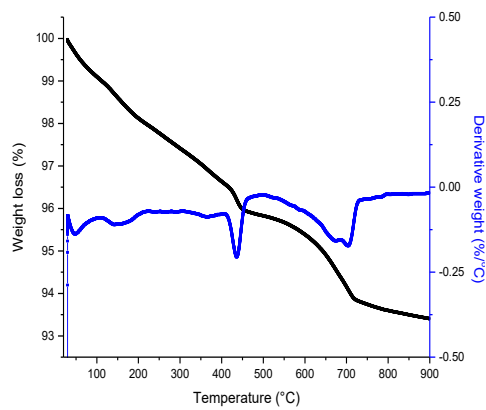
(a) WG0



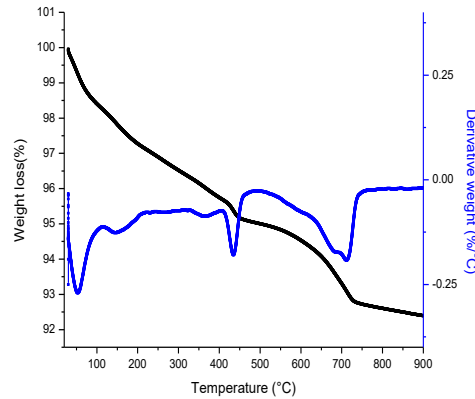
(b) WG18



(c) WG20



(d) WG22



(e) WG24

**Fig. 4.33: TGA / DTA analysis of waste glass concrete samples**

**Fig. 4.33** presents the changes occurring in cement composite when exposed to a gradual rise in temperature (room temperature to 900°C). It has been monitored that percentage weight loss of weakly bound water (CSH, ettringite etc.) for WG0, WG18, WG20, WG22 and WG24 samples were computed as 1.2%, 1.35%, 1.75%, 1.27% and 0.99% respectively. This indicates that growth of weakly bound water marks higher presence for WG20 sample as compared to other mixes. It has been observed from **Table 4.7** that percentage weight loss of calcium hydroxide is lesser for WG20 sample as compared to other samples. This might be due to consumption of calcium hydroxide to form calcium silicate aluminium hydrate due to the presence of fly-ash in cement. Formation of this compound also enhances the mechanical performance of WG incorporated samples.

**Table 4.7: TGA investigated on water cured waste glass concrete samples**

MIX No.	Weight Loss (%)		
	70 - 170°C	225 - 320°C	410 - 470°C
<b>WG0</b>	1.2	0.9	0.64
<b>WG18</b>	1.35	0.86	0.58
<b>WG20</b>	1.75	0.82	0.56
<b>WG22</b>	1.27	0.81	0.67
<b>WG24</b>	0.99	0.69	0.71

#### 4.4.3.4 FTIR Analysis

FTIR spectroscopy has been conducted to investigate bands of molecular groups present in concrete mixes with and without WG at 28 days of curing as shown in **Fig.**

**4.34.** FTIR spectrum can be divided into four regions. These regions are observed in ranges of  $3500 - 1600 \text{ cm}^{-1}$ ,  $1600 - 1400 \text{ cm}^{-1}$ ,  $1100 - 900 \text{ cm}^{-1}$  and  $800 - 400 \text{ cm}^{-1}$ . These bands are characterized to the presence of molecular groups  $\text{Ca(OH)}_2$  (Calcium Hydroxide), OH (Free water),  $\text{CO}_3^{2-}$  (Carbonate), CSH (Calcium Silicate Hydrate) and O-Si-O (Free Silica) respectively. It has also been clear from **Table 4.8** that molecular groups remain almost interminable with respect to their wave number for with and without WG in concrete except for  $\text{Ca(OH)}_2$ . With rise in the percentage of WG as a substitute of fine aggregate free water band decreases due to consumption of free water which delayed hydration process.

Hydration process results into formation of Portlandite which increases up to WG20 incorporation level of WG as shown in **Table 4.8**. The formed Portlandite further evolves into CSH gel with the same extent of polymerization. This results into a denser matrix which ultimately improves the apparent density of concrete mixes as shown in **Fig. 4.26**. This might be the reason for the improved concrete mechanical properties. However, after WG20 replacement level formed Portlandite gets consumed in the generation of CSH gel which results in the fall of Portlandite as shown in above mentioned table.

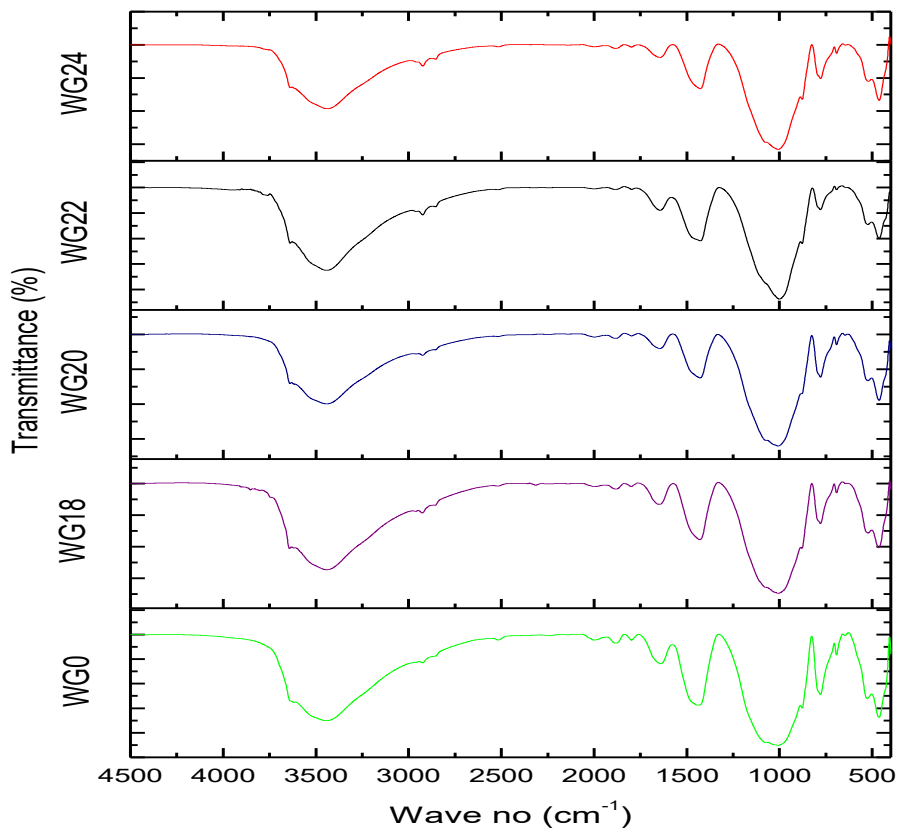


**Fig. 4.34 FTIR analysis of waste glass concrete samples**

**Table 4.8: FTIR analysis on waste glass concrete samples**

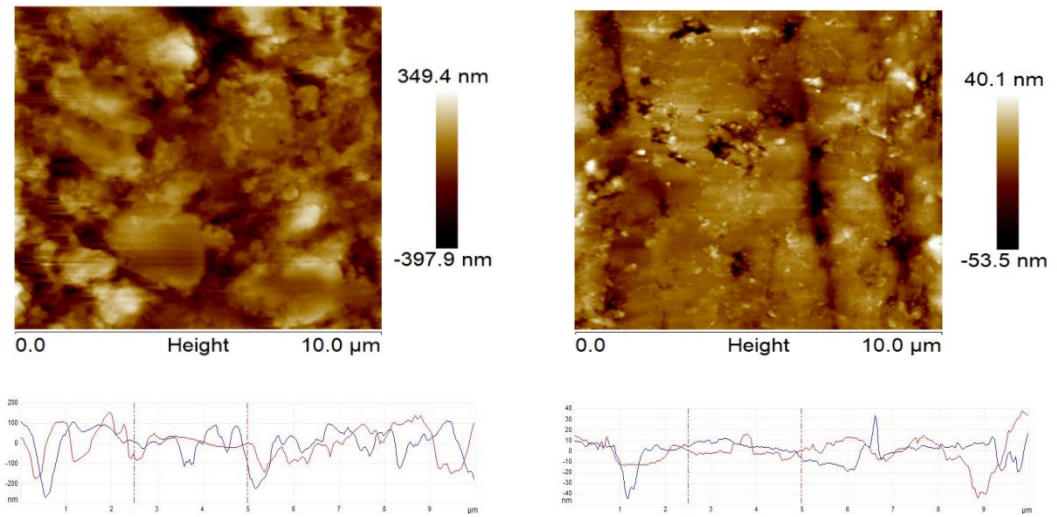
Molecular Group (cm <sup>-1</sup> )	WG0	WG18	WG20	WG22	WG24
Water Band (OH <sup>-</sup> )	3443.38	3441.39	3442.35	3440.10	3438.54
	1643.28	1643.28	1644.27	1643.71	1643.98
Portlandite	3436.30	3441.39	3442.35	3440.66	3440.10
CO <sub>3</sub> <sup>2-</sup>	1442.75	1429.16	1428.39	1426.43	1427.64
CSH	1006.60	1006.60	1007.57	1007.30	1007.52
O-Si-O	879.86	879.36	880.90	878.06	877.77
	779.29	779.18	778.82	779.08	778.57
	463.58	465.54	463.01	463.01	462.90

#### 4.4.3.5 AFM Technique

##### a) Surface Topography

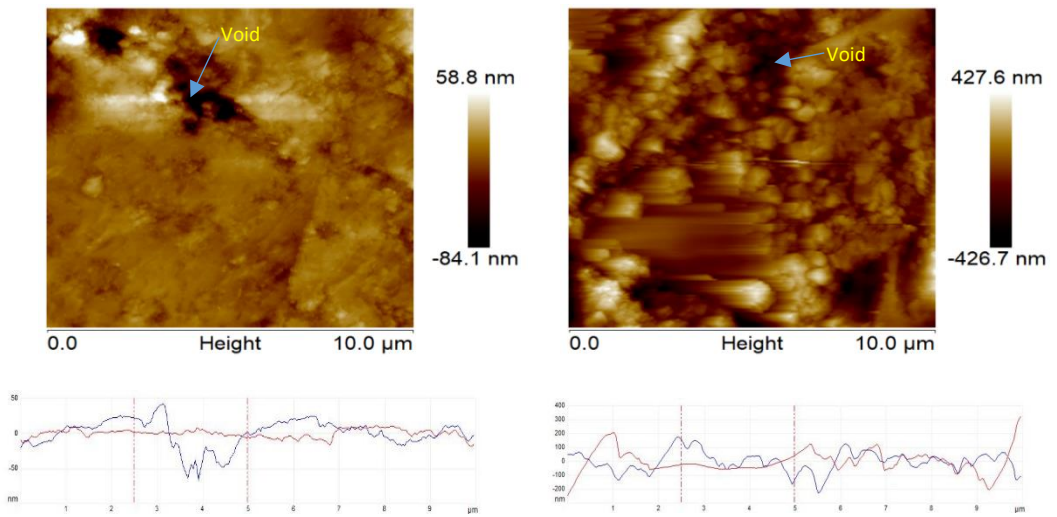
**Fig. 4.35** presents surface topography for WG0, WG18, WG20, WG22 and WG24 samples. Dark spots have been observed in the images which shows the presence of voids at ITZ (Siddique et al. (2017)). NanoScope software was used to identify length and depth of these voids. The average values of length and depth was reported in **Table 4.9**. **Fig. 4.35 (a)** shows the surface topography for WG0 sample. The largest void at top-middle portion of length 0.278  $\mu\text{m}$  and 0.049914  $\mu\text{m}$  depth at scan range of 10  $\mu\text{m}$  was noticed in the same figure. These voids were randomly placed throughout ITZ due to improper bonding between cement matrix and aggregate. This causes variations in surface roughness which has been observed at ITZ layer. The surface topography and roughness distribution curve of WG18 sample is shown in **Fig. 4.35 (b)**. It has been recorded from the image that inclusion of 18% WG aggregate leads to comparatively smoother surface topography of the ITZ layer as compared to WG0 sample. Smoother topography has been observed due to decrease in size of voids as shown in **Table 4.9**. This might be due to filler nature of WG. Roughness curve also shows smoother wave shape with lesser fluctuations. This can be due to improved pozzolanic activity due to incorporation of WG in concrete which results into formation of denser CSH gel at ITZ. Similar observation for augmentation in strength properties was noticed by Metwally (2007) due to pozzolanic reaction between WG and cement matrix.





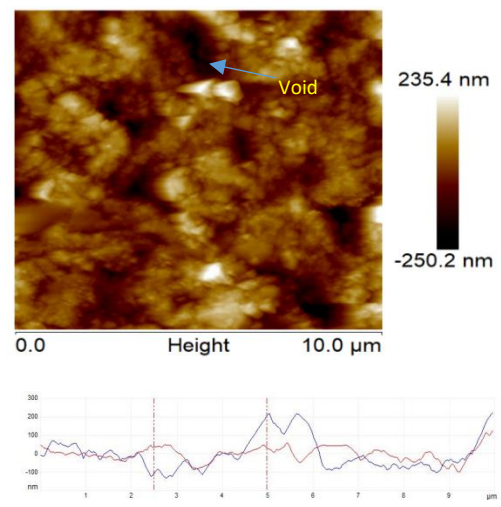
(a) WG0

(b) WG18



(c) WG20

(d) WG22



(e) WG24

**Fig. 4.35: Surface topography with roughness distribution curve of waste glass concrete samples**

It has been pointed out from **Fig. 4.35 (c)** WG20 sample shows highly improved surface topography and roughness curve at 20% substitution level as compared to WG0 and WG18 samples. The surface topography image shows better surface with decreased size of voids. At 10  $\mu\text{m}$  scan range the average length of void is 0.157  $\mu\text{m}$  with 11.319 nm depth. As 20% of natural sand is replaced by WG, plenty of pozzolanic WG fine aggregate results into production of CSH gel at higher amount. This intense formation of CSH gel illustrates smoother and denser ITZ layer. The CSH formed is highly dense and has mushy appearance.

**Fig. 4.35 (d)** presents surface topography image and roughness curve for WG22 sample. The surface topography image at 10  $\mu\text{m}$  scan range shows voids which is dispersed across ITZ. These voids were formed due to excess fine nature of WG which negate the positive pore filling ability at higher substitution level (**Fig. 4.27**). The size of voids has been increased as shown in **Table 4.9**. Due to highly angular shape and sharp edges of WG leads to increase in roughness at ITZ as compared to WG0, WG18 and WG20 samples. Due to increase in voids percentage at ITZ reduction in compressive strength has been observed as shown in **Fig. 4.25**.

**Table 4.9: Average length and depth of voids at ITZ**

Sample	Length ( $\mu\text{m}$ )	Depth ( $\mu\text{m}$ )
WG0	0.278	0.049914
WG18	0.275	0.011379
WG20	0.235	0.000715
WG22	0.299	0.025583
WG24	0.331	0.042129

With inclusion of 24% WG changes has been observed as shown in **Fig. 4.35 (e)**. Surface topography shows the presence of CSH particles which is scattered across ITZ. Increase in percentage of voids was also observed from surface topography image as mentioned above. The size of voids shows higher aspect ratio in terms of length and depth as compared to other samples as shown in **Table 4.9**. It has also been noticed that roughness curve shows more undulations.

#### **b) Roughness**

NanoScope software was used to quantify the surface property by calculating root mean square roughness ( $R_q$ ). This parameter was calculated by taking average value of

surface height profile. The average value of roughness obtained from examination was reported in **Fig. 4.36**. It has been observed that with inclusion of WG in concrete, roughness value decreases up to 20% replacement level as compared to WG0. This change in roughness value is inversely proportional to compressive strength. **Fig. 4.25** shows maximum compressive strength at 20% replacement and minimum roughness value (**Fig. 4.36**). Similar trend for roughness value and compressive strength were also observed by Siddique et al. (2017) for ceramic concrete. The incorporation of fine WG in concrete act as a filler. This improves the bonding between aggregate and cement matrix and improves the quality of ITZ.

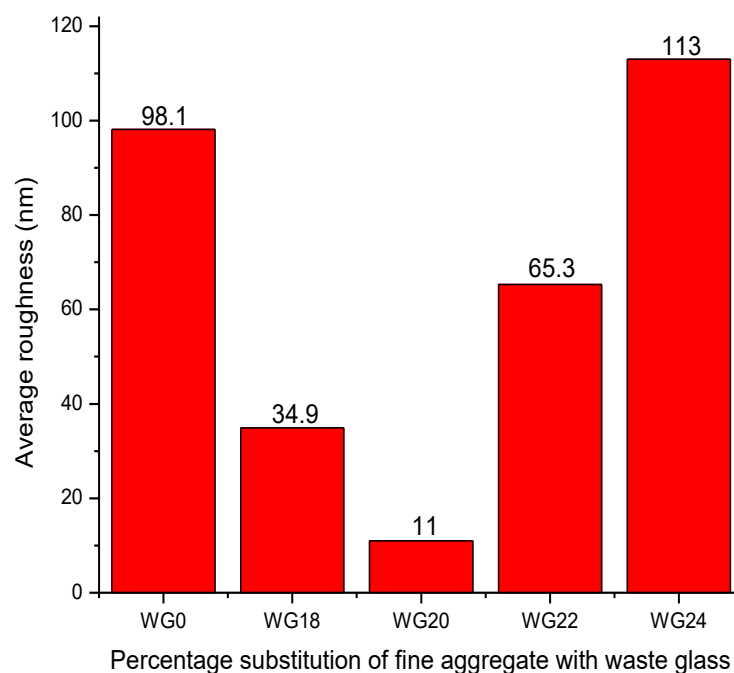


**Fig. 4.36: Average roughness of waste glass concrete samples**

After 20% substitution level increase in roughness value has been observed for WG22 and WG24 samples as shown in above mentioned figure. This rise in roughness value might be due irregular shape and smooth texture which reduces the adhesive strength between WG and cement paste. Decrease in compressive strength might be also due to generation of voids which might have been developed due to excess fine characteristic of WG.

#### **4.5 Concluding Remarks**

In this chapter, CR and WG were utilized individually as a substitute of fine aggregate in concrete mixes and the results were discussed based on its fresh and mechanical

performance. It has been noticed that with inclusion of CR and WG individually as a substitute of fine aggregate workability reduces. Mechanical performance in case of CR incorporated concrete mixes also noticed reduced rise in strength as compared with control sample. However, at 4% substitution level nearby strength was obtained as compared with control concrete and the same was noticed through microstructure. On the other hand, with inclusion of WG rise in strength parameters was noticed up to 21% substitution level and the same has been confirmed by conducting microstructural analysis.

---

**DURABILITY EFFECTS OF WATER ON CONCRETE**

---

**5.1 General**

This chapter portrays the performance of concrete samples prepared with crumb rubber (CR) and waste glass (WG) individually under the action of water. The influence of water on concrete samples was evaluated by conducting water absorption, water permeability (under constant pressure), sorptivity (capillary action), drying shrinkage and freeze and thaw. The list of experiments performed along with techniques used are mentioned in illustration (**Fig. 5.1**).

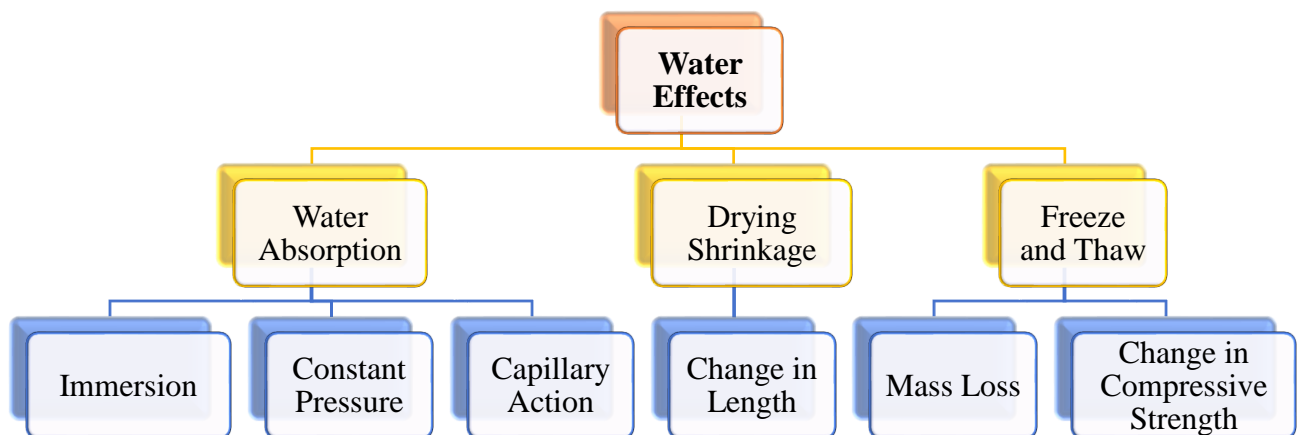


**Fig. 5.1: List of experiments**

**5.2 Experimental Procedure**

The methods employed for performing the experiments listed above are explained below. The test matrix is listed in **Table 5.1**.

**5.2.1 Water Absorption**

This section provides an idea regarding methodology used for conducting water absorption test. This test is further divided into three sub categories through which variation in water absorption can be monitored.

**Table 5.1: Test matrix for durability effects of water on concrete samples**

Type of test	Size of specimen	Specimens tested for each mix	Designation of samples			
<b>Water Absorption</b>			Mix 1	CR0	Mix 1	WG0
• <b>Immersion</b>	100×100×100 mm	3	Mix 2	CR4	Mix 2	WG18
• <b>Constant Pressure</b>	150×150×150 mm	3	Mix 3	CR4.5	Mix 3	WG19
• <b>Capillary Action</b>	100×100×100 mm	3	Mix 4	CR5	Mix 4	WG20
<b>Drying Shrinkage</b>	75×75×300 mm	3	Mix 5	CR5.5	Mix 5	WG21
<b>Freeze and thaw</b>	100×100×100 mm	3			Mix 6	WG22
					Mix 7	WG23
					Mix 8	WG24

### 5.2.1.1 Immersion

Water absorption test was performed as per ASTM C 642 (2008). Three oven dried cubes (100 mm) weight were measured ( $W_5$ ) and then placed in water bath for 48 hours. Water was allowed to drain off and then soaked with dry cloth and final weight ( $W_6$ ) was measured instantly.

$$\text{Water absorption} = \frac{W_6 - W_5}{W_5} \times 100 \quad (5.1)$$

### 5.2.1.2 Constant Pressure

Water permeability was investigated as per DIN 1048 (1991) (**Fig. 5.2**). Three oven dried concrete cube (150 mm) samples were used. A constant water pressure of 0.5 N/mm<sup>2</sup> was applied for 72 hours on concrete specimens. At the end of 72 hours the samples were split into two halves on compression testing machine and the depth of water penetration was recorded.



**Fig. 5.2: DIN permeability apparatus with specimens**

### 5.2.1.3 Capillary Action

Capillary rise of water (sorptivity) was recorded on three oven dried concrete cube (100 mm) specimens after 28 days of curing as per ASTM C1585-13 (2013). Four sides of concrete cube were sealed using wax to resist the penetration of water through side surfaces. Then the initial weight of sealed cube was recorded. After that cubes were placed in water bath such that cubes remain 2 - 5 mm dipped in water and stop watch was started. Rise in capillary action of water in concrete cube was examined for 5 min, 10 min, 20 min, 30 min, 1 hour, 2 hour, 3 hour, 4 hour, 5 hour, 2<sup>nd</sup> day, 3<sup>rd</sup> day and 4<sup>th</sup> day, 5<sup>th</sup> day, 6<sup>th</sup> day and 7<sup>th</sup> day with respect to change in weight.

### 5.2.2 Drying Shrinkage

Drying shrinkage was executed on three concrete prisms (75 mm × 75 mm × 300 mm) of each mix after 28 days of curing as per ASTM C157 (2016). After completion of curing duration, prisms were dried properly, steel bits were mounted on prisms at a spacing of  $212 \pm 1$  mm as shown in **Fig. 5.3**. The change in length was recorded using strain gauge having 0.002 mm least count to record readings at ages of 1, 7, 14, 21, 28, 56, 90, 120, 180, 210, 280 and 365 days.



**Fig. 5.3: Drying shrinkage of specimens**

### 5.2.3 Freeze and Thaw

Freeze and Thaw test was performed on three concrete cubes (100 mm) of each mix after 28 days of curing as per ASTM C666 (2003). The samples were placed in trays filled with water and exposed to the stipulated aggressive condition as shown in **Fig. 5.4**.



**Fig. 5.4: Freeze and thaw apparatus**

First the samples were frozen to  $-18^{\circ}\text{C}$  in 2.5 hours and then the temperature was raised to  $4^{\circ}\text{C}$  in 1.5 hours. This freezing and thawing comprised of one cycle. The samples were subjected to 300 such cycles. At the end of 300 cycles change in weight and compressive strength were monitored and compared with initially measured weight and compressive strength.

### **5.3 Results and Discussion of Part - A: Crumb Rubber**

In this section tests related to water durability effects such as water absorption, drying shrinkage and freeze and thaw are explained below.

#### **5.3.1 Water Absorption**

Water absorption properties of CR concrete samples were examined and explained in the following sections by immersion, constant pressure and capillary action.

##### **5.3.1.1 Immersion**

**Fig. 5.5** presents the percentage of water absorption in concrete and it has been observed that water absorption increases with increase in the percentage of CR in concrete. The water absorption of CR concrete after 28 days of curing for 5.5% replacement is 3.21%, however for control concrete substitution, water absorption is 1.91%. Different authors also reported similar behaviour in their studies (Gupta et al. (2014) and Su et al. (2015)). The increase in water absorption was due to fine nature of CR which results into generation of cracks and voids as shown in **Fig. 4.18**.



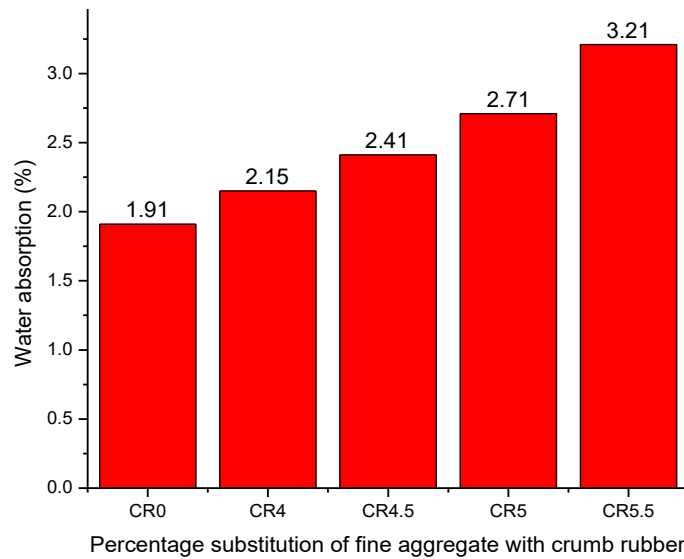


**Fig. 5.5: Water absorption of crumb rubber concrete specimens**

It has been observed from **Fig. 4.13** that percentage of voids ratio also increases with inclusion of CR in concrete mix which allows the water to penetrate inside the concrete. Turatsinze and Garros (2008) reported an increase in porosity of concrete due to increase in voids with 25% replacement of fine aggregates by waste rubber aggregates.

### 5.3.1.2 Constant Pressure

Water permeability is the prime factor which influences the durability of concrete. Using the standard testing environment, the water permeability was calculated in terms of depth of water penetration. **Fig. 5.6** presents the amount of water permeability in the CR concrete. It is clear from the same figure, when inclusion of CR increases from 4% to 5.5% water penetration increases by 32 mm and 40 mm respectively as compared with control concrete (21 mm).

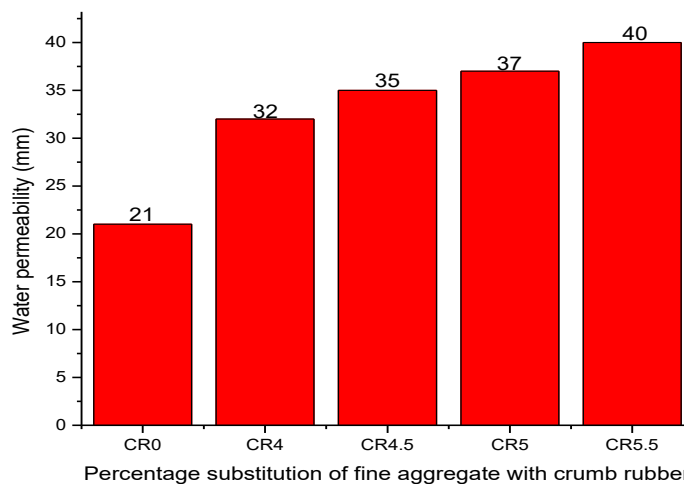


**Fig. 5.6: Water permeability of crumb rubber concrete specimens**

Water permeability of CR concrete increased due to the generation of voids between the CR and cement matrix which allows the water to penetrate to greater depths in concrete as shown in **Fig. 4.18**. Micro-cracks also play important role in water penetration as it provides a continuous path for water to penetrate inside the concrete. **Fig. 4.18 (c)** shows that micro-cracks were mainly developed, where agglomeration of CR has been observed in concrete mix which reduces the bonding between materials. Ganjian et al. (2009) illustrate similar observations for rise in water penetration in concrete mixes, due to weak interlocking and generation of voids between CR and cement paste.

### 5.3.1.3 Capillary Action

Sorptivity was performed to verify the time dependent capillary suction of water as shown in **Fig. 5.7**. It has been observed from same figure that with incorporation of 4% of CR capillary suction of water increases as compared with control mix samples. This rise in capillary suction might be due to generation of voids which allows the water to penetrate inside. However, with further inclusion of CR decrease in capillary rise was monitored. At CR5.5 substitution level capillary rise of water was lesser as compared to control sample. This might be due to lower water absorption of CR which act as a barrier and does not allow capillary rise of water and also due to presence of zinc stearate which is hydrophobic in nature.

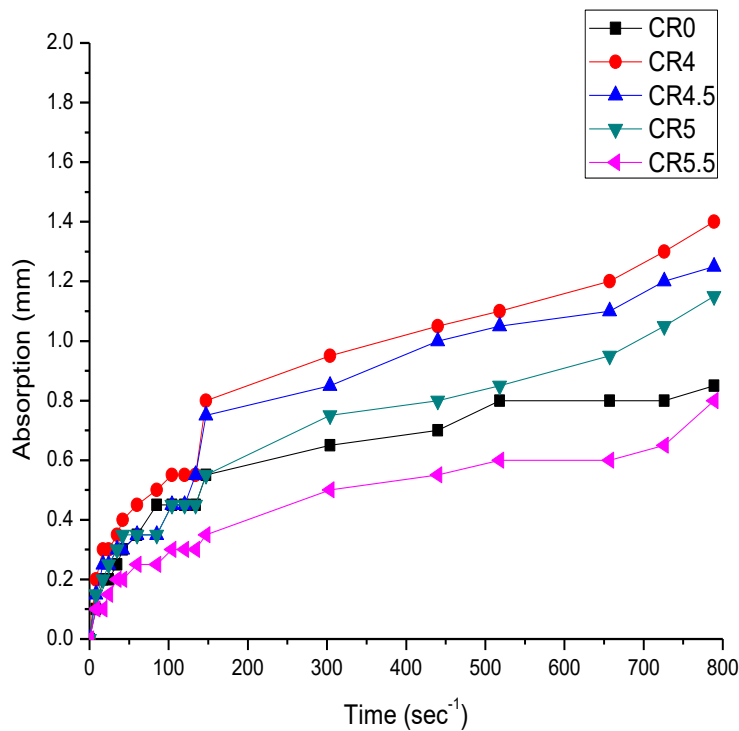


**Fig. 5.7:** Sorptivity of crumb rubber concrete specimens

### 5.3.2 Drying Shrinkage

The variations in drying shrinkage with time (365 days) was observed for CR concrete mixes as shown in **Fig. 5.8**. It has been observed from the same figure that, as the percentage of CR in concrete mixes increases, drying shrinkage also increases. This occurs due to substitution of fine aggregate with CR which is weak and very soft. The increased proportion of CR leads to higher reduction of internal restraints which results into more shrinkage.

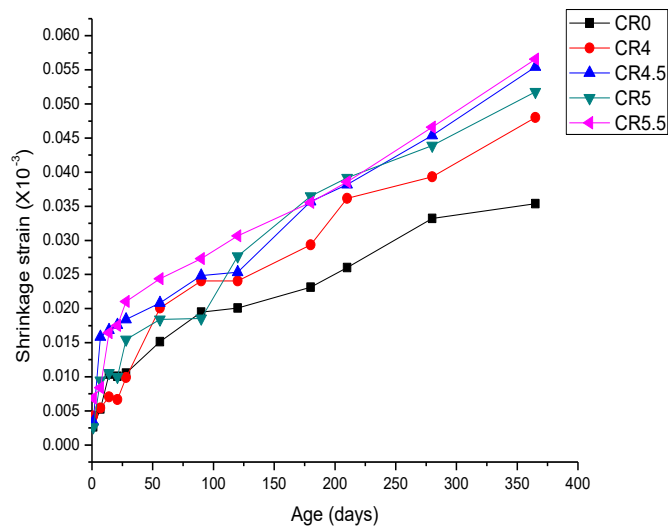


**Fig. 5.8: Drying shrinkage of crumb rubber concrete prisms**

At the age of 365 days, shrinkage strains of CR incorporated concrete mixes CR4, CR4.5, CR5 and CR5.5 were  $480 \times 10^{-6}$ ,  $554 \times 10^{-6}$ ,  $518 \times 10^{-6}$  and  $566 \times 10^{-6}$  respectively. However, for the same period of exposure shrinkage strain recorded for control mix was  $354 \times 10^{-6}$ . This upswing in shrinkage might also be due to increase in porosity due to inclusion of crumb rubber particles. Yung et al. (2013) also reported 95% rise in drying shrinkage when fine aggregate was substituted by rubber powder (0.3 mm and 0.6 mm).

### 5.3.3 Freeze and Thaw

Freeze and thaw property of CR concrete samples were examined and explained in the following sections in terms of mass loss and change in compressive strength.

#### 5.3.3.1 Mass Loss

The mass loss after exposure to freeze and thaw cycles (-18 to 4°C) for CR incorporated concrete mixes are graphically presented in **Fig. 5.9**.

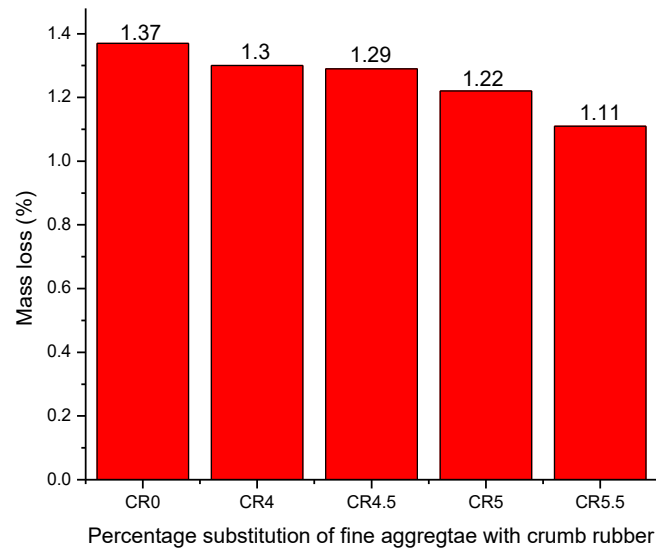
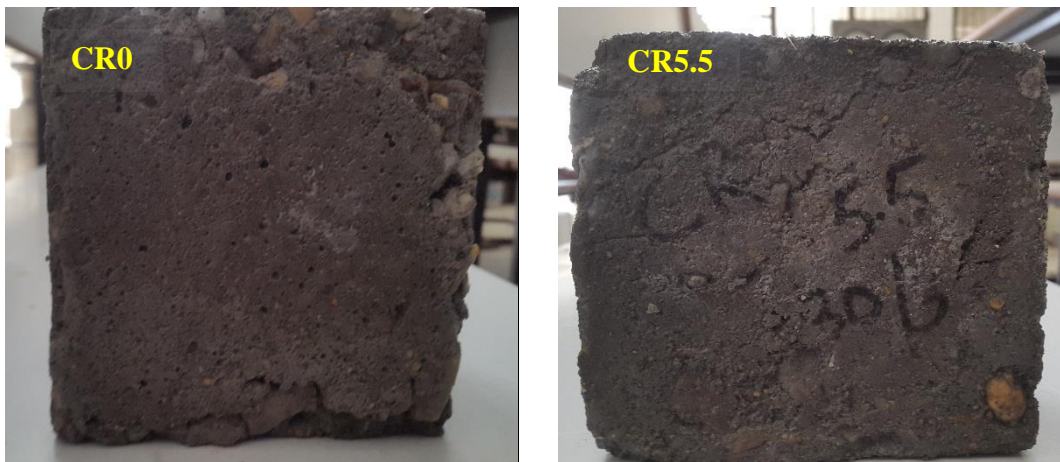


**Fig. 5.9: Mass loss of crumb rubber concrete specimens**

Appearance of samples after exposure to freeze and thaw is shown in **Fig. 5.10**. Inclusion of CR in concrete mixes is accompanied by increase in porosity (**Fig. 4.13**). These excess voids act as cushions for frozen water. Hence, this leads to reduced deterioration of mass when exposed to rapid freezing and thawing.



**(a) CR0**

**(b) CR5.5**

**Fig. 5.10: Freeze and thaw exposure for crumb rubber concrete specimens**

### 5.3.3.2 Change in Compressive Strength

The variation in compressive strength due to freezing and thawing on CR concrete mixes is shown in **Fig. 5.11**.

Performance of control and CR based concrete mixes are measured in terms of compressive strength after 300 cycles as per ASTM C666 (2003). After completion of 300

cycles maximum change in compressive strength was monitored for control mix (26.41%) whereas, CR incorporated mixes show remarkable positive effect. The reduced deterioration in CR based concrete mixes was due to elastic property of CR. This negates the effect of tensile stresses produced during freezing of water inside concrete cubes. This leads to minimum change of 11.68% even at CR5.5 substitution level.

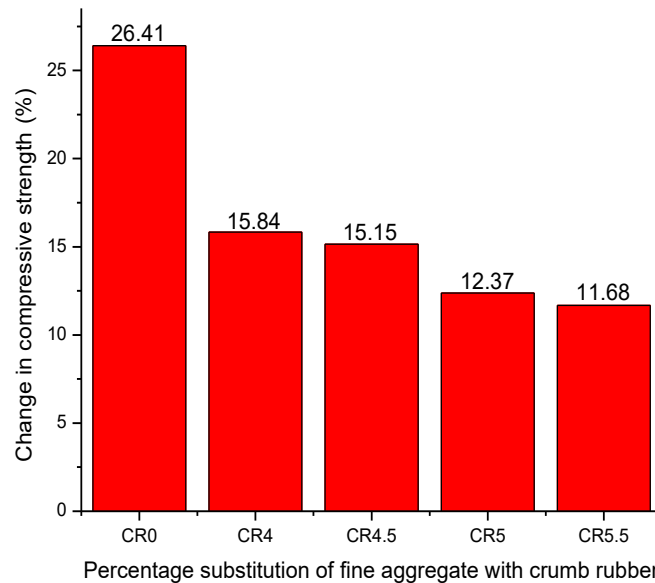


**Fig. 5.11: Change in compressive strength of crumb rubber concrete specimens**

## 5.4 Results and Discussion of Part - B: Waste Glass

### 5.4.1 Water Absorption

Water absorption properties of WG concrete samples were observed and described in the following sections by immersion, constant pressure and capillary action.

#### 5.4.1.1 Immersion

**Fig. 5.12** presents that water absorption increases with increase in the percentage of WG in concrete mixes. The water absorption of WG concrete at 28 days of curing for WG24 replacement is 2.93%, however for WG0 water absorption is 1.91%. The increase in water absorption might be due to highly angular shape and smooth texture of WG which results into generation of voids and cracks. This leads to reduction in adhesive strength between WG and cement paste. The increased percentage of voids and cracks gives passage for water to penetrate inside the concrete. It is clear from **Fig. 4.27** that with increase in substitution level, percentage of voids also increases. Limbachiya (2009)

reported an increase in water absorption as the percentage of WG in concrete increases due to generation of voids.

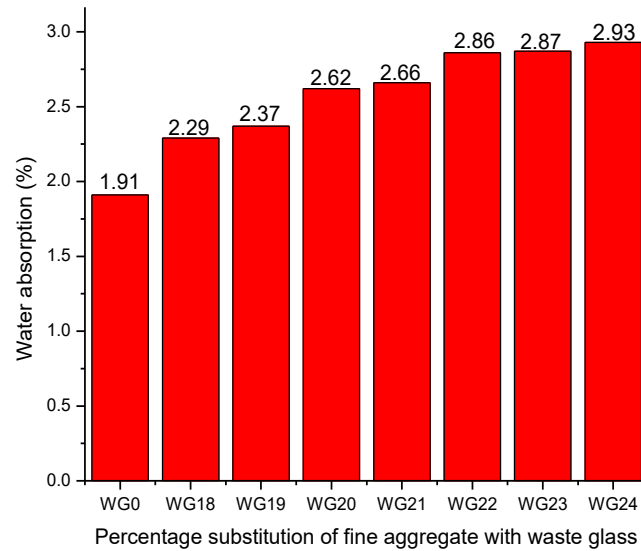


**Fig. 5.12: Water absorption of waste glass concrete specimens**

#### 5.4.1.2 Constant Pressure

Water permeability has been determined in terms of depth of water penetration.

**Fig. 5.13** shows the extent of water permeability in the WG concrete.

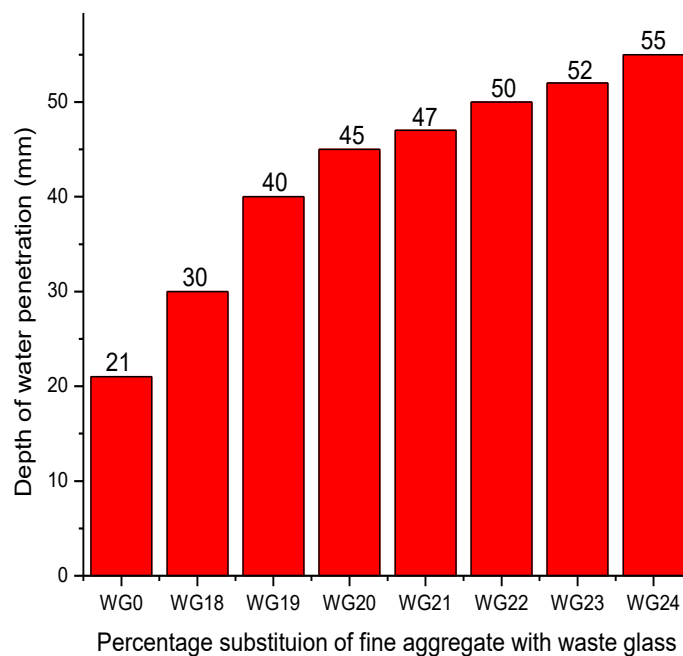


**Fig. 5.13: Water permeability of waste glass concrete specimens**

It has been observed from the same figure that with inclusion of WG20 and WG24 water penetration increases up to 45 mm and 55 mm respectively as compared with control

mix samples (21 mm). Water permeability of WG concrete mix increased due to the generation of voids between the WG and cement paste at the interface which allows the water to penetrate inside the concrete to greater depth. The results agree with the ones reported by Penacho et al. (2014) where substitution of fine aggregate by WG shows similar behaviour for mortar mixes with that of control mix.

### 5.4.1.3 Capillary Action

Sorptivity of concrete specimens with and without WG was carried out on oven dried concrete specimens. Results have been shown in **Fig. 5.14**. It has been observed from same figure that rate of capillary suction of water is time dependent. An increase in quantity of capillary rise of water has been recorded for concrete mixes with WG as compared with control concrete. This increase might be due to porous nature of material to absorb water through capillarity (Tan and Du (2013)). Also, it has been observed from **Fig. 4.27** that as the percentage of WG in concrete increases, percentage of voids also increases. This increase in voids might be due to highly angular shape and smooth texture of WG. Penacho et al. (2014) reported rise in water absorption through capillary action as the percentage of WG increases from 0 – 100% for mortar mixes.

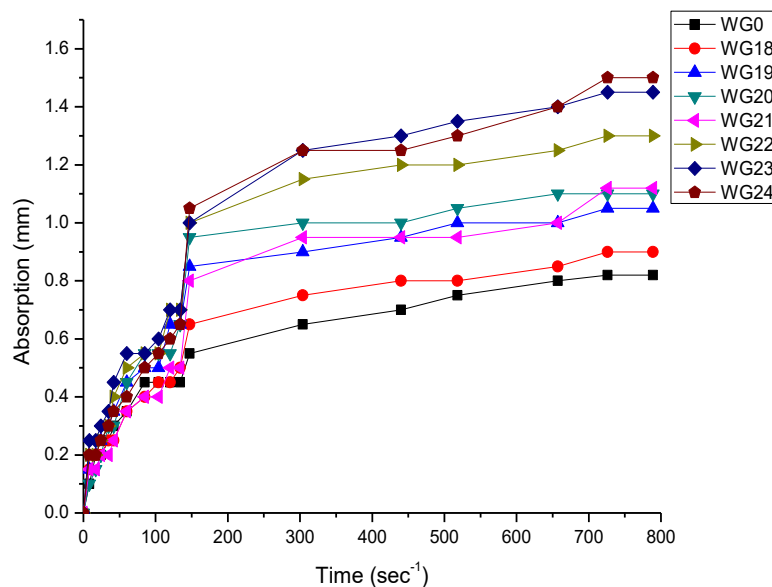


**Fig. 5.14:** Sorptivity of waste glass concrete specimens

### 5.4.2 Drying Shrinkage

The changes in drying shrinkage of concrete prisms for a period of 365 days with and without WG was monitored and is reported graphically in **Fig. 5.15**.

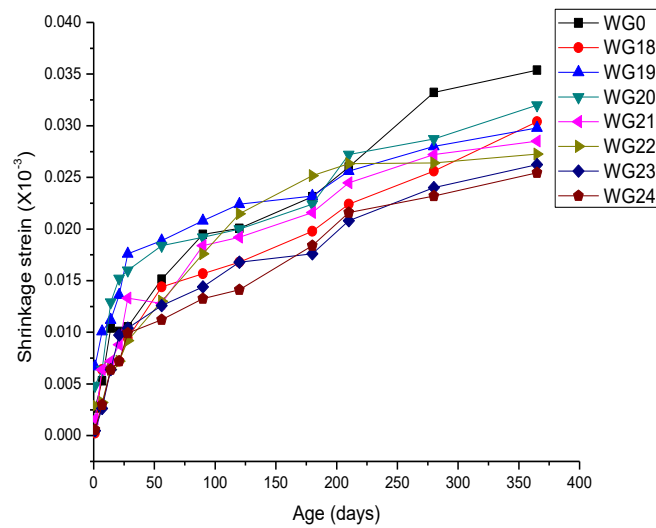


**Fig. 5.15: Drying shrinkage of waste glass concrete specimens**

It has been observed that initially drying shrinkage for WG incorporated mixes was higher as compared to control mix. However, change in trend has been noticed with increased period of exposure. This initial rise in shrinkage might be due to higher fineness of WG. At the age of 365 days, shrinkage strains of WG concrete mixes WG18, WG19, WG20, WG21, WG22, WG23 and WG24 were  $304 \times 10^{-6}$ ,  $278 \times 10^{-6}$ ,  $320 \times 10^{-6}$ ,  $285 \times 10^{-6}$ ,  $273 \times 10^{-6}$ ,  $262 \times 10^{-6}$  and  $254 \times 10^{-6}$  respectively. However, for the same period of exposure shrinkage strain recorded for control mix was  $354 \times 10^{-6}$ .

On later stages of exposure, the decline in drying shrinkage with introduction of WG in concrete mixes is due its higher stiffness. The decrease in drying shrinkage for WG concrete mixes is a positive outcome of using this discarded material as usage of this material reduces the propagation of cracks in concrete structures (Rashad (2014)).

### 5.4.3 Freeze and Thaw

Freeze and thaw property of WG concrete samples were examined and explained in the following sections in terms of mass loss and change in compressive strength.

#### 5.4.3.1 Mass Loss

The mass loss for waste glass incorporated concrete mixes under action of freezing and thawing ( $-18$  to  $4^{\circ}\text{C}$ ) presented in **Fig. 5.16**. After exposure to 300 cycles control and WG concrete mixes shows very less deterioration as shown in **Fig. 5.17**.



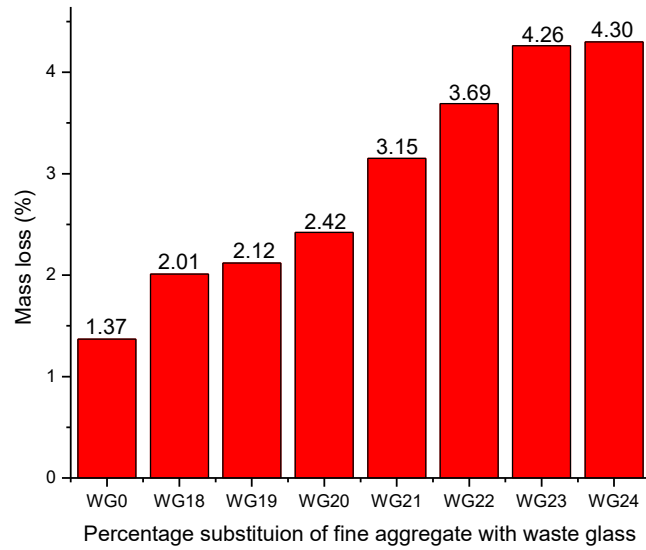


**Fig. 5.16: Mass loss of waste glass concrete specimens**

Slight increase in mass loss has been observed for WG concrete samples after exposure to extreme condition. Increase in mass loss was related with increased water absorption of WG incorporated concrete cubes (Fig. 5.12). This increased water absorption freezes the water and increases tensile stresses. The mass loss was hardly significant as it was only related with scaling out of surface layers. This scaling effect generally occurs when saturated aggregates expands near the surfaces of sample leads to deterioration of nearby cement matrix (Richardson et al. (2012)). This also occurs due to freezing of saturated water in aggregate which boosts pressure owing to failure of nearby cement matrix.

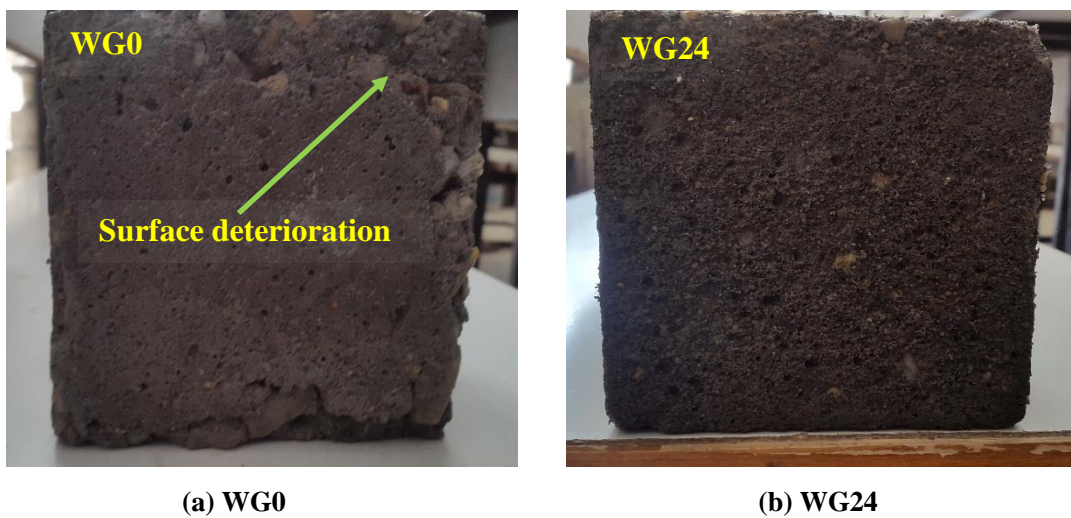


**Fig. 5.17: Freeze and thaw exposure for waste glass concrete specimens**

### 5.4.3.2 Change in Compressive Strength

The changes due to freezing and thawing on WG concrete mixes is reported in **Fig.5.18** after exposure to 300 cycles as per ASTM C666 (2003).

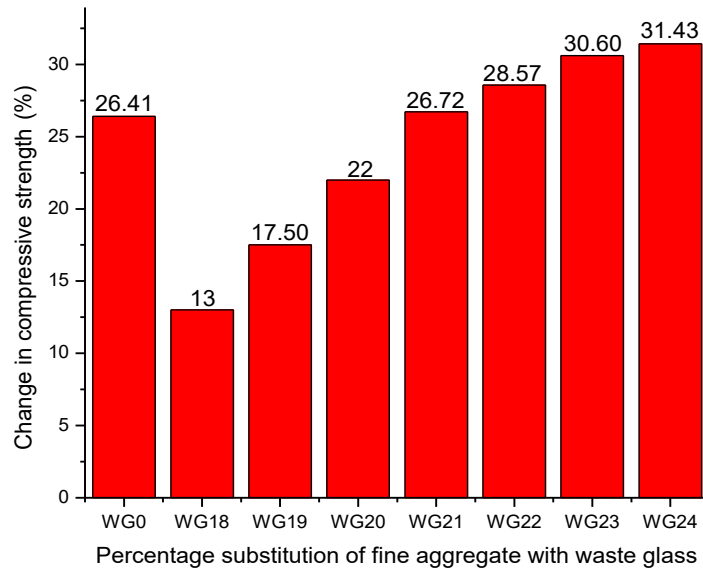


**Fig. 5.18: Change in compressive strength of waste glass concrete specimens**

Results monitored for the concrete mixes WG18 – WG20 substitution level show lower reduction in compressive strength as compared to WG0 mix. In particular for the substitution level of 20%, 22% reduction in compressive strength was noticed as compared to 26.41% for WG0 mix. With inclusion of WG21 in concrete mix, the reduction remains almost constant as compared with WG0 mix. From **Fig. 4.26** it has been observed that apparent density increases up to 21% which reduces susceptibility to damage. However, with further inclusion of WG in concrete mixes shows more reduction in compressive strength as compared to WG0 mix samples. This reduction in WG concrete mixes was due to increased water absorption at initial stage.

### 5.5 Concluding Remarks

In this section, durability effects on concrete cubes with CR and WG individually were noticed under the effect of portable water. Increase in water absorption was noticed for CR incorporated concrete samples as well as for WG concrete samples due to generation of voids. The variations in drying shrinkage with time (365 days) was observed for CR and WG concrete mixes. The results showed that as the percentage of CR in concrete mixes increases, drying shrinkage also increases. This occurs due to substitution of fine aggregate with CR which is weak and very soft when compared to sand. In case of WG

concrete samples initially drying shrinkage was higher but with increase in curing age drying shrinkage reduces due to higher stiffness of WG. When exposed to freezing and thawing cycles CR incorporated samples show positive effect due to elastic nature of rubber however, WG concrete samples show opposing effect.

**LONG TERM DURABILITY PROPERTIES  
AND RESISTANCE TO FIRE**

**6.1 General**

This chapter presents the change in performance of concrete mixes in resisting chemical attack (chloride and acid) and fire exposure when crumb rubber and waste glass are used as fine aggregate. Resistance to corrosion is determined using different tests (Fig. 6.1) such as chloride penetration, carbonation and half-cell potential. The functioning of concrete specimens (with crumb rubber and waste glass) under aggressive conditions (acid attack and fire exposure) are evaluated and compared with control samples in order to justify the usage of these waste materials in concrete. In addition to this, microstructural properties of prepared composites were also investigated through X-ray Diffraction (XRD), Field Emission Scanning Electron Microscopy (FESEM), Thermal Gravimetric Analysis / Differential Thermal Analysis (TGA/DTA) and Fourier Transform Infrared Spectroscopy (FTIR).

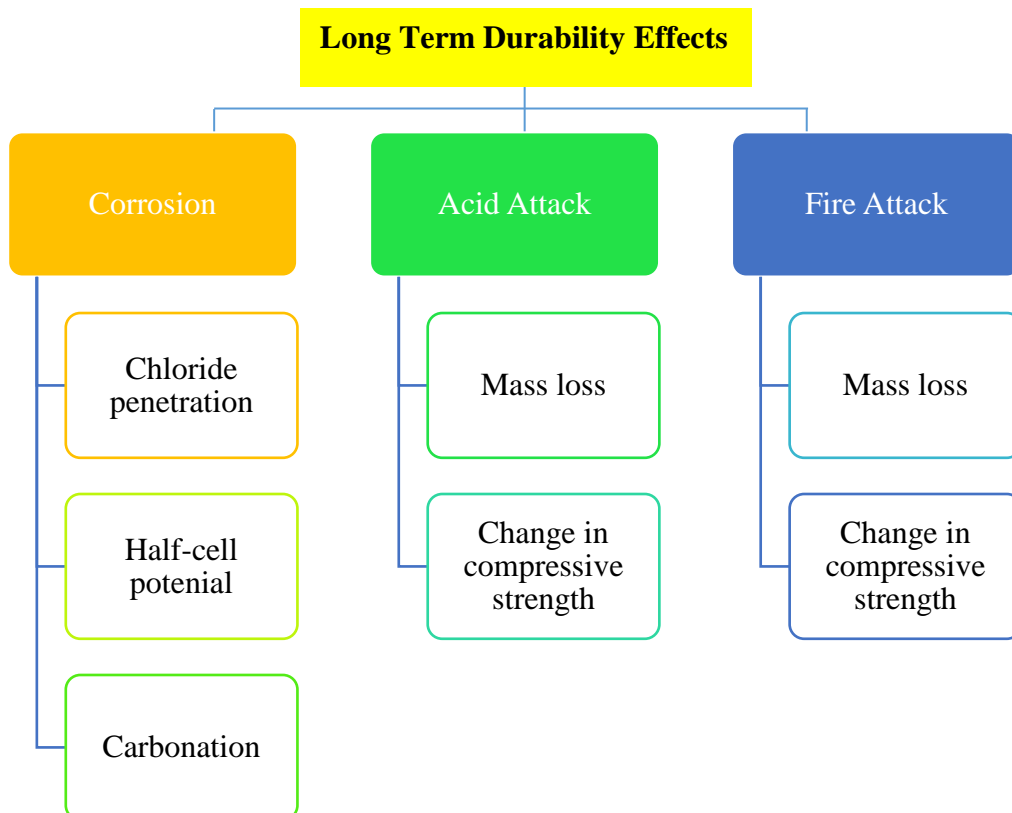


**Fig. 6.1: List of experiments**

## 6.2 Experimental Procedure

The methods employed for performing the experiments listed above are explained below. The test matrix is listed in **Table 6.1**.

**Table 6.1: Test matrix for long term durability effects**

Type of test	Size of specimen	No of specimens tested for each mix	Designation of samples			
<b>Chloride Penetration</b>	100×100×100mm	3	Mix 1	CR0	Mix 1	WG0
<b>Half-cell Potential</b>	115×275×225 mm	3	Mix 2	CR4	Mix 2	WG18
<b>Carbonation</b>	50×50×100 mm	3	Mix 3	CR4.5	Mix 3	WG19
<b>Acid Attack</b>	100×100×100 mm	3	Mix 4	CR5	Mix 4	WG20
<b>Fire Attack</b>	100×100×100 mm	3	Mix 5	CR5.5	Mix 5	WG21
					Mix 6	WG22
					Mix 7	WG23
					Mix 8	WG24

### 6.2.1 Chloride Penetration

To measure the depth of presence of free chloride ions, silver nitrate ( $\text{AgNO}_3$ ) solution spray technique was exercised. After water curing for 28 days, concrete cubes (100 mm) were exposed to 3% sodium chloride solution ( $\text{NaCl}$ ) for a period of 180 days. In order to maintain uniform concentration, chloride solution was recharged after every three weeks. The samples were taken out at an interval of 7, 28, 90 and 180 days from chloride immersion tanks. The cube samples were split into halves and freshly prepared  $\text{AgNO}_3$  (0.1 N<sub>o</sub>) solution was sprayed (Otsuki et al. (1993)). On reaction of  $\text{AgNO}_3$  with free chloride ions present in concrete, results into formation of silver chloride ( $\text{AgCl}$ ) which is white in colour. This change in colour indicates the presence of higher concentration of chloride ions which was more than 0.15% to the weight of cement (Güneyisi and Mermerdaş (2007)). The area where free chloride ions are not present in sufficient concentrations, silver nitrate reacts with hydroxides to form silver oxide ( $\text{AgO}$ ) which is brown in colour.

### 6.2.2 Half-cell Current

Corrosion was monitored on concrete samples (115 mm × 275 mm × 225 mm) cast with three steel bars as shown in **Fig. 6.2**. Prior to positioning of steel bars, surface of steel bars were cleaned properly. The upper single steel bar was positioned at 25 mm from upper end, whereas two other steel bars were positioned at a distance of 125 mm

from upper end spaced at equal distance from end edges. The steel bars of length 380 mm were placed in such a way that projection at both ends of concrete sample remains equal at 50 mm. Neoprene tubes were utilized in order to protect steel bars from external environment which extended into the specimen by 40 mm. Hence, the steel bars were exposed by a length of 200 mm inside the concrete specimens. Ponding was done with Sodium chloride solution (3% concentration) on the top surface of the sample (after 28 days curing and drying for 14 days). To reduce the evaporation of NaCl solution these ponds were sealed using polythene covers. The electrochemical macrocell was formed in concrete due to presence of moisture, penetrated chloride ions and oxygen. Therefore, top bar act as anode and rest two bottom bars act as cathode and current arisen between them.



**Fig. 6.2: Corrosion specimens**

The connections between top and bottom bars were detached and half-cell potential was recorded using copper sulphate electrode as shown in **Fig. 6.3**. The recorded half-cell potential was employed to forecast the chances of corrosion as mentioned in ASTM C876 (2015).



**Fig. 6.3: Half-cell potential**

### 6.2.3 Carbonation

The intensity of carbonation in concrete was recorded as per RILEM CPC 18 (1988). Cubes of size 100 mm were cured for 28 days after which cubes are cut into four parts of 50 mm width and 100 mm length by using concrete cutter. These formed prisms were oven dried for two weeks at 60°C. After drying, these prisms were coated with epoxy paint on their longitudinal faces. After the paint had sufficiently dried, the prisms were placed in a carbonation chamber as shown in **Fig. 6.4**.



**Fig. 6.4: Carbonation chamber**

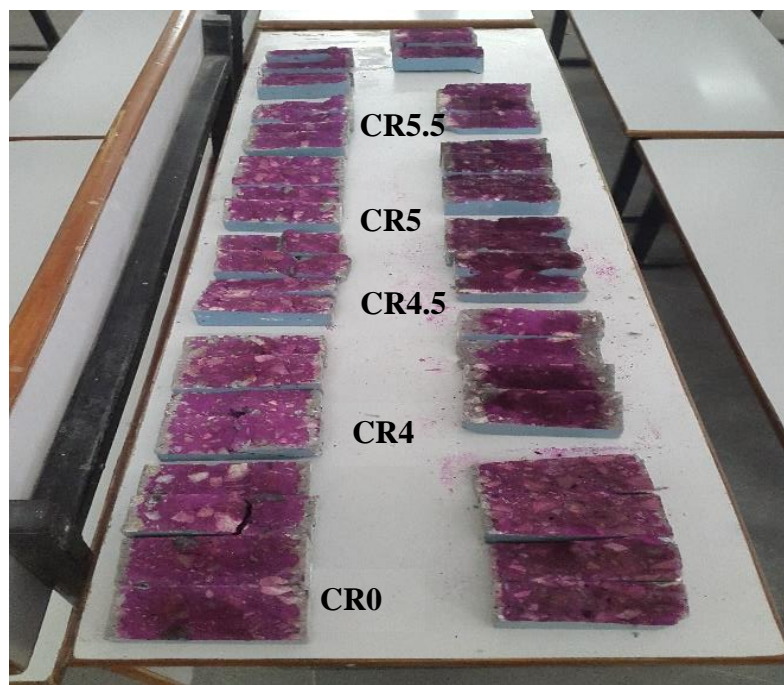


**Fig. 6.5: Carbonated specimens**

The temperature and humidity in this chamber were maintained at  $27 \pm 20^\circ\text{C}$  and 50 - 55%, with a  $\text{CO}_2$  concentration of  $5 \pm 0.2\%$ . Prisms were taken out at stages of 7, 14,

28, 56 and 90 days and split into halves. Phenolphthalein pH indicator (1% phenolphthalein in 70% ethyl alcohol) was sprayed on the split prisms. Carbonated area ( $\text{pH} < 9.2$ ) was identified by the region which remained colourless, whereas the portion of the prism where carbonation did not occur sufficiently turned to pink as shown in **Fig. 6.5**.

#### 6.2.4 Acid Attack

Acid attack test was conducted for 7, 28 and 90 days as per ASTM C267 (1997). As per its recommendation the test method is intended to evaluate the chemical resistance of hydraulic cement concrete under predicted service condition for which 3% sulphuric acid was used to estimate acidic resistance.



**Fig. 6.6: Specimens exposed to acidic environment**

The oven dried concrete cubes (100 mm) were weighed first and then completely submerged in sulphuric acid solution. The solution was changed after every three weeks. Three cubes of each mix were tested after each exposure period. The exposed specimens are shown in **Fig. 6.6**. Change in weight was compared with the initially measured weight. Compressive strength of acid cured specimens has been conducted at respective ages. The load of  $140 \text{ kg/cm}^2/\text{min}$  was applied gradually without any shock as per IS 516 (1959). The achieved results were then compared with the compressive strength of 28 days water cured concrete cubes.



### 6.2.5 Fire Attack

Fire attack test was performed on 28 days water cured specimens as per ISO 834 (1999). The test was planned to measure the effect of standard fire when exposed to elevated temperatures 200 to 800°C at an interval of 200°C. Variation in weight was compared with the initially measured weight. The cube specimens of size 100 mm were heated in gas operated furnace with size of chamber 520 × 520 × 1050 mm as shown in **Fig. 6.7**. During thermal testing, air temperature within the oven was detected with the use of different type-K thermocouples. Compressive strength of fire attacked specimens has been conducted. The load of 140 kg/cm<sup>2</sup>/min was applied gradually without any shock as per IS 516 (1959). The achieved results were then compared with the compressive strength of 28 days water cured concrete cubes and dried at room temperature.

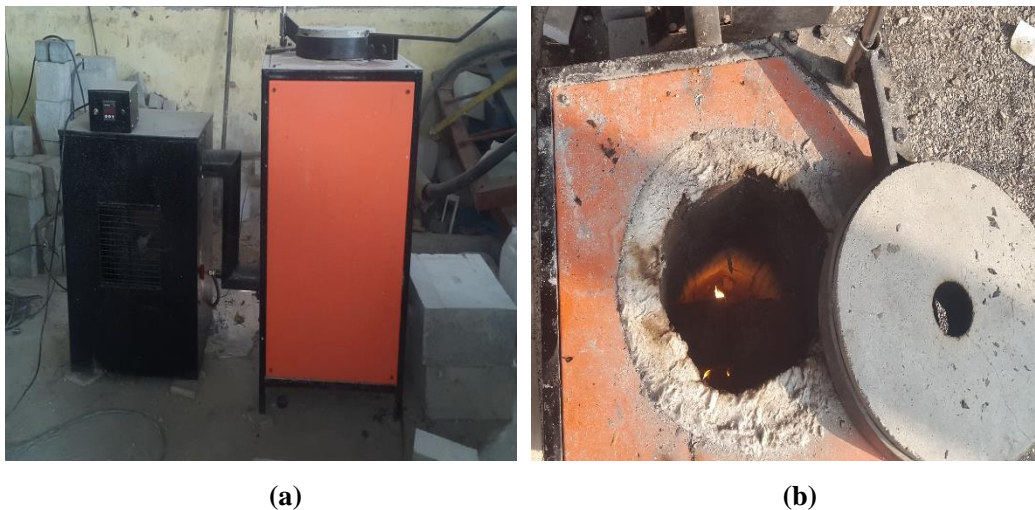


**Fig. 6.7: Fire test apparatus**

### 6.3 Results and Discussion of Part - A: Crumb Rubber

In this section, change in performance of concrete mixes in resisting chemical attack (chloride and acid) and fire exposure are discussed.

#### 6.3.1 Corrosion

In the following section performance of CR concrete samples under influence of chloride attack were explained.

##### 6.3.1.1 Chloride Penetration

The depth of chloride penetration was measured and graphically presented in **Fig. 6.8** after spraying AgNO<sub>3</sub> solution on concrete samples exposed to simulated saline environment. The extent of chloride penetration for CR incorporated concrete presented

in Fig. 6.9. After exposure for 7 days no change has been observed for CR induced concrete mixes whereas, control mix shows penetration of 2 mm. With rise in exposure period (28, 90 and 180 days) decreasing trend for chloride ion penetration has been observed up to CR4.5 mix as compared to control mix. Resistance to chloride penetration was higher up to 4.5% substitution level because crumb rubber particles do not allow the passage of chloride ions.

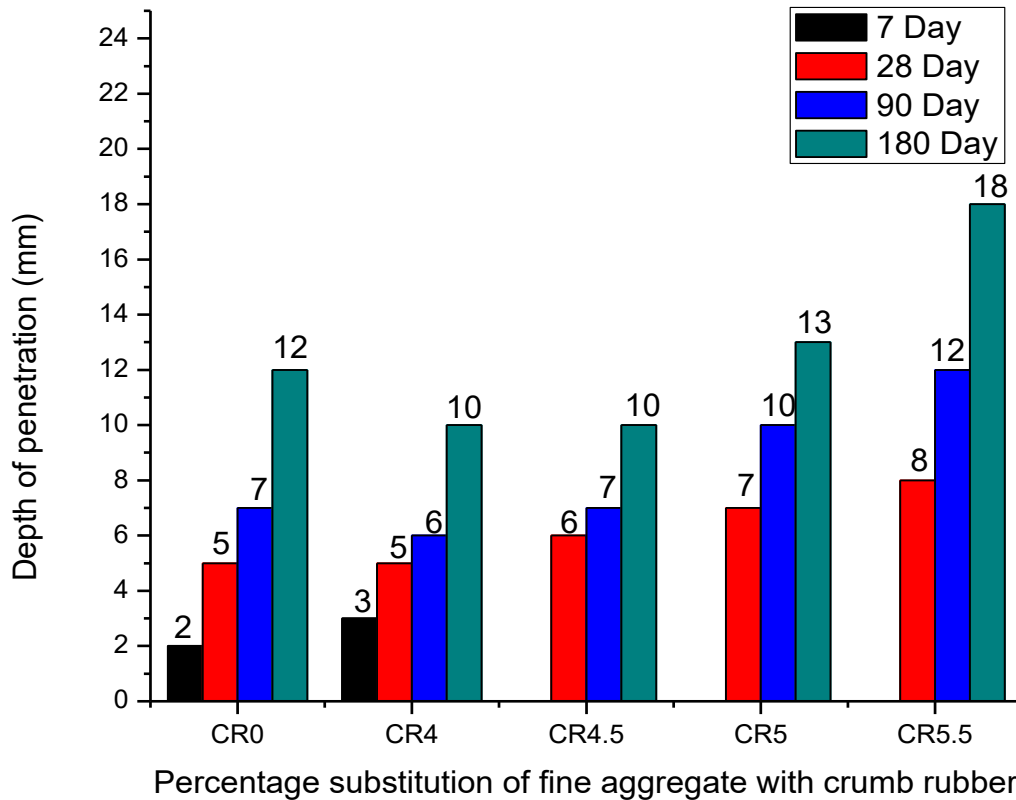


Fig. 6.8: Chloride penetration of crumb rubber concrete specimens

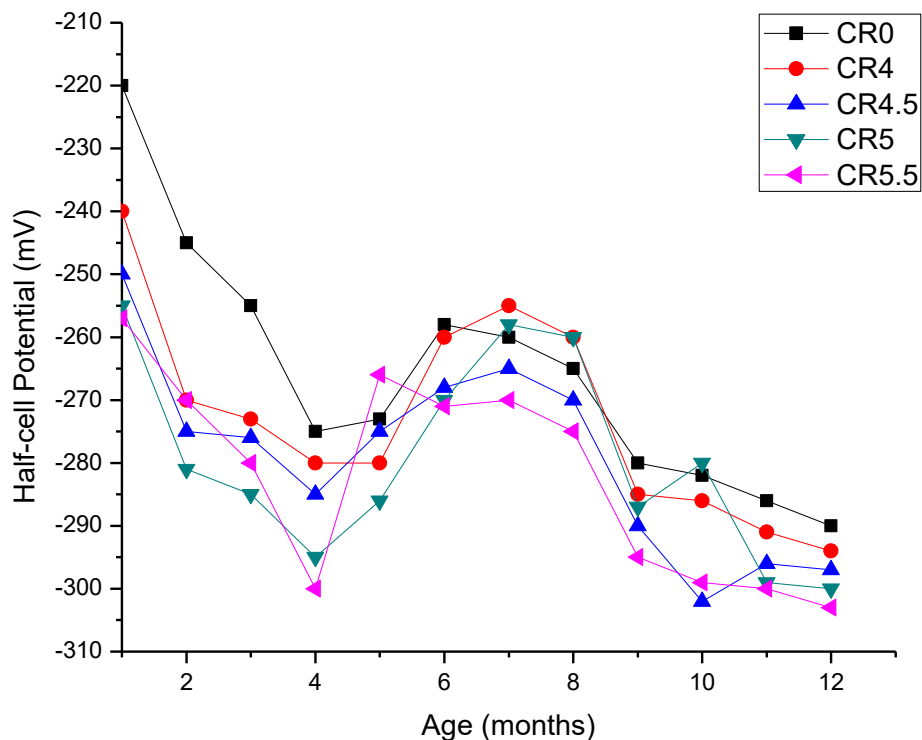


Fig. 6.9: Chloride penetration in crumb rubber concrete specimens

The maximum variation has been examined after 180 days of exposure, where chloride penetration is nearly half for CR4.5 mix (10 mm) as compared with CR5.5 mix (18 mm). This rise in chloride penetration might be due to increase in size and connectivity between the voids which upsurges the chloride penetration for CR5.5 mix as compared to CR4.5 mix. Oikonomou and Mavridou (2009) also reported similar rise in chloride penetration after 5% substitution of fine aggregates with crumb rubber (0.07 – 1 mm).

### 6.3.1.2 Half-cell Potential

The change in half-cell potential with time (up to 12 months) for CR concrete and control concrete mixes has been graphically presented in **Fig. 6.10**. From this figure it can be seen that inclusion of CR imparts higher half-cell potential values right from the initial days of exposure itself. Drastic increase in half-cell potential value is noticed even for the minimal substitution of 4% itself. With increase in substitution rise in potential is recorded. As the duration of exposure progresses, potential values increase to the same extent for all the mixes. CR0 mix reaches the potential of around -270 mV in 4<sup>th</sup> month whereas mix CR4 could attain this at half the exposure period itself. Maximum potential recorded was around -300 mV at a duration of 4 months for the mix CR5.5. As per ASTM C876 (2015) the half-cell values between -200 to -350 mV indicate that it is difficult to judge to what extent corrosion has taken place.



**Fig. 6.10: Half-cell measurements for crumb rubber concrete specimens**

When the exposure period is further stretched potential values reduce for all the mixes in a similar fashion. This change in path might be owing to lack of oxygen due to saturated pores with water which opposes the cathodic reaction. This hinders the movement of electrons as a consequence decreases the corrosion current and potential (Raupach (1996)). This can also be because, the products of corrosion hinder flow of current and stop further corrosion from happening (Vedalakshmi et al. (2008)).

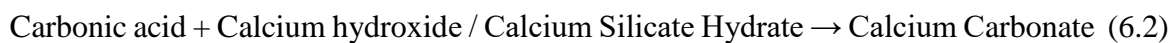
### 6.3.1.3 Carbonation

The effect of carbonation on CR concrete and control mixes is presented in **Fig. 6.11**. A steady rise in carbonation was monitored until the end of test period for all concrete prisms. However, the extent of carbonation is slightly higher for mixes with CR. At the end of 90 days, the depth of penetration for CR0 and CR5.5 concrete mix prisms were recorded as 7.5 mm and 8.6 mm respectively.

When all mixes are compared, rise in carbonation depth might be related to the higher fineness of CR than the fine aggregate it replaces. Thus, increases the porosity of concrete mixes as shown in **Fig. 4.13**. This allows passage for carbon-di-oxide to penetrate inside the prisms to greater depths which reacts with water to form carbonic acid as shown below.



The formed acid further reacts with hydration products (calcium hydroxide and calcium silicate hydrate) and results into production of calcium carbonate as shown by the following chemical reaction.



This consumption of Portlandite is accompanied by fall in pH (Wang et al. (2017)) and hence the colour change is noticed as shown in **Fig. 6.12**.

It can also be pointed out that the maximum carbonation has taken place between 14 and 28 days of exposure for all mixes, however this effect lessens with further increase in exposure period. This is because, on formation of calcium carbonate, the porosity of concrete mixes reduces which prevents further penetration of carbon dioxide.

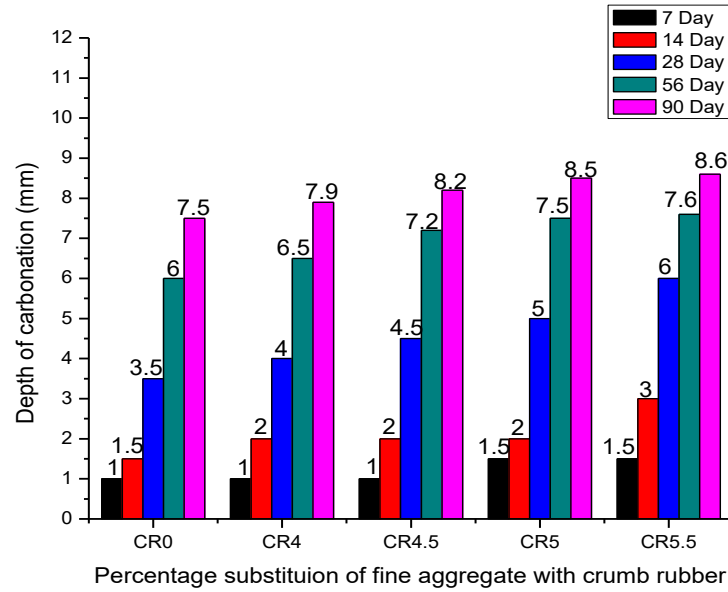


**Fig. 6.11: Depth of carbonation for crumb rubber concrete prisms**

Bravo and De Brito (2012) also noticed rise in carbonation depth when fine aggregate was replaced up to 15% with waste rubber (passing 4 mm). At 15% substitution level carbonation depth increases by 56%. This hike in carbonation depth was due to increased pores between waste rubber and cement matrix.



**Fig. 6.12: Carbonation depth of crumb rubber concrete prisms after exposure to 28 days**

### 6.3.2 Acid Attack

Resistance to acid attack is observed in terms of weight loss and change in compressive strength which are explained in the following section.

### 6.3.2.1 Weight Loss

The change in weight of concrete specimens with and without CR reported in **Fig. 6.13**. It has been observed from same figure that for all mixes the reaction is not catalysed up to 28 days. Acidic exposure after 28 days poisoned the weight of CR0 samples, however for mixes with CR changes remain subdued. Maximum weight loss of 9.06% has been monitored for CR0 samples and 2.32% has been recorded for concrete specimens with CR5.5 after 90 days of acidic exposure. Reduced change in performance has been observed with incorporation of CR in concrete. The segregation of CR was not noticed throughout the process. Reaction between sulphuric acid and calcium hydroxide which is present in concrete results into formation of gypsum (Ismail et al. (1993)).

It has been observed by Monteny et al. (2000) and Monteny et al. (2001) that formation of gypsum plays minor role in deterioration of concrete. However, on further reaction between gypsum and calcium aluminate hydrate leads to the formation of ettringite causes excess deterioration (Lee et al. (2008)). This occurs due to larger volume of ettringite, generating higher inner pressure inside concrete leads to formation of cracks. These cracks make the upper layer of concrete weak which results into spalling. However in modified concrete, CR act as bridge between constituents which prevents the concrete from generation of cracks and surface deterioration (Thomas et al. (2016)).

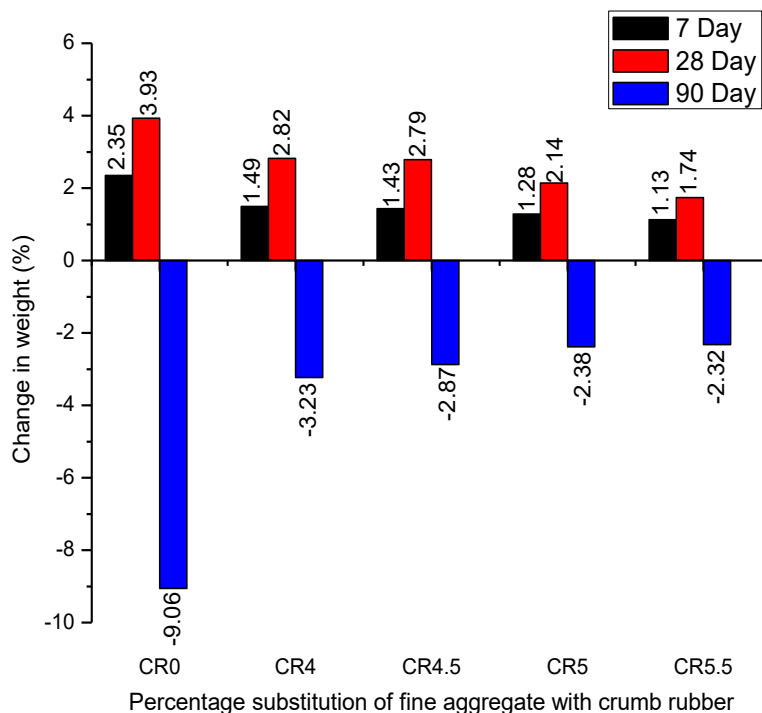


**Fig. 6.13: Change in weight for crumb rubber concrete specimens**

### 6.3.2.2 Change in Compressive Strength

The variation of compressive strength of acid attacked specimens are graphically presented in **Fig. 6.14**. It has been observed from above mentioned figure that increase in compressive strength take place up to seven days of acidic exposure. This might be assumed that ettringite's growth is not harmful and capable of imparting extra filler effect initially (Khyaliya et al. (2017)).

After three weeks when solution was recharged, gradual loss of compressive strength was noted. A maximum compressive strength loss of 53.84 % has been observed for CR0 samples after 90 days of exposure to acidic medium respectively. This reduction in compressive strength might be due to depolymerisation of hydration products (CASH (calcium aluminate silicate hydrate) & CSH (calcium silicate hydrate)). It has also been observed from **Fig. 6.15** that concrete surfaces gets pulpified which results into development of cracks and erosion of surface layers.

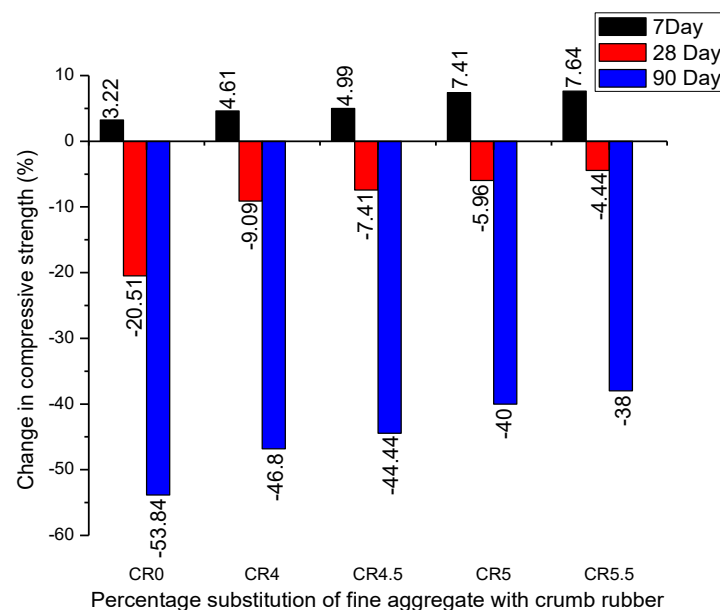


**Fig. 6.14: Change in compressive strength for crumb rubber concrete specimens**

However, with substitution of fine aggregates with CR, the percentage loss of compressive resistance decreases, as replacement level increases. It has been observed from **Fig. 6.14** that fall of 38% has been monitored at 5.5% substitution level which is lower than CR0 samples after exposure in acidic environment for 90 days respectively. This might be due to binding action of CR with concrete constituents (Thomas et al. (2016)). This binding phenomena inhibits that cracking and material separation of concrete.



**Fig. 6.15: Acid attacked crumb rubber concrete samples**

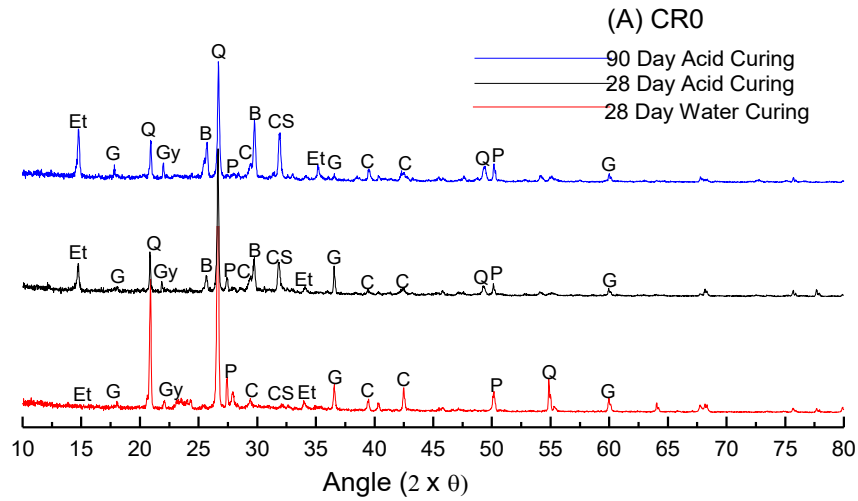
### 6.3.2.3 XRD Analysis

XRD analysis after 28 days of hydration was conducted to identify the mineralogical composition of concrete mixes with and without CR under acidic exposure. In **Fig. 6.16**, four important phases are observed; Quartz ( $\text{SiO}_2$ ) (PDF 01-085-0798), Ettringite (PDF 00-041-1451), Portlandite ( $\text{Ca}(\text{OH})_2$ ) (PDF 01-070-7009) and Gypsum (PDF 00-021-0816).

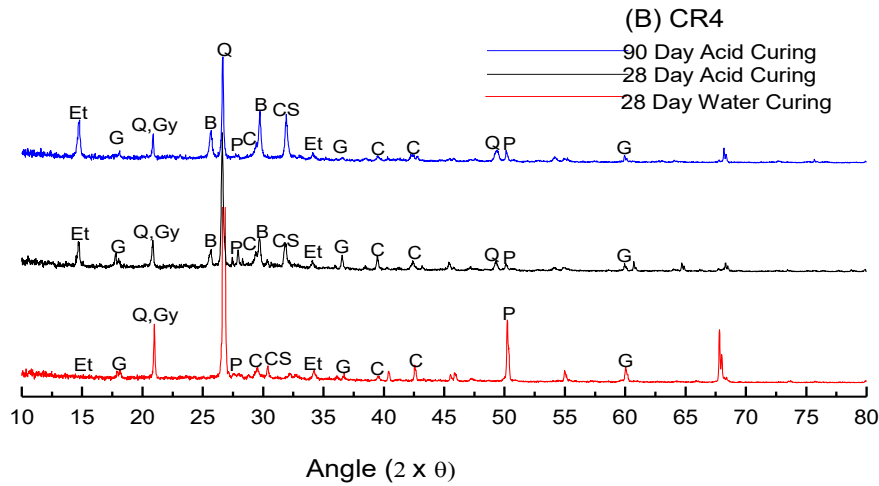
The generation of mineral phases were noticed in concrete specimens by conducting XRD analysis after 28 and 90 days of exposure in acidic medium for CR0, CR4 and CR5.5 samples. This analysis shows the comparison between acidic medium exposed samples spectra to that of 28 days water cured samples. After 28 and 90 days exposure of concrete specimens in acidic medium the relative peak intensities of Portlandite (at  $2\theta = 28.23^\circ, 50.53^\circ$ ) decreases.

This decrease in phases of Portlandite was observed for all mixes after acid curing as compared to reference samples. This change might also be due to reaction between Portlandite and sulphuric acid which results into formation of gypsum (at  $2\theta = 22^\circ$ ). Gypsum was also present in the form of Bassanite. With inclusion of CR lesser formation of gypsum was observed as compared to CR0 mix. This might be due to quick reaction of CR with acid, which decreases change in weight (**Fig. 6.13**) and compressive strength (**Fig. 6.14**). With increase in exposure period in acidic environment, formation of ettringite has been observed for all mixes around  $15^\circ$ . This growth in ettringite is due to reaction between formed gypsum and calcium aluminium hydrate (Samson and Marchand (2007)). The formed ettringite is more pronounced in CR0 mix as compared to CR induced mixes as shown in **Fig. 6.16**.

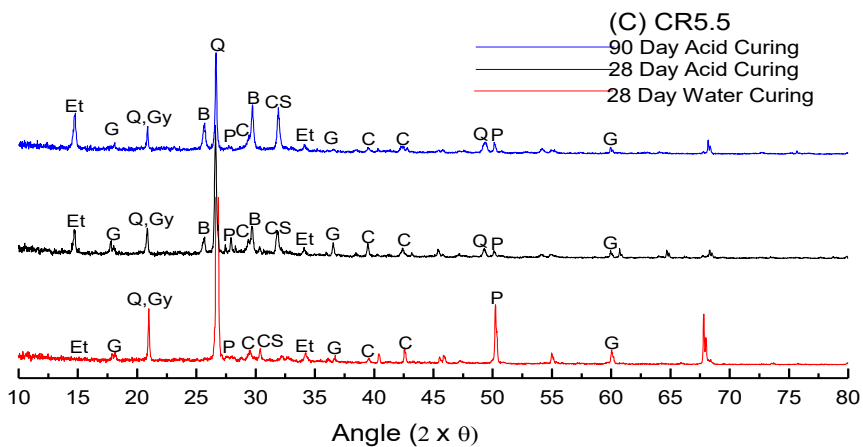




(a) CR0



(b) CR4



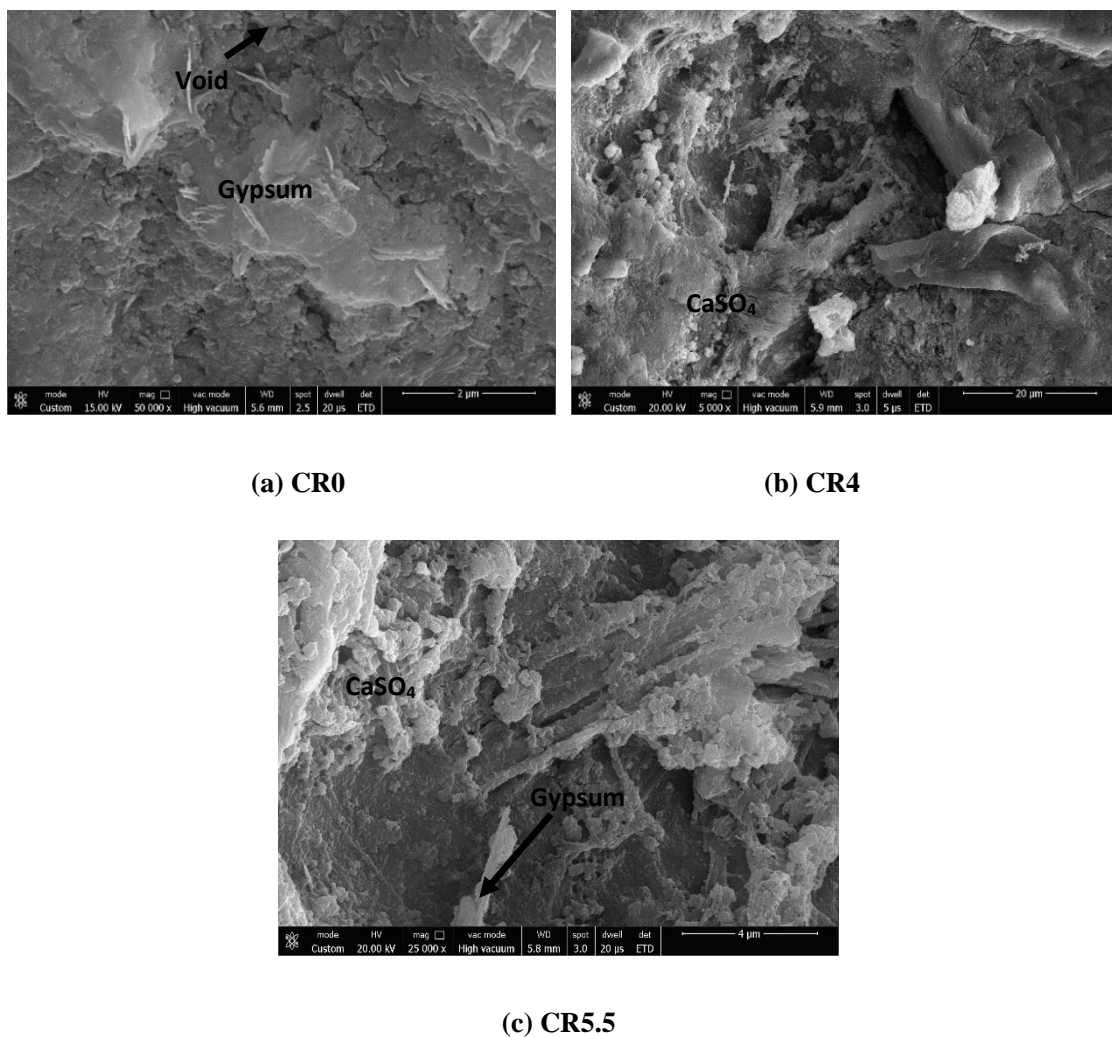
(c) CR5.5

Fig. 6.16: XRD analysis of crumb rubber concrete samples; where, Et - Ettringite, Gy - Gypsum, P-Portlandite, CS - Calcium Silicate Hydrate, Q - Quartz, C - Calcite, B - Brucite

### 6.3.2.4 FESEM Analysis

Microstructural study has also been implemented for CR0, CR4 and CR5.5 samples exposed to acidic environment for 28 days as shown in **Fig. 6.17**. Apart from CSH and CASH gel, formation of gypsum has also been noticed. Gypsum was formed due to reaction between Portlandite and sulphuric acid (Olmstead and Hamlin (1990)).

The presence of gypsum was identified through XRD (**Fig. 6.16**) analysis. Ettringite is not visible in the micrographs but its presence has been noticed through XRD analysis (**Fig. 6.16**) of lower intensity. The incorporated CR in CR4 and CR5.5 mixes react with acid and becomes adhesive (Thomas et al. (2016)). The increased adhesiveness results into lesser material separation and reduced formation of cracks as compared CR0 mix as shown in **Fig. 6.17**. This causes lesser change in weight (**Fig. 6.13**) and compressive strength (**Fig. 6.14**) for CR4 and CR5.5 mixes as compared to CR0 mix.

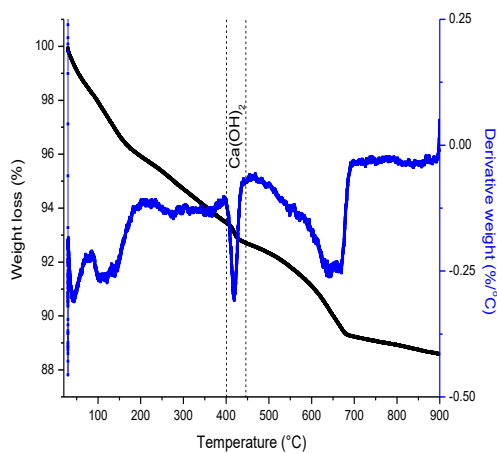


**Fig. 6.17: FESEM analysis for crumb rubber concrete specimens**

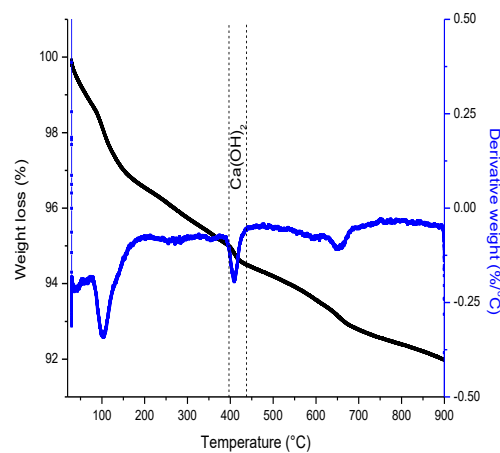
### 6.3.2.5 TGA / DTA Analysis

TGA / DTA thermograms were carried out on CR0, CR4 and CR5.5 mixes after 28 days of curing. The DTA curves (**Fig. 6.18**) show the typical reactions occurring in the cement matrix when subjected to a progressive temperature increase from room temperature up to 900°C. After 28 and 90 days of acid curing the amount of weight loss increases for all mixes as shown in **Table 6.2**.

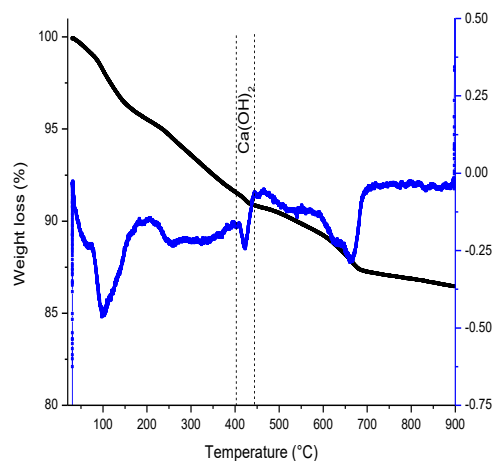
The maximum weight loss was noticed at 28 days of acid curing. The mass loss for CR4 and CR5.5 is more when compared to CR0. This might be due to binding action of CR with ettringite as compared with CR0 mix where ettringite leaches out from concrete. This binding action of CR results into lesser deterioration of mass of concrete (Thomas et al. (2016)). The same has been observed in **Fig. 6.14** where the maximum change in compressive strength was observed for control mix samples.



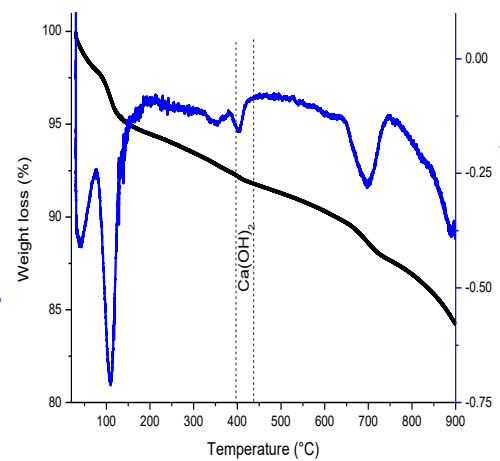
(a) CR0 28 Day Acid curing



(b) CR0 90 Day Acid curing



(c) CR4 28 Day Acid curing



(d) CR4 90 Day Acid curing

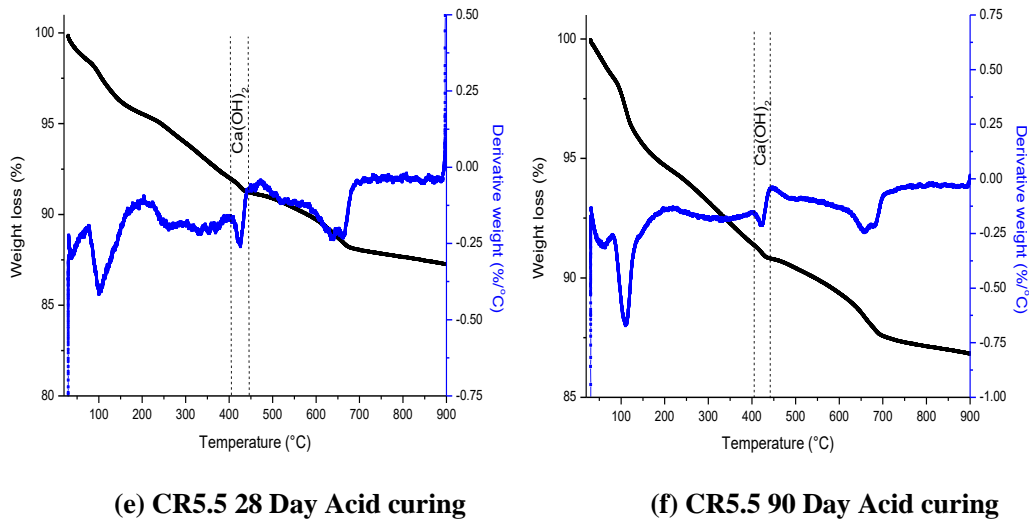


**Fig. 6.18: TGA / DTA analysis for crumb rubber concrete samples**

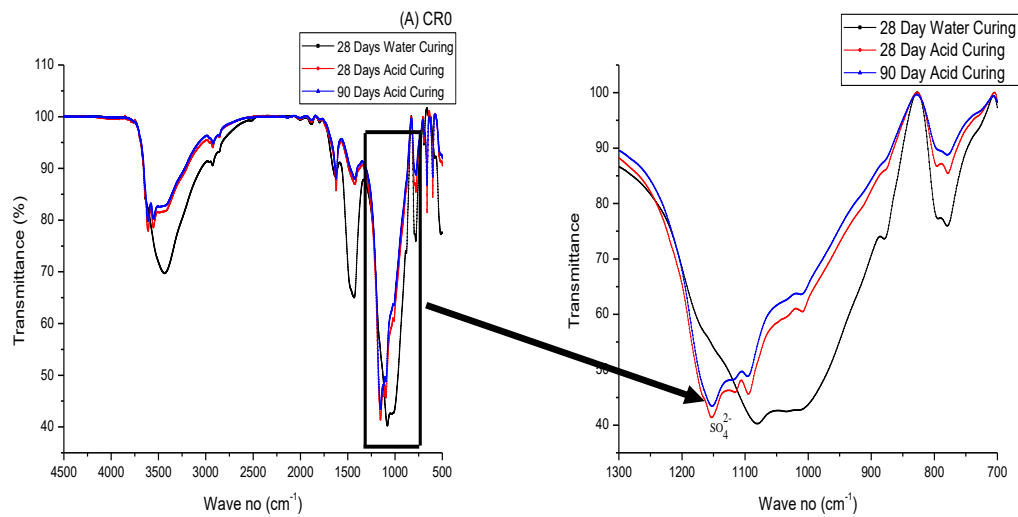
After 28 and 90 days of acid curing maximum degradation of  $\text{Ca}(\text{OH})_2$  has been observed for rubber based concrete mixes as presented in below mentioned **Table 6.2**. This change might be due to quick reaction of sulphuric acid with CR instead of  $\text{Ca}(\text{OH})_2$ . Hence, greater mass loss has been observed for temperature range (410 - 470°C) for mixes with CR as compared to CR0 mix.

**Table 6.2: TGA investigated on crumb rubber concrete samples**

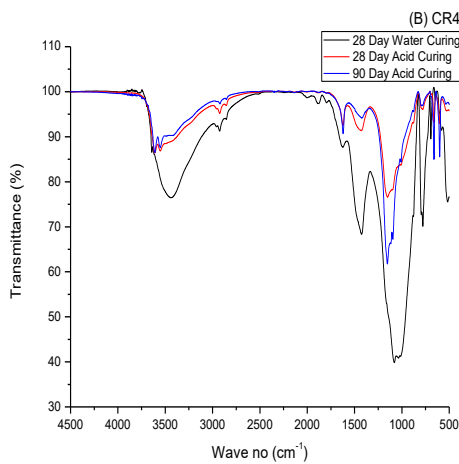
MIX No.	Weight Loss (%)		
	70 - 170°C	225 - 320°C	410 - 470°C
CR0 28 Day	2.34	1.25	0.84
CR0 90 Day	2.11	0.80	0.50
CR4 28 Day	3.21	1.77	0.82
CR4 90 Day	3.39	1.35	0.58
CR5.5 28 Day	3.35	1.80	0.91
CR5.5 90 Day	3.59	1.64	0.69

### 6.3.2.6 FTIR Analysis

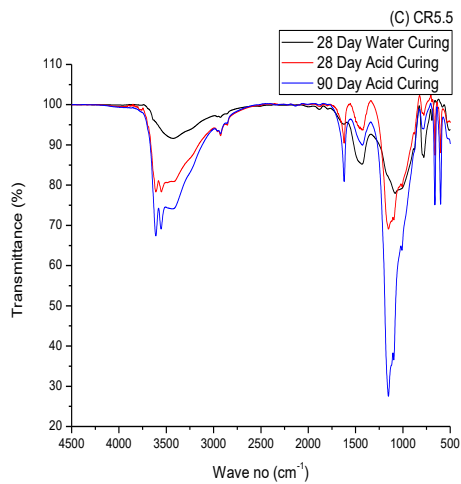
**Fig. 6.19** presents FTIR analysis for CR0, CR4 and CR5.5 samples. The below mentioned figure shows that with increase in exposure period of specimens to acidic medium ( $\text{H}_2\text{SO}_4$ ), ingestion of Portlandite (peak around  $3643\text{ cm}^{-1}$  (Bulatović et al. (2017)) increases.



(a) CR0



(b) CR4



(c) CR5.5

Fig. 6.19: FTIR analysis for crumb rubber concrete samples

Table 6.3: FTIR wave numbers investigated on crumb rubber concrete samples

MIX No.	Molecular Group (cm <sup>-1</sup> )		
	Portlandite	Si-O-Al	SO <sub>4</sub> <sup>2-</sup>
CR0 28 Day Water Curing	3641	1017	-
CR0 28 Day Acid Curing	3611	1008	1153
CR0 90 Day Acid Curing	3610	1006	1152
CR4 28 Day Water Curing	3642	1015	-
CR4 28 Day Acid Curing	3610	1011	1152
CR4 90 Day Acid Curing	3608	1009	1154
CR5.5 28 Day Water Curing	3640	1014	-
CR5.5 28 Day Acid Curing	3610	1010	1151
CR5.5 90 Day Acid Curing	3544	1008	1142

From **Table 6.3** it has been observed that maximum consumption of Portlandite was observed for CR5.5 mix (peak at  $3544\text{ cm}^{-1}$ ) after 90 days of acidic exposure as compared to CR4 (peak at  $3608\text{ cm}^{-1}$ ) and CR0 (peak at  $3610\text{ cm}^{-1}$ ) mixes. The consumed Portlandite results into formation of calcium sulphate. The molecular band observed around  $3465\text{ cm}^{-1}$  indicate the presence of Bassanite mineral ( $\text{CaSO}_4 \cdot 0.5\text{H}_2\text{O}$ ) for exposed specimens (Choudhary et al. (2015)). The presence of this mineral has been justified through XRD analysis (**Fig. 6.16**).

$\text{SO}_4^{2-}$  group generally can be found by a band between the regions at  $1100 - 1200\text{ cm}^{-1}$  (Kloprogge et al. (2002)). The mineral phases identified by XRD analysis shows the existence of  $\text{SO}_4^{2-}$  group such as ettringite and gypsum. The absorption bands around  $1115\text{ cm}^{-1}$ ,  $669\text{ cm}^{-1}$  and  $601\text{ cm}^{-1}$  specifies the presence of gypsum and ettringite (Mollah et al. (2000)). Water present in gypsum can be identified by the presence of band around  $1623\text{ cm}^{-1}$  and  $3549\text{ cm}^{-1}$  (Bulatović et al. (2017)). The presence of these compounds also indicates the consumption of Portlandite. The reduction in wave number of Portlandite for acid cured CR5.5 mix samples was higher as compared to CR4 and CR0 mixes, also be characterized by increase in mass loss for CR5.5 mix around  $410 - 470^\circ\text{C}$  as shown in **Table 6.2**.

### 6.3.3 Fire Test

Resistance to fire attack is observed in terms of weight loss and change in compressive strength which are explained in the following section.

#### 6.3.3.1 Mass Loss

The mass loss was evaluated for CR incorporated concrete specimens after exposure to elevated temperature (from room temperature to  $800^\circ\text{C}$ ) followed by air cooling as shown in **Fig. 6.20**.

From above mentioned figure mass loss has been monitored for all mixes exposed to different temperature conditions. Initially, mass loss mainly related with departure of capillary water. Ramachandran et al. (1981) also mentioned that capillary water tends to disappear from concrete mixes at initial stage. Mass loss at higher temperature might be related with chemically bound water. This water is free when hydration products deteriorates at higher temperature (Demirel and Keleştemur (2010)). Ismail et al. (2011) reported that mass loss at extreme temperature ( $500 - 800^\circ\text{C}$ ) mainly related with thermal disintegration of hydration products. It has been observed from **Fig. 6.21** that CR

decomposes when temperature increases above 300°C. This causes higher mass loss in CR based concrete mixes as compared to control concrete due to flammable nature of CR.

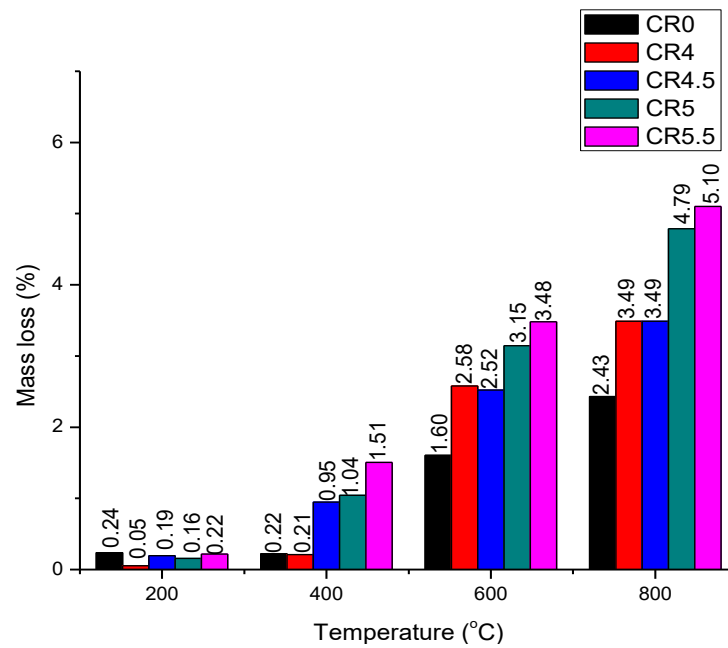


**Fig. 6.20: Mass loss for crumb rubber concrete specimens exposed to fire**

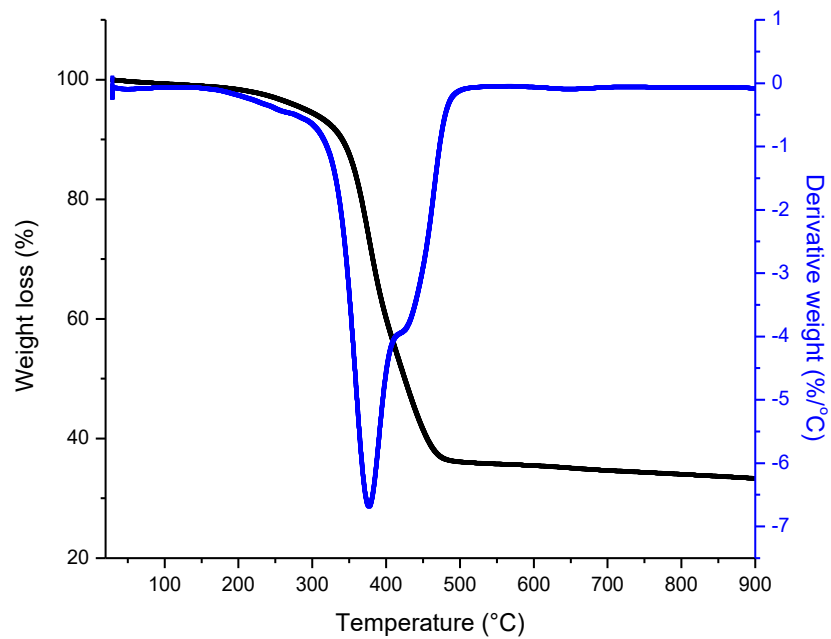


**Fig. 6.21: TGA / DTA analysis of crumb rubber**

### 6.3.3.2 Compressive Strength

The change in performance of concrete behaviour was monitored for with and without CR after exposure to elevated temperature (200°C, 400°C, 600°C and 800°C). This

is graphically presented in **Fig. 6.22**. It has been observed from same figure that with rise in temperature up to 200°C, marginal increase in compressive strength has been observed for all concrete mixes. However, with further rise in temperature fall in compressive strength was noticed. It is also observed that CR starts melting at 170°C, leaves space for water vapour to escape which helps to release the pore pressure and thus reduce prolongs damage on the concrete structure. The enhancement in compressive strength up to 200°C may be also associated with condensed calcium hydroxide and un-hydrated cement (Nadeem et al. (2014)).

With rise in temperature, fall in compressive strength was higher for CR based concrete mixes as compared to control mix. The maximum compressive strength loss has been examined for CR5.5 mix (46.80%) as compared to control mix (32.94%) after exposure at 800°C. It has been observed from TGA (weight loss graph **Fig. 6.21**) of CR that as the temperature crosses 300°C rapid drop in weight has been noticed. It has also been observed for CR based concrete mixes that after completion of test concrete specimens are still ignited until all of the incorporated CR gets fully decomposed at 600 - 800°C. This increases the porosity and hence, results in fall in compressive strength as shown in **Fig. 6.22**.

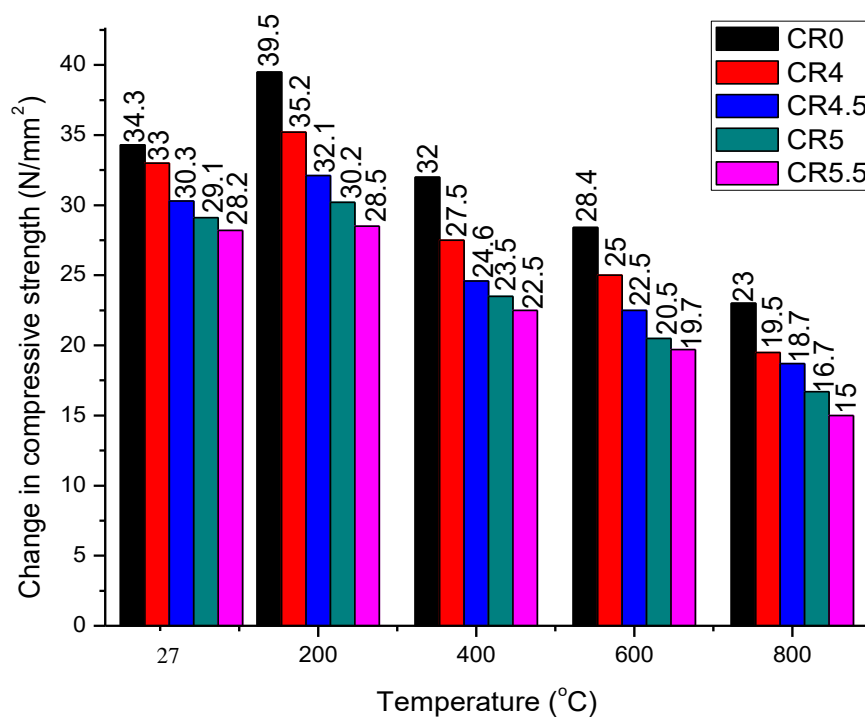
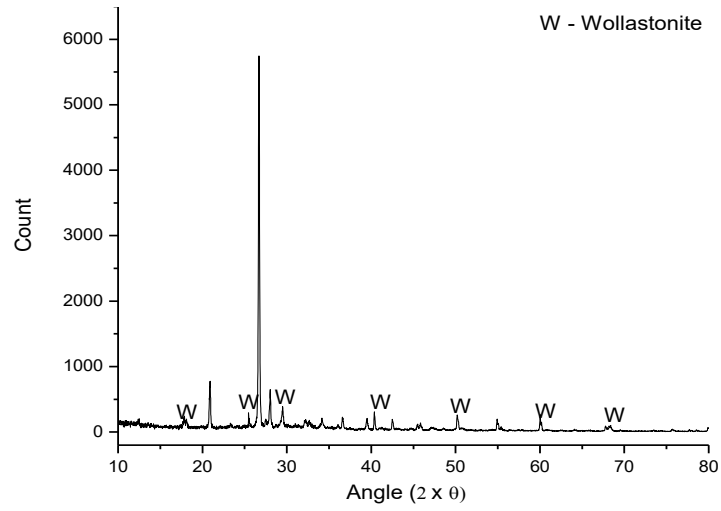
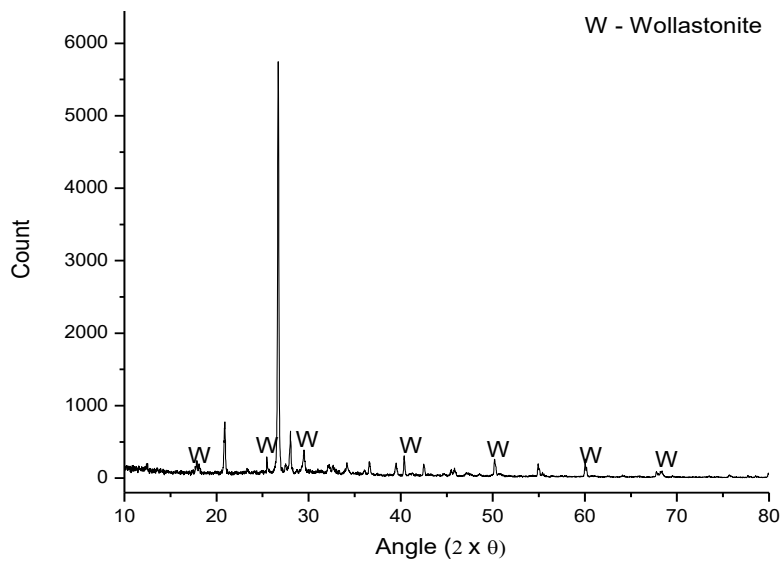


**Fig. 6.22: Change in compressive strength for crumb rubber concrete specimens exposed to fire**

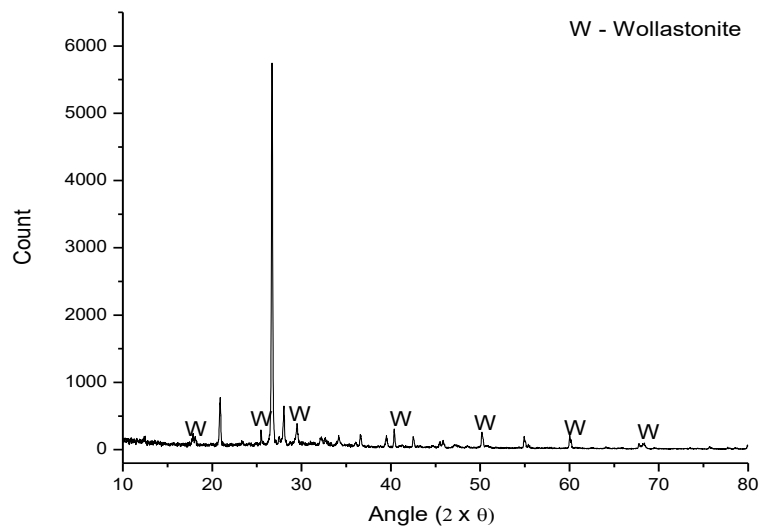




(a) CR0



(b) CR4



(c) CR5.5

Fig. 6.23: XRD analysis of crumb rubber concrete samples exposed to 800°C

At 800°C CSH partially decomposes into wollastonite ( $\text{CaSiO}_3$ ) and same has been detected through XRD analysis as shown in **Fig. 6.23**. Similar observation at 800°C has been observed for CR incorporated concrete mixes. Hence, incorporation of CR at different proportions show some changes at 400°C only and any rise in temperature beyond this does not significantly change the behaviour of concrete mixes as shown in **Fig. 6.22**.

## **6.4 Results and Discussion of Part - B: Waste Glass**

### **6.4.1 Corrosion**

In this part behaviour of WG concrete samples under influence of chloride attack were explained.

#### **6.4.1.1 Chloride Penetration**

The extent of chloride ion penetration for WG incorporated concrete mixes are presented in **Fig. 6.24**. It has been observed that chloride penetration shows adverse behaviour at higher substitution level (21 – 24%) of WG in concrete mix. The level of chloride penetration for WG incorporated concrete samples are presented in **Fig. 6.25**.

Results monitored in the range of 18 – 20% demonstrates better performance as compared to WG0 mix. After 7 days exposure to chloride solution diffused chloride ions show uneven pattern for WG concrete mixes whereas, 2 mm penetration has been observed for WG0 mix. After 28 and 90 days of exposure, penetration of chloride ions for WG20 mix (5 mm) remains consistent as compared to WG0 mix where, hike in penetration has been monitored from 5 to 7 mm respectively. This might be due to a denser internal structure of WG which act as a barrier against chloride ion penetration (Rashad (2014)). However, with further inclusion of WG in concrete mixes (21 – 24%) increase in chloride ion penetration has been observed as compared with WG20 and WG0 mix specimens after 28 and 90 days of exposure respectively. The maximum penetration of 8 and 10 mm has been observed for WG24 as compared to WG20 and WG0 mix respectively. This might be due to the fact that inclusion of WG also increases the voids content apart from densifying the internal microstructure. Hence, in this study even at minimum substitution of 18% leads to generation of voids. These inter-connected capillary voids start playing a dominant role in chloride ion penetration when WG is

substituted above 20%. At higher substitutions the denser cement matrix is not capable of binding chloride ions when compared to WG18.

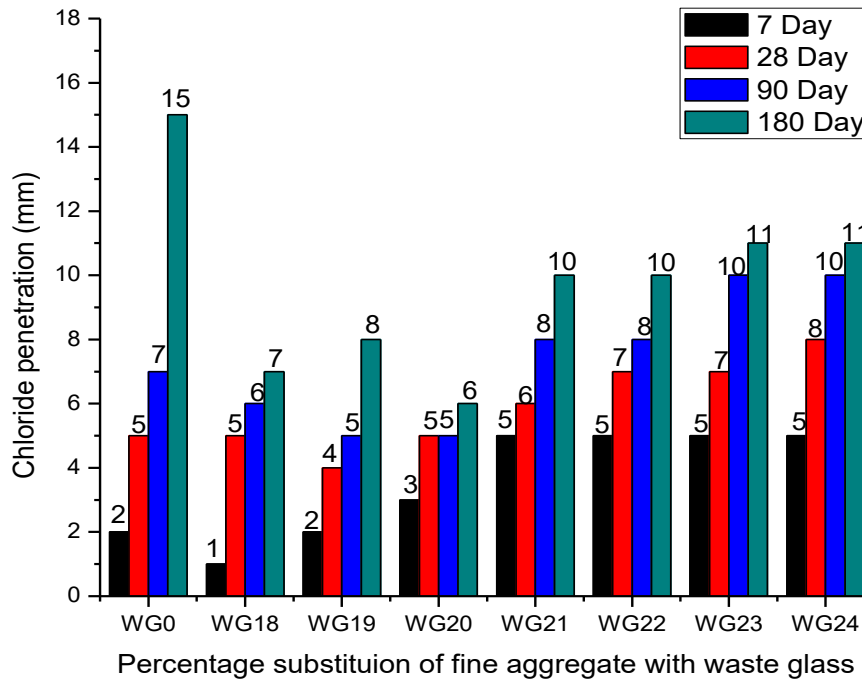


**Fig. 6.24: Chloride penetration for waste glass concrete specimens**

After 180 days of exposure the maximum penetration of chloride ions has been observed for control mix (15 mm) as compared to WG incorporated specimens. It has also been visualized from **Fig. 6.24** that for higher substitution levels no major changes has been observed after 90 days of exposure. Hence, inclusion of WG does not generally vary the performance of concrete mixes through chloride ion penetration.



**Fig. 6.25: Depth of chloride penetration in waste glass concrete specimens**

### 6.4.1.2 Corrosion

The time dependent (12 months) variation of half-cell potential for WG incorporated concrete mixes are graphically reported in **Fig. 6.26**.

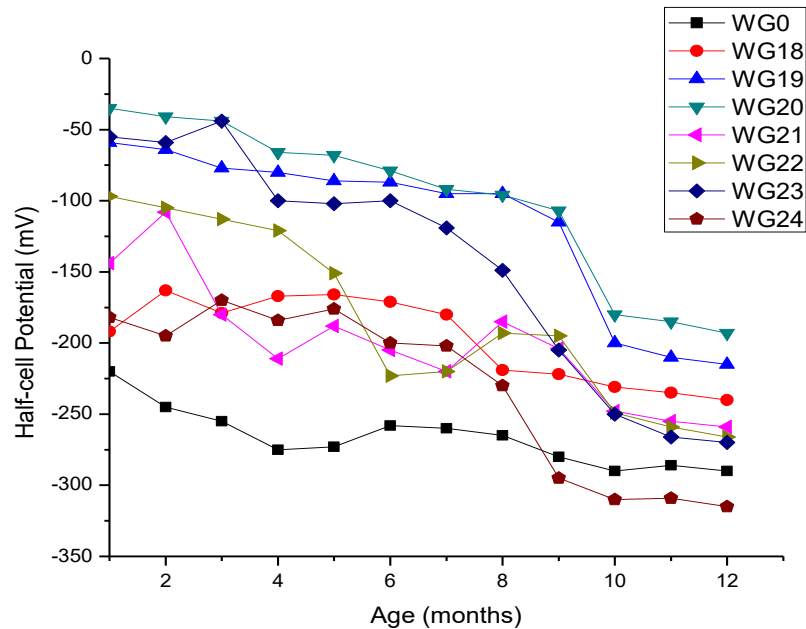


**Fig. 6.26: Half-cell measurements for waste glass concrete specimens**

The initial half-cell potential reading for WG concrete mixes (18 – 24%) lies between 50 to 200 mV. However, WG0 shows higher potential 220 to 250 mV at initial stage. As per ASTM C876 (2015) the half-cell values more negative than -350 mV indicates 90% chances of corrosion.

The maximum potentials for WG0, WG18, WG19, WG20, WG21, WG22, WG23, WG24 mixes were -290 mV, -240 mV, -215 mV, -193 mV, -259 mV, -266 mV, -270 mV and -315 mV after 12 months of exposure. It has been observed from above data that maximum corrosion occurred for control mix samples and minimum for WG20 sample. The results recorded are completely in line with chloride penetration values. In WG21 sample more than -276 mV potential was observed after 3 months of exposure and then decreased afterward. This increase and decrease in half-cell values for concrete mixes noticed here is due to formation of corrosion products on steel bars, which retard the flow of corrosion current (Vedalakshmi et al. (2008)). Secondly, deficiency of oxygen due to saturated voids with water causes cathodic resistance and reduced the flow of electrons as an outcome reduced corrosion current and potential was monitored (Raupach (1996)).

### 6.4.1.3 Carbonation

The influence of carbonation on WG concrete mixes are reported in **Fig. 6.27**. The specimens portraying the depth of carbonation are shown in **Fig. 6.28**.

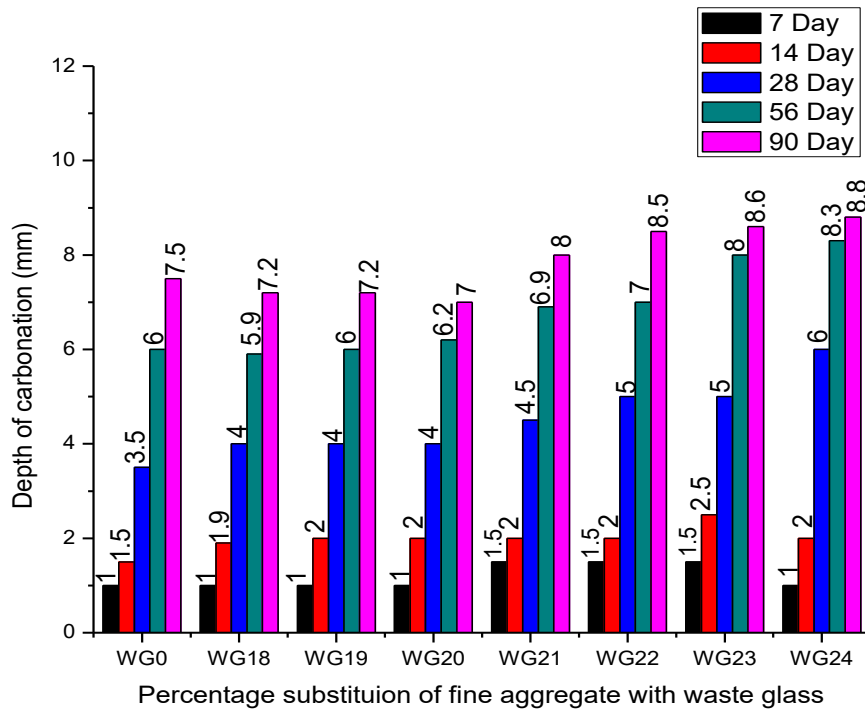


**Fig. 6.27: Depth of carbonation for waste glass concrete prisms**

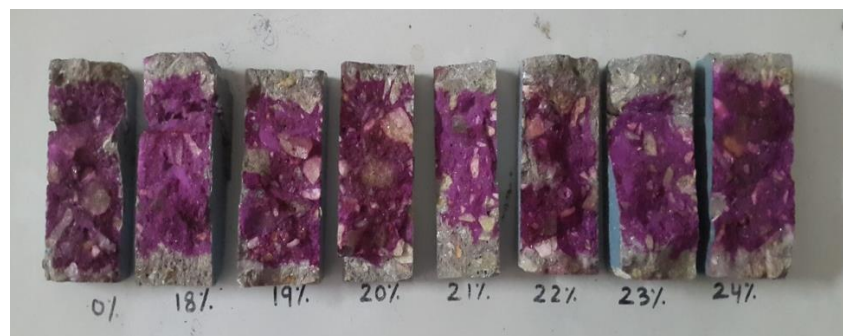


**Fig. 6.28: Carbonation depth of waste glass concrete prisms after exposure to 90 days**

It has been confirmed from **Fig. 6.27** that depth of carbonation remains almost constant up to 20% substitution level for all ages as compared to WG0 mix samples however, further inclusion reduces the resistance of carbonation.

The depth of carbonation remains almost uniform for 7 and 14 days of exposure but some fluctuations have been observed at higher substitution level. These variations might be due to presence of voids which allows effortless penetration of carbon dioxide in concrete samples. The hike in depth of carbonation was monitored at 28 and 56 days of

exposure for waste glass (21 - 24%) concrete mixes. At 90 days, decreasing trend has been observed up to WG20 mix (7mm) as compared to WG0 mix (7.5mm) samples. This might be due to a denser internal structure of WG which act as a barrier against chloride ion penetration (Rashad (2014)). At higher substitution level of 24% (8.8 mm) increased depth of carbonation has been observed. Increase in penetration might also be due to finer nature of WG as compared to fine aggregate it replaces. This reduces the interlocking between constituents and leaves behind cavities, thus amplifies the carbonation.

### 6.4.2 Acid Attack

Resistance to acid attack was conducted for 7, 28 and 90 days of exposure. Changes quantified in terms of weight loss and change in compressive strength are discussed below.

#### 6.4.2.1 Weight Loss

The change in weight of concrete specimens after exposure to acidic environment presented in **Fig. 6.29**. It has been observed from same figure that introduction of WG in concrete mixes reduces the mass loss. Up to 28 days of acidic exposure, increase in mass has been observed for all concrete mixes. This might be due to formation of ettringite which provides extra filler effect.

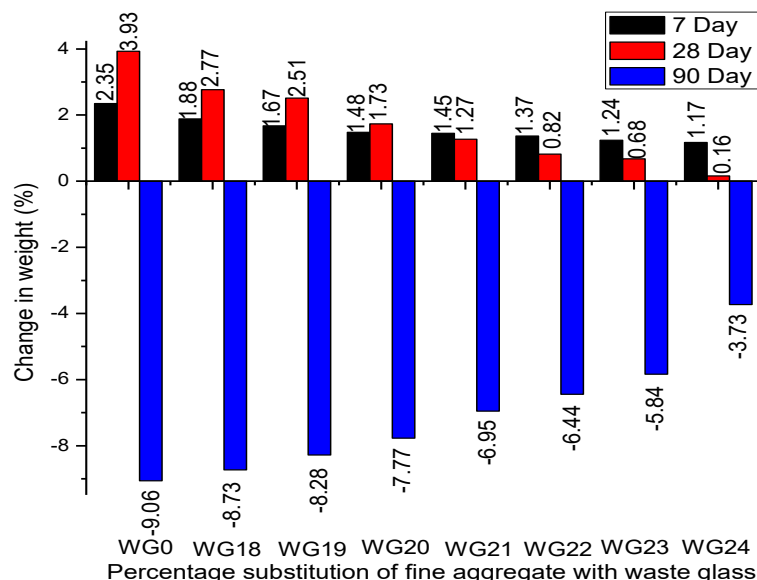


**Fig. 6.29: Change in weight for waste glass concrete specimens**

With rise in exposure period for 90 days, mass loss has been monitored. A maximum loss of 9.06% has been observed for WG0 mix as compared to 3.73% for WG24

mix. The loss in this period is related to deterioration of surface layers. This might be due to lower penetration of acidic solution inside concrete cube because of higher acid resistance WG. Due to this degradation some of the WG particles get exposed to acidic solution. This results into dislodging of WG particles from specimens which causes mass loss. Ling and Poon (2011) also reported comparable performance when WG (60% < 2.36 mm and 40% 2.36 – 5 mm) was incorporated in mortar.

#### **6.4.2.2 Change in Compressive Strength**

The change in compressive strength of acid attacked specimens are reported in **Fig. 6.30**. The sulphate ions of the acidic solution in concrete cubes penetrates through voids and cracks. The exposed samples are shown in **Fig. 6.31**. Rise and fall of compressive strength depend upon the formation of reaction product such as ettringite. It has been observed that after 7 days of exposure WG24 mix showed rise (18.18%) in compressive strength as compared to WG0 mix (3.22%). This increase in compressive strength for WG incorporated mixes might be due to higher porosity which allows more sulphate ions to penetrate inside the concrete cube. The formed reaction product (ettringite) initially act as a filler, hence improves the compressive strength of concrete mixes. With increase in exposure period the maximum decrease in compressive strength has been observed for WG0 mix after 90 days of exposure as compared to WG24 mix. This might be due to higher resistance of WG when compared to river sand it replaces (Wang (2009)). The interconnected voids pose higher rate of sulphate ions penetration for WG0 mix, results into extreme change in compressive strength.

With rise in exposure period filler nature of reaction products tends to decrease as it occupies more volume than the products from which it is formed. This leads to propagation of new cracks, as a consequence reduced compressive strength has been observed for all mixes. It has been observed that acidic exposure for concrete cubes is not monotonous. From **Fig. 6.30** reduced trend has been observed for WG concrete mixes. The maximum decrease of 53.84% in compressive strength has been observed for WG0 mix after 90 days of exposure as compared to 22.39% for WG24 mix. This might be due to higher resistance of WG which does not allow sulphate ions to penetrate greater depths as compared to WG0 mix. The interconnected voids pose higher rate of sulphate ions penetration for WG0 mix, results into extreme change in compressive strength.

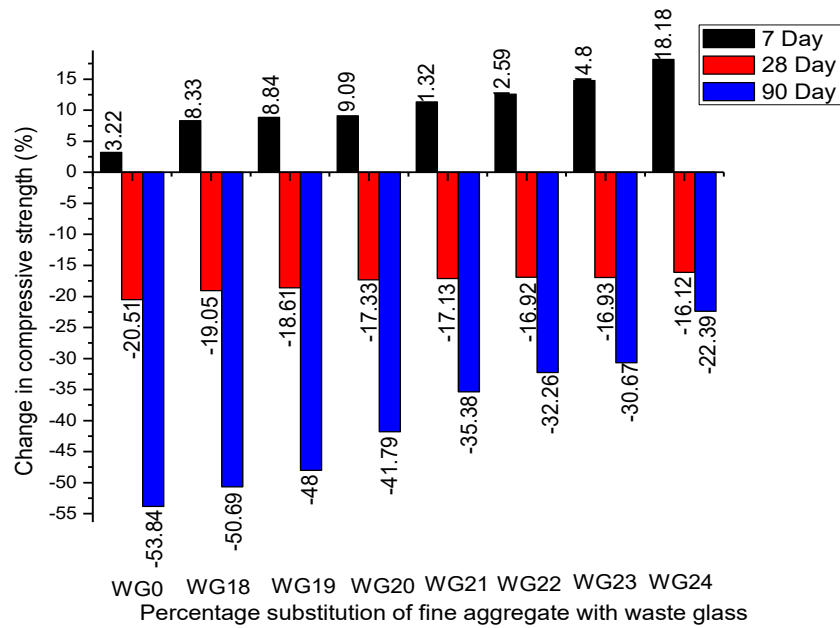


**Fig. 6.30: Change in compressive strength for waste glass concrete specimens**



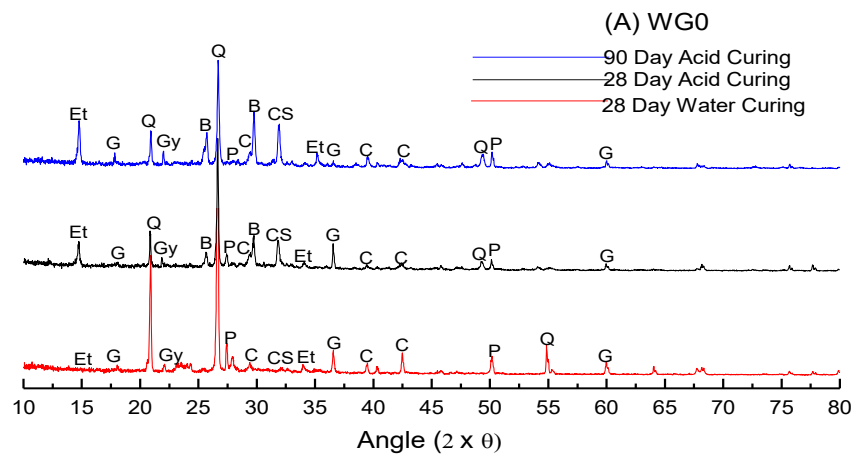
**Fig. 6.31: Acid attacked waste glass concrete samples**

#### 6.4.2.3 XRD Analysis

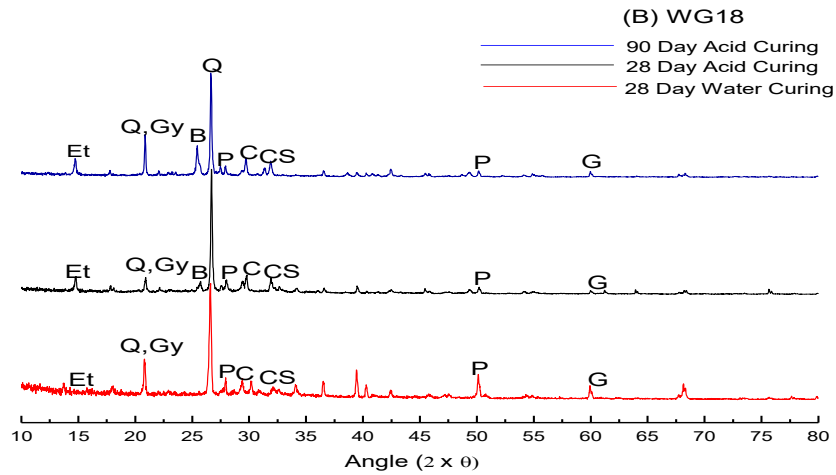
The formed mineral phases were monitored in concrete specimens by conducting XRD analysis after 28 and 90 days of exposure to acidic environment for all the mixes as shown in **Fig. 6.32**. After completion of exposure period in acidic environment, fall in the peak intensities of Portlandite (at  $2\theta = 28.23^\circ, 50.53^\circ$ ) were noticed. This drop-in phases of Portlandite was detected for all acid cured mixes as compared to reference samples. This variation is due to reaction of sulphuric acid with Portlandite which results into



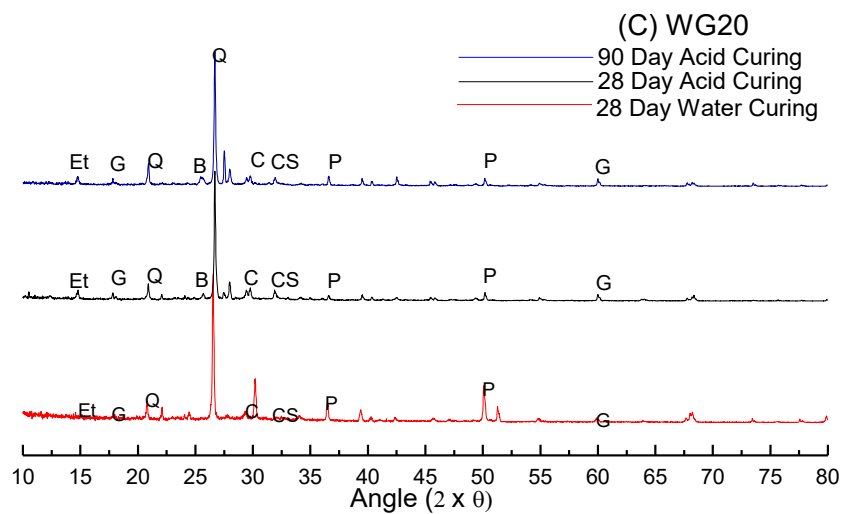
formation of calcium sulphate (at  $2\Theta = 28.23^\circ, 50.53^\circ$ ). Calcium sulphate was detected in the form of Bassanite (at  $2\Theta = 28.23^\circ, 50.53^\circ$ ).



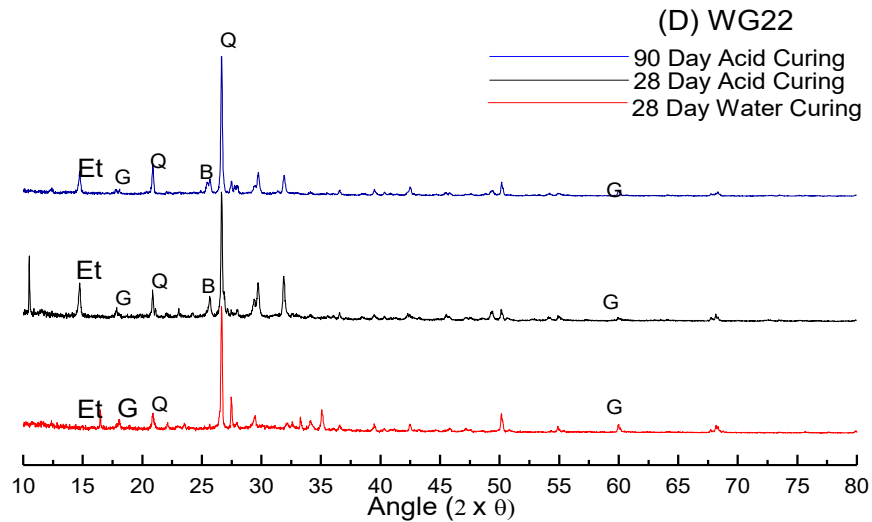
(a) WG0



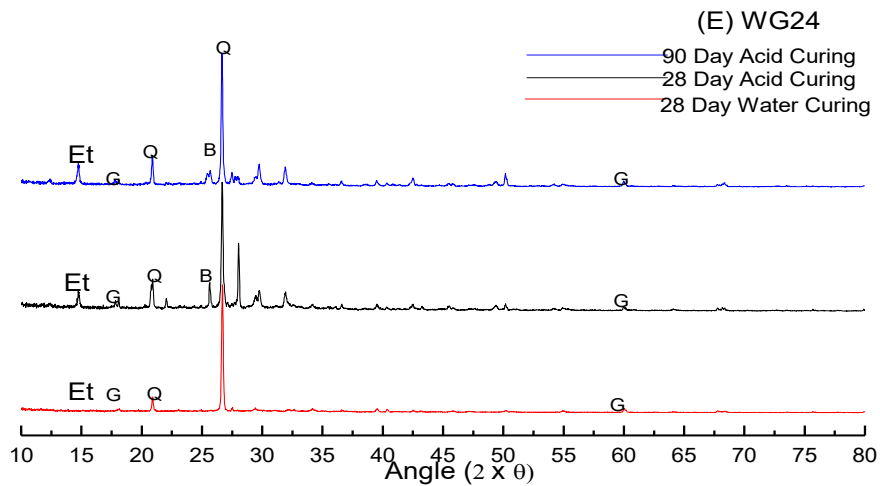
(b) WG18



(c) WG20



(d) WG22



(e) WG24

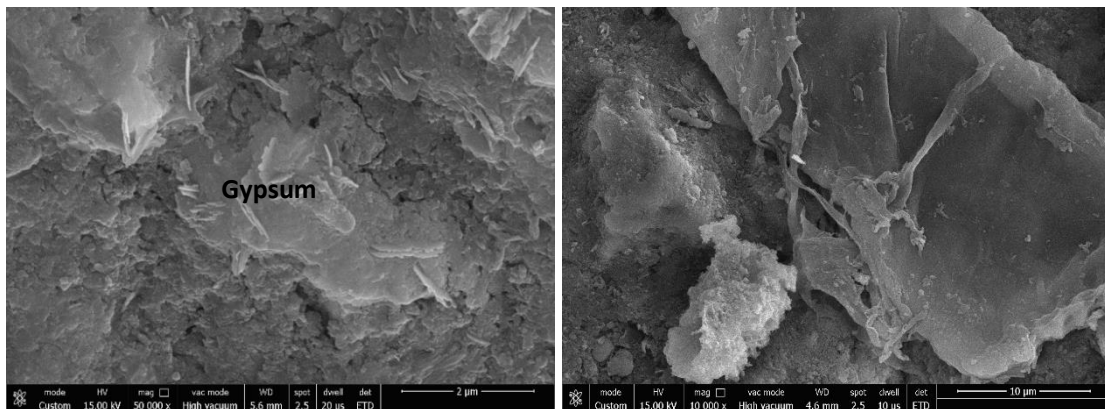
**Fig. 6.32: XRD analysis of waste glass concrete samples; where, Et - Ettringite, Gy - Gypsum, P-Portlandite, CS – Calcium Silicate Hydrate, Q - Quartz, C – Calcite, B – Brucite**

#### 6.4.2.4 FESEM Analysis

Microstructural study has also been executed after 28 days of acidic exposure for WG0, WG18, WG20, WG22 and WG24 samples as shown in **Fig. 6.33**.

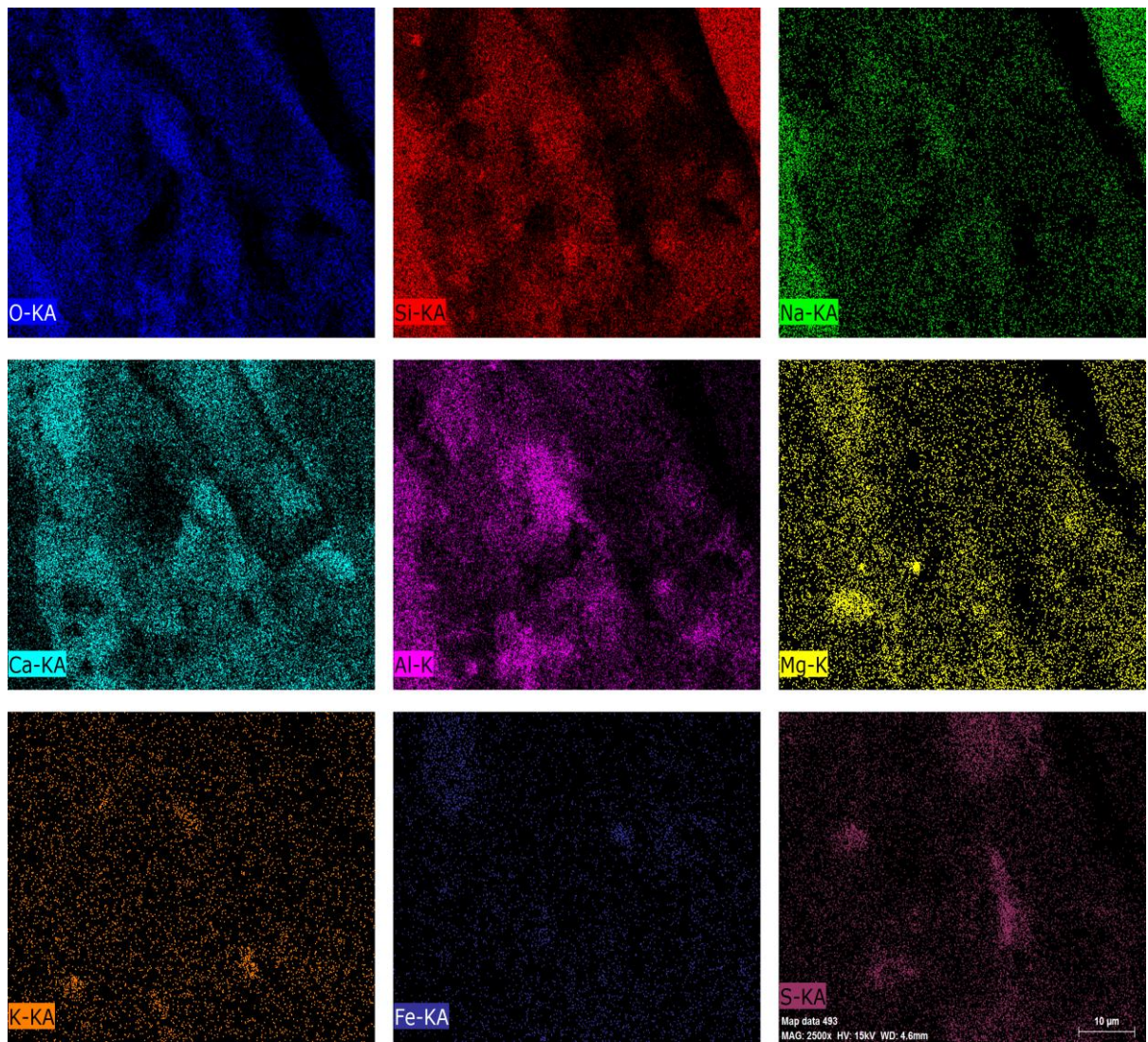
Gypsum was also noticed which was formed due to reaction between Portlandite and sulphuric acid (Olmstead and Hamlin (1900)). The occurrence of gypsum was detected through XRD (**Fig. 6.32**) analysis. Ettringite is also visible in the micrographs and its presence has been noticed through XRD analysis (**Fig. 6.32**). Due to lower reactivity of WG with sulphuric acid as compared with fine aggregate (river sand). This results into lesser change in weight (**Fig. 6.29**) and compressive strength (**Fig. 6.30**) for

WG incorporated mixes as compared to WG0 mix. The formation of compounds mentioned in figure (WG18) are identified by conducting EDAX.

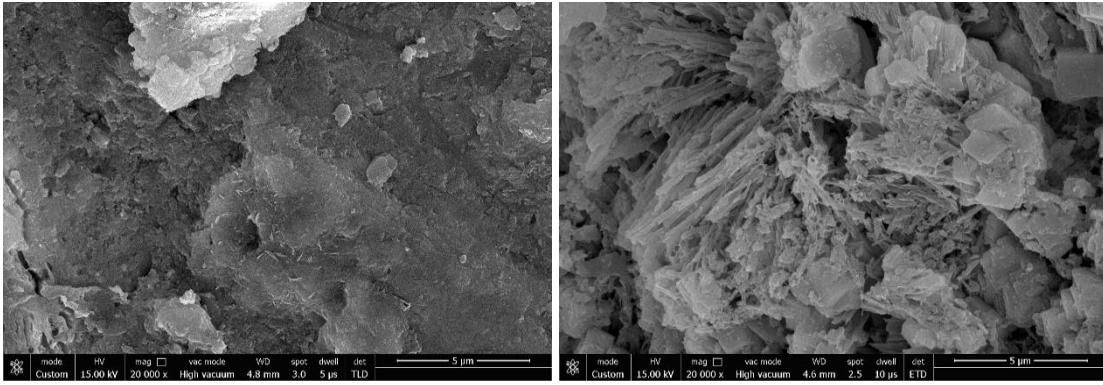


(a) WG0

(b) WG18

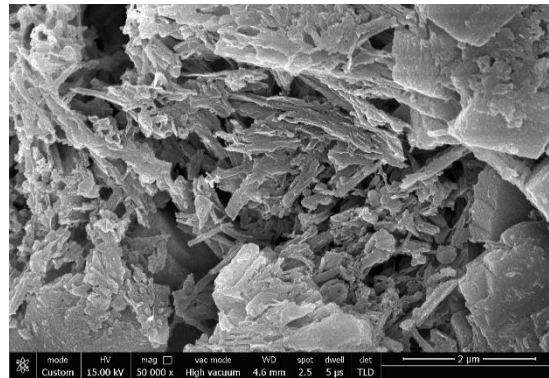


(c) WG18 EDAX



(d) WG20

(e) WG22

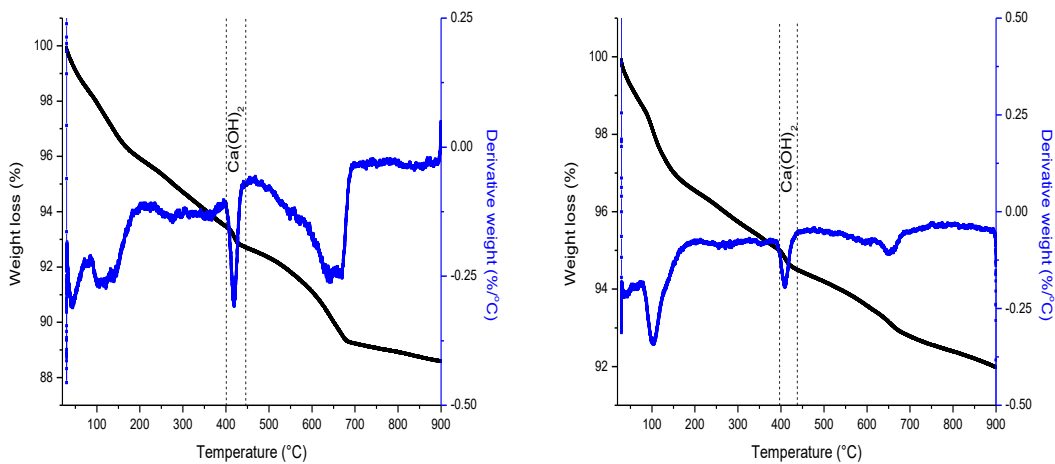


(f) WG24

Fig. 6.33: FESEM analysis of waste glass concrete specimens

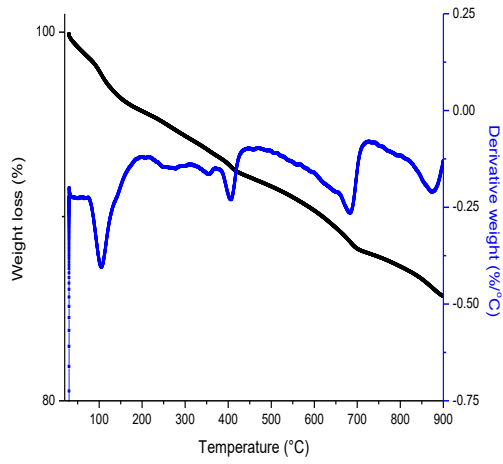
#### 6.4.2.5 TGA / DTA Analysis

TGA / DTA thermograms were performed on WG0, WG18, WG20, WG22 and WG24 mixes for 28 and 90 days of acid curing as shown in Fig. 6.34. After 28 and 90 days of acid curing changes have been observed for all mixes as shown in Table 6.4.

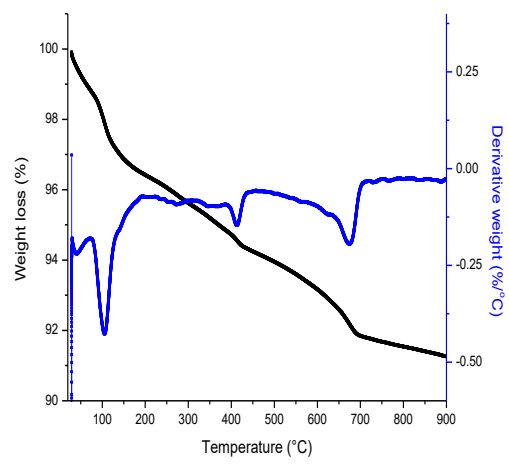


(a) WG0 28 Day Acid Curing

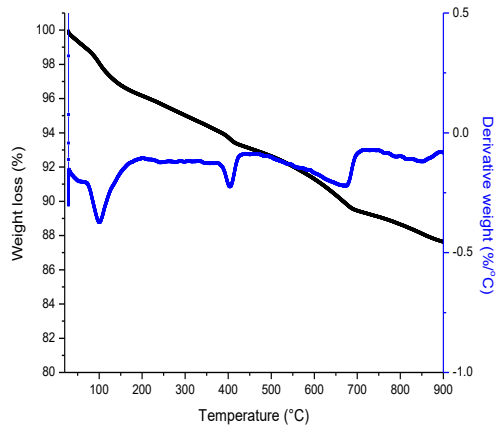
(b) WG0 90 Day Acid Curing



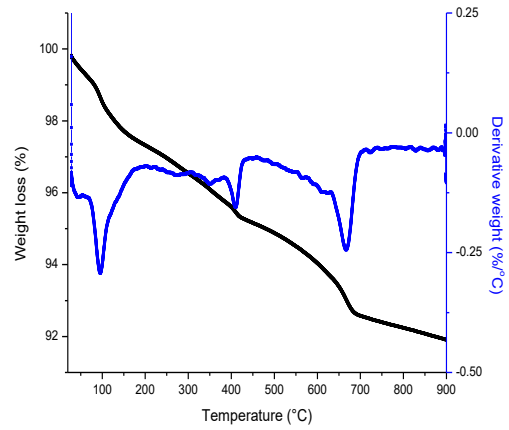
**(c) WG18 28 Day Acid Curing**



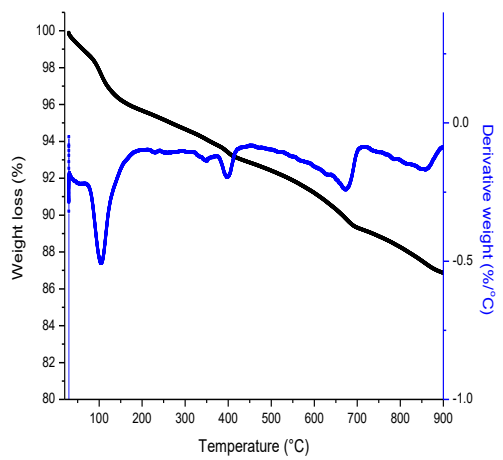
**(d) WG18 90 Day Acid Curing**



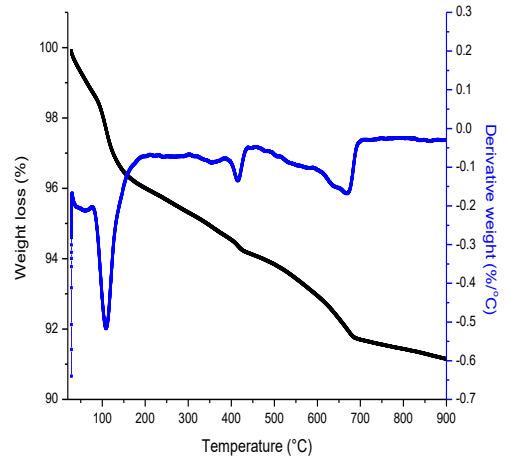
**(e) WG20 28 Day Acid Curing**



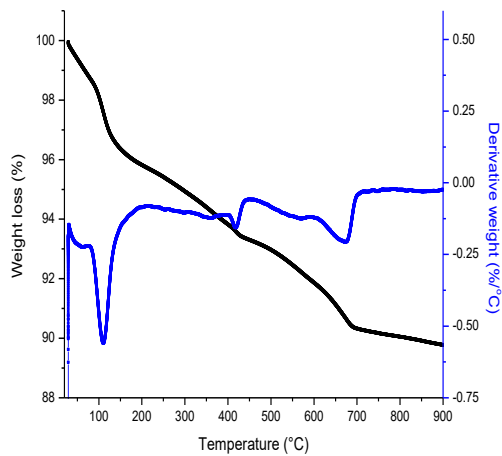
**(f) WG20 90 Day Acid Curing**



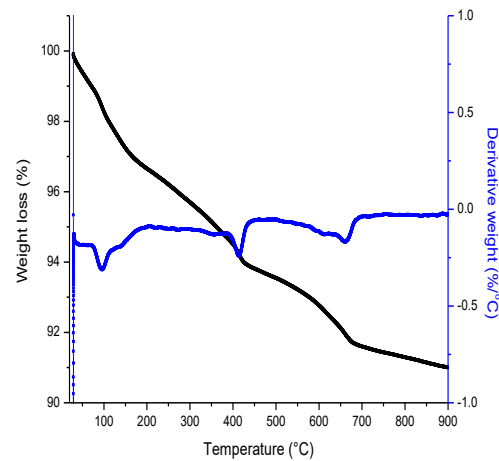
**(g) WG22 28 Day Acid Curing**



**(h) WG22 90 Day Acid Curing**



(i) WG24 28 Day Acid Curing



(j) WG24 90 Day Acid Curing

**Fig. 6.34: TGA / DTA analysis of waste glass concrete samples**

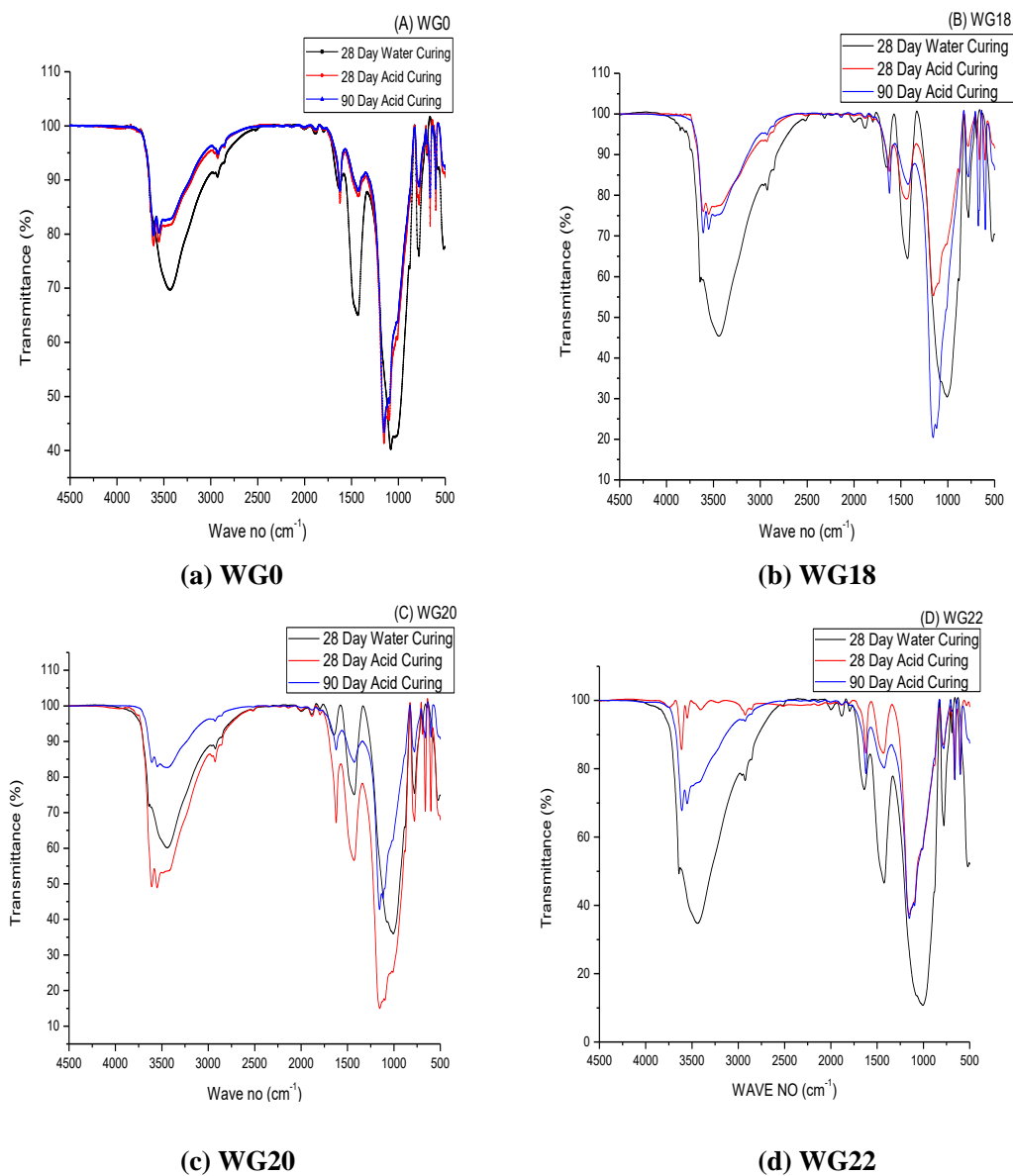
After 28 days of acid curing weight loss increases. The mass loss increases with increase in substitution level at 70 - 170°C. This might be due to presence of un-reactive WG in concrete mixes which becomes adhesive with ettringite. This results into lesser change in compressive strength (**Fig. 6.30**). However, at 410 - 470°C variations have been observed in terms of deterioration of Ca(OH)<sub>2</sub>. The changes remain almost constant for WG incorporated concrete mixes in this temperature range. This is due to pozzolanic nature of WG results into formation of more CSH and CASH gel. This retards the reaction of sulphuric acid with Ca(OH)<sub>2</sub> and results into lesser decomposition.

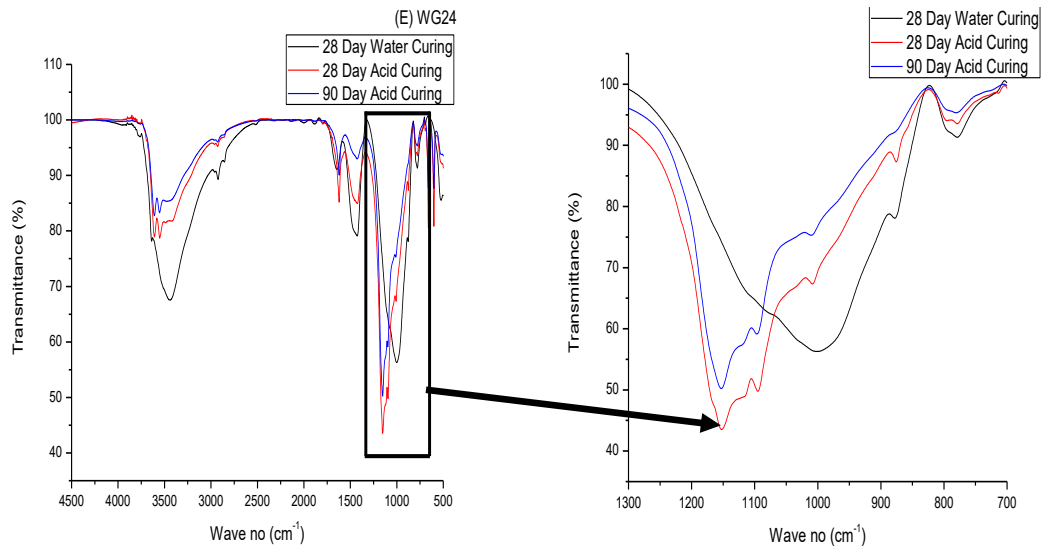
**Table 6.4: TGA investigated on waste glass concrete samples**

MIX No.	Weight Loss (%)		
	70 - 170°C	225 - 320°C	410 - 470°C
WG0 28 Day	2.34	1.25	0.84
WG0 90 Day	2.11	0.8	0.5
WG18 28 Day	2.79	1.14	0.68
WG18 90 Day	1.82	0.57	0.38
WG20 28 Day	2.69	1.41	0.75
WG20 90 Day	2.25	0.82	0.50
WG22 28 Day	2.89	1.03	0.58
WG22 90 Day	2.68	0.69	0.45
WG24 28 Day	2.87	0.94	0.56

### 6.4.2.6 FTIR Analysis

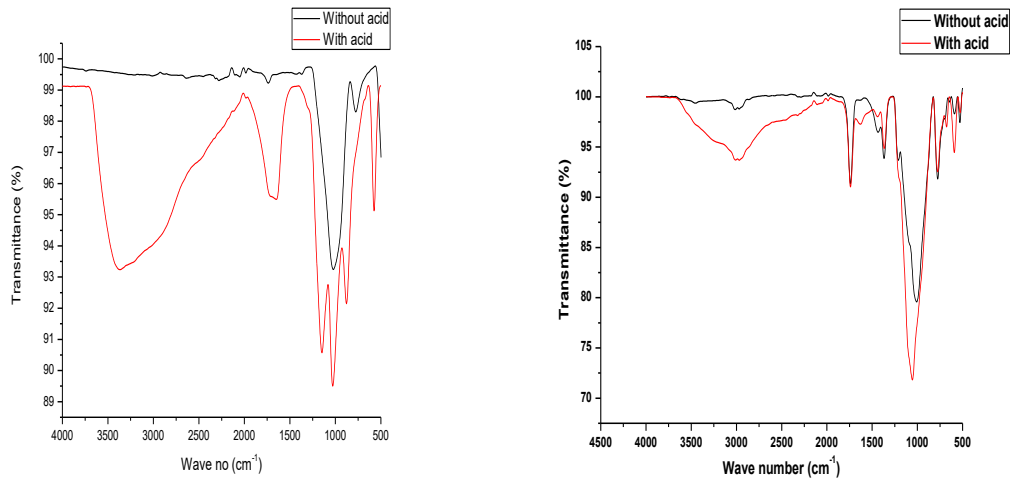
**Fig. 6.35** shows FTIR analysis for WG0, WG18, WG20, WG22 and WG24 samples. The below mentioned figure shows that with increase in exposure period of specimens to acidic medium ( $H_2SO_4$ ), ingestion of Portlandite (peak around  $3643\text{ cm}^{-1}$  (Bulatović et al. (2017))) increases and results into formation of calcium sulphate. This is present in the form of Bassanite mineral ( $CaSO_4 \cdot 0.5H_2O$ ) for exposed specimens (Choudhary et al. (2015)). The presence of this mineral has been verified by XRD analysis (**Fig. 6.32**).





(e) WG24

Fig. 6.35: FTIR analysis of waste glass concrete samples



(a) Waste Glass

(b) River Sand

Fig. 6.36: FTIR analysis of with and without exposed waste glass and river sand

Table 6.5: FTIR wave numbers investigated on waste glass concrete samples

MIX No.	Molecular Group (cm <sup>-1</sup> )		
	Portlandite	Si-O-Al	SO <sub>4</sub> <sup>2-</sup>
WG0 28 Day Water Curing	3641	1017	-
WG0 28 Day Acid Curing	3611	1008	1153
WG0 90 Day Acid Curing	3610	1006	1152
WG18 28 Day Water Curing	3643	1007	-
WG18 28 Day Acid Curing	3608	1017	1153



<b>WG18 90 Day Acid Curing</b>	3609	1016	1157
<b>WG20 28 Day Water Curing</b>	3641	1008	-
<b>WG20 28 Day Acid Curing</b>	3609	1009	1152
<b>WG20 90 Day Acid Curing</b>	3608	1017	1155
<b>WG22 28 Day Water Curing</b>	3643	1008	-
<b>WG22 28 Day Acid Curing</b>	3610	1010	1152
<b>WG22 28 Day Acid Curing</b>	3610	1020	1153
<b>WG24 28 Day Water Curing</b>	3639	1007	-
<b>WG24 28 Day Acid Curing</b>	3608	1008	1152
<b>WG24 28 Day Acid Curing</b>	3609	1011	1152

From **Table 6.5** it has been observed that no significant change changes have been observed in concrete mixes with inclusion of WG. Hence, WG acts superficially. It has also been observed from **Fig. 6.36** that after exposure to acidic condition fine aggregate (river sand) shows more varied changes as compared to WG. This leads to improved behaviour towards weight loss (**Fig. 6.29**) and change in compressive strength (**Fig. 6.30**) with incorporation of WG.

### 6.4.3 Fire Test

Changes observed in terms of weight loss and change in compressive strength after exposure to fire attack are discussed in this section.

#### 6.4.3.1 Mass Loss

The mass loss for WG concrete mixes after exposure to varied temperature (from room temperature to 800°C) was measured and reported in **Fig. 6.37**. Increase in mass has been examined for WG incorporated concrete mixes up to 400°C, whereas control mix samples display reduction in mass. Due to lower water absorption capacity of WG early departure of capillary water makes concrete more compact, thus results into increase in mass as compared to control mix samples (Terro (2006)).

Above 400°C mass loss is be due to chemically bound water due to deterioration of hydration products (Demirel and Keleştemur (2010)). Cooling of concrete cubes to

room temperatures before measuring mass might change the properties of WG from softer and viscous form to solid state (Terro (2006)). This results into lower reduction mass at 800°C even at 22% substitution level as compared to control concrete. At higher substitution levels, mass loss for WG concrete was in-line with control concrete.

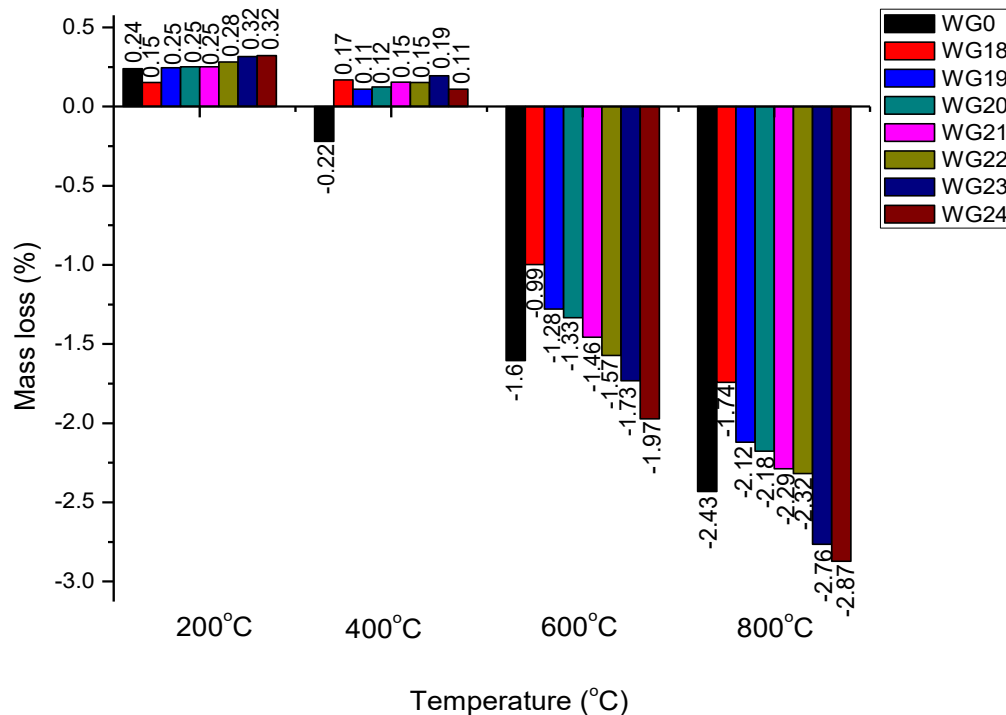


Fig. 6.37: Mass loss of waste glass concrete specimens exposed to fire

#### 6.4.3.2 Compressive Strength

The variation in compressive strength for with and without WG concrete samples have been observed and reported in Fig. 6.38 after exposed to fire at different temperature (200°C, 400°C, 600°C and 800°C). It has been observed that WG incorporated concrete samples shows better performance after exposure to extreme temperature conditions. Increase in compressive strength has been monitored up to 400°C for WG concrete mixes as compared to control sample which illustrates negative performance at 400°C. This hike in compressive strength is due to lower water absorption of WG. Hence, there is lesser amount of water trapped inside mixes with WG. Therefore, on heating lesser amount of pore pressure developed internally. Hence, up to 400°C there is greater compressive resistance up to 20% substitution level.

With rise in temperature decrease in compressive strength has been observed for 600 - 800°C, however the functioning of WG concrete mixes are better than control mix. This might be due to melting of WG which converts its property from solid to viscous. At

viscous form gradation size of WG dominates (Terro (2006)). Since, cubes are allowed to cool at room temperature before compressive test was performed which changes the characteristic of WG from viscous to solid state. During viscous state WG particles fills the voids more uniformly which improves the performance of WG concrete mixes as compared to WG0 sample. At 800°C no other compound was formed other than decomposition of CSH gel to wollastonite ( $\text{CaSiO}_3$ ) and same has been detected through XRD analysis as shown in **Fig. 6.39**.

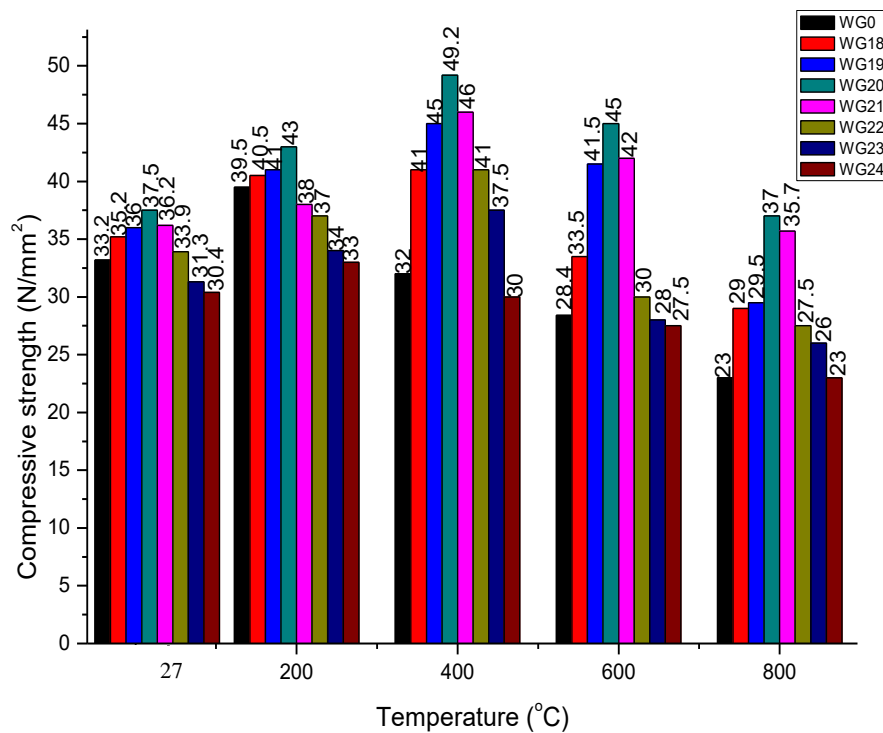
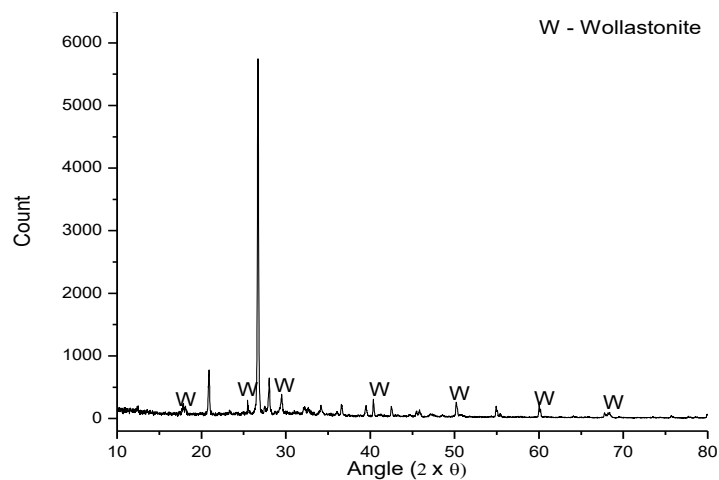
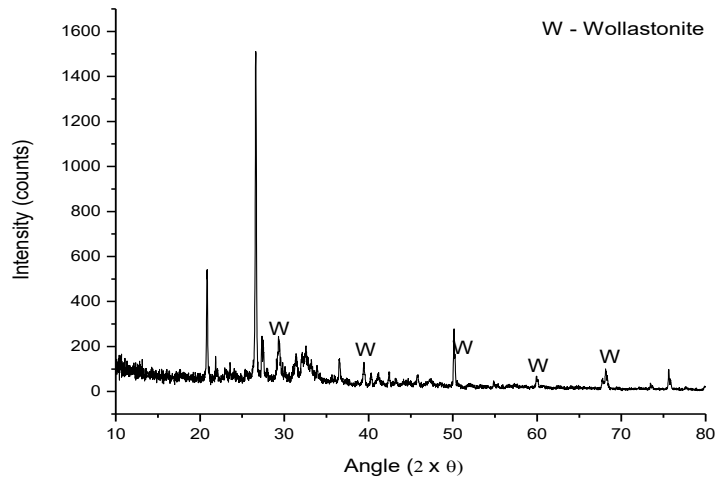


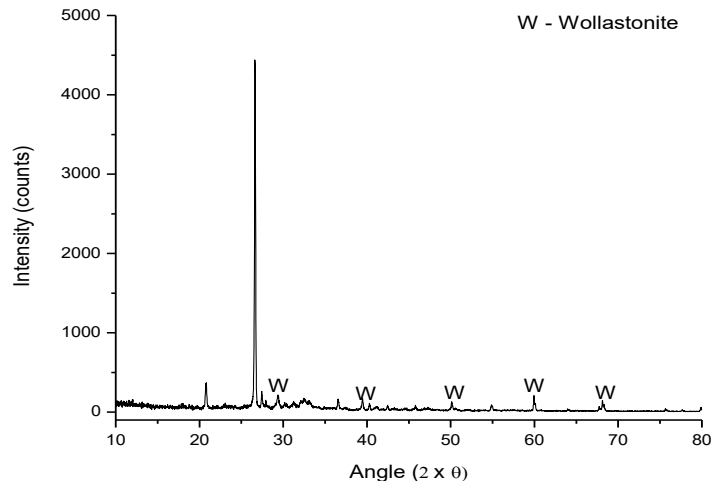
**Fig. 6.38:** Compressive strength of waste glass concrete specimens exposed to fire



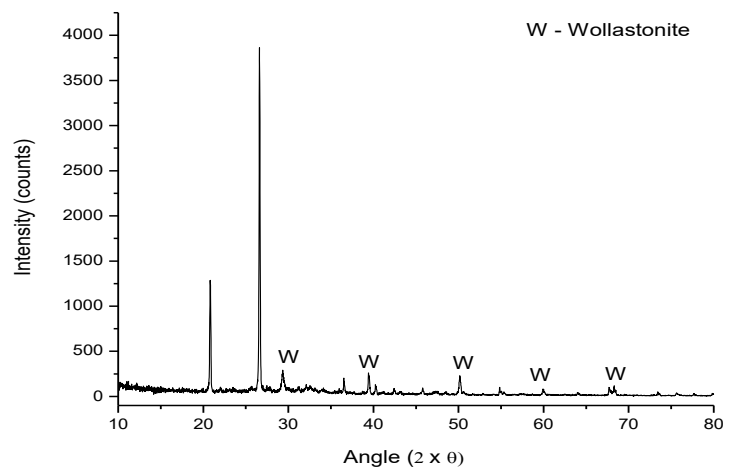
**(a) WG0**



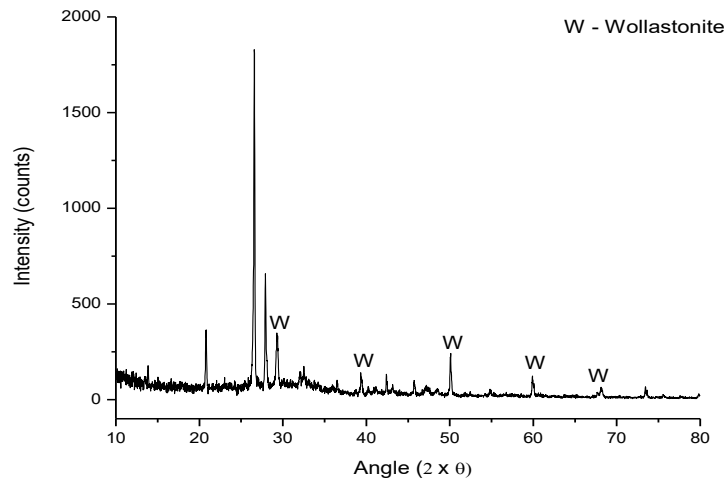
(b) WG18



(c) WG20



(d) WG22



(e) WG24

Fig. 6.39: XRD analysis of waste glass samples exposed to 800°C

### 6.5 Concluding Remarks

In this chapter, long term durability properties were discussed with incorporation of CR and WG individually as fine aggregate in concrete mixes. Various tests on specimens of CR and WG concrete were performed individually to study the effect of corrosion, acid attack and fire exposure. Under these exposure conditions concrete samples show promising results.

---

**CONCLUSIONS & FUTURE SCOPE**

---

**7.1 Summary**

This investigation shows in-depth study on consumption of waste rubber and waste glass individually as fine aggregate at various substitution level in concrete mixes. In the present work M25 grade of concrete mix was prepared using single water / cement ratio (0.4). Waste rubber was utilized in the form of crumb rubber (CR) (600 $\mu$ ) which was produced by mechanical grinding of scrap tyre rubber. The formed CR was substituted with fine aggregate from 4% – 5.5% at an increment of 0.5%. In case of waste glass (WG), mixed coloured beverage bottles were mechanically crushed and particles having size between 150 - 600 $\mu$  were used. The substitution of fine aggregate from WG was used in concrete mixes at varying proportions from 18 –24% in steps of 1%.

Necessary tests were conducted to evaluate the behaviour of concrete mixes. Fresh property was observed by conducting workability (compaction factor) and fresh density. Mechanical performance of concrete was noticed by performing compressive, flexural strength and pull-off tests. Durability studies include water absorption (immersion, under pressure and capillary rise), chloride attack (immersion and corrosion), acid attack, carbonation and abrasion resistance were verified. These samples were also checked when exposed to fire attack and rapid freezing and thawing action. In addition to this, microstructural properties of prepared composites were also investigated through X-ray Diffraction (XRD), Field Emission Scanning Electron Microscopy (FESEM), Thermal Gravimetric Analysis / Differential Thermal Analysis (TGA / DTA), Fourier Transform Infrared Spectroscopy (FTIR) and Atomic Force Microscopy (AFM). From above section of results and discussions comprehending inferences can be drawn.

**7.2 Conclusions****7.2.1 Part – A: Crumb Rubber**

1. Due to fineness of crumb rubber the workability and fresh density of crumb rubber concrete decreases with increase in crumb rubber content.
2. Compressive strength in case of crumb rubber concrete decreases as the quantity of crumb rubber increases. This is due to lower adhesion between rubber and

- cement paste which results in rapid rupture of concrete at the time of loading. This change in compressive strength was also justified by conducting using FESEM.
3. Flexural strength shows reduction with an addition in the proportion of crumb rubber content. This is due to presence of cracks at ITZ which causes weak bonding between the constituent materials.
  4. The hardened density of CR concrete decreases with increase in replacement level. This might be due to increase in porosity of the concrete along with lower specific gravity of crumb rubber as compared to fine aggregates.
  5. The depth of wear increases as the proportion of CR in concrete increases. This decrease in abrasion resistance is due to lower adhesion between CR and cement paste. The depth of wear measured for 5.5% crumb rubber in concrete is lesser than permissible limits as per codal provisions.
  6. Water absorption (immersion, under constant pressure and capillary action) of CR concrete increases with increase in substitution level. The generation of voids and cracks due to larger surface area of CR has led to greater water penetration.
  7. CR particles enhances the drying shrinkage due to increase in elasticity which reduces the internal restraints.
  8. Freezing and thawing exposure shows better performance with inclusion of CR in concrete mixes due to its elastic nature. The change in compressive strength with CR incorporated concrete is 11.68% at 5.5% substitution level as compared to 26.41% for control sample.
  9. The samples exposed to simulated saline environment (immersion and diffusion) shows lower penetration of chloride ion up to 4.5% substitution level beyond which it increases. The decrease in penetration was due to binding of chloride ions by cement. Due to this reaction reduced corrosion was monitored after exposure for 12 months the recorded half-cell potential value is less than 350 mV.
  10. Increased carbonation was noticed with inclusion of CR in concrete mixes. This is because, increase in porosity of concrete mixes which enhances the penetration of carbon dioxide.
  11. The extent of decline in weight and compressive strength has been reduced with inclusion of CR in concrete mixes after exposure to acidic medium. This is due to quick reaction of CR with sulphuric acid which impart adhesiveness, whereas, in control mix ettringite and gypsum were observed which leads to deterioration of

concrete samples. From microstructure it has been observed that CR act as sacrificial material in concrete mixes.

12. Decrease in mass loss and compressive strength was noticed with inclusion of CR when exposed to elevated temperature. It has also been verified through XRD analysis that disintegration of CSH results into formation of wollastonite which reduces the strength of concrete samples.

### **7.2.2 Part – B: Waste Glass**

1. The workability of WG concrete for different proportions decreases with increase in WG content. This decrease in workability is due to sharp edges of WG.
2. On evaluation of compressive strength 21% replacement level of fine aggregate by WG produced the highest performance when compared to control concrete which is despite the increase in void content. This rise also had a denser impermeable pore space which can be credited to the improvement of compressive resistance. However, there is slight increase in crystallization of Portlandite which can be a consequence of better hydration. Micro-structural analysis shows strong interfacial bonding between cement paste and aggregates. Hairline cracks and voids are also seen at the interface, which result in reduction of strength at higher substitution levels of WG.
3. Flexural strength increases for WG concrete up to the same substitution level as mentioned for compressive strength. As seen from FESEM images this increase in flexural strength is due to stronger ITZ.
4. The bulk density of WG concrete decreases as the percentage of replacement level increases. This is the consequence of lower specific gravity of WG.
5. When subjected to abrasion, depth of wear decreases as the proportion of WG in concrete increases. This decrease in abrasion resistance is due to increased adhesion between WG and cement paste up to 21% substitution level.
6. Increase in water absorption (due to immersion), water permeability (at constant pressure) and sorptivity (capillarity rise) of WG concrete has been observed when compared with control concrete. Fine nature of WG leads to generation of permeable pores, which has increased these water absorption characteristics of concrete samples. Also, penetration of water in concrete mix also lies in range of medium permeability as per DIN 1048 (1991).



7. WG particles increase the drying shrinkage at initial stage due to increased water content as a consequence of lower water absorption. However, reduced shrinkage was noticed during later ages for WG incorporated concrete mixes.
8. Inclusion of WG in concrete mixes shows better performance under Freezing and thawing exposure. Concrete mixes shows 22% reduction at 20% substitution level as compared to 26.41% for control sample. However, at 21% shows similar reduction as recorded for control samples. This improved resistance was due to greater initial compressive strength, porosity and. apparent density.
9. The specimens under exposure to simulated saline medium (immersion) presents lower penetration of chloride ions up to 24% substitution level when compared with control mix. This fall in penetration was due to binding action of chloride ions with cement.
10. The specimens exposed to accelerated carbonation attack shows that it is least detrimental up to 20% substitution level. This is due to formation of calcium carbonate which reduces the porosity of concrete mixes and hence prevents further penetration of carbon dioxide.
11. The extent of fall in weight and compressive strength has been reduced with introduction of WG in concrete mixes after exposure to acidic medium. This is due to lower resistivity of WG with sulphuric acid whereas, in control mix ettringite and gypsum were observed, which leads to deterioration of concrete samples. Microstructural analysis also proves that WG act as sacrificial material in concrete mixes.
12. Fall in mass loss and compressive strength was noticed with inclusion of WG when exposed to elevated temperature. It has also been verified through XRD analysis that disintegration of CSH results into formation of wollastonite which reduces the strength of concrete samples.

To summarize the effect of CR on mechanical and durability properties of PPC concrete mixes show healthier performance at 4% substitution level which is comparable with 2.5% replacement in OPC cement concretes. On verifying the durability aspects, at 4% substitution level the residual mechanical performance is far better than control concrete mixes. In line with these results chloride exposure, effect of carbonation also leaves a positive benchmark at this substitution level. Hence, inclusion has been limited

to 4% only. Similar experimental studies were conducted for WG concrete mixes where inclusion of WG proves an optimum substitution level of 21% to be the most beneficial.

Conclusions reported from experimental study shows that fine aggregate can be substituted by CR and WG individually. CR and WG concrete mixes can be used for constructing infill walls (reduced hardened density), can be utilized near to chemical industries where acid rain can occur and with increased resistance towards freezing and thawing action can be employed in cold area.

### **7.3 Future Scope**

1. Effect of crumb rubber and waste glass individually in bi-materials.
2. Test like salt crystallization on concrete specimens under simulated environmental conditions may be executed to understand the performance of these materials.
3. Characterizations like Mercury Intrusion Porosimetry (MIP) and NMR can be conducted on concrete samples (rubber and glass) for better understanding.
4. Behaviour of impact and fatigue on crumb rubber and waste glass concrete mixes.

**Table 7.1: List of concluding results**

SNNo.	Property	Crumb Rubber	Reason	Waste Glass	Reason
1	<b>Workability</b>	Decreases	CR high surface area	Decreases	WG sharp edges
2	<b>Fresh Bulk Density</b>	Decreases	CR lower specific gravity	Decreases	WG lower specific gravity
3	<b>Compressive Strength</b>	Decreases	Lower adhesion CR & cement	Increase up to 21% Beyond 21% decreases	Denser impermeable pores Cracks and voids
4	<b>Hardened Density</b>	Decreases	Increase in porosity	Decreases	WG lower specific gravity
5	<b>Flexural Strength</b>	Decreases	Cracks at ITZ	Increase up to 21% Beyond 21% decreases	Stronger ITZ Cracks
6	<b>Abrasion Resistance</b>	Decreases	Lower adhesion CR & cement	Increases up to 20%	Improved apparent density
7	<b>Pull-off Strength</b>	Approximately same up to 4.5%	Cracks at ITZ	Approximately same up to 21%	Improved mechanical performance
8	<b>Water Absorption</b> 8.1 Immersion 8.2 Constant Pressure 8.3 Capillary Action	Increases	Generation of voids & cracks	Increases	Generation of voids & cracks
9	<b>Drying Shrinkage</b>	Increases	Increase in elasticity	Decreases	WG higher stiffness
10	<b>Freeze and Thaw</b> 10.1 Mass Loss 10.2 Compressive Strength	Better performance up to 5.5%	Elastic property of rubber Void content	Better performance up to 21%	Improved apparent density

11	<b>Chloride Penetration</b> <b>Half-cell Potential</b>	Lower penetration up to 4.5% Corrosion reduced	Binding of chloride ions with cement	Lower penetration up to 24% Corrosion reduced	Binding of chloride ions with cement
12	<b>Carbonation</b>	Increases	Increase in porosity	Decrease up to 20%	Formation of calcium carbonate
13	<b>Acid Attack</b> <b>13.1 Mass Loss</b> <b>13.2 Compressive Strength</b>	Better performance	CR act sacrificially	Better performance	Lower resistivity of WG
14	<b>Fire Attack</b> <b>14.1 Mass Loss</b> <b>14.2 Compressive Strength</b>	Positive effect up to 200°C	CR starts melting after 200°C	Positive effect up to 400°C	Conversion of state of WG from solid to viscous then solid

## REFERENCES

- Ababneh, A.N., 2002. The coupled effect of moisture diffusion chloride penetration and freezing-thawing on concrete durability. Ph.D. Diss. Univ. Color. Boulder, Co. 207.
- Aiello, M.A., Leuzzi, F., 2010. Waste tyre rubberized concrete: Properties at fresh and hardened state. *Waste Manag.* 30, 1696–1704. <https://doi.org/10.1016/j.wasman.2010.02.005>
- AIGFM, 2011. Government & NGO Support in Glass Re-cycling.
- Akçaözoğlu, K., 2013. Microstructural examination of concrete exposed to elevated temperature by using plane polarized transmitted light method. *Constr. Build. Mater.* 48, 772–779. <https://doi.org/10.1016/j.conbuildmat.2013.06.059>
- Al-Akhras, N.M., Smadi, M.M., 2004. Properties of tire rubber ash mortar. *Cem. Concr. Compos.* 26, 821–826. <https://doi.org/10.1016/j.cemconcomp.2004.01.004>
- Al-Tayeb, M.M., Abu Bakar, B.H., Ismail, H., Akil, H.M., 2013. Effect of partial replacement of sand by recycled fine crumb rubber on the performance of hybrid rubberized-normal concrete under impact load: Experiment and simulation. *J. Clean. Prod.* 59, 284–289. <https://doi.org/10.1016/j.jclepro.2013.04.026>
- Araghi, H.J., Nikbin, I.M., Reskati, S.R., Rahmani, E., Allahyari, H., 2015. An experimental investigation on the erosion resistance of concrete containing various PET particles percentages against sulfuric acid attack. *Constr. Build. Mater.* 77, 461–471. <https://doi.org/10.1016/j.conbuildmat.2014.12.037>
- Arliguie, G., Ollivier, J.P., Grandet, J., 1982. Etude de l'effet retardateur du zinc sur l'hydratation de la pate de ciment Portland. *Cem. Concr. Res.* 12, 79–86. [https://doi.org/10.1016/0008-8846\(82\)90101-6](https://doi.org/10.1016/0008-8846(82)90101-6)
- ASTM C 642, 2008. Standard Test Method for Density , Absorption , and Voids in Hardened Concrete. United States: American Society for Testing and Material. <https://doi.org/10.1520/C0642-13.5>.
- ASTM C157, 2016. Standard Test Method for Length Change of Hardened Hydraulic-Cement Mortar and Concrete. Annual Book of ASTM Standards. <https://doi.org/10.1520/C0157>
- ASTM C1585-13, 2013. Standard Test Method for Measurement of Rate of Absorption of Water by Hydraulic Cement Concretes. ASTM International. <https://doi.org/10.1520/C1585-13.2>
- ASTM C267, 1997. Standard Test Methods for Chemical Resistance of Mortars. *Astm i*, 2–7. <https://doi.org/10.1520/C1106-00R12.2>
- ASTM C311, 2003. Standard Test Methods for Sampling and Testing Fly Ash or Natural Pozzolans for Use. *Glass 04*, 1–9. <https://doi.org/10.1520/C0311>
- ASTM C666, 2003. Standard Test Method for Resistance of Concrete to Rapid Freezing and Thawing 1. ASTM C 666 1–6.

- ASTM C876, 2015. ASTM Standard C876. Stand. Test Method Corros. Potentials Uncoated Reinf. Steel Concr. 1–8. <https://doi.org/10.1520/C0876-15.2>
- Avirneni, D., Peddinti, P.R.T., Saride, S., 2016. Durability and long term performance of geopolymer stabilized reclaimed asphalt pavement base courses. *Constr. Build. Mater.* 121, 198–209. <https://doi.org/10.1016/j.conbuildmat.2016.05.162>
- Azevedo, F., Pacheco-Torgal, F., Jesus, C., Barroso De Aguiar, J.L., Camões, A.F., 2012. Properties and durability of HPC with tyre rubber wastes. *Constr. Build. Mater.* 34, 186–191. <https://doi.org/10.1016/j.conbuildmat.2012.02.062>
- Batayneh, M., Marie, I., Asi, I., 2007. Use of selected waste materials in concrete mixes. *Waste Manag.* 27, 1870–1876. <https://doi.org/10.1016/j.wasman.2006.07.026>
- Batayneh, M.K., Marie, I., Asi, I., 2008. Promoting the use of crumb rubber concrete in developing countries. *Waste Manag.* 28, 2171–2176. <https://doi.org/10.1016/j.wasman.2007.09.035>
- Belarbi, A., Dawood, M., Acun, B., 2016. Sustainability of fiber-reinforced polymers (FRPs) as a construction material, Second Edition. ed, Sustainability of Construction Materials. Elsevier Ltd. <https://doi.org/10.1016/B978-0-08-100370-1.00020-2>
- Benazzouk, A., Douzane, O., Langlet, T., Mezreb, K., Roucoult, J.M., Quéneudec, M., 2007. Physico-mechanical properties and water absorption of cement composite containing shredded rubber wastes. *Cem. Concr. Compos.* 29, 732–740. <https://doi.org/10.1016/j.cemconcomp.2007.07.001>
- Benazzouk, A., Mezreb, K., Doyen, G., Goullieux, A., Quéneudec, M., 2003. Effect of rubber aggregates on the physico-mechanical behaviour of cement-rubber composites-influence of the alveolar texture of rubber aggregates. *Cem. Concr. Compos.* 25, 711–720. [https://doi.org/10.1016/S0958-9465\(02\)00067-7](https://doi.org/10.1016/S0958-9465(02)00067-7)
- Bjegović, D., Baričević, A., Serdar, M., 2011. Durability properties of concrete with recycled waste tyres. *Int. Conf. Durab. Build. Mater. Compos.* 1659–1667.
- Borhan, T.M., 2012. Properties of glass concrete reinforced with short basalt fibre. *Mater. Des.* 42, 265–271. <https://doi.org/10.1016/j.matdes.2012.05.062>
- Bravo, M., De Brito, J., 2012. Concrete made with used tyre aggregate: Durability-related performance. *J. Clean. Prod.* 25, 42–50. <https://doi.org/10.1016/j.jclepro.2011.11.066>
- BS 1881, 2003. Testing concrete — Recommendations for the Assessment of Concrete Strength by Near- to - Surface Tests. Bureau of Indian Standards, New Delhi.
- Bulatović, V., Melešev, M., Radeka, M., Radonjanin, V., Lukić, I., 2017. Evaluation of sulfate resistance of concrete with recycled and natural aggregates. *Constr. Build. Mater.* 152, 614–631. <https://doi.org/10.1016/j.conbuildmat.2017.06.161>
- By, O., Khatib, Z.K., Bayomy, F.M., 1999. *R p c c* 11, 206–213.
- Chen, C.H., Huang, R., Wu, J.K., Yang, C.C., 2006. Waste E-glass particles used in cementitious mixtures. *Cem. Concr. Res.* 36, 449–456. <https://doi.org/10.1016/j.cemconres.2005.12.010>

- Choudhary, H.K., Anupama, A. V., Kumar, R., Panzi, M.E., Matteppanavar, S., Sherikar, B.N., Sahoo, B., 2015. Observation of phase transformations in cement during hydration. *Constr. Build. Mater.* 101, 122–129. <https://doi.org/10.1016/j.conbuildmat.2015.10.027>
- Corinaldesi, V., Gnappi, G., Moriconi, G., Montenero, A., 2005. Reuse of ground waste glass as aggregate for mortars. *Waste Manag.* 25, 197–201. <https://doi.org/10.1016/j.wasman.2004.12.009>
- Correia, J.R., Marques, A.M., Pereira, C.M.C., Brito, J. De, 2012. Fire reaction properties of concrete made with recycled rubber aggregate. <https://doi.org/10.1002/fam>
- Dasgupta, T., 2014. Composition of Municipal Solid Waste Generation and Recycling Scenario of Building Materials 1264, 1259–1264.
- De Castro, S., De Brito, J., 2013. Evaluation of the durability of concrete made with crushed glass aggregates. *J. Clean. Prod.* 41, 7–14. <https://doi.org/10.1016/j.jclepro.2012.09.021>
- Demirel, B., Keleştemur, O., 2010. Effect of elevated temperature on the mechanical properties of concrete produced with finely ground pumice and silica fume. *Fire Saf. J.* 45, 385–391. <https://doi.org/10.1016/j.firesaf.2010.08.002>
- DIN 1048, 1991. Testing concrete; testing of hardened concrete (specimens prepared in mould). German Institute for Standardisation (Deutsches Institut für Normung).
- Dong, J.F., Wang, Q.Y., Guan, Z.W., 2013. Structural behaviour of recycled aggregate concrete filled steel tube columns strengthened by CFRP. *Eng. Struct.* 48, 532–542. <https://doi.org/10.1016/j.engstruct.2012.11.006>
- Dong, Q., Huang, B., Shu, X., 2013. Rubber modified concrete improved by chemically active coating and silane coupling agent. *Constr. Build. Mater.* 48, 116–123. <https://doi.org/10.1016/j.conbuildmat.2013.06.072>
- Du, H., Tan, K.H., 2014a. Effect of particle size on alkali-silica reaction in recycled glass mortars. *Constr. Build. Mater.* 66, 275–285. <https://doi.org/10.1016/j.conbuildmat.2014.05.092>
- Du, H., Tan, K.H., 2014b. Concrete with recycled glass as fine aggregates. *ACI Mater. J.* 111, 47–57. <https://doi.org/10.14359/51686446>
- Eldin, N.N., Senouci, A.B., 1994. Measurement and prediction of the strength of rubberized concrete. *Cem. Concr. Compos.* 16, 287–298. [https://doi.org/10.1016/0958-9465\(94\)90041-8](https://doi.org/10.1016/0958-9465(94)90041-8)
- Ganesan, N., Bharati Raj, J., Shashikala, A.P., 2013. Flexural fatigue behavior of self compacting rubberized concrete. *Constr. Build. Mater.* 44, 7–14. <https://doi.org/10.1016/j.conbuildmat.2013.02.077>
- Ganjian, E., Khorami, M., Maghsoudi, A.A., 2009. Scrap-tyre-rubber replacement for aggregate and filler in concrete. *Constr. Build. Mater.* 23, 1828–1836. <https://doi.org/10.1016/j.conbuildmat.2008.09.020>
- Gautam, S.P., Srivastava, V., Agarwal, V.C., 2012. Use of glass wastes as fine aggregate

- in Concrete 1, 320–322.
- Gesoğlu, M., Güneyisi, E., 2007. Strength development and chloride penetration in rubberized concretes with and without silica fume. *Mater. Struct. Constr.* 40, 953–964. <https://doi.org/10.1617/s11527-007-9279-0>
- Gesoğlu, M., Güneyisi, E., Khoshnaw, G., Ipek, S., 2014. Investigating properties of pervious concretes containing waste tire rubbers. *Constr. Build. Mater.* 63, 206–213. <https://doi.org/10.1016/j.conbuildmat.2014.04.046>
- Grinys, A., Sivilevičius, H., Daukšys, M., 2012. Tyre Rubber Additive Effect on Concrete Mixture Strength. *J. Civ. Eng. Manag.* 18, 393–401. <https://doi.org/10.3846/13923730.2012.693536>
- Güneyisi, E., Gesoğlu, M., Özturan, T., 2004. Properties of rubberized concretes containing silica fume. *Cem. Concr. Res.* 34, 2309–2317. <https://doi.org/10.1016/j.cemconres.2004.04.005>
- Güneyisi, E., Mermerdaş, K., 2007. Comparative study on strength, sorptivity, and chloride ingress characteristics of air-cured and water-cured concretes modified with metakaolin. *Mater. Struct. Constr.* 40, 1161–1171. <https://doi.org/10.1617/s11527-007-9258-5>
- Guo, Y.C., Zhang, J.H., Chen, G.M., Xie, Z.H., 2014. Compressive behaviour of concrete structures incorporating recycled concrete aggregates, rubber crumb and reinforced with steel fibre, subjected to elevated temperatures. *J. Clean. Prod.* 72, 193–203. <https://doi.org/10.1016/j.jclepro.2014.02.036>
- Gupta, T., Chaudhary, S., Sharma, R.K., 2014. Assessment of mechanical and durability properties of concrete containing waste rubber tire as fine aggregate. *Constr. Build. Mater.* 73, 562–574. <https://doi.org/10.1016/j.conbuildmat.2014.09.102>
- Hernández-Olivares, F., Barluenga, G., 2004. Fire performance of recycled rubber-filled high-strength concrete. *Cem. Concr. Res.* 34, 109–117. [https://doi.org/10.1016/S0008-8846\(03\)00253-9](https://doi.org/10.1016/S0008-8846(03)00253-9)
- Idir, R., Cyr, M., Tagnit-Hamou, A., 2013. Use of fine glass as ASR inhibitor in glass aggregate mortars. *Cem. Concr. Res.* <https://doi.org/10.1016/j.conbuildmat.2009.12.030>
- Idir, R., Cyr, M., Tagnit-Hamou, A., 2010. Use of fine glass as ASR inhibitor in glass aggregate mortars. *Constr. Build. Mater.* 24, 1309–1312. <https://doi.org/10.1016/j.conbuildmat.2009.12.030>
- IS-4031 (Part V):1988, 1988. Methods of physical tests for hydraulic cement-determination of initial and final setting times. Bur. Indian Stand. New Delhi.
- IS:2386-7, 1963. Methods of Test for Aggregates for Concrete , Part VII : Alkali Aggregate Reactivity 8–11.
- IS:2386 (Part III), 1963. Method of Test for aggregate for concrete. Bur. Indian Stand. New Delhi (Reaffirmed 2002).
- IS:2386 (Part IV), 1963. Method of Test for aggregate for concrete. Bur. Indian Stand. New



Delhi (Reaffirmed 2002).

- IS:9103, 1999. Specification for Concrete Admixture BIS:9103-1999, New Delhi, India.
- IS 1199, 1959. Methods of Sampling and Analysis of Concrete. Bureau of Indian Standards, New Delhi.
- IS 1237, 2012. Cement Concrete Flooring Tiles - Specification. Bureau of Indian Standards, New Delhi.
- IS 1489 ( Part 1 ), 2015 Portland Pozzolana Cement — Specification Part 1 Fly Ash Based ( Fourth Revision ), New Delhi.
- IS 383, 2016. Coarse and Fine Aggregate for Concrete — Specification. Bureau of Indian Standards, New Delhi.
- IS 4031 ( Part 4 ), 1988. Indian Standard methods of physical tests for hydraulic cement.
- IS 516, 2004. IS 516 -1959: Method of Tests for Strength of Concrete. Bureau of Indian Standards, New Delhi.
- Ismail, M., Elgelany Ismail, M., Muhammad, B., 2011. Influence of elevated temperatures on physical and compressive strength properties of concrete containing palm oil fuel ash. *Constr. Build. Mater.* 25, 2358–2364. <https://doi.org/10.1016/j.conbuildmat.2010.11.034>
- Ismail, N., Nonaka, T., Noda, S., Mori, T., 1993. Effect of carbonation on microbial corrosion of concretes. *Doboku Gakkai Ronbunshu* 133–138. [https://doi.org/10.2208/jscej.1993.474\\_133](https://doi.org/10.2208/jscej.1993.474_133)
- Ismail, Z.Z., AL-Hashmi, E.A., 2009. Recycling of waste glass as a partial replacement for fine aggregate in concrete. *Waste Manag.* 29, 655–659. <https://doi.org/10.1016/j.wasman.2008.08.012>
- ISO 834, 1999. Fire-resistance tests — Elements of building construction 1999.
- Jamil, M., Kaish, A.B.M.A., Raman, S.N., Zain, M.F.M., 2013. Pozzolanic contribution of rice husk ash in cementitious system. *Constr. Build. Mater.* 47, 588–593. <https://doi.org/10.1016/j.conbuildmat.2013.05.088>
- Jani, Y., Hogland, W., 2014. Waste glass in the production of cement and concrete - A review. *J. Environ. Chem. Eng.* 2, 1767–1775. <https://doi.org/10.1016/j.jece.2014.03.016>
- Joseph, A., Dwayne, A., Stephen, L., 1997. Decreasing concrete sewer pipe degradation using admixtures. *Mater. Perform.* 36, 51–56.
- Jun, Z., Dongwei, H., Haoyu, C., 2011. Experimental and Theoretical Studies on Autogenous Shrinkage of Concrete at Early Ages. *Concrete* 23, 312–320. [https://doi.org/10.1061/\(ASCE\)MT.1943-5533.0000171](https://doi.org/10.1061/(ASCE)MT.1943-5533.0000171).
- Khaloo, A.R., Dehestani, M., Rahmatabadi, P., 2008. Mechanical properties of concrete containing a high volume of tire-rubber particles. *Waste Manag.* 28, 2472–2482. <https://doi.org/10.1016/j.wasman.2008.01.015>

- Khyaliya, R.K., Kabeer, K.I.S.A., Vyas, A.K., 2017. Evaluation of strength and durability of lean mortar mixes containing marble waste. *Constr. Build. Mater.* 147, 598–607. <https://doi.org/10.1016/j.conbuildmat.2017.04.199>
- Klopprogge, J.T., Schuiling, R.D., Ding, Z., Hickey, L., Wharton, D., Frost, R.L., 2002. Vibrational spectroscopic study of syngenite formed during the treatment of liquid manure with sulphuric acid. *Vib. Spectrosc.* 28, 209–221. [https://doi.org/10.1016/S0924-2031\(01\)00139-4](https://doi.org/10.1016/S0924-2031(01)00139-4)
- Kou, S.C., Poon, C.S., Chan, D., 2008. Influence of fly ash as a cement addition on the hardened properties of recycled aggregate concrete. *Mater. Struct.* 41, 1191–1201. <https://doi.org/10.1617/s11527-007-9317-y>
- KPMG, 2007. Glass and Ceramics market & opportunities. IBEF.
- Lee, G., Poon, C.S., Wong, Y.L., Ling, T.C., 2013. Effects of recycled fine glass aggregates on the properties of dry-mixed concrete blocks. *Constr. Build. Mater.* 38, 638–643. <https://doi.org/10.1016/j.conbuildmat.2012.09.017>
- Lee, S.T., Hooton, R.D., Jung, H.S., Park, D.H., Choi, C.S., 2008. Effect of limestone filler on the deterioration of mortars and pastes exposed to sulfate solutions at ambient temperature. *Cem. Concr. Res.* 38, 68–76. <https://doi.org/10.1016/j.cemconres.2007.08.003>
- Limbachiya, M.C., 2009. Bulk engineering and durability properties of washed glass sand concrete. *Constr. Build. Mater.* 23, 1078–1083. <https://doi.org/10.1016/j.conbuildmat.2008.05.022>
- Ling, T.C., Poon, C.S., 2013. Effects of particle size of treated CRT funnel glass on properties of cement mortar. *Mater. Struct. Constr.* 46, 25–34. <https://doi.org/10.1617/s11527-012-9880-8>
- Ling, T.C., Poon, C.S., 2011. Properties of architectural mortar prepared with recycled glass with different particle sizes. *Mater. Des.* 32, 2675–2684. <https://doi.org/10.1016/j.matdes.2011.01.011>
- Ling, T.C., Poon, C.S., Kou, S.C., 2011. Feasibility of using recycled glass in architectural cement mortars. *Cem. Concr. Compos.* 33, 848–854. <https://doi.org/10.1016/j.cemconcomp.2011.05.006>
- Liu, F., Zheng, W., Li, L., Feng, W., Ning, G., 2013. Mechanical and fatigue performance of rubber concrete. *Constr. Build. Mater.* 47, 711–719. <https://doi.org/10.1016/j.conbuildmat.2013.05.055>
- Malik, M.I., Bashir, M., Ahmad, S., Tariq, T., Chowdhary, U., 2013. Study of concrete involving use of waste glass as partial replacement of fine aggregates. *IOSR J. Eng.* 3, 2250–3021. <https://doi.org/10.9790/3021-031130615>
- Marques, A.M., Correia, J.R., De Brito, J., 2013. Post-fire residual mechanical properties of concrete made with recycled rubber aggregate. *Fire Saf. J.* 58, 49–57. <https://doi.org/10.1016/j.firesaf.2013.02.002>
- Mathew, N.M., 2010. Rubber products manufacturing industry in India : Current trends and future prospects, 7–10.

- Metwally, I.M., 2007. Investigations on the Performance of Concrete Made with Blended Finely Milled Waste Glass. *Adv. Struct. Eng.* 10, 47–53. <https://doi.org/10.1260/136943307780150823>
- Mohammed, B.S., Anwar Hossain, K.M., Eng Swee, J.T., Wong, G., Abdullahi, M., 2012. Properties of crumb rubber hollow concrete block. *J. Clean. Prod.* 23, 57–67. <https://doi.org/10.1016/j.jclepro.2011.10.035>
- Mollah, M.Y.A., Yu, W., Schennach, R., Cocke, D.L., 2000. A Fourier transform infrared spectroscopic investigation of the early hydration of Portland cement and the influence of sodium lignosulfonate. *Cem. Concr. Res.* 30, 267–273. [https://doi.org/10.1016/S0008-8846\(99\)00243-4](https://doi.org/10.1016/S0008-8846(99)00243-4)
- Monteny, J., De Belie, N., Vincke, E., Verstraete, W., Taerwe, L., 2001. Chemical and microbiological tests to simulate sulfuric acid corrosion of polymer-modified concrete. *Cem. Concr. Res.* 31, 1359–1365. [https://doi.org/10.1016/S0008-8846\(01\)00565-8](https://doi.org/10.1016/S0008-8846(01)00565-8)
- Monteny, J., Vincke, E., Beeldens, A., De Belie, N., Taerwe, L., Van Gemert, D., Verstraete, W., 2000. Chemical, microbiological, and in situ test methods for biogenic sulfuric acid corrosion of concrete. *Cem. Concr. Res.* 30, 623–634. [https://doi.org/10.1016/S0008-8846\(00\)00219-2](https://doi.org/10.1016/S0008-8846(00)00219-2)
- Mukul, 2010. Sustainable concrete with scrap tyre aggregate. *NBMCW* 1–17.
- Murari, K., Siddique, R., Jain, K.K., 2014. Use of waste copper slag, a sustainable material. *J. Mater. Cycles Waste Manag.* 17, 13–26. <https://doi.org/10.1007/s10163-014-0254-x>
- Nadeem, A., Memon, S.A., Lo, T.Y., 2014. The performance of Fly ash and Metakaolin concrete at elevated temperatures. *Constr. Build. Mater.* 62, 67–76. <https://doi.org/10.1016/j.conbuildmat.2014.02.073>
- Oikonomou, N., Mavridou, S., 2009. Improvement of chloride ion penetration resistance in cement mortars modified with rubber from worn automobile tires. *Cem. Concr. Compos.* 31, 403–407. <https://doi.org/10.1016/j.cemconcomp.2009.04.004>
- Oliveira, L.A.P. De, 2008. Mechanical and Durability Properties of Concrete with Ground Waste Glass Sand.
- Olmstead, W., Hamlin, H., 1990. Converting portions of the Los Angeles outfall sewer into a septic tank, *Eng. News.* <https://doi.org/10.1007/3-540-27710-2>
- Onuaguluchi, O., Panesar, D.K., 2014. Hardened properties of concrete mixtures containing pre-coated crumb rubber and silica fume. *J. Clean. Prod.* 82, 125–131. <https://doi.org/10.1016/j.jclepro.2014.06.068>
- Otsuki, N., Nagataki, S., Nakashita, K., 1993. Evaluation of the AgNO<sub>3</sub> solution spray method for measurement of chloride penetration into hardened cementitious matrix materials. *Constr. Build. Mater.* 7, 195–201. [https://doi.org/10.1016/0950-0618\(93\)90002-T](https://doi.org/10.1016/0950-0618(93)90002-T)
- Ozbay, E., Lachemi, M., Sevim, U.K., 2011. Compressive strength, abrasion resistance and energy absorption capacity of rubberized concretes with and without slag. *Mater. Struct. Constr.* 44, 1297–1307. <https://doi.org/10.1617/s11527-010-9701-x>

- Pacheco-Torgal, F., Ding, Y., Jalali, S., 2012. Properties and durability of concrete containing polymeric wastes (tyre rubber and polyethylene terephthalate bottles): An overview. *Constr. Build. Mater.* 30, 714–724. <https://doi.org/10.1016/j.conbuildmat.2011.11.047>
- Papadakis, V.G., Fardis, M.N., Vayenas, C.G., 1992. Hydration and carbonation of pozzolanic cements 89(2), 119–130.
- Pappu, A., Saxena, M., Asolekar, S.R., 2007. Solid wastes generation in India and their recycling potential in building materials. *Build. Environ.* 42, 2311–2320. <https://doi.org/10.1016/j.buildenv.2006.04.015>
- Park, S.B., Lee, B.C., Kim, J.H., 2004. Studies on mechanical properties of concrete containing waste glass aggregate. *Cem. Concr. Res.* 34, 2181–2189. <https://doi.org/10.1016/j.cemconres.2004.02.006>
- Pelisser, F., Zavarise, N., Longo, T.A., Bernardin, A.M., 2011. Concrete made with recycled tire rubber: Effect of alkaline activation and silica fume addition. *J. Clean. Prod.* 19, 757–763. <https://doi.org/10.1016/j.jclepro.2010.11.014>
- Penacho, P., De Brito, J., Rosário Veiga, M., 2014. Physico-mechanical and performance characterization of mortars incorporating fine glass waste aggregate. *Cem. Concr. Compos.* 50, 47–59. <https://doi.org/10.1016/j.cemconcomp.2014.02.007>
- Peng, G.F., Bian, S.H., Guo, Z.Q., Zhao, J., Peng, X.L., Jiang, Y.C., 2008. Effect of thermal shock due to rapid cooling on residual mechanical properties of fiber concrete exposed to high temperatures. *Constr. Build. Mater.* 22, 948–955. <https://doi.org/10.1016/j.conbuildmat.2006.12.002>
- Pereira, E., Medeiros, M.H.F. de, 2012. Ensaio de “Pull Off” para avaliar a resistência à compressão do concreto: uma alternativa aos ensaios normalizados no Brasil. *RIEM - IBRACON Struct. Mater. J.* 5, 757–780. <https://doi.org/10.1590/S1983-41952012000600003>
- R. Siddique, 2008. *Waste Materials and By-Products in Concrete*, Springer. Springer, Berlin, Heidelberg. [https://doi.org/https://doi.org/10.1007/978-3-540-74294-4\\_7](https://doi.org/https://doi.org/10.1007/978-3-540-74294-4_7)
- R. Vidya Sagar, B.K. Raghu Prasad (2012). Damage limit states of reinforced concrete beams subjected to incremental cyclic loading using relaxation ratio analysis of AE parameters. *Construction and Building Materials*, 35, 139–148.
- Raghavan, D., Huynh, H., Ferraris, C.F., 1998. Workability, mechanical properties, and chemical stability of a recycled tyre rubber-filled cementitious composite. *J. Mater. Sci.* 33, 1745–1752. <https://doi.org/10.1023/A:1004372414475>
- Rajabipour, F., Maraghechi, H., Fischer, G., 2010. Investigating the Alkali-Silica Reaction of Recycled Glass Aggregates in Concrete Materials. *J. Mater. Civ. Eng.* 22, 1201–1208. [https://doi.org/10.1061/\(ASCE\)MT.1943-5533.0000126](https://doi.org/10.1061/(ASCE)MT.1943-5533.0000126)
- Ramachandran, V.S., Feldman, R.F., Beaudoin, J.J., 1981. *Concrete science treatise on current Research*. London Heyden Son Ltd. Philadelphia, USA 317.
- Rashad, A.M., 2014. Recycled waste glass as fine aggregate replacement in cementitious

- materials based on Portland cement. *Constr. Build. Mater.* 72, 340–357. <https://doi.org/10.1016/j.conbuildmat.2014.08.092>
- Raupach, M., 1996. Chloride-induced macrocell corrosion of steel in concrete - Theoretical background and practical consequences. *Constr. Build. Mater.* 10, 329–338. [https://doi.org/10.1016/0950-0618\(95\)00018-6](https://doi.org/10.1016/0950-0618(95)00018-6)
- Richardson, A.E., Coventry, K.A., Ward, G., 2012. Freeze / thaw protection of concrete with optimum rubber crumb content. *J. Clean. Prod.* 23, 96–103. <https://doi.org/10.1016/j.jclepro.2011.10.013>
- RILEM CPC 18, 1988. Measurement of hardened concrete carbonation depth.
- Roy, S.K., Poh, K.B., Northwood, D. o., 1999. Durability of concrete—accelerated carbonation and weathering studies. *Build. Environ.* 34, 597–606. [https://doi.org/10.1016/S0360-1323\(98\)00042-0](https://doi.org/10.1016/S0360-1323(98)00042-0)
- Samson, E., Marchand, J., 2007. Modeling the transport of ions in unsaturated cement-based materials. *Comput. Struct.* 85, 1740–1756. <https://doi.org/10.1016/j.compstruc.2007.04.008>
- Segre, N., Joekes, I., 2000. Use of tire rubber particles as addition to cement paste. *Cem. Concr. Res.* 30, 1421–1425. [https://doi.org/10.1016/S0008-8846\(00\)00373-2](https://doi.org/10.1016/S0008-8846(00)00373-2)
- Sha, W., O’Neill, E.A., Guo, Z., 1999. Differential scanning calorimetry study of ordinary Portland cement. *Cem. Concr. Res.* 29, 1487–1489. [https://doi.org/10.1016/S0008-8846\(99\)00128-3](https://doi.org/10.1016/S0008-8846(99)00128-3)
- Shah, S.G., Ray, S., Chandra Kishen, J.M., 2014. Fatigue crack propagation at concrete-concrete bi-material interfaces. *Int. J. Fatigue* 63, 118–126. <https://doi.org/10.1016/j.ijfatigue.2014.01.015>
- Shao, Y., Lefort, T., Moras, S., Rodriguez, D., 2000. Studies on concrete containing ground waste glass. *Cem. Concr. Res.* 30, 91–100. [https://doi.org/10.1016/S0008-8846\(99\)00213-6](https://doi.org/10.1016/S0008-8846(99)00213-6)
- Siddique, S., Shrivastava, S., Chaudhary, S., 2017. Lateral force microscopic examination of interfacial transition zone in ceramic concrete. *Constr. Build. Mater.* 155, 688–725. <https://doi.org/10.1016/j.conbuildmat.2017.08.080>
- Simon, K., Chandra, K., 2016. Effects of Microcracks in the Interfacial Zone on the Macro Behavior of Concrete. *Proc. 9th Int. Conf. Fract. Mech. Concr. Concr. Struct.* <https://doi.org/10.21012/FC9.074>
- Singh, S., Khan, S., Khandelwal, R., Chugh, A., Nagar, R., 2016. Performance of sustainable concrete containing granite cutting waste. *J. Clean. Prod.* 119, 86–98. <https://doi.org/10.1016/j.jclepro.2016.02.008>
- Sivakumar Babu, G.L., Chouksey, S.K., Reddy, K.R., 2013. Approach for the use of MSW settlement predictions in the assessment of landfill capacity based on reliability analysis. *Waste Manag.* 33, 2029–2034. <https://doi.org/10.1016/j.wasman.2013.05.018>
- Skariah, B., Chandra, R., Kalla, P., Cseteneyi, L., 2014. Strength , abrasion and permeation

- characteristics of cement concrete containing discarded rubber fine aggregates. *Constr. Build. Mater.* 59, 204–212. <https://doi.org/10.1016/j.conbuildmat.2014.01.074>
- Son, K.S., Hajirasouliha, I., Pilakoutas, K., 2011. Strength and deformability of waste tyre rubber-filled reinforced concrete columns. *Constr. Build. Mater.* 25, 218–226. <https://doi.org/10.1016/j.conbuildmat.2010.06.035>
- Su, H., Yang, J., Ling, T.C., Ghataora, G.S., Dirar, S., 2015. Properties of concrete prepared with waste tyre rubber particles of uniform and varying sizes. *J. Clean. Prod.* 91, 288–296. <https://doi.org/10.1016/j.jclepro.2014.12.022>
- Su, N., Chen, J.S., 2002. Engineering properties of asphalt concrete made with recycled glass. *Resour. Conserv. Recycl.* 35, 259–274. [https://doi.org/10.1016/S0921-3449\(02\)00007-1](https://doi.org/10.1016/S0921-3449(02)00007-1)
- Sukontasukkul, P., Chaikaew, C., 2006. Properties of concrete pedestrian block mixed with crumb rubber. *Constr. Build. Mater.* 20, 450–457. <https://doi.org/10.1016/j.conbuildmat.2005.01.040>
- Sukontasukkul, P., Tiamlom, K., 2012. Expansion under water and drying shrinkage of rubberized concrete mixed with crumb rubber with different size. *Constr. Build. Mater.* 29, 520–526. <https://doi.org/10.1016/j.conbuildmat.2011.07.032>
- Syed, a D.P., Quadri, R., 2013. Effective Utilization of Crusher Dust in Concrete Using Portland Pozzolana Cement. *Int. J. Sci. Res. Publ.* 3, 1–10.
- Taha, B., Nounu, G., 2009. Utilizing Waste Recycled Glass as Sand/Cement Replacement in Concrete. *J. Mater. Civ. Eng.* 21, 709–721. [https://doi.org/10.1061/\(ASCE\)0899-1561\(2009\)21:12\(709\)](https://doi.org/10.1061/(ASCE)0899-1561(2009)21:12(709))
- Taha, B., Nounu, G., 2008. Properties of concrete contains mixed colour waste recycled glass as sand and cement replacement. *Constr. Build. Mater.* 22, 713–720. <https://doi.org/10.1016/j.conbuildmat.2007.01.019>
- Taha, M.M.R., Asce, M., El-wahab, M.A.A., 2009. Mechanical , Fracture , and Microstructural Investigations 20, 640–649.
- Tan, K.H., Du, H., 2013. Use of waste glass as sand in mortar: Part i - Fresh, mechanical and durability properties. *Cem. Concr. Compos.* 35, 118–126. <https://doi.org/10.1016/j.cemconcomp.2012.08.028>
- Terro, M.J., 2006. Properties of concrete made with recycled crushed glass at elevated temperatures. *Build. Environ.* 41, 633–639. <https://doi.org/10.1016/j.buil.2005.02.018>
- Thomas, B.S., Gupta, R.C., Panicker, V.J., 2016. Recycling of waste tire rubber as aggregate in concrete: Durability-related performance. *J. Clean. Prod.* 112, 504–513. <https://doi.org/10.1016/j.jclepro.2015.08.046>
- Topçu, I.B., Canbaz, M., 2004. Properties of concrete containing waste glass. *Cem. Concr. Res.* 34, 267–274. <https://doi.org/10.1016/j.cemconres.2003.07.003>
- Turatsinze, A., Garros, M., 2008. On the modulus of elasticity and strain capacity of Self-Compacting Concrete incorporating rubber aggregates. *Resour. Conserv. Recycl.* 52, 1209–1215. <https://doi.org/10.1016/j.resconrec.2008.06.012>

- Turgut, P., Yahlizade, E.S., 2009. Research into Concrete Blocks with Waste Glass. *Int. J. Civ. Environ. Eng.* 1, 203–209.
- Turki, M., Zarrad, I., Bretagne, E., Quéneudec, M., 2012. Influence of Filler Addition on Mechanical Behavior of Cementitious Mortar-Rubber Aggregates: Experimental Study and Modeling. *J. Mater. Civ. Eng.* 24, 1350–1358. [https://doi.org/10.1061/\(ASCE\)MT.1943-5533.0000512](https://doi.org/10.1061/(ASCE)MT.1943-5533.0000512)
- Uygunoğlu, T., Topçu, I.B., 2010. The role of scrap rubber particles on the drying shrinkage and mechanical properties of self-consolidating mortars. *Constr. Build. Mater.* 24, 1141–1150. <https://doi.org/10.1016/j.conbuildmat.2009.12.027>
- V.Sanjeev Kumar, 2018. Stop rubber dumping ; set import price , says industry, Hindu News Paper. Hindu News Paper.
- Vedalakshmi, R., Rajagopal, K., Palaniswamy, N., 2008. Longterm corrosion performance of rebar embedded in blended cement concrete under macro cell corrosion condition. *Constr. Build. Mater.* 22, 186–199. <https://doi.org/10.1016/j.conbuildmat.2006.09.004>
- Vipulanandan, C., Amani, N., 2018. Characterizing the pulse velocity and electrical resistivity changes in concrete with piezoresistive smart cement binder using Vipulanandan models. *Constr. Build. Mater.* 175, 519–530. <https://doi.org/10.1016/j.conbuildmat.2018.04.196>
- Wang, H.Y., 2009. A study of the effects of LCD glass sand on the properties of concrete. *Waste Manag.* 29, 335–341. <https://doi.org/10.1016/j.wasman.2008.03.005>
- Wang, Y., Nanukuttan, S., Bai, Y., Basheer, P.A.M., 2017. Influence of combined carbonation and chloride ingress regimes on rate of ingress and redistribution of chlorides in concretes. *Constr. Build. Mater.* 140, 173–183. <https://doi.org/10.1016/j.conbuildmat.2017.02.121>
- Weeks, C., Hand, R.J., Sharp, J.H., 2008. Retardation of cement hydration caused by heavy metals present in ISF slag used as aggregate. *Cem. Concr. Compos.* 30, 970–978. <https://doi.org/10.1016/j.cemconcomp.2008.07.005>
- Wongkeo, W., Chaipanich, A., 2010. Compressive strength, microstructure and thermal analysis of autoclaved and air cured structural lightweight concrete made with coal bottom ash and silica fume. *Mater. Sci. Eng. A* 527, 3676–3684. <https://doi.org/10.1016/j.msea.2010.01.089>
- Xie, Z., Xiang, W., Xi, Y., 2003. ASR Potentials of Glass Aggregates in Water-Glass Activated Fly Ash and Portland Cement Mortars. *J. Mater. Civ. Eng.* 15, 67–74. [https://doi.org/10.1061/\(ASCE\)0899-1561\(2003\)15:1\(67\)](https://doi.org/10.1061/(ASCE)0899-1561(2003)15:1(67))
- Xue, J., Shinozuka, M., 2013. Rubberized concrete: A green structural material with enhanced energy-dissipation capability. *Constr. Build. Mater.* 42, 196–204. <https://doi.org/10.1016/j.conbuildmat.2013.01.005>
- Yilmaz, A., Degirmenci, N., 2009. Possibility of using waste tire rubber and fly ash with Portland cement as construction materials. *Waste Manag.* 29, 1541–1546. <https://doi.org/10.1016/j.wasman.2008.11.002>
- Yuksel, C., Ahari, R.S., Ahari, B.A., Ramyar, K., 2013. Evaluation of three test methods

for determining the alkali-silica reactivity of glass aggregate. *Cem. Concr. Compos.* 38, 57–64. <https://doi.org/10.1016/j.cemconcomp.2013.03.002>

Yung, W.H., Yung, L.C., Hua, L.H., 2013. A study of the durability properties of waste tire rubber applied to self-compacting concrete. *Constr. Build. Mater.* 41, 665–672. <https://doi.org/10.1016/j.conbuildmat.2012.11.019>

Zheng, L., Huo, X.S., Yuan, Y., 2008. Strength, Modulus of Elasticity, and Brittleness Index of Rubberized Concrete. *J. Mater. Civ. Eng.* 20, 692–699. [https://doi.org/10.1061/\(ASCE\)0899-1561\(2008\)20:11\(692\)](https://doi.org/10.1061/(ASCE)0899-1561(2008)20:11(692))

Zhu, X., Miao, C., Liu, J., Hong, J., 2012. Influence of crumb rubber on frost resistance of concrete and effect mechanism. *Procedia Eng.* 27, 206–213. <https://doi.org/10.1016/j.proeng.2011.12.445>



### **Brief Biodata of the Author**

**1. Name:** Kunal

**2. Address:** H.No 278/3 Jail Road, Mandi, Himachal Pradesh - 175001.

**Email:** kunal\_bisht@yahoo.co.in

**Phone:** +91-6350631706

### **3. Educational Qualifications**

1. B-tech (Civil Engineering with specialization in Infrastructure Development): University of Petroleum & Energy Studies, Dehradun, Uttarakhand.

2. M.E (Structural Engineering): Thapar University, Patiala, Punjab.

### **4. List of Publications**

#### **Journals - Published**

1. Kunal Bisht, P.V. Ramana.2017. "Evaluation of mechanical and durability properties of crumb rubber concrete." *Construction and Building Materials* 155 (2017) 811-817.
2. Kunal Bisht, P.V. Ramana.2018. "Sustainable production of concrete containing discarded beverage glass as fine aggregate." *Construction and Building Materials* 177 (2018) 116-124.
3. Kunal Bisht, and P.V. Ramana.2019. "Waste to resource conversion of crumb rubber for production of sulphuric acid resistant concrete." *Construction and Building Materials* 194 (2019) 276-286.

#### **Conferences-**

1. Kunal Bisht, P.V. Ramana, The waste materials as partial replacement of fine aggregate in concrete-outlet, Structural Engineering Convention (SEC-2016) CSIR-SERC, Chennai, INDIA. 21-23 December 2016.
2. Ramana P.V., Bisht K, Pathak D, Gupta R, Mechanical properties of concrete exposed to burning, ICCMS-2016, IIT Bombay, Mumbai, India 27<sup>th</sup> June – 1<sup>st</sup> July 2016.